AD-A174 012 ENERGY TRAPPING RELEASE AND TRANSPORT IN THREE DIMENSIONAL ENERGETIC SOLI..(U) MICHIGAN TECHNOLOGICAL UNIV HOUGHTON A B KUNZ 30 JUN 86 N00014-81-K-0620 1/4

UNCLASSIFIED F/G 7/3 NL

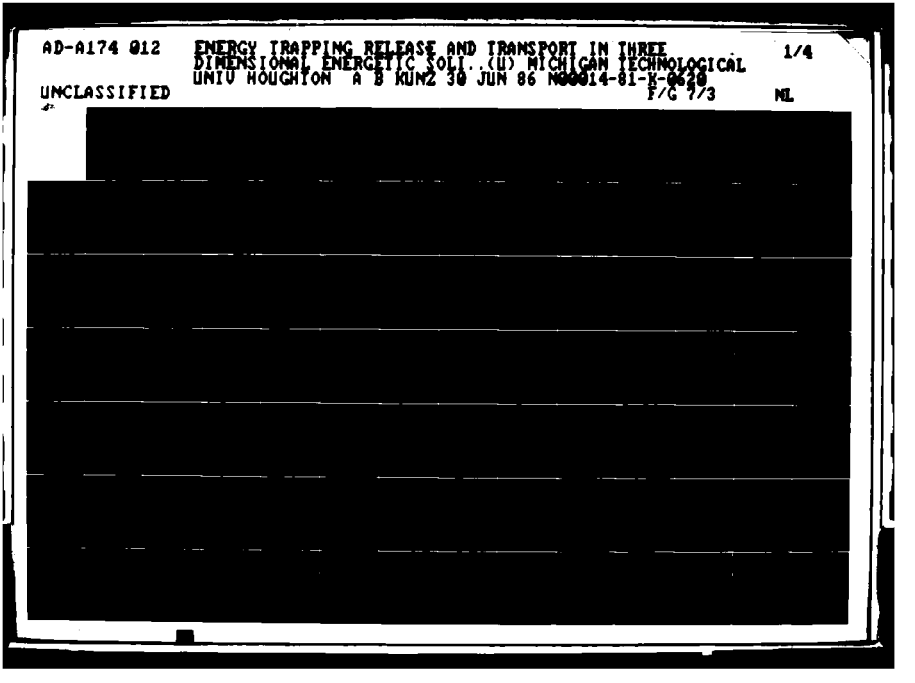

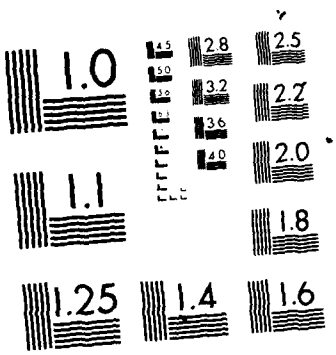

SECURITY CLASSIFICATION OF THIS PAGE (When Data Entered)

REPORT DOCUMENTATION PAGE

READ INSTRUCTIONS BEFORE COMPLETING FORM

1. REPORT NUMBER	2. GOVT ACCESSION NO	3. RECIPIENT'S CATALOG NUMBER

4. TITLE (and Subtitle)

Energy Trapping, Release, and Transport in Three-Dimensional Energetic Solids and Molecular Crystals.

5. TYPE OF REPORT & PERIOD COVERED

Final report 1 July 1981-30 June 1986

6. PERFORMING ORG. REPORT NUMBER

7. AUTHOR(s)

A. Barry Kunz, Presidential Professor and Head Department of Physics

8. CONTRACT OR GRANT NUMBER(s)

ONR-N-00014-81-K-0620

9. PERFORMING ORGANIZATION NAME AND ADDRESS

Michigan Technological University
Houghton, MI 49931

10. PROGRAM ELEMENT, PROJECT, TASK AREA & WORK UNIT NUMBERS

11. CONTROLLING OFFICE NAME AND ADDRESS

Office of Naval Research
Arlington, VA 22217

12. REPORT DATE

30 Jun 86

13. NUMBER OF PAGES

14. MONITORING AGENCY NAME & ADDRESS (if different from Controlling Office)

15. SECURITY CLASS. (of this report)

Unclassified

15a. DECLASSIFICATION DOWNGRADING SCHEDULE

16. DISTRIBUTION STATEMENT (of this Report)

Approved for public release: distribution unlimited.

17. DISTRIBUTION STATEMENT (of the abstract entered in Block 20, if different from Report)

18. SUPPLEMENTARY NOTES

19. KEY WORDS (Continue on reverse side if necessary and identify by block number)

Energetic Solids, molecular solids, clusters, defects, impurities, ICECAP.

20. ABSTRACT (Continue on reverse side if necessary and identify by block number)

In this report we describe development and implementation of a general theoretical approach to describing the properties of defects and impurities in non-metallic solid systems as well as its bulk properties. This approach combines fully correlated, fuly self-consistent electronic structure determination of the electrical and mechanical properties associated with neutral or charged defects/impurities in or on a non-metal. The system remote from the defect is described by the shell model which incorporates self-consistently, host polarization and distoration. This results in our being able to obtain absolute

DD FORM 1 JAN 73 1473 EDITION OF 1 NOV 65 IS OBSOLETE

SECURITY CLASSIFICATION OF THIS PAGE (When Data Entered)

20. continued

energies of the impurity ions in the host and their interaction. The model is free of adjustable or undefines parameters. This project is of non-trivial magnitude and the current computer implementation, which is functional in our laboratory, consists of a program, ICECAP, which is about 100,000 statements long. This program is the result of extensive collaboration between our group and that of Prof. J.M. Vail, University of MAnitoba, and of Dr. A.M. Stoneham, Harwell, AERE.

A1

Final Technical Report on Grant
ONR-N-00014-81-K-0620

1 July 1981 - 30 June 1986

"Energy Trapping, Release and Transport in Three Dimensional Energetic Solids and Molecular Crystals"

A. Barry Kunz, Principal Investigator
Presidential Professor and Head
Department of Physics
Michigan Technological University
Houghton, MI 49931

Other Senior Investigators Participating in this project:
D. R. Beck, Professor, Physics, MTU
R. S. Weidman, Associate Professor, MTU
T. O. Woodruff, Senior Scientist, Hughes Aircraft

Abstract

In this report we describe development and implementation of a general theoretical approach to describing the properties of defects and impurities in non-metallic solid systems as well as its bulk properties. This approach combines fully correlated, fully self-consistent electronic structure determination of the electrical and mechanical properties associated with neutral and charged defects/impurities in or on a non-metal. The system remote from the defect is described by the shell model which incorporates self-consistently, host polarization and distortion. This results in our being able to obtain absolute energies of the impurity ions in the host and their interaction. The model is free of adjustable or undefined parameters. This project is of non-trivial magnitude and the current computer implementation, which is functional in our laboratory, consists of a program, ICECAP, which is about 100,000 statements long. This program is the result of extensive collaboration between our group and that of Professor J.M. Vail, University of Manitoba, and of Dr. A.M. Stoneham, Harwell, AERE.

Summary of Project

This project, since its beginning, has been dedicated to understanding the fundamental properties that control the electronic structure and also, ultimately, the chemical properties of energetic and other molecular solids. This project began envisioning the need to understand the fundamental electronic structure of energetic materials. This was, and to an extent still remains, an area in which there are very few definitive studies. The normal methodology employed by researchers in the area of solid state physics would be to attempt to determine the electron energy band structure of such systems and it was here that this project began. Immediately, there is a point of contention, namely what model should one adopt for describing the electronic energy band structure of such a system. Conventional solid state wisdom would imply that one should begin with a general first principles methodology called density functional theory. However, past experience in applying density functional theory to materials with similiar electrical properties to most of the energetic materials, that is, to molecular systems such as the solid rare gases or other insulating systems such as the alkali halides has indicated that the density functional methods provide an extremely poor initial guess as to the band structure of the systems involved. Therefore, the likelihood of obtaining a qualitatively correct and certainly a quantitatively correct description of the electronic properties of such systems is highly unlikely. It has also been known for some time, due to in part the early studies of this principal investigator that Hartree-Fock methodologies, although cumbersome, in application to metallic or near matallic systems are nonetheless capable of providing extremely accurate descriptions of the electronic properties of insulating systems including the solid rare gases in the alkali halides. It is with these methodologies therefore, that we decided to begin.

The type of electronic properties that one would wish to describe accurately for the bulk of materials include the following. We would like to have an accurate description of the shape and widths of the occupied electronic energy bands. We would like to have a good estimate of the non-occupied or virtual energy bands and shapes, in particular, since their width extends from the point of inception to the positive infinite. We are interested principally in an accurate description of the density of states and also the absolute energy value at which the onset of these continuous bands begin.

Next, we would like to obtain an accurate description of the optical spectroscopy of such systems. This does not just include some kind of a convolution of the electronic occupied with the electronic virtual bands, but also includes those modifications caused by the coulomb correlations provided by the interaction of an outgoing electron, that is, the electron being excited with the net positive hole left behind in the valence band. Such excited states in solid state physics are normally termed excitons and it was with these problems that we began.

In order to begin we initially sought to verify our methodologies which consisted of the use of many body perturbation theory on top of an unrestricted Hartree-Fock calculation and so our initial starting point was with the free space methane molecule itself. In this study which is described fully in appendix A we determined a basis set which was proven

accurate to be able to account for the total correlation and total system energy of the methane molecule to within 2 tenths of an eV of the experimental value. This is a calculation that was roughly comparable in accuracy to the best available in the literature at that time. In addition, this calculation was pushed through to provide a description of the methane excited state spectrum. This again is fully described in appendix A, however, it is my intent to call attention to one very significant and important fact which arose from this study and that is in systems that contain extremely light and mobile ions such as the hydrogen nuclei or protons in the methane molecule that the vibrational amplitude of such protons is sufficient that there is considerable overlap in the vibronic wave functions of Frank-Condon type excited states and those of reduced symmetry. In fact, it has been demonstrated here with the extremely accurate calculations available that the methane molecule relaxes directly into a lowered symmetry than the ground state and it is these states which in fact dominate the excited states spectrum not the Frank-Condon states as we normally expect. This is carefully documented in appendix A. Subsequent to the study on the methane molecule we began a description of the local states of the methane solid by constructing a cluster consisting of a central cell methane molecule and the surrounding twelve nearest neighbor methanes. This is a cluster consisting of 65 atoms in all. Again, studies were made of the ground excited state, and spectral predictions including relaxations into modified geometry excited states were obtained. From this we began to construct an electron energy band model for methane. Orbitals obtained from the molecular calculation were employed here and appropriate block states were obtained from them in the Hartree-Fock limit and as corrected by a use of the electronic polaron which is really a weakly modified many-body perturbation theory method described by this author approximately ten or twelve years in the past. These band structures and their band gaps, band shapes and widths are described in full in appendix B. In addition in appendix B we will also find a description of the excited states of the methane system. The excited states of the methane system, compaired with those that are measured experimentally, are found to be excitations into relaxed, lowered symmetry geometries not into the ideal geometry of the methane crystal itself. Therefore, the important lesson of the molecular study is found to apply here also. We believe that this is a significant result and represents, to our knowledge, the first time the solid state calculation where it was demonstrated that localized excited states of different nuclear symmetry than the ground state were dominant in obtaining a spectrum for the system. Subsequent to this, there have been measurements of the virtual densities of state for the methane solid made at the University of Sherebrook in Canada. We are happy to report that these studies confirm the results of the calculation. Particularly pleasant in our view is the fact that the calculations were performed well in advance of the measurements. We realized at this point that traditional solid state band theory was not going to provide a sufficient basis for all of the necessary studies one needs and wishes to do on energetic materials. At this point we recognized that the real problems did indeed concern those properties which did not appear to be simply periodic in the usual band theory sense. An example has also been given, namely in necessity of including distortions in excited nuclear geometries. Therefore, we decided to abandon further studies

based entirely upon translation of periodicity using, at best, weak perturbated methods to modify this and to directly incorporate localization in further calculations.

A next study performed was a study beginning with the nitro-methane molecule and then extending to clusters of nitro-methane molecules meant to simulate properties that could happen in the solid. A very complete description of this is given in appendix C and is a reproduction of a thesis submitted by Dave Lucas a graduate student entirely supported by this project which was recently completed. In the case of the nitro-methane following on the methane there were no significant surprises of the nature elucidated by the methane study. However, there were some features of this calculation that I would like to draw your attention to, which are fully documented in the appendix C. These are that the quality of normal Hartree-Fock basis sets applied for studies in nitro-methane have in all likelyhood been less than optimal. In this particular study as is seen in appendix C we were able to obtain a substantial reduction in the Hartree-Fock ground state energy over other calculations that are available. While it is true that much of the energy is undoubtedly described to core electron it is also true that in other studies in the absence of counterpoise type methodologies descriptions of binding and bond energies are likely to be in reasonable error. In addition to this, we are also able, even on this not particularly heavy system, to see some effects, we believe, of the size consistency problem. That is of current concern in areas of quantum chemistry or solid state physics. That has led some workers to adoptions of coupled clustered or many-body perturbation techniques. This is reported and described thoroughly in appendix C, Prios work uses techniques such as complete single-double CI's have been reported. Furthermore, Davidson techniques have been used in general to take those results and extrapolate them to what is a presumed correlation limit. Nonetheless, you will see that the simple size consistent methods, generally, considerably enhance the size of the presumed correlation energies for this molecule. This causes us to question both the validity of the CI method at least in its limited sense as applied to this class of system, let alone heavier systems and also to the validity and utility of the Davidson extrapolation techniques. We believe that the use of such methodologies should be further studied and more convincing cases made either for their validity or their non-validity. Certainly, on the basis of the results demonstrated for nitro-methane there is a sufficient reason to question the utility of these methods for further extension in this type of area unless more complete CI type calculations can be effected.

Finally, we have begun the development of the method which will provide for a general description of the properties of defects in and the defects on other properties of non-metallic systems. This general method which was described rather thoroughly in our last annual technical report is termed the ICECAP method. The ICECAP method has recieved a much more complete analysis since then and an internally consistent method of application has been developed that should be applicable to the general class of non-metallic solid. This methodology including the exact handling of the boundary region between the classical and semi-classical region and the quantum mechanical region is thoroughly described in a thesis reproduced in appendix D by another student partially supported by this contract. In this appendix you will

see the full theoretical development of the ICECAP methodology and a preliminary result for a very sensitive system consisting of the lithium impurity in a potassium chloride host. The dominant problem here is that the lithium, because of its small size does not sit at the center of the well, but goes off center distorting the surrounding well and hopping back and forth. Even though this method is applied and this is certainly a preliminar application which has not shown capable of producing the exact frequencies, it has been capable of providing fairly accurate estimates for the barries to the migration and also a set key quantities as a Greuneiseu parameter. We believe that this development will be of significant affect in future studies related to energetic and other non-metallic solids and we believe that in general the ICECAP implementation which is driven by and built on the previous developments reported here is, in fact, a significant advance in the area of non-metallic and certainly energetic materials.

In summary then, we believe that this project has had a considerable amount of success in developing, understanding and improving the methodologies available to us for understanding energetic materials. We have come up with an accurate and effective description of the bulk band structure properties of such materials, presumably a two dimensional slab type implementation would also permit accurate description of the surface properties of such materials. We have demonstrated that we have developed extremely accurate methods, even at the molecular level for describing things such as total energies, excitation energies, even changes of geometry upon excitation. Finally, we have discovered the need for, and provided an implementation of, a very exact method for studying defects in impurity properties in the general class of non-metallic materials.

Appendix A:

Dynamic Effects in the Excited Spectrum of Gaseous Methane

J. Phys. B: At. Mol. Phys. 17 (1984) 2159–2168. Printed in Great Britain

Excitation energies for the lowest triplets and singlet–triplet splittings in gas-phase methane including many-body effects

Donald R Beck and A Barry Kunz†

Physics Department, Michigan Technological University, Houghton, MI 49931, USA

Received 31 January 1984

Abstract. Using second-order Moller–Plesset perturbation theory, we have calculated or estimated (=est) the geometries (we allow for Jahn–Teller distortion) and excitation energies, ΔE, of the five lowest triplets all associated with the $2p \rightarrow 3s$ transition of CH_4 to be: C_{2v}, D_{2d}, C_{3v}, D_{4h}, T_d (unrelaxed) with $\Delta E = 8.74$, 8.95, 9.30 (est), 9.89 (est) and 10.41 eV. The C_{2v} and T_d singlets are found to be 0.33 and 0.22 eV above the respective triplets. Based on these results, two experimental singlet features at 9.65 eV and 10.33 eV are assigned to the D_{4h} and T_d geometries.

1. Introduction

There is much current interest in how energy is localised and released in van der Waals molecular crystals, of which solid methane is almost an ideal representative due to its relative theoretical simplicity and because it is best characterised experimentally (Righini *et al* 1981 and references therein). One hypothesis (Kunz 1983) is that the lower lying excitons (electronic excited states, in molecular language), play a fundamental role in energy localisation in such solids.

Due to the nature of the chemical bonding (van der Waals) of the solid there should be considerable similarity between solid and gas, as is confirmed by direct comparisons of the fundamental spectral region from threshold ($\leqslant 8.5$ eV) to about 14 eV (Brongersma and Oosterhoff 1969, Koch and Skibowski 1971, Lombos *et al* 1967a, b, Ditchburn 1955, Harshbarger and Lassettre 1973). So it is clear that knowledge gained about gas-phase excitons will be significantly transferable to the solid phase especially as regards basis set construction (very small, yet accurate sets are obviously needed) and the role electron correlation plays for excitation energies. Moreover gas-phase results are necessary to establish gas–solid phase trends in conjunction with results already available on the rare gases (Moore 1949, Baldini 1962). Finally gas-phase results are valuable in studying the effects of hydrostatic pressure on excitonic properties.

Because of the computational method adopted, most of our attention will be directed towards the triplet excitons (we should note that triplet excitons may have been already observed in the solid (Brongersma and Oosterhoff 1969)). As the molecule is to be eventually part of a solid, our greatest interest is in equilibrium geometries, including Jahn–Teller distortions of the ground-state T_d symmetry upon excitation.

† Permanent Address: Physics Department, University of Illinois, Urbana, IL 61801, USA.

0022-3700/84/112159 + 10$02.25

A survey of the existing gas-phase literature reveals only a few fairly crude results (Pauzet *et al* 1972, Williams and Poppinger 1975) for the lowest ($2p \rightarrow 3s$) triplet (with no investigation of Jahn–Teller effects); although the singlets have been somewhat better investigated (Gordon and Caldwell 1979 and references therein, Pauzet *et al* 1972, Williams and Poppinger 1975) much of the extra attention has been focused away from the equilibrium region.

In this work a much more thorough examination of the lowest gas-phase triplet is presented using many-body methods, and including the effect of Jahn–Teller distortion. Singlet–triplet splittings for the lowest excitons are obtained at the Hartree–Fock level and used to partially clarify identification of some of the experimental features. Finally, a small but well optimised correlated basis set has been developed which is suitable for cluster modelling of the solid.

2. Hartree–Fock methods and results

While there are numerous methods of demonstrated practical utility for treating many-body effects in the gas phase, our choice will be restricted to those which also offer the greatest practical utility when applied to the cluster. Our current preference, based in earlier experience (Kunz and Klein 1978, Beck 1981), work reported here, and work in progress on the methane cluster as well as atomic excitation energies is to use for a zeroth-order result the unrestricted Hartree–Fock (UHF) solution for the triplets. ($\approx 0.5\%$ contamination of S at the UHF level was observed; the ground state was pure $S = 0$) to which we apply second-order Rayleigh–Schrödinger perturbation theory to correct for correlation effects (extension to third and fourth orders is in progress).

We will represent the triplets with a single Slater determinant, whose elements are one-electron functions which are products of a pure spin and orbital function. The orbital functions, which are not artificially constrained to be eigenstates of orbital operators, are expressed as linear combinations of known atomic orbitals (i.e., the standard LCAO method is used). The AO are themselves fixed linear combinations of primitive (elementary) Gaussian functions (the process of establishing the combinations is called contraction), associated with a unique type ($s, x, y, z, xx, \ldots, xz, xxx, \ldots$, etc) and centre with exponent, ζ. Once the AO are established, the UHF procedure self-consistently obtains the coefficients preceding the AO, for each MO. The computer algorithms used to perform this task involve the 'labels and integrals' package of the POLYATOM code (Csizmadia *et al* 1964, Neumann *et al* 1971) and a UHF algorithm, developed primarily by one of us (ABK). In order to increase the flexibility of this approach with regard to the cluster calculations, we have revised the integral package so that LCMO calculations can be done (i.e., contraction over Gaussians of different types and/or centres can be carried out).

In specifying the set of contracted AO, we will use a notation of which the following is an illustration: [5, 1/1, 1/1 : 2/1 : 1]. This is shorthand for using two contracted s functions centred on C (consisting of 5 and 1 primitives respectively), two p on C (one primitive each), and one d on C (one primitive). Additionally, there is one s function on H (two primitives), one p there (one primitive) and one s midway (unless otherwise specified) between C and H (one primitive).

Our calculations began with the [7, 2, 1/4, 1] set of Dunning and Hay (1977) (nb the next to last ζ, of this work should be 0.4962 and not 4.4962) which were originally

contracted from the 9s5p, in our notation [1, 1, 1, 1, 1, 1, 1, 1, 1/1, 1, 1, 1, 1], set of Huzinaga (1965), which we then partially uncontracted to (5, 1, 1, 1, 1/1, 1, 1, 1). To this set, the four H-centred s primitives of Meyer (1973), and one s-bond function were added. The position and exponent of the bond function was then optimised for the T_d ground state, and the UHF results contracted with minimal loss (only the H contraction associated with the 1s orbital was excluded). The results of this process are shown in table 1.

Table 1. Contracted[a] AO from Gaussian basis sets for CH_4.

	C				H		
ζ_s	C(1s)	C(2s)	ζ_p	C(2p)	ζ_s	C_s	C_2
4233.0	0.001 2184	−0.000 242	18.16	0.010 2025	20.04	0.004 2886	0.005 2455
634.9	0.009 3299	−0.001 8534	3.986	0.063 5277	3.02	0.030 1889	0.036 9433
146.1	0.045 3934	−0.009 0173	1.143	0.165 9428	0.6806	0.093 394	0.117 8185
42.5	0.154 4574	−0.030 6828	0.3594	0.308 178	0.185	0.027 1863	0.151 9823
14.19	0.358 4029	−0.071 1964	0.1146	0.131 6705			
5.148	0.436 7437	0.147 1277	2.9				
1.967	0.147 1753	0.050 2061	15.5				
0.4962	0.001 1586	0.335 5736					
0.1533	0.001 384	0.414 0564					
0.022							
4.4							
8.7							

[a] The 'HF space' consists of 18 AO and 70 primitives, to which we add 24 correlation functions. The C s and p virtuals are shown in the table. In addition, the virtual space includes a d ($\zeta_d = 0.6$) and an f ($\zeta_f = 0.5$) centred on C. The HF space also includes an s function centred at the bond midpoint ($\zeta_s = 1.0$). For the C_{2v} geometry, the larger r_{CH} has a bond function with $\zeta = 0.75$.

In an attempt to check the valence space saturation for the ground state, the following function types were added to the set of table 1 one (in the absence of the correlation f functions) at a time and exponent optimised: d on C ($\zeta = 0.3, -0.001$ au lower), f on C ($\zeta = 0.4, -0.002$ au lower); p on H ($\zeta = 0.75, -0.002$ au lower) and p at the bond midpoint ($\zeta = 0.45, -0.001$ au lower). Due to over-completeness of basis sets, interference of different effects, etc, we can not simply add these lowerings together to produce a better value. On the other hand, by directly comparing the Huzinaga and Saki (1969) 11s7p set with the 9s5p set (Huzinaga 1965) we found that about −0.003 au is 'lost'. Detailed comparison of the two sets shows that this is to be associated with the 1s electrons, which are of no chemical concern. Comparison of our UHF ground-state results with the accurate calculations of others (Meyer 1973, Ortenburger and Bagus 1975, Frisch *et al* 1980, Bartlett and Purvis 1980) shows (table 2) that we do quite well, and the remarks above suggest the bulk of the discrepancy lies in the deep core region. The basis of table 1 also includes the diffuse s of the excited state and the correlation primitives. These additions had little effect on the UHF ground-state energy. Also included in this table is an estimate of the HF limit (Ermler and Kern 1974, Pople *et al* 1976) for the ground state.

The triplets of interest to us may loosely be described as those associated with a 2p to 3s transition on C. From previous (Meyer 1973, Dixon 1974) work on CH_4^+

Table 2. Hartree–Fock energies, E, in au.

State	Method	E(au)	r_{CH}(au)	<HCH (deg)	Basis
ground T_d	UHF[b]	−40.195 17		109.47	6–31 G*[a]
ground T_d	UHF[c]	−40.206 59	2.065	109.47	(531/31)[a]
ground T_d	UHF[d]	−40.207 68	2.05	109.47	[9,9,1,1,1/5,1,1/1/1:4,4:1]
ground T_d	RHF[e]	−40.209 037	2.05	109.47	[9,9,1,1,1/5,1,1/1,1/1:4,4/1:1]
ground T_d	RHF[f]	−40.214 178	2.050	109.47	C: 12s6p3d1f/H: 6s1p/CH: 1s
ground T_d	RHF[g]	−40.214 834	2.066	109.47	
ground T_d	Est. limit[h]	−40.219			
Triplets					
unrelaxed T_d	UHF[d]	−39.840 762	2.05	109.47	[9,9,1,1,1/5,1,1/1/1:4,4:1]
relaxed T_d	UHF[d]	−39.846 921	2.149	109.47	[9,9,1,1,1/5,1,1/1/1:4,4:1]
D_{2d}	UHF[d]	−39.896 76	2.1105	140.8	[9,9,1,1,1/5,1,1/1/1:4,4:1]
C_{2v}	UHF[d]	−39.909 494	2.035; 2.221	121.9; 56.3	[9,9,1,1,1/5,1,1/1/1:4,4:1]

[a] Basis set notation is that of the original authors.
[b] Frisch *et al* (1980). The equilibrium distance was obtained from the UHF minimum.
[c] Bartlett and Purvis (1980).
[d] This work. Basis set of table 1 (NBF = 42).
[e] This work. On C, ε_d' ($\zeta_d' = 0.2$) and on H, ε_p ($\zeta_p = 0.50$) were added to the basis of table 1 (NBF = 60).
[f] Meyer (1973).
[g] Ortenburger and Bagus (1975).
[h] *Ermler and Kern* (1974), Pople *et al* (1976).

and the excited singlets (Gordon and Caldwell 1979), it is clear that strong Jahn–Teller effects may be expected in the excited state, which suggests we investigate several different geometries. We choose to look at a subset of those which Meyer (1973) looked at: namely the T_d (relaxed and unrelaxed: the latter is likely to give the largest Franck–Condon factors), and C_{2v} and D_{2d} as these were the two Meyer (1973) found lowest in energy. Because our ultimate interest is in the solid, the equilibrium regions of the potential energy surfaces are of greatest interest.

The UHF calculations for the unrelaxed excited state began with the original (prior to the contraction shown in table 1) ground-state basis, to which a diffuse C-centred s was added, and then optimised. Subsequent to this, an additional s and p primitive was placed on the C atom and both optimised—with little effect. These were then removed. Finally, the calculation was redone, using the contracted ground-state orbitals of table 1 and the optimised diffuse s, with the net result that the energy was raised 0.006 au.

For the three excited states whose geometry could vary, geometrical optimisation was performed (UHF level), beginning with the CH_4^+ bond angles and distances (Meyer 1973). Typically, bond angles were varied in increments of 5°, and distances in increments of 0.1 au. In all cases, the CH_4^+ geometries (Meyer 1973) were found optimal. For C_{2v} it was found that the longer bond distance had a bond exponent optimised of $\zeta_s = 0.75$, while the shorter one had the 'standard' value of $\zeta_s = 1.0$. (The positions of the bond functions were optimised as well; all were found to be at the midpoint of the bond.)

Our final UHF results for the excited triplets are presented in table 2. It may be noted that the relative ordering of the results is the same as it is for the ion (Meyer

1973). In this table, two extra C s, p and one extra C d and f primitive GTO appear in the basis which produced the quoted result. These are required by and optimised for, the correlation part of the problem. Their presence at this stage is due to formal requirements of the theory (they must contribute to formation of the UHF, or zeroth-order, Hamiltonian). In fact their presence is also efficacious at the UHF level, for on average they lower the UHF triplet energies by about -0.008 au (probably their largest contribution occurs from symmetry-breaking polarisation effects associated with individual MO).

3. Correlation method and results

We choose to correlate our results using second-order Rayleigh–Schrödinger perturbation theory with the UHF energy operator used as a zeroth-order Hamiltonian—a process called unrestricted Moller–Plesset theory (UMP2) by some (Pople *et al* 1976). For us, the method possesses several attractions: (i) it is accurate, yet computationally inexpensive enough to be applied to the clusters of interest, (ii) it requires less decision making—as opposed to, for example, the symmetry-adapted independent-electron pair approximation (SA-IEPA) we applied before (Beck 1981). This advantage will remain in the short term, until enough experience is gained to expedite the decision-making process (to this end, a full analysis, by pairs, is routinely output as part of the correlation run), (iii) it is generally what is called (Pople *et al* 1978) 'size consistent' (as is SA-IEPA), and (iv) extension to higher orders can be made with some ease (Bartlett and Purvis 1980, Pople *et al* 1978).

In UMP2, the correlation energy $E^{(2)}_{\text{corr}}$, is given by (Bartlett and Purvis 1980):

$$E^{(2)}_{\text{corr}} = -\frac{1}{4}\sum_{ij}^{\text{occ}}\sum_{ab}^{\text{virt}} D^{-1}_{abij}\langle ij||ab\rangle^2. \tag{1}$$

where

$$D_{abij} = \varepsilon_a + \varepsilon_b - \varepsilon_i - \varepsilon_j \tag{2}$$

and

$$\langle ij||ab\rangle = \int\int \psi_i^*(1)\psi_j^*(2)\frac{1}{r_{12}}(\psi_a(1)\psi_b(2) - \psi_b(1)\psi_a(2))\,\mathrm{d}\tau_1\,\mathrm{d}\tau_2. \tag{3}$$

In the above, the i, j subscripts refer to the occupied UHF spin–orbitals, and the a, b subscripts to the unoccupied UHF spin–orbitals (called 'virtuals'). The ψ are the output molecular spin–orbitals obtained from the self-consistent UHF process, and the ε are the corresponding eigenvalues. The absence of single excitations in equation (1) presumes that a 'good' UHF solution has been constructed.

By far the most computationally expensive part of evaluating equation (1) is transformation of the integrals from the AO form to the MO form. We have constructed an algorithm to do this which replaces each of the quadrupole sums with four linear sums (e.g. Shavitt 1977), uses random-access scratch files, makes full use of the symmetry of partially transformed integrals, establishes a threshold for the AO integrals below which they are discarded (prior to transformation), and which uses an unpacked set of labels. For the final function space which consists of 84 orbitals (42 in each spin space), typical computation times were about 10 h on the VAX 11/750 equipped with a floating-point accelerator.

In developing a correlated basis, our procedure was to contract the UHF solutions as much as possible (see § 2), to allow maximum control over virtual space convergence. A set of primitive Gaussians was then added to this set to represent the virtuals (at the UHF stage). The exponents of this virtual set were initialised by forcing the $\langle r \rangle$ for the primitive GTO to be the same as the $\langle r \rangle$ for the carbon 2s and 2p functions, as suggested earlier (Beck and Nicolaides 1978). These were then optimised by minimising the *valence* part of $E_{corr}^{(2)}$ for the ground state. In almost all cases, the optimum exponent was very close to the initial one, as had been suggested. It should be noted that for each *virtual* type, GTO are just about as good as Slater-type orbitals (Meyer 1973, Beck and Nicolaides 1978) i.e., as rapidly convergent; about 70–80% of a pair's l-dependent correlation energy is obtained with a single primitive.

The virtual correlation set was developed with two general principles in mind: (i) it must be small enough to be used in the cluster, yet (ii) accurate enough to account for the triplet excitation energy as well. We began with a single optimised virtual s, p and d centred on carbon, which gave us a gap (to unrelaxed T_d) of 10.42 eV, and which yielded a ground-state UMP2 valence correlation energy of −0.1357 au. As will be seen from table 4, this excitation energy is in excellent agreement with our final value—and it is in fact this set which has been used in the cluster calculations.

In order to test how converged the set was, and to provide a benchmark test of the method, our virtual set was further augmented in two stages. First, an extra s and p were added, along with one f virtual; all were centred on C and exponent optimised. This set (42 AO) turned out to be the standard gas phase one—and all triplet as well as the ground-state (see table 3) correlation energies were obtained using it. It can be seen from table 4 that the T_d gap changed by only 0.01 eV.

To provide a benchmark test on the ground state, this set was then augmented with an extra exponent optimised C d ($\zeta_d' = 0.2$) and p on the H ($\zeta_p = 0.50$), and

Table 3. Correlation energies[a] (in au) for CH_4.

State	Method	Valence	All electron
Ground state T_d	UMP2[b]	−0.1640	−0.2018
Ground state T_d	RMP2[c]	−0.1826	−0.2224
Ground state T_d	UMP2[d]		−0.18980
Ground state T_d	UMP2[e]	−0.1373	—
Ground state T_d	PNO-CI[f]		−0.2442
Ground state T_d	Expt[g]	−0.240	−0.293
Triplets			
Unrelaxed T_d	UMP2[b]	−0.1484	−0.1863
Relaxed T_d	UMP2[b]	−0.1415	−0.1794
D_{2d}	UMP2[b]	−0.1461	−0.1840
C_{2v}	UMP2[b]	−0.1410	−0.1789

[a] Geometries and basis sets as shown in table 2.
[b] This work; NBF = 42 (see table 1).
[c] Adding v_d' on C. v_p on H (see footnote e, table 2). Done at the restricted level.
[d] Bartlett and Purvis (1980).
[e] Frisch *et al* (1980).
[f] Meyer (1973).
[g] Pople and Binkley (1975).

Table 4. Theoretical excitation energy (in eV) ΔE to lowest triplets.

Upper state	Method	ΔE
Unrelaxed T_d	UMP2[a]	10.41
	E2[b]	10.53
	EOM[c]	9.97
	UHF[a]	9.98
	S-CI[d]	11.40
	S-CI[c]	10.55
Relaxed T_d	UMP2[a]	10.43
	UHF[a]	9.82
D_{2d}	UMP2[a]	8.95
	UHF[a]	8.46
C_{2v}	UMP2[a]	8.74
	UHF[a]	8.11

[a] This work. Correlated values do not include excitations from the K shell. For the ground state, NBF = 42 results were used.
[b] Pauzet *et al* (1972).
[c] Williams and Poppinger (1975).
[d] Kohda-Sudoh and Katagiri (1978); single excitation CI.

correlated using the RHF variant of the code (called RMP2). (Formally, there is no difference between UHF and RHF correlation for closed-shell ground states; computationally there is a significant saving because there are half as many MO orbital functions.) This lowers the correlation energy by about -0.02 au as shown in table 3 (RMP2).

Let us analyse these RMP results for the ground state. Firstly they surpass the other two theoretical results (Frisch *et al* 1980, Bartlett and Purvis 1980) cited using this method (as do the respective UHF results; see table 2). Next, our RMP2 result for the $\varepsilon_{1s\uparrow,1s\downarrow}$ pair is -0.863 eV (1 au $\sim$27.211 61 eV). If we assume that this should be essentially the $1s^2$ pair energy for the carbon atom, which is about 1.1 eV, we see an error of about -0.009 au has been made in this pair. Of course, a substantial error in this pair is *not* unexpected when we recall our virtual exponents were optimised for the valence part of the correlation energy. A direct comparison with the valence space PNO-CI results of Meyer (1973) whose results include certain of the effects of higher order perturbation theory indicates a valence space error of approximately -0.012 au (see also table 3).

Both Frisch *et al* (1980) and Bartlett and Purvis (1980) have estimated that contributions of third- and fourth-order perturbation theory lower the ground-state energy by -0.022 to -0.023 au (Bartlett and Purvis (1980) also contend that the primary effect of basis-set improvement is on the UHF and UMP2 contributions, which seems reasonable so long as two reasonably accurate sets are being compared, as appears to be the case here).

Pople and Binkley (1975) have provided us with an estimate of the total experimental correlation energy of CH_4, with relativistic and zero-point vibration effects removed. Specifically, for all electrons they estimate about -0.293 au of correlation energy is present (based on Emler and Kern (1974), Pople *et al* (1976) and the UHF limit). In the above, we have accounted for -0.222 (UMP2) -0.021 (UMP2 error) -0.022 (third and fourth order) $= -0.265$ au, leaving us -0.028 au short.

4. Excitation energies and singlet–triplet splittings

In table 4, the triplet excitation energies obtained by UHF and UMP2 methods are presented. It can be seen that correlation typically increases the gap some 0.5 to 0.6 eV. We feel that the triplets have a larger error associated with them then does the ground state, due to the loss due to contraction (however some of the loss of about +0.006 au may be recovered via the virtual s and p centred on C), the spin impurity, and the fact that the virtual set has been optimised for the ground state (pair energies associated with the 3s orbital will be most sensitive to this). If this error were larger than that for the ground state, then our excitation energies would be larger than the exact results. To check the size of the relative error, we have computed the $2p^2\ ^3P \rightarrow 2p3s\ ^3P^o$ excitation energy of the C atom using the CH_4 basis with the result that our value is only 0.08 eV larger than experiment (Moore 1949). Similar errors in other atomic excitation energies obtained using this method are found.

We may also compare our gaps with the related ones obtained by Meyer (1973) for the CH_4^+ states (ionisation process). Using C_{2v} as a reference, his PNO-CI D_{2d} is +0.0062 au higher, ours (excitation) is +0.0077 au, his unrelaxed T_d is 0.062 au and ours is 0.061 au higher. On the other hand, our 'relaxed' T_d is actually slightly *higher* than our unrelaxed value after correlation (at the UHF level, the ordering is reversed; recall geometry optimisation was performed at this level). This appears to be a clear manifestation of the errors referred to above.

In table 4, the lowest triplet excitation energy has also been compared with the theoretical work of other approaches which were all computed using methods and/or basis sets of perhaps less intrinsic merit. None the less, there are two other theoretical values fairly close to our results—one obtained by Pauzet *et al* (1972) using second-order perturbation theory and one by Williams and Poppinger (1975) using single-excitation CI.

Rather than formulate and implement a UHF-based approach to open-shell singlets, we will use an RHF approach implemented with the codes of Goddard *et al* (1972). The results of doing this with the basis of table 1, without any virtuals (NBF = 18), are shown in table 5. Typically the singlet–triplet splittings are 0.2–0.3 eV which are in good agreement with most other *ab initio* theoretical work (Pauzet *et al* 1972, Williams and Poppinger 1975, Kohda-Sudoh and Katagiri 1978). They also agree well with the splittings observed (Moore 1949) in atomic C and Ne, for the 2p3s configuration.

We finally turn to the question of comparing our predictions with experiment. We first note that there are at least two more geometries with triplets potentially below the T_d triplet (see Meyer 1973). These are the C_{3v} and D_{4h} geometries and *if* the spacings of CH_4^+ are maintained (as they *were* for C_{2v}, D_{2d} and T_d), their *estimated* positions would be at 9.30 and 9.89 eV respectively. The relative ordering of the triplets is then C_{2v}, D_{2d}, C_{3v}, D_{4h}, T_d with excitation energies 8.74, 8.95, 9.30 (est), 9.89 (est) and 10.41 eV (unrelaxed) with singlets presumably lying 0.2–0.3 eV above these.

Harshbarger and Lassettre (1973) have measured the electron impact spectra and found a broad diffuse spectra which is difficult to deconvolute in the 8.55–10.95 eV region. This region possesses two maxima, one at 9.65 eV and one at 10.33 eV which they ascribe to a $2p \rightarrow 3s$ transition (see also Koch and Skibowski 1971). Based on energy considerations we might assign these to the D_{4h} and T_d geometries respectively (a more conclusive assignment would involve simultaneous comparison of oscillator strengths; however, accurate *ab initio* theoretical ones seem currently unavailable).

Table 5. Theoretical singlet–triplet splittings (eV), ΔE_{st}.

Species/state	Method	ΔE_{st} (eV)
CH_4, unrelaxed T_d	RHF[a]	0.215
	S–CI[b]	0.21
	E2[d]	0.34
	EOM[c]	0.27
	S–CI[e]	0.41
CH_4, C_{2v}	RHF[a]	0.330
C atom, 2p3s	Expt[c]	0.202
Ne atom, 2p3s	Expt[c]	0.225

[a] This work (see text).
[b] Moore (1949).
[c] Kohda-Sudoh and Katagiri (1978); single excitation CI.
[d] Pauzet *et al* (1972).
[e] Williams and Poppinger (1975).

Brongersma and Oosterhoff (1969) believe they have directly seen transitions to two triplets at 8.8 and 11.0 eV. This large splitting (0.7–1.0 eV) is supported by Katagari and Sandorfy's (1966) semi-empirical calculations but is in obvious contradiction to all *ab initio* results. Kohda-Sudoh and Katagiri (1978) suggest that the larger splitting would occur *if* the excited state orbital had a significant valence (i.e. compact) component. However, an alternative explanation consistent with both the measurement and theory is possible—namely, that the triplets have been assigned to the wrong singlets. The 8.8 eV triplet feature could well be assigned to the C_{2v} singlet and the 9.80 to the D_{4h} feature; under these circumstances, the splitting would be no more than a few tenths of an eV.

Acknowledgments

The authors acknowledge partial support of this research by the US Navy Office of Naval Research under contract ONR-N-00014-81-K-0620. They also thank Mr Joseph Boisvert for his help in developing the MBPT code. DRB thanks the US National Science Foundation for a grant (#PRM-8111589) which provided computer equipment used during the course of this work.

References

Baldini G 1962 *Phys. Rev.* **128** 1562–7
Bartlett R J and Purvis G D III 1980 *Phys. Scr.* **21** 255–65
Beck D R 1981 *Int. J. Quantum Chem.* S **15** 521–38
Beck D R and Nicolaides C A 1978 *Excited States in Quantum Chemistry* ed C A Nicolaides and D R Beck (Dordrecht: Reidel) pp 105–42
Brongersma H H and Oosterhoff L J 1969 *Chem. Phys. Lett.* **3** 437–44
Csizmadia I G, Harrison M C, Moskowitz J W, Seung S, Sutcliffe B T and Barrett M P 1964 *Quantum Chemistry Program Exchange* **11** 47
Ditchburn R W 1955 *Proc. R. Soc.* A **229** 44–62
Dixon R N 1974 *Mol. Phys.* **20** 113–26

Dunning T H Jr and Hay P J 1977 *Method of Electronic Structure Theory* ed H F Schaefer III (New York: Plenum) pp 1–27
Emler W C and Kern C W 1974 *J. Chem. Phys.* **61** 3860–2
Frisch M J, Krishnan R and Pople J A 1980 *Chem. Phys. Lett.* **75** 66–8
Goddard *et al* 1972 unpublished
Gordon M S and Caldwell J W 1979 *J. Chem. Phys.* **70** 5503–14
Harshbarger W R and Lassettre E N 1973 *J. Chem. Phys.* **58** 1505–13
Huzinaga S 1965 *J. Chem. Phys.* **42** 1293–302
Huzinaga S and Saki Y 1969 *J. Chem. Phys.* **50** 1371–81
Katagari S and Sandorfy C 1966 *Theor. Chim. Acta.* **4** 203–23
Koch E E and Skibowski M 1971 *Chem. Phys. Lett.* **5** 429–32
Kohda-Sudoh S and Katagiri S 1978 *Bull. Chem. Soc. Japan* **51** 94–7
Kunz A B 1983 *Phys. Rev.* B **28** 3465–73
Kunz A B and Klein D L 1978 *Phys. Rev.* B **17** 4614–9
Lombos B A, Sauvageau P and Sandorfy C 1967a *J. Mol. Spectrosc.* **24** 253–69
—— 1967b *Chem. Phys. Lett.* **1** 382–4
Meyer W 1973 *J. Chem. Phys.* **58** 1017–35
Moore C E 1949 *Atomic Energy Levels* vol I (Washington, DC: US Govt Printing Office)
Neumann D R, Basch H, Kornegay R L, Synder L C, Moskowitz J W, Hornback C and Liebman S P 1971 *Quantum Chemistry Program Exchange* **11** 199
Ortenburger I B and Bagus P S 1975 *Phys. Rev.* A **11** 1501–3
Pauzet F, Ridard J and Levy B 1972 *Mol. Phys.* **23** 1163–78
Pople J A and Binkley J S 1975 *Mol. Phys.* **29** 599–611
Pople J A, Binkley J S and Seeger R 1976 *Int. J. Quantum Chem.* S **10** 1–19
Righini R, Maki K and Klein M L 1981 *Chem. Phys. Lett.* **80** 301–5
Shavitt I 1977 *Methods of Electronic Structure Theory* ed H F Schaefer III (New York: Plenum) pp 189–275
Williams G R J and Poppinger D 1975 *Mol. Phys.* **30** 1005–13

Appendix B:

Band Theory and Excitonic Effects in Energetic Solids:

Example of Solid Methane

THEORY OF THE ELECTRONIC STRUCTURE AND OPTICAL PROPERTIES OF ORGANIC SOLIDS: COLLECTIVE EFFECTS*

A. Barry Kunz

Department of Physics and Materials Research Laboratory
University of Illinois at Urbana-Champaign
Urbana, Illinois 61801, U.S.A.

Abstract: In this series of lectures we briefly consider two complimentary approaches to the study of organic solids: The method of simulation by finite clusters of molecules, and the methods of energy band theory. In both cases, the initial starting point is the Hartree-Fock method, which, as expected, turns out to be inadequate for any reasonable level of quantitative accuracy. Solids, being essentially infinite sized systems, restrict our choice of correlation methods to those which are size consistent. We are furthermore interested in properties such as optical excitation and need to be able to obtain the finite difference between extensive total energies. This further restricts our choices. Methods based upon ordinary Rayleigh-Schrodinger Perturbation-Theory are chosen and extensive results for solid CH_4 are used as an illustration.

*This research has been funded in part by the U. S. Navy Office of Naval Research, ONR-N-0014-81-K-0620, in cooperation with the Department of Physics, Michigan Technological University, and by the National Science Foundation, DMR-80-20250 in cooperation with the Materials Research Laboratory of the University of Illinois.

I. Introduction.

Theoretical studies on the electronic structure of three dimensional solids have largely excluded the organic or molecular solids. The vast majority of existing calculations have been performed for the solid rare gases.[1] More complicated molecular solids, such as those with two or more atoms per molecu-

J. Ladik et al. (eds.), Quantum Chemistry of Polymers - Solid State Aspects, 83–99.

lar unit, or more than one molecular unit per unit cell, have been largely ignored. The principal exception to this tendency has been for solid I_2. It should be further noted, that the interest in solid H_2 stems largely from interest in its possible transformation to a monatomic metal, exhibiting high temperature BCS type superconductivity.[2] In addition, a recent resurgance of interest in the solid rare gases has been generated by speculations that "low" pressure (~0.3 M bar) metal phases of solid Xe might exist.[3] In addition, some theoretical studies on solid N_2[4] and H_2O[5] exist. In addition, quite a few studies on properties of polymer systems exist.[6] There are probably many reasons for the neglect of this interesting and technologically interesting class of solids. Several of the reasons are likely related to the complicated and at times ill-defined crystal structure of such systems and the associated difficulties in constructing adequate theoretical models. A second and perhaps more serious problem relates to the question of which approach one might use to determine the electrical structure. As an example, the spectrum of solid CH_4 has been determined over an energy range of 8 to about 35 eV. The fundamental spectral region of from threshold (>8.5 eV) to about 14 eV shows marked similarity in both solid and gas phase. It is generally conceded that the gas phase spectra in this energy region is dominated by transitions from the bonding to antibonding bound state orbitals or to Rydberg series like transitions.[7] It seems reasonable to expect that the crystalline spectrum is likely to be similarly dominated by transitions to bound rather than free final states. That is we do not expect the contributions from energy band theory to play a major role in the low lying excitations of solid CH_4. On the other hand the spectral region above 14 or so eV may well be dominated by band to band transitions and this may account for the apparent differences between the high lying spectrum of gas phase CH_4 and solid CH_4. Similar considerations apply to many other molecular solids.

The previous theoretical study on solid methane lends credibility to this argument, as the calculation of Piela, Pietronero, and Resta finds a band gap in excess of 27.2 eV for solid methane.[8] It is not likely that this result is quantitatively accurate as these authors used a very abbreviated basis set in their calculation and found the conduction results to be highly sensitive to the virtual basis set. A further source of error in this early study is the use of the Hartree-Fock approximation uncorrected for any correlation corrections. Similar studies by Mickish and Kunz on the somewhat similar solid rare gases have found that the Hartree-Fock method consistently overestimates the band gap of these systems by about 4 or 5 eV.[1] In addition all band methods are inaccurate, in that, all neglect

the formation of local excited states called excitons.

We believe new approaches are needed if one is to truly interpret the electronic structure of such systems as solid Methane. Recent theoretical results of Kunz and Flynn have demonstrated that it is possible to include the effect of electron-hole interaction and exciton formation without violating Bloch's theorem in calculations of the optical properties of such divergent solids as LiF and Mg or Ca. This is accomplished by means of a degenerate perturbative calculation using the $\vec{k}$-conserved one body valence to conduction band excitations as a basis.[9] This model retains the periodic symmetry of the lattice avoiding complications introduced by the use of finite cluster models to describe the local excitations. These finite cluster models, nonetheless, are useful and accurate approximates as we shall see. The formulationm of the problem in this way by Kunz and Flynn causes one to wish to begin with Hartree-Fock descriptions of the solid since a well defined Many-Body wavefunction is needed. The Hartree-Fock model neglects all correlations and the limited basis set used to describe excitonic effects does not describe properly the relaxation or polarization properties of the system. In these lectures, the correlation effects are incorporated by means of a simple Many Body Perturbation Theory Model (MBPT). The necessary theoretical methods are described in Section II. The numerical calculations are described in Section III, and conclusions are given in the final section.

II. Theoretical Development

The initial step in this development is the choice of the Hartree-Fock method. This choice is largely determined by the need to perform extensive correlation calculations in addition to the initial Hartree-Fock study. To facilitate development, we employ variants on the familiar Linear-Combination-of-Atomic-Orbitals method (LCAO). In the case of cluster calculations, these AO's are first rotated into molecular orbitals (MO's) spanning the entire cluster, and in the case of the band calculations, the AO's are rotated into MO's spanning the crystallographic unit cell. This rotation into MO's is advantageous because for unit cells of ever increasing size or complexity, an adequate description in terms of AO's yields rather large secular determinants. The LCMO scheme reduces substantially the size of the secular determinant. This method was first introduced by Piela et al.[8] for studies on solid methane. In such a simple case the basis set for the occupied orbitals is reduced from 9 to 5 orbitals. Furthermore, the MO's may contain polarization functions in them and therefore yield far greater accuracy than a much larger set of AO's.

The essential features of this approach is this. Let each unit cell be divided into molecules (real ones or not), and we devise a basis set to represent the MO's of these molecules. The primitive basis set used are spherical-harmonic Gaussian Type Orbitals (GTO's) centered about different origins, and have the form

$$\chi_i(\vec{r}-\vec{R}_i) = \exp\,[-Z_i(\vec{r}-\vec{R}_i)^2]\; Y_\ell^m\,(\theta,\phi). \qquad (1)$$

The $\vec{R}_j$ are the origins about which these functions are centered and need not be an actual nuclear site, the Y_ℓ^m are the usual spherical harmonics. The orbital exponent Z_i is chosen by energy minimization. The MO's in turn are just linear combinations of these GTO's,

$$\phi_j\,(\vec{r}-\vec{R}_\alpha) = \sum_i\; a_i^j\;\chi_i(\vec{r}-\vec{R}_i), \qquad (2)$$

The $\vec{R}_\alpha$'s are the locations of the molecules in the system. From the MO's, one forms Bloch orbitals which span the entire system:

$$\psi_j(\vec{k},\vec{r}) = N^{-1/2}\;\sum_\alpha\; e^{i\vec{k}\cdot\vec{R}_\alpha}\;\phi_j(\vec{r}-\vec{R}_\alpha). \qquad (3)$$

The MO's (Eq. (2)) or the Bloch functions (Eq. (3)) form the basis by which we solve the HF problem or its extensions.

The first point is that the Hartree-Fock equation need be solved self-consistently. For a finite molecular cluster, this is achieved by conventional iterative means. However, the infinite periodic system imposes special difficulties. These are simply that the occupied canonical Bloch orbitals are infinite in number and therefore enumerating the contribution of each orbital to the Fock operator imposes a strain on ones computer budget. Two options are available. The first is to use a finite mesh in $\vec{k}$- space and use some form of quadrature to construct the Fock operator. The second is to rotate into a basis set of local orbitals.[10,11,12] In the early stages, both methods were tried with negligible differences in numerical result between them. However, at the current stage of our code development, the local orbitals method enjoys a substantial speed advantage.

The intent of the present study is to obtain spectroscopic information and hence we need examine the meaning of the energy bands. The occupied bands are the negative of the ionization energy for that band for the state of wave vector $\vec{k}$. The virtual bands are similar representations for the electron affinities. In this event one is assuming the use of the Hartree-Fock eigenvalue and also of Koopmans' theorem as is

usually done. The essential physics here refers to ionization properties, not to excitation properties of the n-electron system.

In order to improve upon the Hartree-Fock results one must include correlation corrections. In doing this, initially the author will maintain the same physical definition for the energy bands as in the Koopmans' case. That is, the bands now become quasi-particle bands in which the energy of an occupied level is the negative of the energy needed to create it, and the energy of the virtual states are the negative of the energy recovered in creating it. This is in keeping with the earlier usage of the electronic polaron model and its extensions as discussed by Pantelides et al.[13,14,15]

It is now necessary to discuss correlation corrections. The first problem is that of size consistency (The total energy is an extensive quantity).[16,17] In fact the total energy of an infinite solid is infinite and only the energy/molecule is finite. Unfortunately, the energy change upon ionization is also finite and the energy change/molecule vanishes. That is the energy difference is still finite. Similar considerations apply to excitations of the n-electron system. A simple classical way to view this is to realize that the size of the wave created by hurling a brick into a pond is largely independent of the size of the pond. Therefore we must establish a size consistent framework for the system total energies in such a way that formally we can obtain differences in extensive quantities, cancelling the infinities before we compute finite differences. Alternately, we may reduce the size of the systems so that total energy determinations are possible.

Let us work in a local representation here. This is appropriate since many molecular solids are filled shell systems. For notational simplicitiy, designate the Wannier function $W_{iN}(\vec{r})$ as the i^{th} Wannier function about site $\vec{R}_N$. Form a complete set of Wannier orbitals describing the ground state of the neutral, N-electron solid in the Hartree-Fock limit. We will use them to generate the ion states as well. For a system of N-electrons the Hamiltonian is

$$H = \sum_{i=1}^{n} -\frac{\hbar^2}{2m}\nabla_i^2 - \sum_{i=1}^{N}\sum_{I=1}^{M}\frac{Z_I e^2}{|\vec{r}-\vec{R}_I|} + \frac{1}{2}\sum_{i=1}^{N}\sum_{j=1}^{N}\frac{1}{}\frac{e^2}{|\vec{r}_{ij}|} \qquad (4)$$

The electronic has mass m, and is charge e, Z_I is the atomic number of the nucleus at site I. The i^{th} electron has coordinate $\vec{r}_i$ and the I^{th} nucleus has coordinate $\vec{R}_I$. In terms of Wannier Functions, in the single determinant limit, the energy of the system is

$$E_N = \sum_{ij}^{(N)} \langle w_{iI} | -\frac{\hbar^2}{2m}\nabla^2 - \sum_{J=1}^{M} \frac{Z_J e^2}{|\vec{r}-\vec{R}_j|} | w_{iI}\rangle \qquad (5)$$

$$+ \frac{1}{2}\sum_{ij}^{(N)} \sum_{IJ} \langle w_{iI} w_{jJ} | \frac{e^2}{r_{12}} | w_{iI} w_{jJ}\rangle - \langle w_{iI} w_{jJ} | \frac{e^2}{r_{12}} | w_{jJ} w_{iI}\rangle \Big\}$$

The symbol (N) on the summation implies sums over all states in the occupied N electron space. To keep the physics of the energy bands discussed earlier we need to look at the N-1 and N+1 electron system next.

Let the ground state of the N-electron Hartree-Fock system be designated as $|N\rangle$ and let a^+_{pI}, a_{pI} create or destroy a Wannier function at site I with other quantum numbers p. We adopt the conventive that quantum numbers i, j, k etc., refer to occupied orbitals, a, b, c to virtual orbitals and o, p, q to either/both. A Slater determined of the N-1 body system is

$$|N-1;\ jB\rangle \quad a_{jB}|N\rangle \qquad (6)$$

This will by symmetry adapted later. The energy expectation value of this state is simply

$$E^{jB}_{N-1} = E_N - \langle w_{jB}|F(N)|w_{jB}\rangle \qquad (7)$$

Here F(N) is simply the N-electron ground state Hartree-Fock operator. Similarly one may obtain the off diagonal matrix elements between two states $|N-1, iA\rangle$ and $|N-1, jB\rangle$. These are:

$$D^{iAjB}_{N-1} = \langle w_{jB}|F(N)|w_{iA}\rangle. \qquad (8)$$

One may project on the state $|N-1, jb\rangle$ to form a proper translational invariant Bloch function, $\psi^{N-1}_j(\vec{k})$:

$$\psi^{(N-1)}_j(\vec{k}) = \sum_B \frac{1}{\sqrt{M}} e^{i\vec{k}\cdot\vec{R}_B} |N-1;\ jB\rangle \qquad (9)$$

In terms of eqs (5)-(9) one may construct a band structure in terms of Wannier-functions and Slater determinante for the occupied orbitals. These are yet uncorrelated. One may treat the N+1 body states similarly. Furthermore, recognizing that E_N in eq (11) is infinite and also irrelevant, since energy changes are needed, we proceed to define E_n as 0, and thus simplify our computation.

A framework is needed in order to simply correlate this problem since the simple single Slater determinants $|n-1, jB\rangle$ are highly degenerate, and within a band, the $\psi_j(\vec{k})$ are nearly degenerate. Consider the problem in a general framework initially. H is a Hamiltonian,

$$H = H_o + V. \tag{10}$$

We assume that the eigenstates of H_o are known as

$$H_o\phi_i = w_i\phi_i. \tag{11}$$

The projector onto a given eigenstate of H_o say ϕ_i is P_i and is given as

$$P_i = |\phi_i><\phi_i|.$$

Furthermore a projector onto the first n states say is $\bar{P}$ and

$$\bar{P} = \sum_{i=1}^{n} |\phi_i><\phi_i| = \sum_{i=1}^{n} P_i. \tag{12}$$

Assume we order our eigenfunction of H_o so that the states of interest lie in the range 0 to n. Furthermore no other states are degenerate with these states. Now let us solve the desired equation:

$$H\psi = E\psi = (H_o+V)\psi. \tag{13}$$

Let us chose a w_j for $1 \leq j \leq n$, then:

$$(1-\bar{P})(H_o-w_j)\psi = (1-\bar{P})(E-w_j-V)\psi \tag{14}$$

One may commute $(1-\bar{P})$ with H_o-w_j and proceed to see

$$\psi = \bar{P}\psi + (H_o-w_j)^{-1}\ (1-\bar{P})\ (E-w_j-V)\psi. \tag{15}$$

Furthermore;

$$P_i\psi = \pi_i\phi_i,\ \pi_i = <\phi_i|\psi>,$$

so that

$$\bar{P}\psi = \sum_{k=1}^{n} \pi_k\phi_k = \phi. \tag{16}$$

Therefore

$$\left[1 - (H_o-w_j)^{-1}\ (1-\bar{P})(E-w_j-V)\right]\psi = \phi. \tag{17}$$

If one defines

$$T = \left\{1 - (H_o-w_j)^{-1}\ (1-\bar{P})(E-w_j-V)\right\}^{-1}, \tag{18}$$

then

$$\psi = t\phi. \tag{19}$$

Furthermore one can show that

$$(E-w_i)\,\pi_i = \sum_{k=1}^{n} \pi_k\,\bar{V}_{ik}, \tag{20}$$

where

$$\bar{V}_{ik} = \langle\phi_i|VT|\phi_k\rangle. \tag{21}$$

Eqs. (20) and (21) define a perfectly good algebraic eigenvalue equation for the system energies. To proceed further, one expands the inverse appearing in T. That is,

$$VT = N + V\frac{1}{H_o - w_j}(1-\bar{P})(E-w_j-V) + \ldots\,. \tag{22}$$
$$= \bar{V},$$

or

$$\bar{V}_{ik} = V_{ik} + \sum_{a=N+1}^{\infty} \frac{a}{w_j - w_a} V_{ia}\,V_{ak}. \tag{23}$$

The structure of the eigenvalue problem defined by Eqs (20), (21) and (23) is now clear. The matrix elements to lowest approximation are similar to those of second order R.S.P.T. and this is clearly a size consistent approach. If all the eigenvectors in the first n are degenerate, one recovers normal degenerate perturbation theory. Consider our problem, where we use Wannier functions, this framework makes our approach clear. First correlate the single Slater determinant of Wannier functions, then proceed with Bloch symmetry projection to remove the degeneracy. The N-body wavefunction has proper Bloch symmetry for closed band systems. By using a proper choice of A in the Adams-Gilbert local orbital formulation called A^W one may obtain Wannier orbitals.[11] The actual choice of A^W is not important, only that such exist. Then

$$[F + PA^W P]\,w_{iI} = \varepsilon_{iI} w_{iI} \tag{24}$$

The first order Fock-Dirac density matrix is ρ. From this one constructs a zero order Hamiltonian. For a system of M-electrons, H_o is defined as

$$H_o = \sum_{i=1}^{M} [F(\vec{r}_i) + \rho_i A_i^W \rho_i] \tag{25}$$

and then the perturbation, V becomes

$$V \equiv H - H_o \tag{26}$$

$$E(N) = E_N + \sum_{iI>jJ}^{(N)} \sum_{aA>bB} \frac{|V_{iIjJ}^{aAbB}|^2}{\epsilon_{iI}+\epsilon_{jJ}-\epsilon_{aA}-\epsilon_{aB}}. \tag{27}$$

Here the summation (N) indicates all Wannier orbitals in the N-electron state. The matrix element is simply

$$V_{iIjJ}^{aAbB} = \langle w_{iI} w_{jJ} | \frac{e^2}{r_{12}} | w_{aA} w_{bB} \rangle - \langle w_{iI} w_{jJ} | \frac{e^2}{r_{12}} | w_{bB} w_{aA} \rangle \tag{28}$$

The N-body orbitals will be used to describe both the N-1 and N+1 body states. Brillouin's theorem is not valid for such states. Consider first the N-1 body problem. Let Wannier orbital w_{iB} be deleted from the N-body ground state. Then to second order one finds that

$$E(N-1,iB) = E_n - D_{N-1}^{iBiB} + \sum_{jI}^{(N+1)} \sum_{aA} \frac{|F(N-1;iB)_{jI}^{aA}|^2}{\epsilon_{jI}-\epsilon_{aA}} + \sum_{kK>jJ}^{(N-1)} \sum_{aA>bC} \frac{|V_{kK,jJ}^{aAbB}|^2}{\epsilon_{kK}+\epsilon_{jJ}-\epsilon_{aA}-\epsilon_{bC}}. \tag{29}$$

In Eq (19) the V is still as defined in Eq (18) and F(N-1;iB) is obtained by deleting terms referring to orbital w_{iB} from F(N). Therefore

$$F(N-1;iB)_{jI}^{aA} = \langle w_{jI} | F(N-1,iB) | w_{aA} \rangle. \tag{30}$$

One proceeds in like fashion for the N+1 electron case, adding W_{CB} to the N electron state.

$$E(N+1;cB) = E_N + D_{N+1}^{cBcB} + \sum_{jJ}^{(N+1)} \sum_{aA} \frac{|F(N+1,cB)_{jJ}^{aA}|^2}{\epsilon_{jJ}-\epsilon_{aA}} + \sum_{jJ>kK}^{(N+1)} \sum_{aA>dD} \frac{|V_{jJkK}^{aAdD}|^2}{\epsilon_{jJ}+\epsilon_{kK}-\epsilon_{aA}-\epsilon_{\alpha D}} \tag{31}$$

In Eq (21) V remains as in Eq (18) and F(N+1;cB) is obtained by adding terms referring to orbital w_{cB} to the N-electron Fock operator.

One may obtain the physically interesting energy differences from these expressions. The ionization potentials are defined by E(N) - E(N-1;iB). This difference called

here Δ_{iB} is given as

$$\Delta_{iB} = D_{N-1}^{iBiB} + -\sum_{jJ}^{(N-1)} \sum_{aA} \frac{|F(N-1,iB)_{jJ}^{aA}|^2}{\epsilon_{jJ} - \epsilon_{aA}}$$

$$+ \sum_{jJ\neq iB}^{(N)} \sum_{aA>cC} \frac{|V_{iBjJ}^{aAcC}|^2}{\epsilon_{iB}+\epsilon_{jJ}-\epsilon_{aA}-\epsilon_{cC}} - \sum_{jJ>kK\neq iB} \sum_{aA} \frac{|V_{jJkK}^{iBaA}|^2}{\epsilon_{jJ}+\epsilon_{kK}-\epsilon_{iB}-\epsilon_{aA}} \quad (32)$$

Likewise the electron affinity terms are obtained by letting $\Delta_{CB} = E(N+1;CB)-E(N)$. Then

$$\Delta_{cB} = D_{N+1}^{cBcB} + \sum_{jJ}^{(N+1)} \sum_{aA} \frac{|F(N+1,\ CB)_{jJ}^{aA}|^2}{\epsilon_{jJ} - \epsilon_{aA}} + \sum_{iI}^{(N+1)} \sum_{aA>dD\neq cB}$$

$$\frac{|V_{iIcB}^{aAdD}|^2}{\epsilon_{iI} + \epsilon_{cB} - \epsilon_{aA} - \epsilon_{dD}} - \sum_{iI>jJ}^{(N+1)} \sum_{aA\neq cB} \frac{|V_{iIjJ}^{cBaA}|^2}{\epsilon_{iI} + \epsilon_{jJ} - \epsilon_{cB} - \epsilon_{aA}} \quad (33)$$

It is these formulas we will use in this study.

One final piece is needed to complete this theory. This is to include the actual effect of electron-hole interaction upon excitation. An accurate method of doing this for both tightly bound or loosely bound excitations has been recently given by Kunz and Flynn.[9]

The essential point is to use the Hartree-Fock bands as a basis set after incorporation of correlation corrections into the band energies. The Fock ground state $|N\rangle$ is then used to describe schematically the process. Let $\alpha_v(\vec{k})$ *annihilate* a valence electron of wavevector $\vec{k}$ and let $\alpha_c^+(\vec{k})$ create a conduction electron of wavevector $\vec{k}$. Consider the state then:

$$|N,\vec{k}\rangle = \alpha_c^+(\vec{k})\ \alpha_v(\vec{k})\ |N\rangle \quad (34)$$

It is only states like this which can be reached from the ground state via optical processes. Furthermore all such ground states $|N,\vec{k}\rangle$ correspond to the same total crystal wavevector; that of the ground state. The most general excited state that one may access is then $|N, E\rangle$, where

$$|N,e\rangle = \sum_{\vec{k}} a_{\vec{k}}\ |N,\vec{k}\rangle \quad (35)$$

In this sum, the ground state $|N\rangle$ is excluded because it differs in parity from the excited state. By finding the $a_{\vec{k}}$ and $\langle N, E|H|N, E\rangle$, one may determine the spectrum of the solid including electron-hole interaction. This is achieved by means of a CI calculation among the states $|N, \vec{k}\rangle$. The formation of such ex-

citon states is not an extensive property and size consistency is not a problem as demonstrated by Kunz and Flynn.[9] Exact implementation of such an infinite CI is of course impossible and we use a finite number of states, some 270 configurations. A second approximation is made as well. This is to truncate the coulomb interaction at the boundary of a unit cell. This is not unreasonable for tightly bound excited systems as in the case of CH_4 particularly since the large lattice constant (11.14 au) encloses a substantial volume in a unit cell. The dominant consequence of this is to allow the formation of only a single bound exciton, not an entire Rydberg series below the bands. However when the coefficients a_k are used to evaluate the optical response one finds substantial adjustment over the Hartree-Fock results. These changes are due to the redistribution of oscillator strength to the bottom of the conduction band due to the inclusion of electron-hole interaction.

The alternate approach employed is to use a finite molecular cluster simulation. This is also done using the method of local orbitals. In this case one partitions the system into the cluster and the environment. The environment imposes itself on the cluster by means of a bounding potential. The methods of doing this are well represented in the literature, and a general approach is given by Kunz and Klein[18] which need not be repeated here. Correlation is imposed using the technique of this section and in particular eqs. (20), (21) and (23) as needed. For non-degenerate states of course, these reduce to ordinary second order RSPT. Most cases considered here are not degenerate in the cluster limit, but for those cases for which degeneracy is a problem, we have found the full approach to be very powerful.[19]

III. Results for Solid CH_4

A Gaussian basis set was first developed for the CH_4 molecule in free space and then reoptimized for the crystal to allow accurate description of the energy bands, occupied and virtual. It was found easy to obtain accurate valence bands, but that the conduction bands were quite sensitive to the choice of outer orbital. The variational principal applies to the solution of the one particle states in a LCMO formalism, and the selection of the basis is quite easy. In practice, the conduction bands are found to be stable against small changes in basis set. The valence structure here agrees well with that obtained after corrections to formalism by Piela *et al.*[8,20,21] The conduction bands are in very poor agreement however. This is due to the far too restrictive basis set employed in the Piela *et al.*[8] calculation of the virtual bands. In performing this calculation, some idealizations are needed. A lattice constant of 11.14 au,

in agreement with Piela et al. is used and the C sub lattice is fixed as a fcc one as per experiment. The four H's form in tetrahedra about the C in a unit cell. In the real world, the tetrahedra do not allign from one cell to another but have orientational disorder. We, as did Piela et al. fix the H's in an ordered fcc lattice as well. The current calculation uses the same geometry as does Piela et al. The C-H distance is obtained computationally from Beck[22] and for a lattice constant of 11.14 au, the equilibrium constant, is essentially the same C-H distance as in the free molecule.

Although the Hartree-Fock band results overestimate any reasonable band gap, they do reduce the Piela gap by about 13.6 eV however,[8] and one need add correlation along the lines suggested in Section II. In performing the correlation correction computations, the author deviates from the ideals expressed in the preceding section to the extent that instead of solving for a set of rather complicated, orthogonal Wannier functions as implied by the derivations, one approximates these by a set of local orbitals. In obtaining these the unit on which localization occurs is the CH_4 molecule is used, and also the appropriate multicenter localization.[23] These orbitals are quite local, the valence-valence overlaps being 0.03 or less here. First order overlap corrections are made in the inter molecular terms for further precision. Due to the procedure adopted, all orders of overlap in the large intra molecular overlaps are included exactly. The inclusion of these corrections is essential if one wishes to achieve quantitative accuracy. In evaluating the perturbation sums, d orbitals on the C atom and p orbitals on the H atoms were added to the band structure basis set. The effect of the several contributions to Eqs (32) and (33) are given in Table 1. There we call the second term on the right hand sides of Eqs (32) and (33) the relaxation and the sum of the second and third terms, which come from two electron virtual excitations, clearly represent correlation terms.

The energy bands for CH_4 including correlation are shown in Figure 1. The density of electron states is also seen in these figures. As is clear from these figures, the band gap is indirect and from Γ_{15v} to $X_{5'C}$. The direct gap is at the X point and is $X_{5'v}$ to $X_{5'C}$. The correlated indirect gap is found to be 13.0 eV, and the correlated direct gap is found to be 13.3 eV.

Finally, one computes the position of the exciton levels in CH_4. This is accomplished using the method given in Section II which has been more fully described in Ref. 9. In this calculation the coulomb interactive is treated as a one molecule interaction. The effective electron-hole interaction is here computed to be 5.4 eV. This is the value of the V_0 discussed in

Table 1

Contributions to the ionization potential and electron affinity of solid CH_4 are shown as a function of lattice parameter. Results are given for the correlation correction and the relaxation correction. Results are in eV.

a	11.14 au	10.50 au	10.00 au
valence correlation	0.1 eV	0.2 eV	0.4 eV
valence relaxation	1.2 eV	1.2 eV	1.2 eV
conduction correlation	-.7 eV	-.8 eV	-.9 eV
conduction relaxation	~0.0 eV	~0.0 eV	~0.0 eV
net gap change	-2.0 eV	-2.2 eV	-2.5 eV

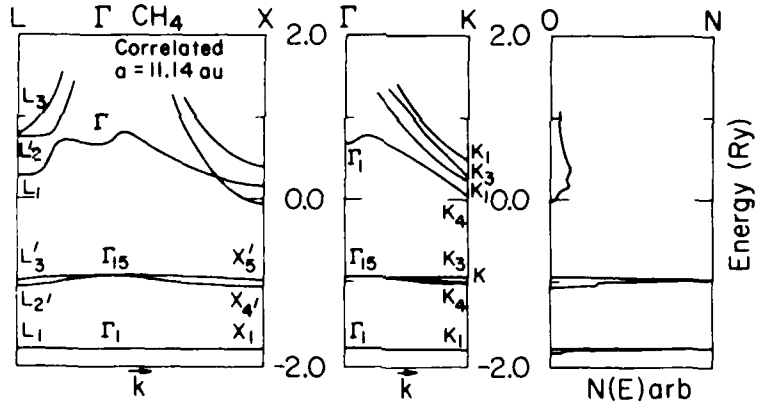

Figure 1 The correlated band structure of solid CH_4 and density of states in shown for lattice parameter = 11.14 au.

Ref. 9. Using this value, the exciton is found to be at 10.9 eV. The optical spectrum of Koch and Skibowski[24] does find a spectral peak at 11.0 eV and this may well be our exciton. A more quantitative analysis of the optical response is not possible at this time because the highest valence and lower conduction bands are of like symmetry and the techniques developed in Ref. 9 and currently available do not permit a calculation of the optical response for the case in which the band to band transitions are dipole forbidden only the positions. Therefore, the author reluctantly contents himself with using only the $\vec{k}$ conserved joint density of states in comparison with the measured reflectance spectrum shown in Figure 2.[24] As is clear from this figure, even if one were to include the exciton at 11.0 eV, a fair degree of discrepancy remains. This is largely at low energy. This discrepancy is expected. A similar result is seen in the free CH_4 molecule and is due to the mobility of the H nuclei and their large zero point motion. The excited CH_4 molecule can lower its energy by about 1.6 eV by relaxing from ideal T_D geometry to D_{2h} geometry. Due to large zero point motion it may be possible to excite from the ground state T_D geometry directly into the relaxed, distorted D_{2h} geometry directly. This certainly appears to be the case in the free molecule and a discussion of this is being prepared by Beck and Kunz.[25] If one assumes the same type of Jahn-Teller distortion is present in the solid, a distorted exciton line would then appear at about 9.3 eV. This is shown as a dotted line in Figure 1. Since the first experimental peak in solid CH_4 lies at 9.6 eV, this inclusion greatly enhances the comparison of theory and experiment. In addition the low energy continuous spectrum between about 12 and 14 eV would be enhanced in strength by the redistribution of oscillator strength due to exciton formation as was seen in LiF.[9]

Large scale cluster calculation for bulk CH_4 (13 molecules or 65 atoms) and for the CH_4 surface (9 molecules or 45 atoms), including all electrons and correlation via the perturbative route, have been recently performed by Beck.[26] These calculations are for the excitons alone and tend to confirm the energy band results qualitatively and quantitatively. The specific details of the perturbation treatment for large systems is well described in the literature.[27]

IV. Conclusions

The essential conclusions are few and simple. These are one can construct a satisfactory, self-consistent Hartree-Fock band structure for molecular solids, including the conduction bands, if one carefully optimizes the basis set. If one wishes

to obtain quantitative comparisons with experiment, the inclusion of correlation corrections is essential. Furtherm re, in describing the ion states in terms of the neutral system orbitals corrections termed relaxation corrections are needed. It is seen here, using a Wannier basis, how such arise and may be included. It is also seen that inclusion of electron-hole interaction is needed if one is to quantitatively study the optical spectrum. In addition, due to the light mas of H one need also be prepared to include Jahn-Teller distortion if one is to be fully quantitative.

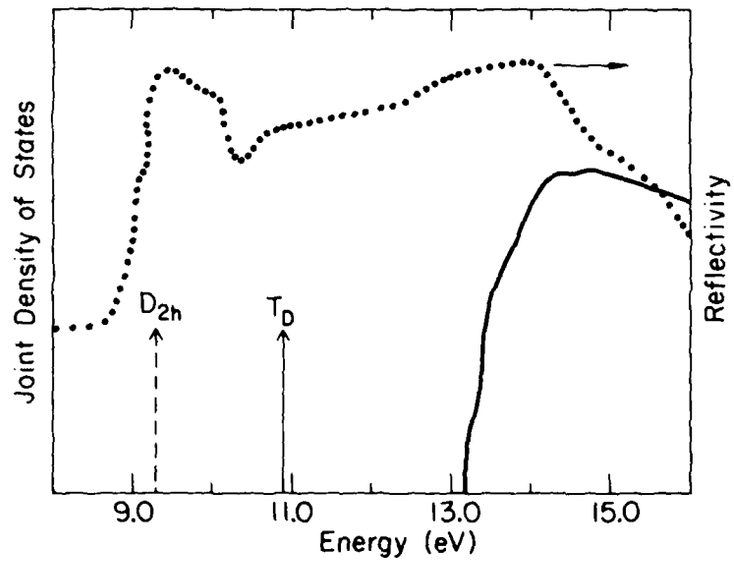

Figure 2 The optical joint density of state is shown for solid CH_4 along with the T_D geometry exciton position and probable D_{2h} geometry exciton. The optical reflectivity of Ref. 24 is also shown

References

1. A. B. Kunz and D. J. Mickish, Phys. Rev. B 8, 779 (1973); and references contained therein.

2. A. Zunger, J. Phys. Chem. Solids 36, 229 (1975); G. Pastori-Parraviccini, F. Piccini and L. Resca, Phys. Stat. Sol. 60, 801 (1972); E. L. Pollack, T. A. Bruce, G. V. Chester and J. A. Krumhansl, Phys. Rev. B 5, 4180 (1972); J. A. Krumhansl and S. Y. Wu, Phys. Rev. B 5, 4155 (1972); D. M. Gray and A. B. Gray, Phys. Rev. B 19, 5329 (1979); L. Kumar, H. J. Monkhorst and J. Oddershede, Int. J. Quant. Chem. 12, 145 (1978); C. Friedli and N. W. Ashcroft, Phys. Rev. B 16, 662 (1977).

3. D. A. Nelson and A. L. Ruoff, Phys. Rev. Lett. 42, 383 (1979); M. Ross and A. K. McMahon, Phys. Rev. B 21, 1658 (1980); A. K. Ray, S. B. Trickey, R. S. Weidman and A. B. Kunz, Phys. Rev. Lett. 45, 933 (1980); A. K. Ray, S. B. Trickey and A. B. Kunz, Sol. St. Comm. 41, 351 (1982).

4. E. Huler and A. Zunger, Phys. Rev. B 12, 5878 (1975); A. Zunger, Mol. Phys. 28, 713 (1976).

5. E. Huler and A. Zunger, Chem. Phys. 13, 433 (1975).

6. See for example, Quantum Theory of Polymers, J-M Andre, J. Delhalle and J. Ladik, eds. D. Reidel Co. Dordrecht (1978).

7. R. W. Ditchburn, Proc. Roy. Soc. 229A, 44 (1955); P. H. Metzger and G. R. Cook, J. Chem. Phys. 41, 642 (1964).

8. L. Piela, L. Pietronero and R. Resta, Phys. Rev. B 7, 5321 (1973).

9. A. B. Kunz and C. P. Flynn, J. Phys. C. 16, 1659 (1983); Phys. Rev. Lett. 50, 1524 (1983).

10. W. H. Adams, J. Chem. Phys. 34, 89 (1961); 37, 2009 (1962).

11. T. L. Gilbert in Molecular Orbitals in Chemistry, Physics and Biology, P. O. Lowdin and B. Pullman, eds. (Academic Press, 1964).

12. A. B. Kunz, Phys. Stat. Sol. (b) 36, 301 (1969); Phys. Rev. B 7, 5364 (1973); B 8, 1690 (1973).

13. Y. Toyazawa, Progr. Theoret. Phys. (Kyoto) 12, 421 (1954).

14. A. B. Kunz, Phys. Rev. B 6, 606 (1972).

15. S. T. Pantelides, D. J. Mickish and A. B. Kunz, Phys. Rev. B 10, 2602 (1974).

16. D. J. Thouless, The Quantum Mechanics of Many-Body Systems, (Academic Press, 1961).

17. E. R. Davidson and D. W. Silver, Chem. Phys. Lett. 52, 403 (1977).

18. A. B. Kunz and D. L. Klein, Phys. Rev. B 17, 4614 (1978).

19. P. Goalwin, P. Keegstra and A. B. Kunz, unpublished research results.

20. A. B. Kunz, Phys. Rev. B 9, 5330 (1974).

21. L. Piela, L. Pietronero and R. Resta, Phys. Rev. B 9, 5332 (1974).

22. D. R. Beck, unpublished research results.

23. A. B. Kunz, Phys. Rev. B 26, 2056 (1982); B. 26 2070 (1982).

24. B. H. Lombos, P. Sauvageaw and C. Sandorfy, Chem. Phys. Lett. 1, 382 (1967); E. E. Koch and M. Skibowski, Chem. Phys. Lett. 9, 29 (1972).

25. D. R. Beck and A. B. Kunz, ONR report, unpublished.

26. D. R. Beck, ONR report, unpublished.

27. R. J. Bartlett and I. Shavitt, Chem. Phys. Lett. 50, 190 (1977); R. J. Bartlett, J. Shavitt and G. D. Purvis, III, J. Chem. Phys. 71, 281 (1979); R. J. Bartlett and G. D. Purvis, III, Ann. of the N.Y. Academy of Sciences 367, 62 (1981).

Appendix C:

Some Theoretical Calculations for Nitromethane

THE ELECTRONIC STRUCTURE OF NITROMETHANE (CH_3NO_2)

By

DAVID J. LUCAS

B.S., Michigan State University, E. Lansing, Michigan, 1975.
M.S., Michigan Technological University, Houghton, Michigan, 1977.

A DISSERTATION

Submitted in partial fulfillment of the requirements

for the degree of

DOCTOR OF PHILOSOPHY

(Metallurgical Engineering/Physics of Solids)

MICHIGAN TECHNOLOGICAL UNIVERSITY

1986

This dissertation, "The Electronic Structure of Nitromethane (CH_3NO_2)", is hereby approved in partial fulfillment of the requirements for the degree of DOCTOR OF PHILOSOPHY in the field of Metallurgical Engineering under the Physics of Solids option.

DEPARTMENT Metallurgical Engineering

Donald R Beaab

Thesis Advisor

Floyd Ahlgren

Head of Department

Date 8/25/58

ABSTRACT

THE ELECTRONIC STRUCTURE OF NITROMETHANE (CH_3NO_2)

David J. Lucas
Department of Metallurgical Engineering
Department of Physics
Michigan Technological University
Houghton, Michigan
1986

Ab initio methods are used to investigate the electronic structure of the energetic molecule, nitromethane, in the gas phase as well as in dimer, trimer and small cluster (central molecule plus 8 near-neighbors) configurations in the crystal geometry. Both ground and excited states are investigated, resulting in the lowest reported energy for the ground state, confirmation of a low-lying excited state, and never before reported work on ground and excited states in configurations of more than one molecule. The dipole moment of the free molecule is calculated and compares favorably with experiment. Electronic transition moments and oscillator strengths for the ground to first excited state reported are calculated and interpreted. The ordering of the outer orbitals for the free molecule calculated in this work supports previous semi-empirical work and conflicts with experimental results, all of which are subject to difficult interpretation.

An investigation is also carried out on the effect of a

single free charge on the carbon-nitrogen bond strength of the molecule. It is shown that with the free ion situated at a location where a neighbor molecule would exist in the crystal configuration, this bond, on the central molecule, may be strengthened or weakened by nearly 0.2 eV out of a total calculated bond energy of 2.57 eV.

Work on both the CH_3 and NO_2 fragments is also discussed, the NO_2 results being the lowest yet reported energies for the ground state.

A methodology and approximations are discussed for working with more than one molecule. It is found that scrubbing of integrals over atomic functions to a tolerance of 10^{-6} yields excellent results for the dimer when compared to the case where all integrals are included.

ACKNOWLEDGMENTS

I would like to express considerable thanks to my thesis advisor, Dr. Donald R. Beck, without whose help this work would not have been possible. His knowledge of Hartree-Fock and many-body perturbation theory and their applications to atomic and molecular systems was invaluable. I also received a basic knowledge of atomic physics from his discussions with me on his work in this field. I appreciate the fact that he was always ready and willing to help and make suggestions to me concerning the course of this work. I hope some of his programming skills, which are considerable, have rubbed off on me.

Thanks are in order for Dr. A. Barry Kunz, head of the Department of Physics. His dynamic enthusiasm and direct responsibility for much of the work being done in the department as well as for the scientific computing capability at Michigan Tech yield a fine environment in which to do research and has resulted in outstanding growth in the department over the past several years.

A special thanks is extended to the Department of Metallurgical Engineering and Dr. Lloyd A. Heldt, Dr. Donald E. Mikkola and Dr. Thomas H. Courtney. They have given us a free hand in pursuing research in physics while allowing us to be associated with their department and this is deeply appreciated.

I also wish to thank my committee members, some of who were mentioned above, but also Dr. Samson A. Marshall as well as Dr. Jong K. Lee and Dr. Christopher Woodward for being willing to accept committee responsibility on such short notice. Another thanks to Chris for his professional help in our discussions on the subject of molecular physics and for his friendship.

I thank Ron Winsauer and his group in the Center of Experimental Computation at Michigan Tech for maintaining an excellent environment for large scale computation and to Gloria Strieter, Julie Walter and Helene Hiner in the physics department for allowing me such free access to the use of the p.c.'s.

A very special thanks is extended to Dr. S. F. Trevino of the National Bureau of Standards in Gaithersburg, Maryland. He was considerate enough to give me an extensive tutorial on the method of obtaining molecular coordinates from neutron diffraction data. His professional and courteous response to my inquiries were of tremendous help and are very deeply appreciated.

Finally, I would like to thank my wife, Marsha, for allowing me to pursue this goal and putting up with me.

This work was funded by the U.S. Navy Office of Naval Research under contract ONR-N-00014-81-K-0620.

TABLE OF CONTENTS

LIST OF TABLES

Chapter 3
Computational Methods

Chapter 4
Results for the Nitromethane Monomer

Chapter 5
Nitromethane Dimer Calculations

Appendices

LIST OF FIGURES

Chapter 3
Computational Methods

Chapter 4
Results for the Nitromethane Monomer

Chapter 5
Nitromethane Dimer Calculations

Appendices

LIST OF ORBITAL PLOTS

LIST OF ABBREVIATIONS

au.....atomic units
CASSCF.....complete active space self-consistent field
CI.....configuration interaction
CNDO.....complete neglect of differential overlap
CP.....counterpoise
DZ.....double zeta
EGS.....extended Gaussian set
eV.....electron volt
gs.....ground state
GTO.....Gaussian type orbital
GVB.....generalized valence bond
HF.....Hartree-Fock
hy.....hartrees (energy units)
LCAO.....linear combination of atomic orbitals
MBPT.....many-body perturbation theory
MCHF.....multi-configurational Hartree-Fock
MO.....molecular orbital
MRDCI.....multi-reference determinant configuration interaction
PDZ.....polarized double zeta
PE or PES.....photoelectron spectroscopy
RHF.....restricted Hartree-Fock
RSPT.....Rayleigh-Schroedinger perturbation theory
SCF.....self-consistent field
SD.....Slater determinant
s-t.....singlet-triplet
STO.....Slater type orbital
UHF.....unrestricted Hartree-Fock

Chapter 1

Introduction

The theoretical study of the electronic structure of nitro compounds (XNO_2) is interesting from both the computational and practical points of view. These compounds are highly reactive [1] because of the nature of the electronic structure of the NO_2 group and modifications to the structure that occur for different forms of X (i.e., BH_2, CH_3, H, NH_2). Nitromethane (CH_3NO_2) is an explosive material. We study the electronic nature of nitromethane with the hope of better understanding the initiation and sustenance of the detonation process. It is the theoretically simplest compound of this type in practical use. Both the NO_2 group and CH_3 group are known as radicals because they contain unpaired electrons which allow them to be reactive.

These compounds are characterized by low-lying excited electronic states (excitons)[1]. It has been proposed by A.B. Kunz (1983)[2] that excitons play a key role in energy localization within these compounds and therefore may be fundamentally related to the detonation process. Kleier and Lipton [1] indicate that excitons can cause weakening of the N-O bonds in the compound with the possibility of bond scissioning.

Work has been done by Zerilli and Toton [3] on shock induced molecular excitation in solids. Their shock wave study involved the excitation of low-lying vibrational states in energetic solids and indicate that relaxation time for thermal equilibration of the

internal modes in the energetic molecule is the controlling factor in the initiation of reactions. Excitations of vibrational modes by optical phonons in nitromethane occur at frequencies of about 10^{14} sec^{-1}. The shock wave produces acoustic phonons which raise the temperature of the lattice through acoustic vibrational branches (i.e., excite intermolecular modes in the weakly interacting system) while leaving the optical branches (intramolecular vibrations) at the initial temperature. The critical issue is the rate at which acoustic mode energy is transferred to the intramolecular modes.

Rotational excitations and their pressure dependence have also been studied.[4-6] The relation of these excitations to the detonation process is not indicated although these modes can be excited by acoustic phonons and therefore may be intrinsically related to shock-induced detonation.

Tsai and Trevino[7-9] have done molecular dynamics studies on the initiation and propagation of the detonation process in energetic molecular crystals. These studies involved the hypothetical heating of one end of a molecular crystal capable of undergoing exothermic dissociation. The heating leads to dissociation of molecules and subsequent propagation of a shock wave leading to the detonation of the crystal.

Shock wave experiments by Guirguin, et.al.[10] investigated the decomposition of gaseous nitromethane. They indicate several different pathways by which the molecule can decompose following an initial step of breaking the C-N bond of several molecules and

observing the effect of the products (CH_3 and NO_2) on other molecules in the gas.

Although, as indicated above, the excited vibrational and rotational states of nitromethane have been studied, little work has been done on its low-lying excited electronic states. These states can be attained by photon absorption in the uv region. Experimentally, photo-electron (PE) absorption studies were performed on nitromethane in 1960 by Nagakura[11]. He observed an absorption band at 270 nm (4.6 eV) but attributed it to a nitromethyl anion in the solution. In 1971, PE work[12] showed a band at 220 nm (5.6 eV) due to an excitation in nitromethane. Rabalais[13] saw the band at 270 nm and also one at 198 nm (6.3 eV)

In 1959, McEwen[14] performed semi-empirical calculations on nitromethane, indicating a host of possible transitions at relatively low energies. Kleier and Lipton[1] performed what they called "approximate ab initio" calculations using a minimal basis set and also found several low-lying excited states, but indicate little confidence in their energies, although they feel the ordering of the states they found is correct. No work has been done on nitromethane excitons using extended basis sets and electron correlation calculations and no one has investigated the effects of the crystal environment on excitons when compared to the molecule in the gaseous phase.

Ab initio studies using extended basis sets and electron correlation have been done on other smaller energetic crystals. Particularly noteworthy is the work done by Beck and Kunz[15] on the

methane molecule (CH_4) and the solid simulation. They demonstrate the ability to apply cluster techniques (to be discussed later) to energetic systems and obtain excellent quantitative results.

Ab initio calculations on energetic molecules, while important in helping to gain insights into the electronic behavior, are also interesting and challenging from the computational point of view. The Unrestricted Hartree-Fock method used in this study is an iterative technique which leads to a self-consistent field approximation for the molecular system. When applied to energetic systems such as nitromethane, there is sometimes a tendency for the method to exhibit erratic behavior and difficulty in gaining convergence to an appropriate state. Although it is said to have a relatively simple chemical structure[10] (it being one of the simplest explosives in terms of chemical composition) it is a rather large and complicated system when speaking in terms of ab initio calculations. Also, there is little symmetry in the molecule with which to help reduce the size of the calculation. The task of investigating a cluster of nitromethane molecules using ab initio techniques is a formidable one and in fact, ab initio calculations of this size have rarely been attempted.

Finally, a comment should be made on the relationship of this study to energy transport and localization in solids. There are many mechanisms by which energy transfer can occur.[16] Two well known mechanisms are resonant energy transfer and the exciton. Usually, these two phenomena can be distinguished. The first

involves electromagnetic coupling between molecules with the possibility of the creation of a phonon to conserve energy. The second involves the creation of electron-hole pairs which may move about the lattice. Excitons may experience scattering, radiative decay, dissociation or trapping, all of which result in energy transfer within the crystal. [17]

This work primarily involves the ab initio study of nitromethane's electronic structure in both the ground and excited states. Included in this investigation are studies of both the CH_3 and NO_2 fragments, electronic structure of nitromethane dimers and trimers oriented in near-neighbor crystal geometries and a discussion of the procedure and difficulties involved in working with a cluster of 9 near-neighbor nitromethane molecules in the crystal configuration. The primary focus in this work is to see how near-neighbors affect the electronic structure of the molecule of interest. Also, an investigation into the effects of free charges at specific lattice locations on the strength of the carbon-nitrogen bond in the central mclecule will be discussed as will the dipole moment. None of the mechanisms mentioned in the previous paragraph will be investigated in this work other than a brief look at the transition probability (oscillator strength) between the ground and first excited state in the molecule.

Chapter 2

Theoretical Techniques

Hartree-Fock Theory

In order to undertake the formidable task of calculating the properties of solids, one necessarily must make some approximations. We are primarily interested in the nature of the electronic characteristics of materials. One can divide the problem up into two parts involving the motion of the nuclei (or ions in a lattice) and the electrons (see Madelung [18] for a more complete discussion).

The Hamiltonian is, upon neglecting external fields and relativistic effects:

$$H = H_{el} + H_{nuc} + H_{el\text{-}nuc} \tag{2.1}$$

where in atomic units ($|e|=\hbar=m_e=1$),

$$H_{el} \quad \text{(electron)} = \sum_{i=1}^{n} -\frac{1}{2}\nabla_i^2 \quad + \frac{1}{2}\sum_{i\neq j}^{n} \frac{1}{\left|\bar{r}_i - \bar{r}_j\right|} \tag{2.2}$$

where n is the number of electrons and $\bar{r}$ defines the electron coordinates.

$$H_{nuc}(\text{nuclei}) = -\sum_{i=1}^{N} \frac{1}{2M_i}\nabla_i^2 + \frac{1}{2}\sum_{j\neq k}^{N} \frac{Z_j Z_k}{\bar{R}_{jk}} \qquad (2.3)$$

where the two terms represent the kinetic energy and nuclear repulsion energy and N, M_i, Z and R represent the number of nuclei, nuclear mass, charge and position, respectively.

$$H_{el\text{-}nuc}(\text{electron-nuclei}) = -\sum_{k=1}^{N}\sum_{i=1}^{n} \frac{Z_k}{|\bar{R}_k - \bar{r}_i|} \qquad (2.4)$$

The decoupling of the Hamiltonian is usually justified by the adiabatic approximation (Born-Oppenheimer method).[19] Due to the large mass difference between the electrons and nuclei, the nuclei are slow to respond to changes in electron configurations while the electrons respond to changes in nuclear positions almost instantaneously.

To describe the motion of the electrons we can replace $H_{el\text{-}nuc}$ by $H^0_{el\text{-}nuc}$ involving only the average positions of the nuclei.[18]

The Schroedinger equation for electron motion is then

$$(H_{el} + H^0_{el\text{-}nuc})\psi(\bar{r}) = E_{el}\psi(\bar{r}) \qquad (2.5)$$

assuming the total wavefunction, Ψ, can be approximated by a product of nuclear (ϕ) and electron (ψ) wavefunctions[20] and the nuclei are assumed fixed in position at their mean values. Ψ is a

function of the electron's position and spin.

Hartree-Fock theory (HFT) approximates ψ as a finite linear combination of Slater determinants, i.e.,

$$\psi = \Sigma\ C_i \Delta_i \tag{2.6}$$

where Δ_i is a Slater determinant.[21] The Slater determinant[22] (SD) is a convenient way to invoke the Pauli Exclusion Principle. The minimal approximation here is to use only a single SD which consists of products of spin orbitals, ϕ_i:

$$\Delta = \frac{1}{\sqrt{n!}} \begin{vmatrix} \phi_1(1) \ldots \phi_n(1) \\ \vdots \quad\quad \vdots \\ \phi_1(n) \ldots \phi_n(n) \end{vmatrix} \tag{2.7}$$

where the prefactor is for normalization purposes, n is the number of electrons, the subscripts refer to electrons and the ϕ are functions of position ($\bar{r}$) of the electrons. This determinant allows for all possible permutations of electrons since each electron is equally likely to occur in any spin orbital due to their indistinguishability. Also, upon exchanging two electrons, one interchanges two columns resulting in a change of sign for Δ, i.e., the wavefunction is antisymmetric with respect to the interchange of two particles. If two electrons have the same space and spin coordinates, two columns of Δ are identical and the wave function vanishes. We use the unrestricted variant of HF

wave function vanishes. We use the unrestricted variant of HF theory, where no symmetry restrictions are imposed on ϕ other than that they be eigenstates of $\hat{s}_z$ (electron spin) .

A single determinant of doubly occupied orbitals is an appropriate representation of a totally symmetric singlet ground state of an atom or molecule ('closed shell'). Most molecular ground states are of this type.[23]

It can be shown that the expectation value of the energy for a given Hamiltonian and wave function is an upper bound to the energy of the first state of corresponding symmetry [23]:

$$E = \frac{\langle \Delta \mid H \mid \Delta \rangle}{\langle \Delta \mid \Delta \rangle} \geq E_1 \text{(energy of lowest state)}. \qquad (2.8)$$

Application of the variation method allows one to minimize the energy yielding the best approximation to the wavefunction in the energy sense. In this case, the ϕ's are varied until the minimum energy occurs.

We have:

$$\frac{\delta}{\delta}\frac{E}{\phi_i} = 0 \qquad (2.9)$$

It can be shown that the spin orbitals, ϕ_i, can be assumed to be orthonormal without loss of generality in what is to follow.[21]

The Hamiltonian is, from above, in atomic units:

$$H = -\sum_{k=1}^{n} \frac{1}{2} \nabla_k^2 + \sum_{k=1}^{N} \sum_{i=1}^{n} \frac{Z_k}{|\bar{R}_k - \bar{r}_i|} + \frac{1}{2} \sum_{\substack{k,l \\ k \neq l}} \frac{1}{|\bar{r}_k - \bar{r}_l|} \qquad (2.10)$$

This can be written in the abbreviated form,

$$H = \sum_{i=1}^{n} F_i + -\frac{1}{2} \sum_{i \neq j}^{n} g_{ij} \qquad (2.11)$$

where F_i is the one electron operators and g_{ij} contains the two electron operators (coulomb and exchange).

The energy may then be written as:

$$E = \sum_{i=1}^{n} \langle \phi_i(1) | F | \phi_i(1) \rangle + -\frac{1}{2} \sum_{i,j}^{n} (\langle \phi_i(1)\phi_j(2) | g_{12} | \phi_i(1)\phi_j(2) \rangle - \langle \phi_i(1)\phi_j(2) | g_{12} | \phi_j(1)\phi_i(2) \rangle) \qquad (2.12)$$

and $\langle \Delta | \Delta \rangle = 1$.

Use of the energy variational principle with variation of E with respect to the ϕ_k^* and the necessity of invoking Lagrange multipliers to implement the constraint of orthonormality of the solutions results in the following:

$$fn = E + \sum_{i,j} \lambda_{ij} \int \phi_i^* \phi_j \, d\tau \qquad (2.13)$$

where fn is the functional to be varied, E is the energy expression in equation (2.12), λ_{ij} is a Lagrange multiplier and the integration is over the electron's spatial coordinates.

The variation

$$\frac{\delta fn}{\delta \phi^*} = 0 \qquad (2.14)$$

results in the following equation:

$$\int d\tau_1 \delta\phi_k^*(1)\{F_1\phi_k(1) + \sum_j [\int \phi_j^*(2) g_{12} \phi_k(1)\phi_j(2) d\tau_2 - \int \phi_j^*(2) g_{12} \phi_j(1)\phi_k(2) d\tau_2] + \sum_j \lambda_{kj}\phi_j(1)\} = 0 \qquad (2.15)$$

Since the terms within { } are independent and the variation $\delta\phi_k^*(1)$ is arbitrary, it follows that:

$$F_1\phi_k(1) + \sum_j [\int \phi_j^*(2)\phi_j(2) d\tau_2 \phi_k(1) - \int \phi_j^*(2) g_{12} \phi_k(2) d\tau_2 \phi_j(1)] + \sum_j \lambda_{kj} \phi_j(1) = 0 \qquad (2.16)$$

A unitary transformation of ϕ_j can be found which diagonalizes the λ_{kj} matrix (i.e., $\sum \lambda_{ij}\phi_j(1) \rightarrow \lambda_{kk}\phi_k$). The λ_{kk} are the energy eigenvalues (E_k) for the ϕ_k orbital.

Finally, one can write the Hartree-Fock equation:

$$F_1\phi_k(1) + \sum_j \left(\int \phi_j^*(2)\phi_j(2)d\tau_2\, \phi_k(1) - \int \phi_j^*(2)g_{12}\phi_k(2)d\tau_2\phi_j(1)\right) = E_k\phi_k(1) \qquad (2.17)$$

This can be written in the simplified form,

$$H^{scf}\phi_k = E_k^{scf}\phi_k \qquad (2.18)$$

where H^{scf} is the self-consistent field Hamiltonian operator. The set of integro-differential equations is solved iteratively since the Hartree-Fock Hamiltonian operator is a function of the solutions, ϕ_k.

For molecular calculations, one expands the ϕ_k in terms of a set of analytic basis functions. Since it is not possible to use a mathematically complete set of functions, we can obtain only approximate solutions to the HF equations. The best (lowest energy) single determinant wave function constructed within a finite basis set is the self-consistent field (SCF) wavefunction[24]

Restrictions on symmetry of the spin orbitals and equivalence of spin up and spin down space lead to solutions of the equations which are the Restricted Hartree-Fock wavefunctions.[24] Unrestricted HFT, used for most calculations in this thesis, does not force these types of requirements, allowing for more flexibility in the SCF wavefunction and a lower energy. These

wavefunctions are not eigenfunctions of orbital angular momentum.

The UHF theory is useful in studying excitation energies in that it is not necessary to force spin up and spin down spaces to be identical. If one begins with a closed shell ground state and excites a spin down electron into the spin up space, one may perform a UHF calculation on this determinant. The resulting energy and wavefunction are the best single determinant description of the (new) excited state (which differs in symmetry from the closed shell ground state). The energy difference between the two states is the excitation energy for the new state (ΔSCF method).

The UHF calculations performed in this work utilize the linear combination of atomic orbitals (LCAO) approximation in constructing the spin orbitals.

$$\Phi_i = \Sigma\, c_{ij}\, \chi_j \qquad (2.19)$$

The χ_{ij} in this work were Gaussian-type orbitals (GTO's) of the form,

$$\chi_j = a_j \left[x^l\, y^m\, z^n \exp\{-b_j r^2\}\right] \quad (25) \qquad (2.20)$$

The a_j and b_j are input parameters in the sequence of codes used to calculate the integrals over atomic orbitals and the x, y, and z, raised to their respective powers indicate the type of atomic

orbital (s,p,d etc.).

The χ_j are what are called primitive Gaussians. The iteration time in the UHF procedure is heavily dependent on the number of Gaussian functions used. Calculations carried out using primitive functions can become very time consuming depending on the size of the basis set.[26] Contracted functions consist of fixed linear combinations of primitives.[27] Use of contracted functions only requires the calculation of the orbital coefficients of the contracted functions at the SCF stage (the a_j can be absorbed into the c_{ij} for a given function). One can use a large number of primitives within a function which enables one to take advantage of the analytic properties of Gaussians, while allowing the orbital to span a reasonable part of configuration space and yet keep the iteration time down. The disadvantage of contracted functions is that the integrals over atomic orbitals become more complicated and time is lost during their calculation. Usually, however, this is a one step calculation since the integrals are saved and the large gain in SCF computation time generally outweighs the loss in integrals calculation time.

GTO's have the advantage over Slater-type orbitals (STO's) in that integrals involving GTO's are generally much easier to perform. However, STO's are capable of describing the orbitals in a more physically realistic manner and one usually needs relatively more GTO's than STO's to obtain comparable results.

Electron Correlation

Electron correlation effects are corrections to independent electron models or orbital theories of molecular electronic structure.[28] In the Hartree-Fock approximation, the motion of each electron is solved for in the presence of the average potential created by the remaining electrons and therefore neglects instantaneous repulsions between electrons. The contribution to the total energy due to instantaneous repulsions is called the correlation energy (E_c).[29] This energy is usually accepted to be the difference between the Hartree-Fock energy and the exact non-relativistic energy of the system.[26]

The method employed in this work to calculate E_c is many-body perturbation theory (MBPT). (Technically, second order Rayleigh-Schroedinger perturbation theory is used here. RSPT and MBPT are identical to 2nd order. The difference lies in higher orders where RSPT has size-inconsistent terms which mutually cancel in the higher orders, resulting in a size-consistent theory. MBPT is based on the Linked Diagram Theorem (see Wilson, ref. 28) and involves only size-consistent terms. RSPT is an N electron theory whereas MBPT is RSPT specialized to spin orbitals.) Although E_c is usually a small percentage of the total energy of a system, it is often larger than the energy needed to break many chemical bonds.[28] Since energy differences between states of systems are of primary importance, and since different states do not generally

have the same electronic structural characteristics and perhaps even different relative atomic geometries (in molecules), the electron correlation energy of two states is not the same and does not entirely cancel upon subtraction.

We assume [21] the Hamiltonian to be split into two terms, one which yields known solutions;

$$H_o \Phi_j = W_j \Phi_j \qquad (2.21)$$

and the other (V) assumed to be small such that the total Hamiltonian is given as;

$$H = H_o + V \qquad (2.22)$$

The perturbation, V, represents an addition to the energy of the unperturbed system and is the difference between the exact energy of the system and the approximate (Hartree-Fock in this case) energy.

$$V = H - H_o \qquad (2.23)$$

Note that H is the exact non-relativistic Hamiltonian and H_o may be any Hamiltonian for which known solutions exist.

H_o is the Hartree-Fock Hamiltonian. The zeroth order energy

is the Hartree-Fock energy:

$$E_j^{0} = W_j = \langle \Phi_j \mid H_o \mid \Phi_j \rangle \qquad (2.24)$$

The 1st order correction is the expectation value of the perturbation for the unperturbed state;

$$E_j^{(1)} = \langle \Phi_j \mid V \mid \Phi_j \rangle = V_{oo} \qquad (2.25)$$

and

$$E_j^{0} + E_j^{(1)} = E_{HF} \qquad (2.26)$$

However, the second order correction can be shown to require the wavefunction corrected to first order;

$$E_j^{(2)} = \langle \Phi_j \mid V \mid \Phi_j^{(1)} \rangle \qquad (2.27)$$

where $\Phi_j^{(1)}$ is the first order wavefunction.

In principle, one could solve the equation

$$(H_o + V)\,\Psi = E\,\Psi \qquad (2.28)$$

or equivalently,

$$(H_o - W)\,\Psi = (E - V - W)\,\Psi \qquad (2.29)$$

to get Ψ by using the inverse operator $(H_o - W)^{-1}$. However, the possibility exists that this operator could be singular. Therefore

we need to project out of Ψ the part of the wavefunction proportional to Φ ($H_o\Phi_j = W_j\Phi_j$) so that singularities will not occur. The projection operator (1-P) defined for an arbitrary function (F) as

$$(1-P)\ F \ = \ F - \langle\Phi \mid F\rangle\Phi \qquad (2.30)$$

does this.

It can be shown that P commutes with H_o. Then equation 2.29 becomes;

$$(H_o - W_j)(1-P_j)\Psi_j = (1-P_j)(E_j - V - W_j)\Psi_j \qquad (2.31)$$

assuming no degeneracies. Invoking intermediate normalization ($\langle\Phi_j|\Psi_j\rangle=1$) and using the fact that $P_j\Psi_j = \Phi_j$, equation (2.31) can be solved for Ψ_j (an expansion of the inverse of Ψ_j's prefactor is also necessary) resulting in the following expression for Ψ_j;

$$\Psi_j \ = \ \Phi_j + \frac{1}{(H_o-W_j)}(1-P_j)(E_j-W_j-V)\Phi_j \ +$$

$$\frac{1}{(H_o-W_j)}(1-P_j)(E_j-W_j-V)\frac{1}{(H_o-W_j)}(1-P_j)(E_j-W_j-V)\Phi_j$$

$$+ \text{ higher order terms} \qquad (2.32)$$

Note that care is taken when expanding to preserve the proper order of the operators. Simplification of equation 2.32 is possible since E_j and W_j can be factored through to yield expressions such as $(1-P_j)\Phi_j$ which have been shown to be zero above. To first order in V including $\Psi_j^{(0)}$ $(= \Phi_j)$ we have;

$$\Psi_j^{(1)} = \Phi_j - \frac{1}{(H_o-W_j)}(1-P_j)V\Phi_j \qquad (2.33)$$

This is the corrected wavefunction necessary to calculate the second order correction to the energy.

From equation 5 we have;

$$E_j^{(2)} = \langle\Phi_j|V|\Psi_j^{(1)}\rangle = -\langle\Phi_j|V|\frac{1}{(H_o-W_j)}(1-P_j)V\Phi_j\rangle \qquad (2.34)$$

Both operators $(H_o-W_j)^{-1}$ and $(1-P_j)$ can be shown to be hermitian. Also, it is useful to introduce the identity element;

$$\mathbb{1} = \sum_k |\Phi_k\rangle\langle\Phi_k| \qquad (2.35)$$

where the Φ_k is a complete set of functions.

$$E_j^{(2)} = -\sum_k \langle\Phi_j|V|\Phi_k\rangle\langle\Phi_k|\frac{1}{(H_o-W_j)}(1-P_j)V|\Phi_j\rangle \qquad (2.36)$$

For $k=j$, $(1-P_j)\Phi_k=0$ as shown above.

For $k\neq j$, $(1-P_j)\Phi_k=\Phi_k$

Using the hermiticity and commutivitiy of $(1-P_j)$ and $(H_o-W_j)^{-1}$ we have

$$E_j^{(2)} = -\sum_{k\neq j} \langle\Phi_j|V|\Phi_k\rangle\langle\frac{1}{(H_o-W_j)}(1-P_j)\Phi_k|V|\Phi_j\rangle$$

$$= -\sum_{k\neq j} \langle\Phi_j|V|\Phi_k\rangle\frac{1}{(W_k-W_j)}\langle\Phi_k|V|\Phi_j\rangle \qquad (2.37)$$

Using a more compact notation we write;

$$E_j^{(2)} = \sum_{k\neq j} -\frac{V_{jk}V_{kj}}{(W_o-W_k)} \qquad (2.38)$$

to second order in the perturbation, V.

If Φ_o is the total zeroth order wave function (Hartree-Fock in this case), the total correlation energy is then;

$$E = W_{oo} + V_{oo} + \sum_{k\neq j} -\frac{V_{ok}V_{ko}}{(W_o-W_k)} \qquad (2.39)$$

to second order in V.

It can be shown that;

$$\langle\Delta_k|V|\Delta_k\rangle = -\frac{1}{2}\sum_{i,j\in\Delta_k}\{\langle\Phi_i(1)\Phi_j(2)|\frac{1}{r_{12}}|\Phi_i(1)\Phi_j(2)\rangle - \langle\Phi_i(1)\Phi_j(2)|\frac{1}{r_{12}}|\Phi_j(1)\Phi_i(2)\rangle\}$$

$$= -\frac{1}{2}\sum_{i,j} J_{ij;ij} \qquad (2.40)$$

where Δ_k is a Slater determinant whose elements are orthonormal spin orbitals.

The second order expression has matrix elements of the form $V_{ok} = \langle \Delta_o | V | \Delta_k \rangle$ where Δ_o represents the Hartree-Fock space. The $E_2^{(2)}$ expression contains all possible double excitations due to instantaneous repulsions of electron pairs in the HF space to possible configurations in virtual space (Δ_k). Since unrestricted Hartree-Fock is used, it can be shown that single excitations (matrix elements between two determinants differing by one spin-orbital) vanish. The only surviving terms occur where Δ_k differs from Δ_o in two spin orbitals (i,j (HF) go to a,b (virtual)). Each $J_{ij;ij}$ then is replaced by $J_{ij;ab}$ and the sums must go over all occupied pairs (i,j) and all virtual pairs (a,b). Also, the total energy difference between the HF and virtual space for a given pair is $\epsilon_i + \epsilon_j - \epsilon_a - \epsilon_b$ which replaces the denominator in the second order expression.

Combining all of the above we have;

$$E^{(2)} = -\frac{1}{4} \sum_{i<j} \sum_{a<b} \frac{|J_{ij;ab}|^2}{(\epsilon_i + \epsilon_j - \epsilon_a - \epsilon_b)} \qquad (2.41)$$

Bartlett and Purvis [30] showed that 60 to 70 percent of the total correlation energy and 70 to 80 percent of the valance shell correlation energy in simple molecules could be provided using contracted HF basis sets augmented by well chosen virtual functions. A finite basis set of m functions is used in the calculation. There are n occupied solutions and m-n virtual

solutions to the HF calculation. The summations go from 1 to n for the occupied space and from n+1 to m for the virtual space. The virtual space created in the UHF calculation is not suitable for investigating electron correlation effects or excited states. They represent states of an (n+1) electron system (negative ion).[31] That is, they describe state of an electron moving in the field of the neutral molecule whereas an excited state of the molecule would have the electron moving in the field of the n-1 other electrons. Therefore the HF virtuals are removed by contracting over basis functions and the virtual space is rebuilt and designed to minimize the correlation energy. This is done by forcing the functions of the virtual space to spatially overlap the functions of the HF space by appropriate choice of the exponent in the virtual GTO's. A good starting point for this exponent is proposed by Beck and Nicolaides.[30] Their expression,

$$\langle r \rangle = \frac{2}{3} \times \frac{4}{5} \times \cdots \times \frac{2n}{2n-1} \quad \frac{1}{(2\Pi a)^{1/2}} \qquad (2.42)$$

gives the virtual space exponent, a, as a function of the expectation value of the orbital you wish to overlap. The integer n is representative of the angular momentum of the virtual orbital (n=1,2,3, etc. for l=s,p,d etc.).

For atomic calculations, the application of this expression is straightforward. For example, given the neon atom ($1s^2 2s^2 2p^6$), possible double excitations are:

$$2s2p \rightarrow VsVp + VpVd + VdVf$$

For neon, <r> is about 1 au for the 2s and 2p orbitals. Application of equation 2.42 would yield a=0.63662 for the V_s exponent and this would be the starting point in the creation of the Vs correlation space. Exponent optimization would then be done to find the minimum value of the correlation energy. The application of equation 2.42 to molecular systems such as nitromethane is not quite so useful since molecular orbital construction is based upon combinations of atomic orbitals. However, one can maximize the overlap to the largest atomic constituent and use this as a starting point in the creation of the virtual space.

Counterpoise Method

The counterpoise method (CP) evolved [33] to reduce the error in calculating medium range interatomic or intermolecular potentials. One primary source of error was attributed to basis set superposition.[34] Traditionally, the binding energy of a dimer was calculated as follows:

1) Calculate the energy of the separate molecules at infinite separation where each molecule is characterized by its own basis set.

2) Combine the basis sets and calculate the total energy of the dimer at the equilibrium intermolecular separation (which may have to be determined by energy optimization).

3) The difference in energy, $E(\text{dimer})-\{E_1(\infty) + E_2(\infty)\}$ gives the binding energy of the system.

This method, however, does not yield accurate results when compared to experiment.[35] The error results from the fact that the calculations on separate molecules were not strictly comparable to that of the dimer. The dimer calculation contains compensation, using orbitals (basis functions) located on one center, for the deficiency of the wavefunction in the neighborhood of the second center (and vice versa).[34]

The correct calculation is to allow the presence of the basis

functions of the second molecule (without its associated nuclear charge) when calculating the energy of the first molecule and doing the same for calculations on the second molecule. The individual calculations are then comparable to the dimer calculation in that all functions are present all the time as are their effects on the energy and orbital structure of both molecules.

The effect of basis set superposition error, while often times small, is extremely important in work where intermolecular potentials are small. Kolos and co-workers [36] used the CP method effectively in work on the methane dimer. Dacre's work [34] indicates that basis set superposition error should be considered when calculating small correlation effects. The inclusion of this effect in his work did not tend to overcompensate but resulted in a more accurate description of the system in which he was working.

The CP method was found to be useful in the work presented in this thesis under several circumstances. It was an aid when making comparisons between all-electron versus pseudopotential calculations for both the CH_3 and NO_2 groups in nitromethane and also in helping to converge the nitromethane molecule when using pseudopotentials by using CP Hartree-Fock orbitals as input guesses for the two pieces.

Chapter 3

Computational Methods

Calculations on nitromethane were done in two stages: 1) gas phase (free molecule) and 2) molecular groups (dimers and trimers with work begun on a cluster of 9 molecules).

In order to perform some of the calculations, modifications of existing Fortran codes was necessary as will be discussed below. All calculations were done using Michigan Tech University's Center for Experimental Computation Floating Point System FPS/164 Max in conjunction with a Digital Equipment Corporation Vax 11/750. The FPS/164 is an attached processor which uses the VAX as a host for access purposes. It has provided computational speed-ups by factors of six to ten times over the VAX depending upon the stage of the calculations.

Gas phase calculations were done using the Labels and Integrals portions of the POLYATOM [37] sequence of codes as well as unrestricted Hartree-Fock (UHF) and many-body perturbation theory (MBPT) codes developed by A.B. Kunz and modified by D.R. Beck. These codes were adapted for FPS use by students at the University of Illinois. [38] The MBPT code was run in a mode that allowed for only part of the calculation to be done on the FPS since at that time it did not have sufficient memory to handle the entire calculation. D.R. Beck made additional modifications to this code to provide for corrections to spin eigenvalues. Dimer and trimer

calculations were done using the same codes except without correlation.

Cluster calculations required extensive program modifications and some code development by the author in view of the approximations which were used. No correlation calculations were done due to size and time limitations. A key approximation, neglect of neighbor-neighbor (n-n) interactions, forced extensive restructuring of the way in which input files were handled at the UHF stage. Also, in order to facilitate storage of labels and integrals, codes had to be written which scrubbed the integrals while at the same time created small labels flag files which contained information to help recreate the labels files while being much easier to store. A cluster calculation used to be performed by setting up the entire cluster in the labels and integrals input files, calculate all integrals and then perform the UHF calculation using the labels and integrals (2 separate files). Three hundred and thirty seven basis functions were used in the preliminary cluster calculations (9 nitromethane molecules). This would require the computation of about 1.6×10^9 integrals. It took 6 hours to calculate 8×10^6 integrals on the FPS, therefore over 200 hours (8.3 days) of cpu would be needed for the total calculation. It is difficult to estimate the amount of time per iteration that would be required at the UHF stage. However, it could be up to 8 days per iteration based on comparisons of single molecule to dimer calculations.

It is clear that the neglect of n-n interactions was

necessary in order to make calculations at all feasible using current computing capabilities. Eight separate dimer calculations were done, a dimer consisting of the central molecule plus one neighbor. This resulted in eight separate labels and integrals files. The integrals involving pure central site functions had to be removed from all but one of the integrals and labels files. This step was actually done at the labels stage where no label which involved purely the central site was included in the list. The integrals also were scrubbed to a 10^{-6} tolerance in absolute value (to be justified later). Once scrubbed, the integrals were stored on disk since it was impractical to recalculate them each time a run was desired (6 hours of cpu per dimer). The labels calculation was relatively inexpensive (about 20 minutes of cpu per dimer). However, since the integrals had been scrubbed and since the labels files were larger than the integrals files, (and therefore requiring a lot of disk space also), it was necessary to create an intermediate flag file which was much smaller than the labels file but contained enough information to help recreate the scrubbed labels file at a later stage. [Note: If the tolerance had not been invoked, all that would have been necessary was to recalculate the labels and use the entire labels file each time.] Renumbering of the new labels had to be done in order to convert the eight separate dimer runs into one cluster run. One other modification had to be done to the potential energy integrals for the central site. These had to be calculated in the presence of all the eight neighbors at once and stored in a separate file.

This file was read whenever the UHF code needed one electron integrals from the central site.

The block diagrams of figures 3.1 through 3.4 will clarify the above comments. Figure 3.1 represents the normal sequence of events in carrying out the UHF procedure. Figures 3.2 through 3.4 show the necessary modifications to this procedure in order to work on the nitromethane cluster. The UHF code had to be modified to handle the new file structure.

Neglecting n-n interactions, the total number of two electron (2e) integrals is approximately 56 X 10^6. The tolerance criteria reduces this number to about 12 X 10^6. The storage requirements for the eight separate integrals files and labels flag files was about 200,000 blocks of disk out of an 880,000 block disk (475 Mbytes). If the labels themselves had been stored as well, the requirement would have increased by a factor of 2. The UHF stage took about 45 minutes per iteration with 337 basis functions and 12 million integrals.

Finally it should be mentioned that several other ideas were explored to help limit the problem size. These included heavy contractions of neighbor basis functions, neglect of any integrals involving more than two centers (up to four centers are possible in the 2 electron integrals) under the assumption that these would be small, and use of local symmetry operations on Gaussian primitives within a spin orbital during the calculation of integrals to reduce the total number of integrals. Integrals code modifications by D.R. Beck to investigate the latter of these

ideas indicate that some savings could be made in the total number of integrals that need to be calculated but that the savings were not great enough for nitromethane to warrant further investigation at this time. Also, it was determined that the neighbor molecules could be described well enough without the necessity of having to use heavily contracted functions (which increase the calculation time of integrals). Finally, it was decided that neglect of all n-n interactions was a more consistent first order approximation than the neglect of multicenter integrals.

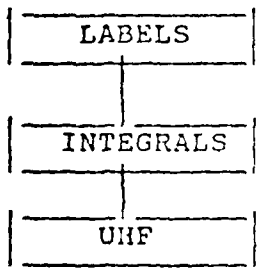

Give list of one and two electron labels for the entire cluster.

Calculate all integrals over atomic basis functions based on the labels.

Calculate energy and eigenvectors of the cluster

Figure 3.1 Block diagram of the normal procedure.

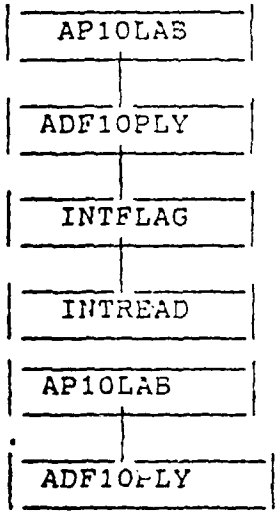

Calculate labels for dimer 1 (D1). A dimer consists of the central molecule + one neighbor.

Calculate integrals for D1.

Scrub and save the integrals file (P01) and create the labels flag file (L01)

Remove any pure central one electron labels and integrals from P01.

Calculate the one electron labels for the central molecule only.

Calculate the one electron integrals for the central site in the presence of the charge of all the neighbors. Note, the one electron labels are stored on and read from the integrals tape at the UHF stage. The one electron labels need not be saved.

Figure 3.2 Preparation of special labels and integrals files for Dimer 1.

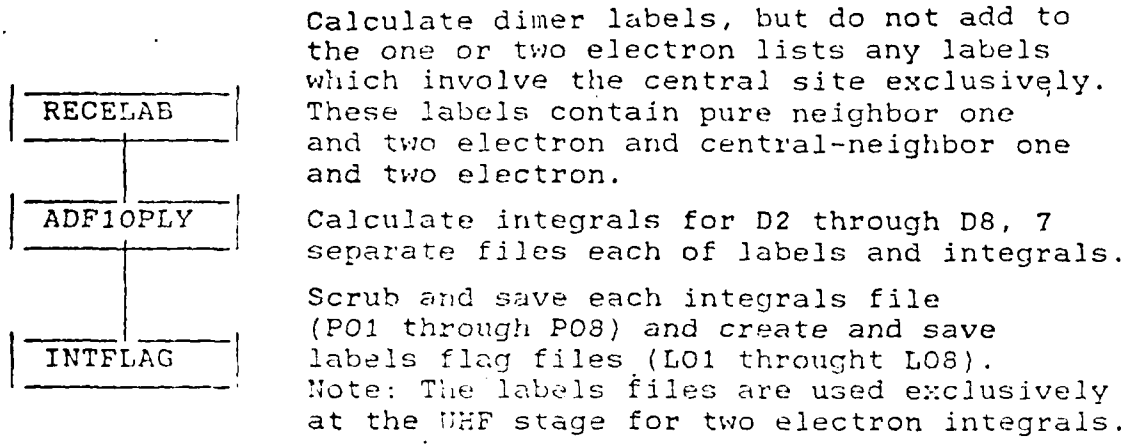

Figure 3.3 Preparation of integrals files and labels flag files for the other 7 dimers of the cluster.

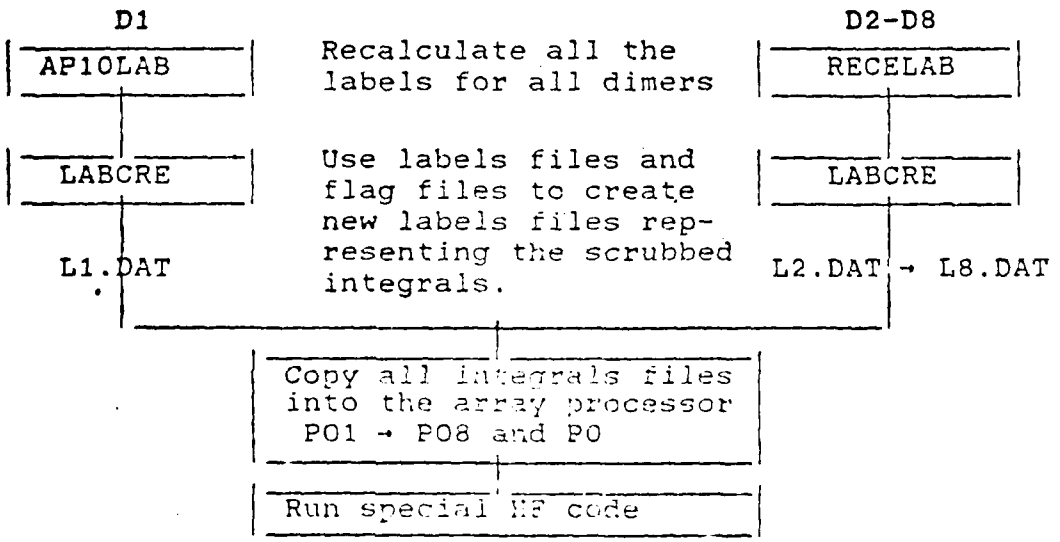

Figure 3.4 *Procedure for running the cluster with the special file structure.*

The codes INTFLAG, LABCRE and INTREAD were created by the author. RECELAB is a modification of the existing labels code as is AP1OLAB. NIAUHF is a modification of the existing Hartree-Fock code. The only change required for the integrals code was to redimension it to handle a single dimer of 92 functions. Table3.1 is a summary of the files used and their contents when running the modified system of codes.

Table 3.1

Files and Contents When Using Special Codes

	pc1e	pc2e	pn1e	pn2e	c-n1e	c-n2e
P0	X					
P01 ↓ P08		X	X	X	X	X

p=pure
c=central
n=neighbor
1e=one electron
2e=two electron

Chapter 4

Results for the Nitromethane Monomer

Gas phase calculations for nitromethane were performed using the geometry determined by Cox and Waring.[39] Figure 4.1 is a schematic diagram of the molecule. The only symmetry operations that can be used to reduce the number of integrals is:

1.) Reflection in the x-y plane (applies to the entire molecule.

2.) Reflection in the x-z plane (applies to the $C-NO_2$ group).

3.) Two-fold rotation about the x axis ($C-NO_2$ group).

4.) Three-fold rotation about the x axis (CH_3 group).

The system has a total of 32 electrons (16 spin up, 16 spin down for the ground state).

Basis Sets

This section will briefly describe the basis sets used in all the calculations performed on the molecule.

Initially a Dunning[40] (3s,2p), (7,1,1/4,1) contraction of Huzinaga's[41] (9s,5p) primitive set for the oxygens, nitrogen and carbon with Dunnings (2s), (4,1) contraction of Huzinaga's 4s set

STRUCTURE OF NITROMETHANE

CH_3NO_2

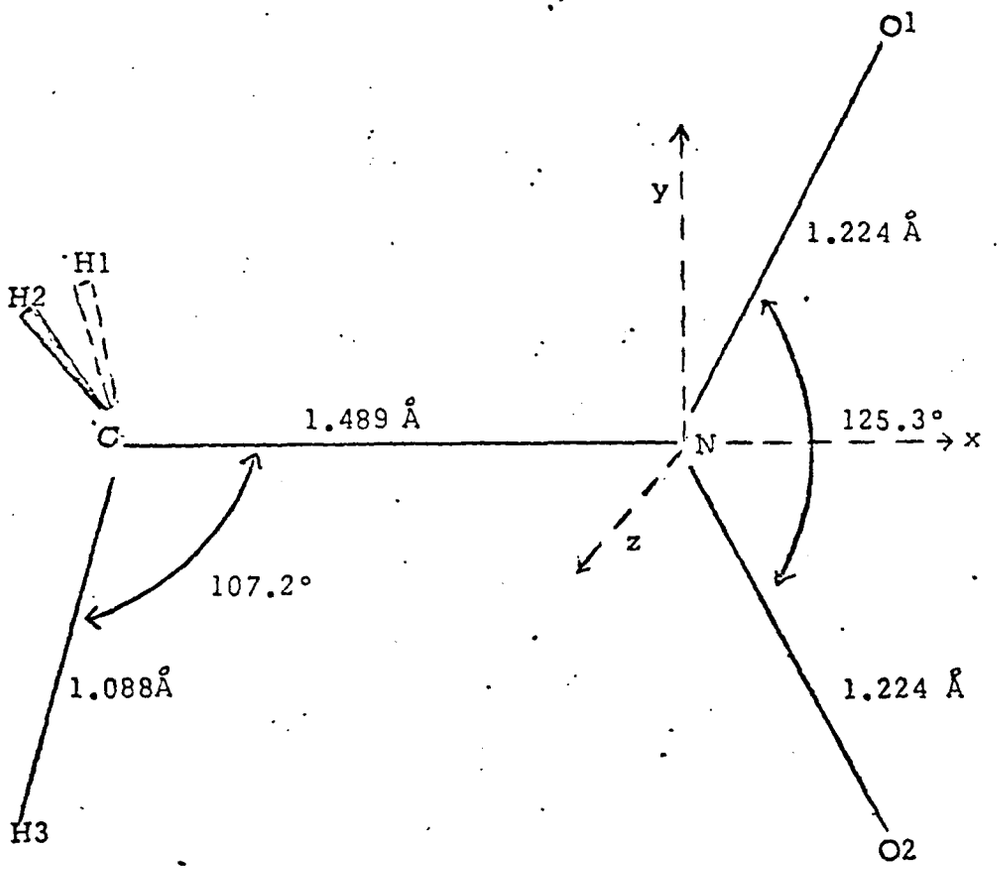

Ref. Cox and Waring: J. Chem. Soc. Far. Trans. 68, 1060: 1972

Figure 4.1

was used for the hydrogens (The notation (7,1,1/4,1) indicates the 3s functions consisted of 7,1 and 1 primitive Gaussians, the 2p functions of 4 and 1 primitives, etc.). Also, s bond functions were placed midway between atoms on the six main bonds (C-N, N-O1, N-O2, C-H1, C-H2, C-H3). For various reasons, this set evolved to 57 functions (adding p bond functions), 81 functions (adding d correlation functions on each atom except the hydrogens) and 84 functions (upon uncontracting the s functions on O1, O2 and N {(7,1,1) → (6,1,1,1)}. Some experimentation was done on each of these basis sets, including exponent optimization. Appendix C contains listings of the basis sets used in calculations throughout this work.

A comment concerning the usefulness of exponent optimization is in order. The basis sets used in the molecular calculations are optimized for the individual atoms in the system. However, this does not mean that these functions, when brought together to form a molecule, will be energy optimized. It is sometimes useful to vary some of the more diffuse exponents in the molecule on an individual basis to see if a lower energy results. An example of this occurs in the calculation of a low-lying excited state of nitromethane (to be discussed in more detail later). Figure 4.2 shows how variation of the z exponents on the oxygen and nitrogen atoms on an individual basis cause the energy to drop somewhat. For the oxygen z functions, the minimum energy did occur at the original value of the exponent (Energy= -243.5876 Hy). However,

OPTIMIZATION OF THE EXPONENTS ON THE OXYGEN AND NITROGEN Z FUNCTIONS
(EXCITED STATE)

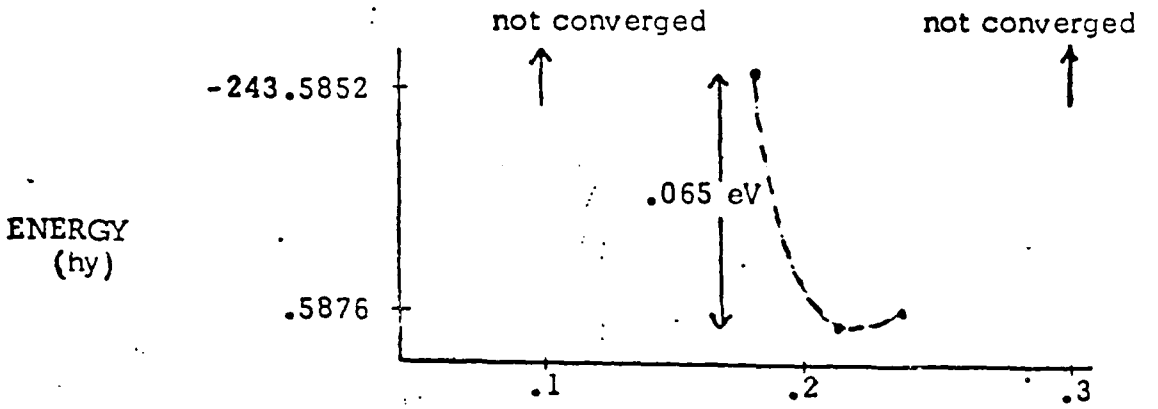

OXYGEN Z EXPONENT (ORIGINALLY 0.2137)

NOTE: THE MINIMUM ENERGY OCCURS AT THE ORIGINAL VALUE

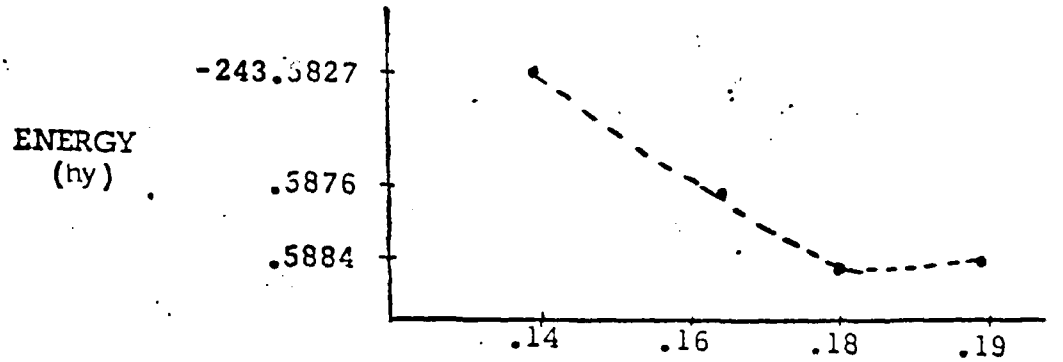

NITROGEN Z EXPONENT (ORIGINALLY 0.1654)

NOTE: THE MINIMUM ENERGY OCCURS AT Z=0.18

Figure 4.2

an additional 0.0008 Hy (0.022 eV) at the HF stage was acquired by changing the z exponent of nitrogen from 0.1654 to 0.1800, which appeared to yield a minimum. In this example, the gain is small, but this may not always be the case. Ditchfield, Hehre and Pople [42] have done work in basis set optimization for both atoms and molecules. Their work involved the variation of both the coefficients and exponents in minimal basis sets whose functions consisted of sums of Gausssian type functions (GTOs).

As stated earlier, GTOs are generally easier to work with than STOs. Others (Stewart [43], Clark and Miller [44], Adams [45] and Hillier [46] and co-workers) have done some work on Gaussian approximations to STOs using various fitting schemes resulting in a mixture of fair to poor results. Ditchfield's work indicates that a few well-chosen GTO's can yield very good results.

Ground State Characteristics of the CH_3NO_2 Monomer

A basis set of 81 functions was used to study the ground state (gs) of the monomer. This set evolved from the 48 function set derived from Dunning's [40] basis sets. It is interesting to see how the energy varied as more basis functions were added to the set. Table 4.1 compares the gs energy, including electron correlation effects (2nd order MBPT) for 48, 57 and 81 function sets which were previously described. At the HF stage there was a large decrease in energy of about 0.058 Hy (~ 1.58 eV) from 48 to

57 functions and an additional decrease of 0.025 Hy (~ 0.68 eV) upon going to 81 functions. This demonstrates the importance of the p bond functions and diffuse d functions in acquiring the minimal energy state. The d functions, which were added as polarization functions helped lower the energy considerably at the HF stage. This shows the importance of polarization functions in properly describing systems in which atoms are brought together to form molecules. There was also a large lowering in energy due to electron correlation. From 48 to 57 functions a gain of ~0.081 Hy (2.18 eV) was made while the 81 function set picked up an additional 0.089 Hy (2.45 eV). It is quite clear that the p bonds and diffuse atom-centered d's are extremely important as there are substantial energy gains at both the HF and MBPT levels when they are added.

Table 4.2 shows previous work done on the monomer gs. It should be noted that the 57 function set used in this work is well below the energy reported by anyone else at the HF stage. Both Murrell and Murdoch use the same geometry as in this work. However, Mezey's work involved geometry optimization to his basis set, resulting in some slight differences in bond lengths and angles. No attempt was made here to optimize the gs geometry.

Kaufman's work utilizes the crystal geometry of Trevino[60] which differs slightly from that of the free molecule. Her work consisted of varying the C-N bond length distance and involved calculations at 4 different stages of accuracy; SCF, CI,

Table 4.1

Energy (hy) Comparison Between Basis Sets

Basis Functions	48	57	81
Energy (HF)	-243.640710	-243.698453	-243.723297
Correlation (MBPT)	-0.429168	-0.509799	-0.598611
Total Energy	-244.069878	-244.208252	-244.321908
Spin (S)	0.412	0.338	0.345

Table 4.2

Comparison of Ground State Energies: Nitromethane Monomer

Reference	Energy (hy)	Method
Murrell (47)	-243.2590	SCF-MO, DZ nocor
Mezey (48)	-243.2630	STO w/4.31 EGS,nocor
Murdoch (49)	-243.2721	SCF-MO/4.31 EGS,nocor
Kaufman (50)	-243.6505	CASSCF
Kaufman (50)	-243.5903	SCF, 49 con. GT fns
Kaufman (50)	-243.8135	MRD-CI, 4449 SCs
Kaufman (50)	-243.8749	Ext. CI
Kaufman (50)	-243.8962	Full CI estimate
This work	-243.7233	SCF-MO,81fns,151GPs
This work	-244.3219	SCF+MBPT 81/151

SCF=self consistent field, DZ=double zeta, nocor=no correlation, STO=Slater type orbitals, EGS=extended Gaussian set, CASSCF=complete active space SCF, con.=contracted, GT=Gaussion type, fns=functions, MRD-CI=multireference determinant configuration interaction, SCs=selected configurations, Ext. CI=extrapolated configuration interaction, GPs=Gaussian primitives. Kaufman's values calculated at equilibrium C-N distance (2.8 au).

extrapolated CI and a full CI estimate. The extrapolated CI calculation is an approximate way in which to add in the effects of other configurations. She also shows work using Complete Active Space SCF (CASSCF) and was interested in determining the configurations necessary to yield accurate descriptions of the system along the decomposition pathway of the C-N bond.

It is interesting to note that the energy shown by this author (-244.321915 Hy SCF+MBPT) is about 0.426 Hy below Kaufman's 'full CI' estimate. At first glance this is rather startling in that full CI is supposed to account for all possible excitations and the total energy of the system. Several comments are in order here. The correlation energy for CH_3, as given by Pople [63] is -0.248 au. A CI calculation done by Schaefer [64] using a small basis set gives a correlation energy for NO_2 as -0.357 au. When accounting for the CH_3NO_2 bond energy, the total correlation energy for the system is at least -0.7 au. Neither Kaufman's or this work has reached that value although the correlation energy reported here (-0.598611 au) is quite a bit more than that reported by Kaufman. It should also be noted that Kaufman also used a much smaller basis set (55 functions) than used in this work. It is unlikely that the calculated second order correction in this work has overshot the true value. Added configurations (MCHF) would have the effect of lowering this author's HF energy. Kaufman tries to account for the multiconfiguration nature of the system whereas this work does not. However, the SCF value

reported here is above the full CI estimate made in Kaufman's work (this is reasonable). Also, CI is not a size consistent theory. The Davidson equation used by Kaufman is an approximate correction for size consistency (see Paldus [52]) whereas MBPT is already a size consistent theory. The second order MBPT correction is complete.

A problem does arise in the calculation of the spin of the gs. Nitromethane has 32 electrons and is a closed shell molecular gs (S = 0 where S is the spin). Spin calculations at the HF stage yield values on the order of 0.35. An attempt was made to determine corrections to spin values at the MBPT stage. D.R. Beck modified the MBPT code to calculate spin corrections using the corrected first order wave function. Table 4.3 shows that these corrections were small. Indications in other work (Kauffman [53], Marynick [54] and Kleier [1]) are that a better description of the nitromethane system is one of mixed configurations, requiring multi-configurational Hartree-Fock techniques. No attempt was made here to carry out MCHF calculations. A method proposed by A.B. Kunz [55] indicates that spin purification using projection operators may lower the energy of the gs by up to 1.0 eV.

A restricted Hartree-Fock calculation was performed using the output of the 84 function UHF run as input. This run resulted in an RHF energy of -243.715959 (0.0072 Hy or 0.196 eV above the UHF value), spin = 0 (as expected) and orbital composition very similar to the UHF run. Furthermore, the output of this RHF run

was input as a UHF run. The result was a spin=0 UHF state at the same energy as in the RHF run, i.e., 0.196 eV above the original UHF gs. Table 4.4 compares the 16 occupied spin up orbital energies and general characteristics of these runs. A brief word on notation is in order. Nitromethane has 2 oxygen atoms (denoted O1 and O2, see Figure 4.1), 1 nitrogen atom (N), 1 carbon atom (C) and 3 hydrogen atoms (H1, H2 and H3). O1S refers to the s type orbital on oxygen 1, etc. The orbitals labelled 'Z' are p function orbitals with lobes in the z direction as referred to the schematic diagram of the molecule (Figure 4.1). It should be noted that none of the point group or local symmetry operations transform the z functions into x or y functions. Therefore, only x-y mixing with orbitals will occur, the z orbitals being separate (H1S and H2S may also occur within the z orbitals since these transform in the same way as the z functions). There are 3 z-type occupied orbitals. The orbitals which are unlabelled as to type consist of mixtures of p or s functions on different sites, or combinations of p+s functions, attributable to the presence of a dipole moment within the molecule.

By studying Table 4.4 it is very difficult to determine what characteristics cause the RHF and UHF results to be so different in overall energy and spin and particularly why the UHF run with RHF input didn't converge to the lowest energy at the UHF stage. The general characteristics of all three runs are very similar.

Table 4.5 compares orbital energy differences between the

Table 4.3

MBPT Corrections to Spin

	48 Basis	57 Basis
UHF S^2 *	0.603	0.452
MBPT Correction	-0.021	0.006
S^2 Total	0.582	0.458
Spin (S)	0.412	0.338

* $S^2 = S(S+1)$

Table 4.4

Orbital Comparisons, Nitromethane Monomer, UHF vs RHF

Ground State Energies Converged to 10^{-6}

All Energies in hartrees

Orb.	84 fn RHF E=-243.71596 Spin =0	81 fn UHF E=-243.72329 Spin=0.35	84 fn UHF E=-243.72316 Spin=0.35	84 fn UHF→RHF E=-243.71596 Spin=0
1	-20.6128 O1s	-20.6302 O1s	-20.6324 O1s	-20.6123 O2s
2	-20.6092 O2	-20.6061 O2s	-20.6084 O2s	-20.6093 O1s
3	-15.8655 Ns	-15.8055 Ns	-15.8109 Ns	-15.8656 Ns
4	-11.3215 Cs	-11.3075 Cs	-11.3084 Cs	-11.3216 Cs
5	-1.6083	-1.6015	-1.6016	-1.6083
6	-1.4016	-1.3985	-1.3986	-1.4016
7	-1.1053	-1.0877	-1.0878	-1.1053
8	-0.8681	-0.8656	-0.8654	-0.8681
9	-0.7538	-0.7483	-0.7485	-0.7538
10	-0.7383 Z	-0.7465 Z	-0.7464 Z	-0.7383 Z
11	-0.7330	-0.7290	-0.7287	-0.7330
12	-0.6260	-0.6170	-0.6172	-0.6260
13	-0.6066 Z	-0.6093 Z	-0.6093 Z	-0.6066 Z
14	-0.4954	-0.5121	-0.5123	-0.4955
15	-0.4941	-0.4890	-0.4891	-0.4942
16	-0.4536 Z	-0.4631 Z	-0.4634 Z	-0.4536 Z

original UHF run, the RHF run and the second UHF run (UHF1 refers to the original run, RHF1 refers to the original RHF run and UHF2 to the second UHF run). This table indicates that the RHF1 and UHF2 runs are almost identical in orbital energy. Also, 11 of the 16 orbitals in these two runs are lower in energy than their counterparts in UHF1. All but orbital 3 (NS) are within about 0.5eV of their counterparts. NS is quite different in energy (1.49 eV). A comparison of atomic orbital (ao) coefficients in molecular orbital (MO) 3 between RHF1 and UHF2 shows them to be identical to 5 decimal places (as is to be expected). Comparison of this MO between UHF1 and UHF2 shows all 84 coefficients to be identical to at least 3 decimal places. The largest coefficients are those belonging to NS. Table 4.6 compares the major coefficients in UHF1 and UHF2 for MO 3. The coefficients other than 33 and 34 are so small they are essentially negligible. Again, it is difficult to determine where the differences in these two runs occur.

A comparison of the z orbitals (10,13 and 16) reveals some interesting features. Table 4.5 shows energy differences of -0.22 eV, -0.07 eV and -0.27 eV for each of these (UHF1-UHF2). Table 4.7 shows all major contributing coefficients to these 3 orbitals. MO 10 is a reasonably well matched orbital between the two. However, there are some substantial differences in orbital make-up for MO 13 and MO 16, particularly in the O2Z, NZ and CZ contributions. MO 13 for UHF1 has much less O2Z and NZ character

Table 4.5

Orbital Energy Differences, UHF vs RHF, 84 Functions

Orbital		ΔE(UHF1-RHF1) hy.	(eV)	ΔE(UHF1-UHF2) hy.	(eV)
1	O2s	-0.0196	-0.53	-0.0197	-0.542
2	O1s	0.0008	0.022	0.0009	0.02
3	Ns	0.0546	1.49	0.0547	1.49
4	Cs	0.0131	0.36	0.0132	0.36
5		0.0067	0.18	0.0067	0.18
6		0.0030	0.080	0.0030	0.08
7		0.0175	0.48	0.0175	0.48
8		0.0027	0.07	0.0027	0.07
9		0.0053	0.140	0.0053	0.14
10	Z	-0.0081	-0.27	-0.0081	-0.27
11		0.0043	0.12	0.0043	0.12
12		0.0088	0.24	0.0088	0.24
13	Z	-0.0027	-0.07	-0.0027	-0.07
14		-0.0169	-0.46	-0.0168	-0.45
15		0.0050	0.14	0.0051	0.14
16	Z	-0.0098	-0.27	-0.0098	-0.27

Table 4.6

Nitromethane MO3: UHF1 vs UHF2 Coefficients

Coeff.	UHF1	UHF2	Type
33	0.593736	0.593838	Ns
34	0.445983	0.446088	Ns
35	0.001786	0.001039	Ns
36	0.000895	0.000753	Ns
44	0.000081	0.000294	Nd
50	0.000968	0.000763	Cs
52	0.000527	0.000422	Cx
67	0.000318	0.000774	BNO1x

AD-A174 012 ENERGY TRAPPING RELEASE AND TRANSPORT IN THREE DIMENSIONAL ENERGETIC SOLI..(U) MICHIGAN TECHNOLOGICAL UNIV HOUGHTON A B KUNZ 30 JUN 86 N00014-81-K-0628 2/4

UNCLASSIFIED F/G 7/3 NL

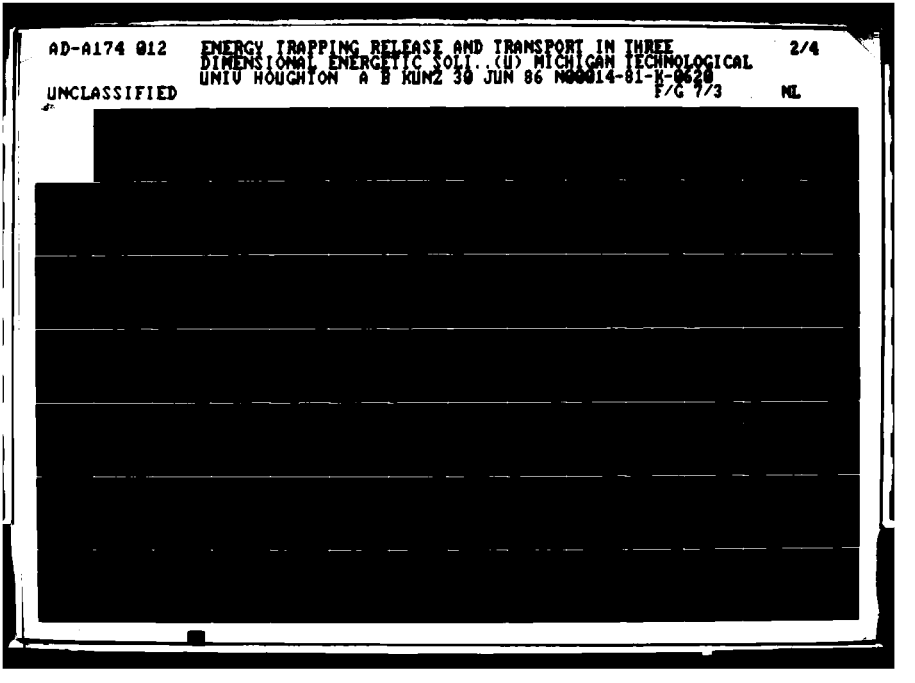

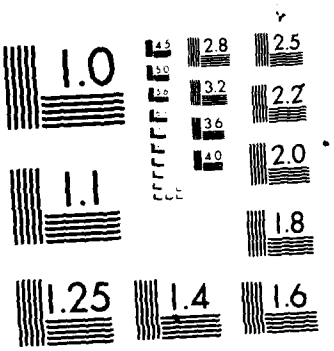

Table 4.7

Z-Type MO Coefficients; UHF1 vs UHF2, 84 Functions.

Coeff #	Type	MO 10		MO 13		MO 16	
		UHF1	UHF2	UHF1	UHF2	UHF1	UHF2
17	O1z	-0.451	-0.278	0.344	0.194	0.489	0.512
18	O1z	-0.154	-0.098	0.147	0.081	0.282	0.291
19	O2z	-0.162	-0.275	0.024	0.207	-0.377	-0.502
20	O2z	-0.058	-0.096	0.012	0.092	-0.209	-0.291
41	Nz	-0.424	-0.439	0.073	0.207	-0.369	-0.001
42	Nz	-0.133	-0.143	0.028	0.086	-0.197	0.013
56	Cz	-0.195	-0.247	-0.467	-0.450	0.112	-0.012
57	Cz	-0.031	-0.042	-0.117	-0.118	-0.003	-0.062
76	H1s	0.095	0.122	0.272	0.273	-0.093	0.003
77	H1s	0.021	0.028	0.082	0.085	-0.089	-0.052
78	H2s	-0.095	-0.122	-0.272	-0.273	0.092	-0.003
79	H2s	-0.021	-0.028	-0.082	-0.085	0.089	0.052
82	BCH1s	0.006	0.009	0.013	0.019	-0.006	0.001
83	BCH2s	-0.006	-0.009	-0.018	-0.019	0.006	-0.001

where MO 16 for UHF1 has much more NZ and CZ character. These outer orbitals will be discussed in more detail in the next section.

From the energy variational viewpoint, UHF1 is the best ground state since its energy is lower the UHF2 by 0.2 eV. It has not been determined in this study if the UHF2 result is actually an excited state of this system. However, since UHF functions are supposed to be spin eigenfunctions and since this is a closed shell molecular system, UHF2 is a more accurate description of the system from the energy/spin viewpoint if it truly is the ground state. In any event, the spin differences must be tied up in the difference in character of these outer orbitals. It should be noted that the RHF value of -243.715959 (with correct spin) is also lower than any previously reported UHF or RHF value.

Outer Orbital Characteristics

There has been some discrepancy on the ordering of the outer orbitals of nitromethane. Experimental work (photoelectron spectroscopy (PES)) done by Kobayashi [57] (1977), Dewar [56] and Rabalais [11] (1972) indicate that the outermost occupied MO is a bonding σ-type orbital of a_1 symmetry while the second orbital is an anti-bonding π-type orbital of a_2 symmetry (see Appendix B for a brief discussion of these symmetry and bond types). The π orbitals are what were referred to as the z orbitals which are

perpendicular to the x-y plane of the molecule. However, Fujikawa [58] (1974) indicates these two are reversed. Orbital assignments in both Fujikawa's and Kobayashi's work were initially determined using CNDO methods (Complete Neglect of Differential Overlap) and both indicated that the π anti-bonding orbital was the least bound. Kobayashi's mistrust of CNDO methods caused him to reverse the assignment based on experimental results of PES on nitrobenzene. Fujikawa (while comparing ultraviolet and x-ray spectra of nitromethane) did not reverse the assignment but commented that these bands are superimposed on one another in the x-ray spectrum, leaving one to question his assignment of these orbitals. Rabalais also reassigned the top orbitals (originally based on INDO calculations) and made the σ orbital outermost. Semi-empirical work done by McEwan [14] in 1959 also assigns the π orbital as outermost with a statement indicating the difficulty in ordering such closely spaced orbitals. Work done by Murrel[147] and co-workers in 1975 suggest that the π,σ ordering is correct based on the small energy difference between the a_1 (π) and a lower-lying orbital of b_2 symmetry. The a_1, a_2, b_2 ordering suggested by Kobayashi and Rabalais requires a 3.4 eV difference in energy between the a_1 and b_2 orbitals based on their band energies. Murrel indicates all semi-empirical work done on nitromethane shows this splitting to be small (nearly degenerate) and therefore the a_2 orbital could not possibly lie between them. They use Koopman's Theorem and neglect correlation, two approximations

which could result in errors of level assignment not to mention energy values. Niemeyer [59] also places the π orbital as the outermost. He uses CNDO methods also. As questionable as some of these theoretical methods may be from the accuracy point of view, work done by this author assigns the order a_2 (π), a_1 (σ) for the two outermost orbitals, in agreement with the semi-empirical work. At the UHF-MBPT stage, these orbitals are only about 0.7 eV apart. The orbital b_2 lies another 0.63 eV below the a_1 orbital. Since the RHF work done by this author on the ground state also results in the same ordering for these orbitals support is given to previous theoretical work on the system. However, a wavefunction which is corrected to first order may really be necessary to determine the orbital ordering with confidence.

Plots For Ground State Molecular Orbitals

13, 14, 15, 16

The following pages display molecular orbital wavefunction amplitude plots for the four outermost MO's of nitromethane. Both RHF and UHF plots are shown. All diamonds in the diagrams represent atoms of the molecule not lying in the plot plane. Any 'x' represents an atom of the molecule in the plot plane. All plots have contours spaced every 0.05 au within the range of ±1.0 au for the wavefunction. Solid lines indicate positive regions of the wavefunction while dashed lines indicate negative regions.

UHF MO 13 shows a strongly localized π orbital on carbon with a weaker lobe on nitrogen. RHF MO 13 has a much stronger contribution at the nitrogen atom. Both are of b_1 symmetry. MO's 14 and 15 are of a_1 in both the RHF and UHF calculations. There is very little difference between the UHF and RHF orbitals in this case. The orbitals are bonding at the oxygen lobes with strong x-y character. MO 16 shows the largest discrepancy between the UHF and RHF runs. UHF shows the π orbitals of a_2 symmetry localized on the oxygen atoms but it also shows a strong nitrogen contribution (See Orbital Plot 10) whereas the RHF run shows no nitrogen contribution (The x-z plot for 16 RHF which would show the nitrogen contribution is not shown here because it contained no information, i.e., no localization at all on the nitrogen atom.). It is probably this orbital at the UHF stage which causes the spin to be incorrect.

Rabalais [13] shows the top three orbitals as having symmetry a_1, a_2, b_2. Both UHF and RHF runs indicate them to be a_2, a_1, a_1, i.e., an orbital of b_2 symmetry does not show up here. The a_2 orbitals are anti-bonding as are the b_2 orbitals. Orbitals of a_1 symmetry are bonding. The a_1 orbitals shown here are similar to the one shown schematically by Rabalais [13] except he indicates that the oxygen lobes have less tilt with respect to the x-axis. Both up and down spin spaces were shown for UHF orbitals 14 and 15 to indicate the orbital symmetry.

The lack of an orbital of b_2 symmetry poses a problem in that

two experimentalists claim it is there (Rabalais [13] and Kobayashi [57]). However, Fujikawa [58] merely characterizes these three outer orbitals as lone-pairs, one out-of-plane and two in-plane. This is essentially what is shown in the orbital plots.

Orbital Plot 1

X-Z Plane

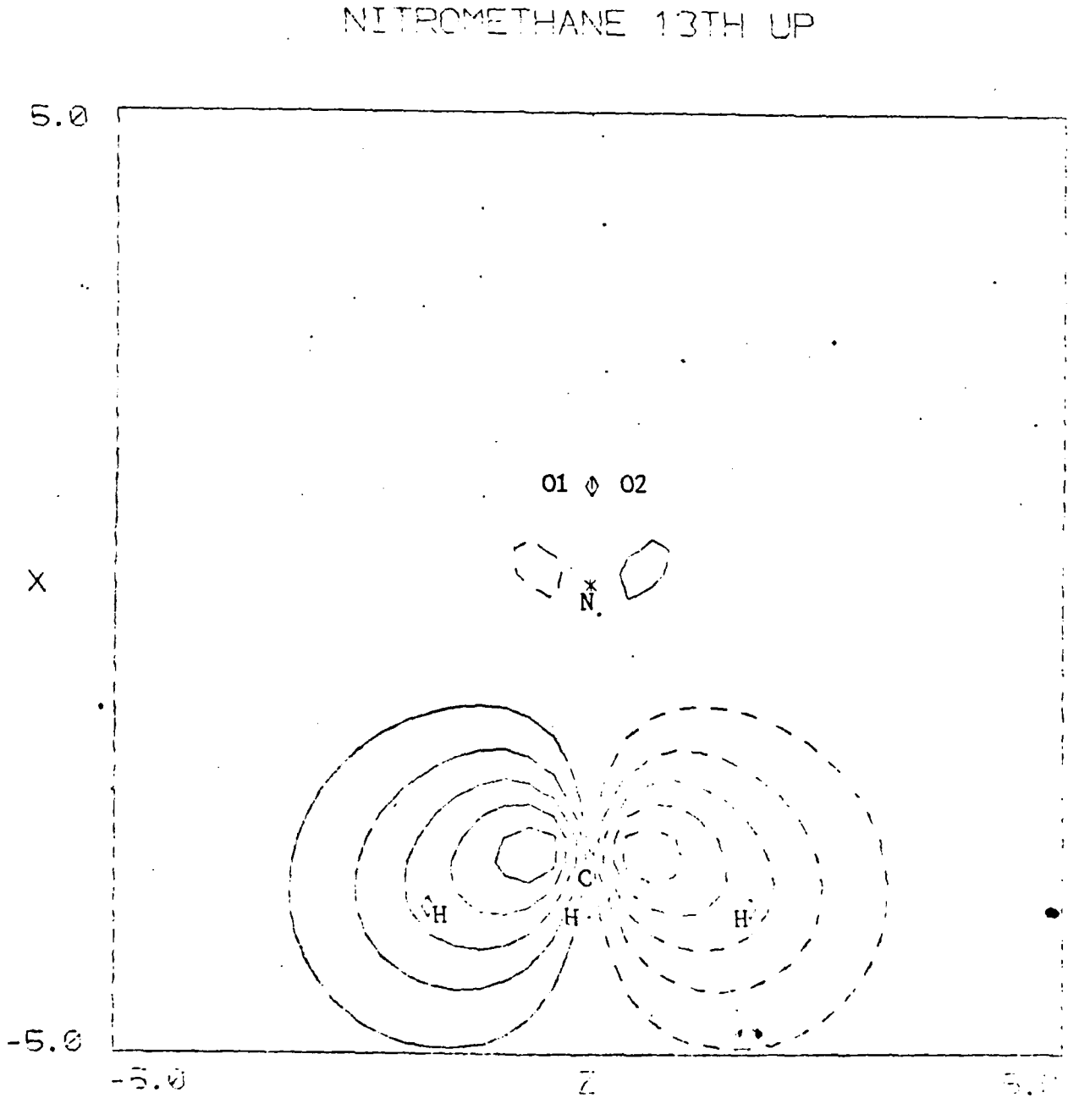

Orbital Plot 2

. X-Z Plane

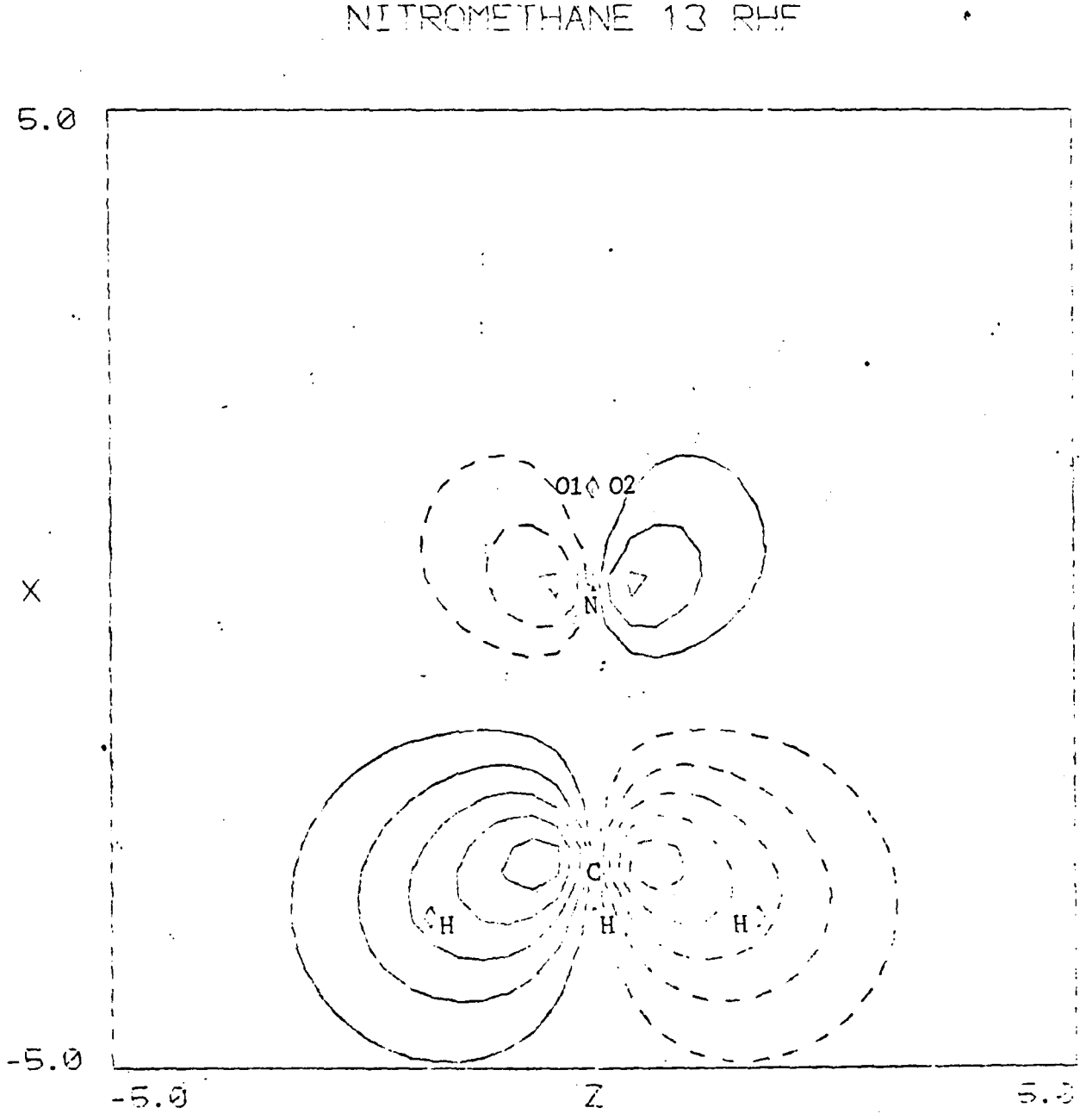

Orbital Plot 3

X-Y Plane

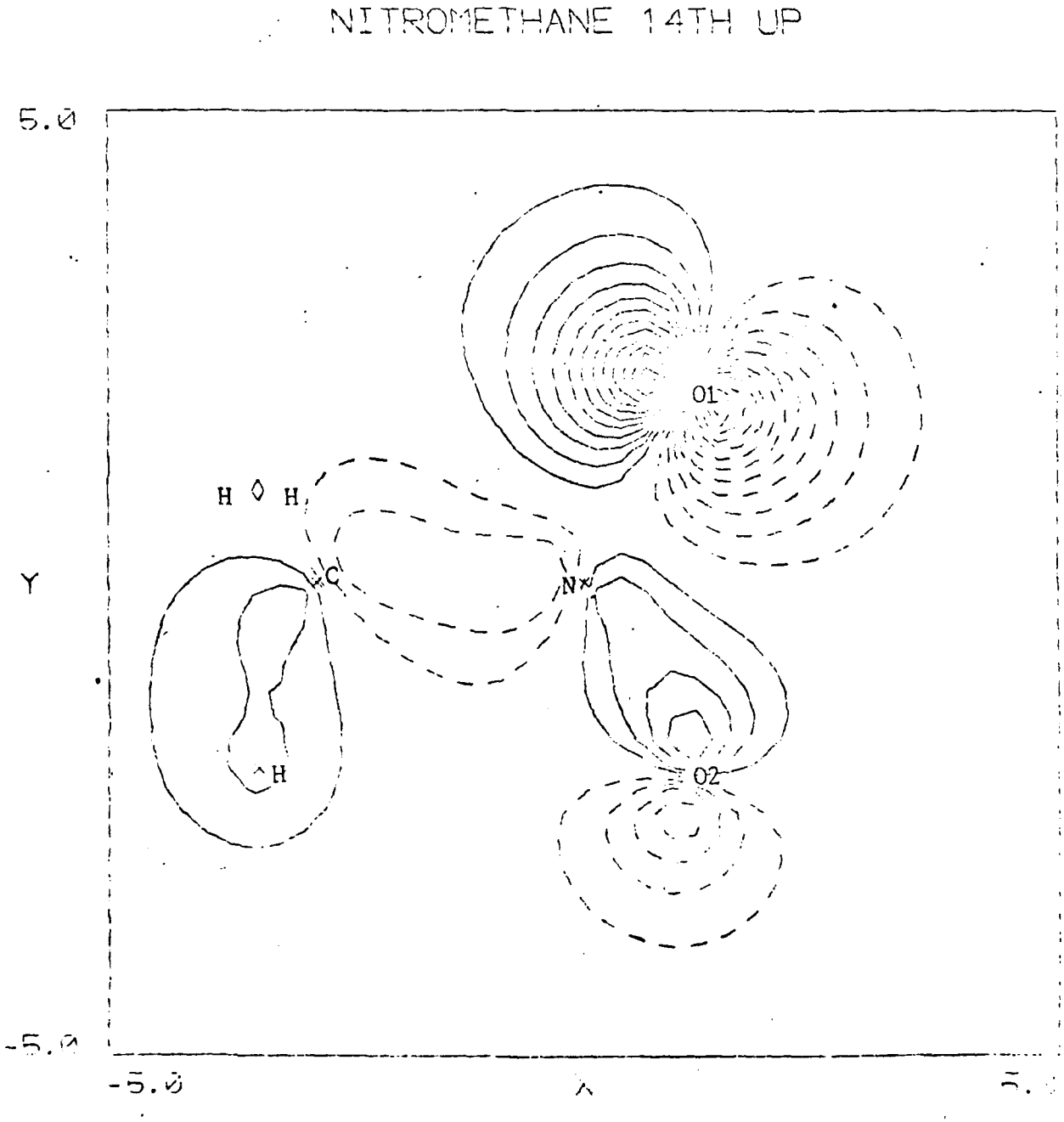

Orbital Plot 4

X-Y Plane

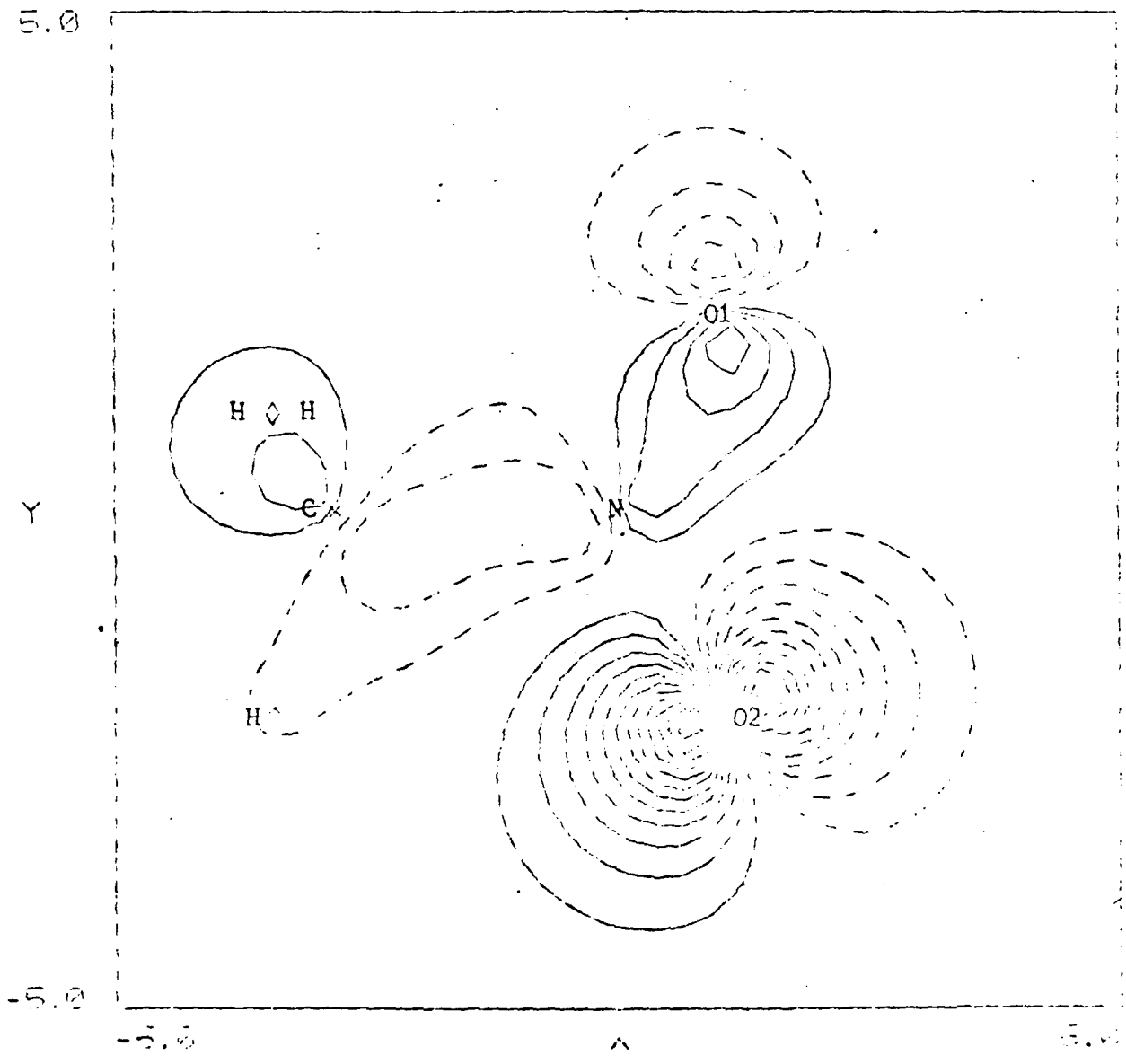

Orbital Plot 5

X-Y Plane

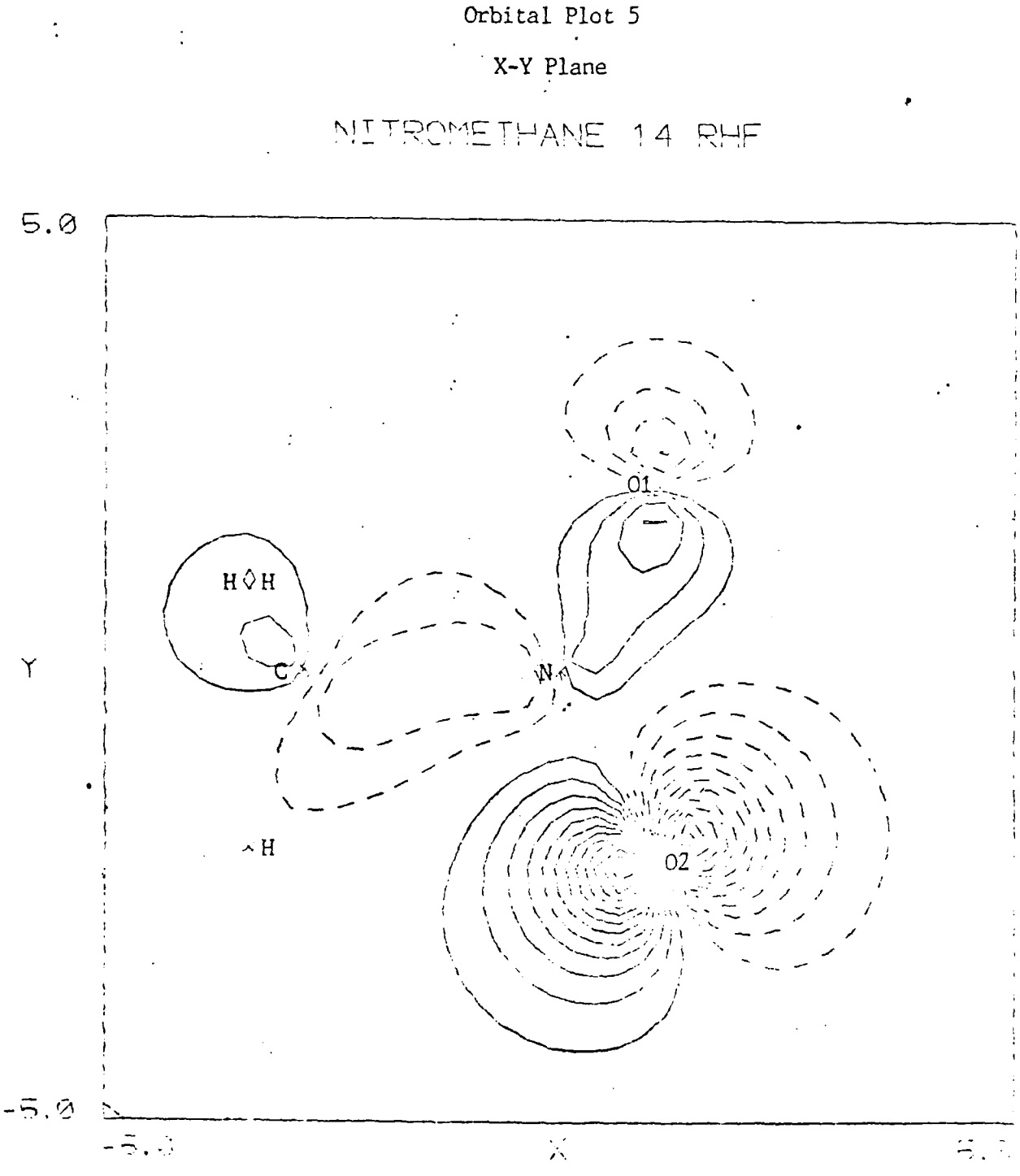

Orbital Plot 6

X-Y Plane

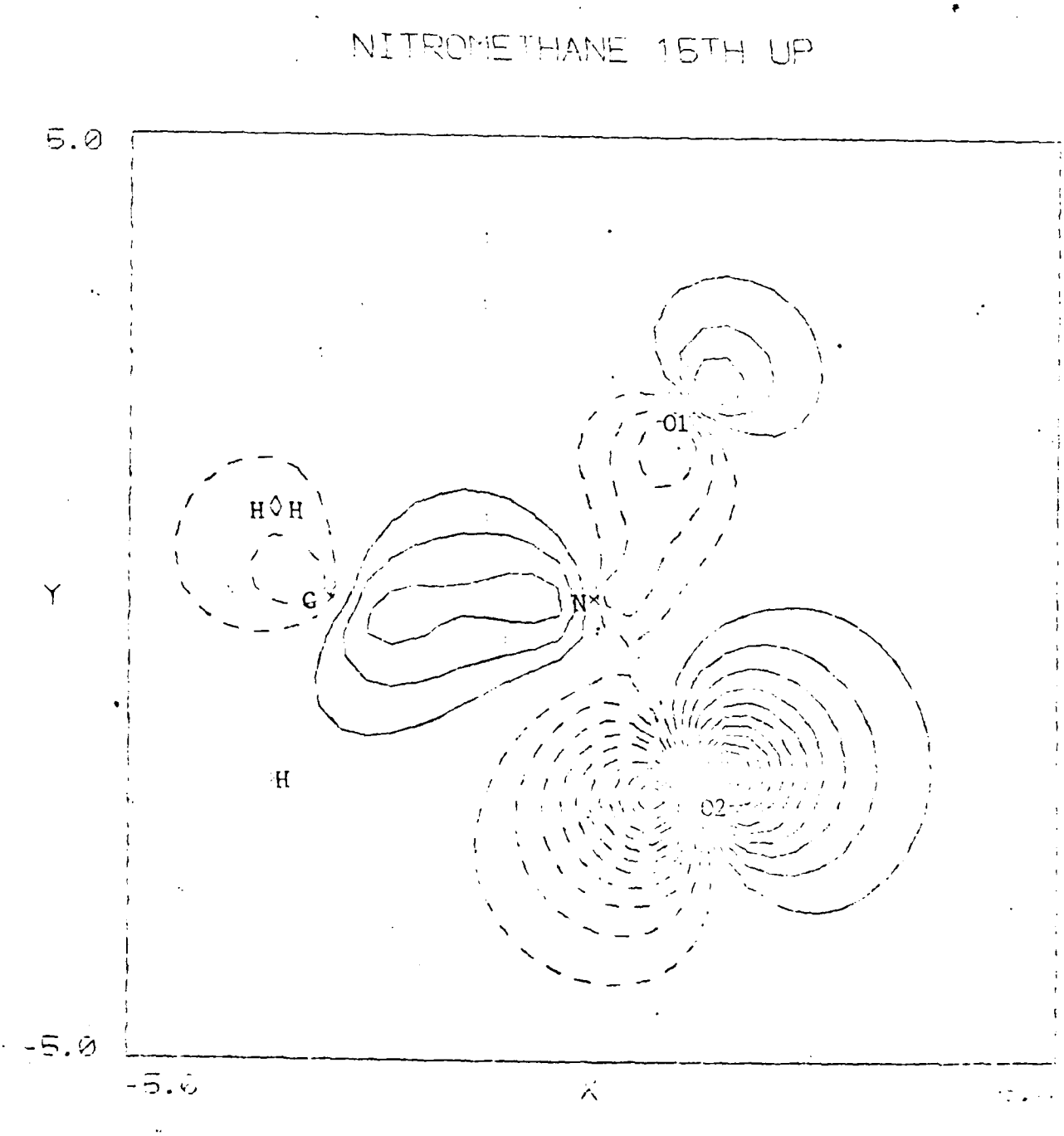

Orbital Plot 7

X-Y Plane

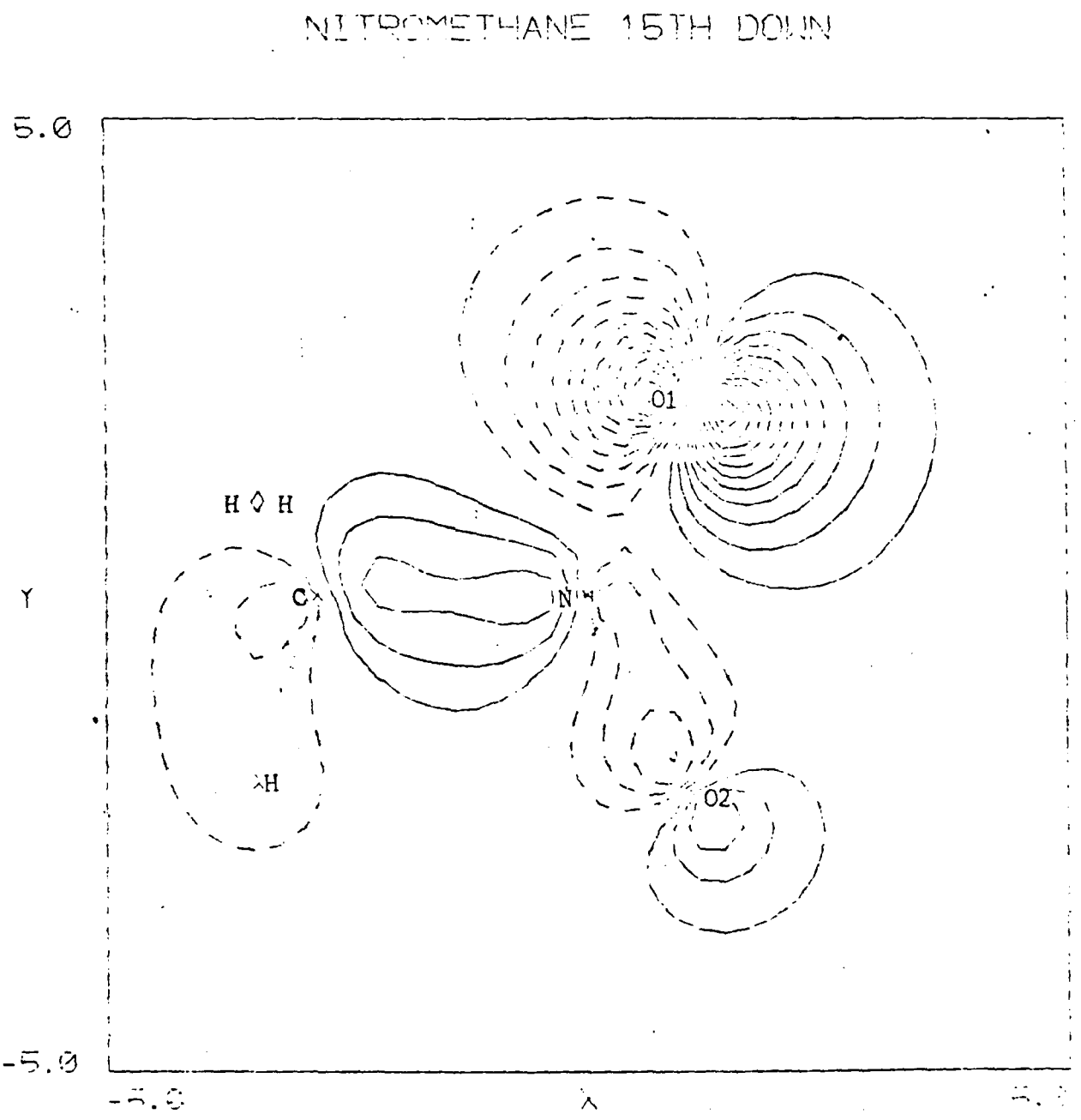

Orbital Plot 8

X-Y Plane

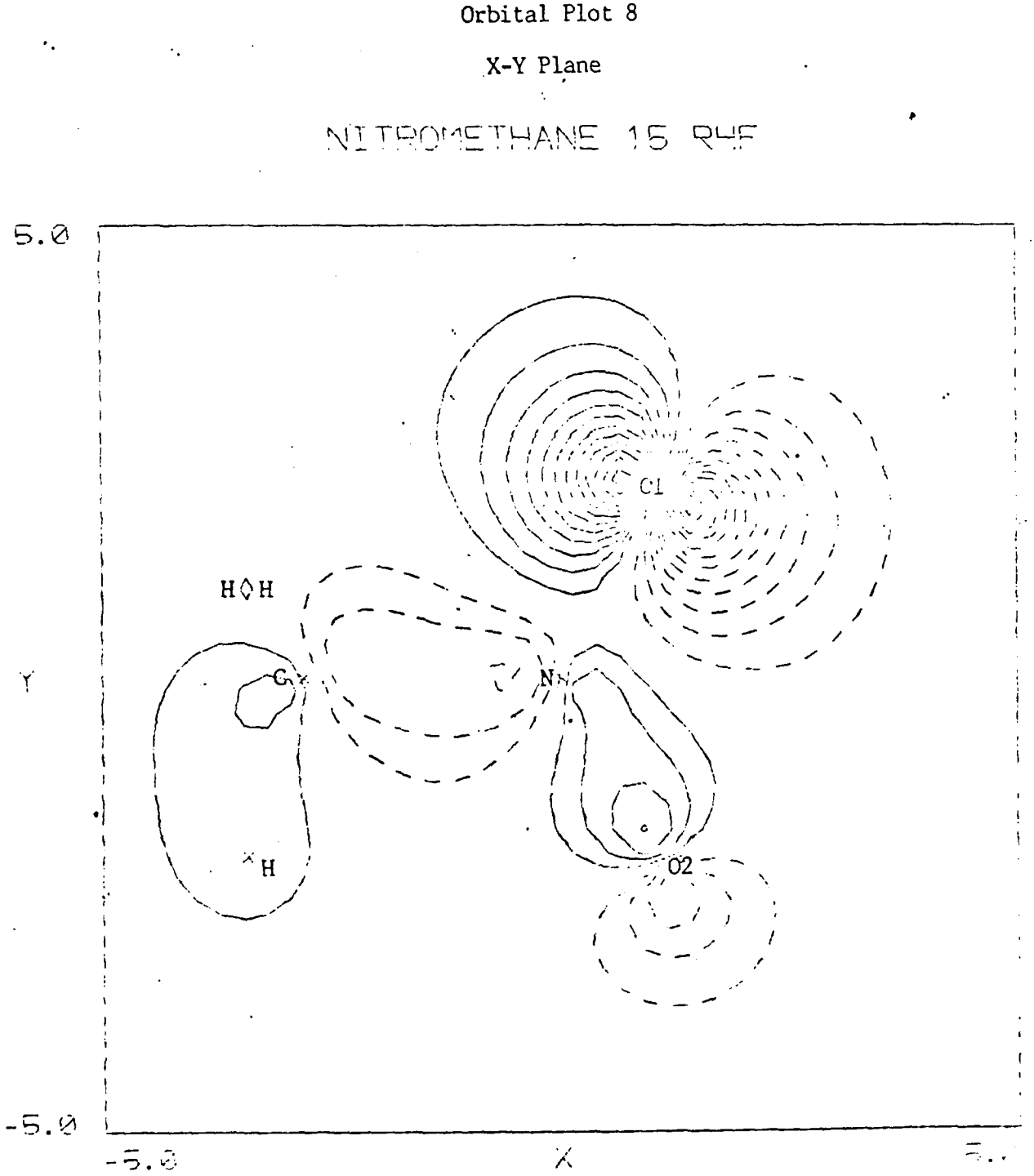

Orbital Plot 9

O1-O2 Plane

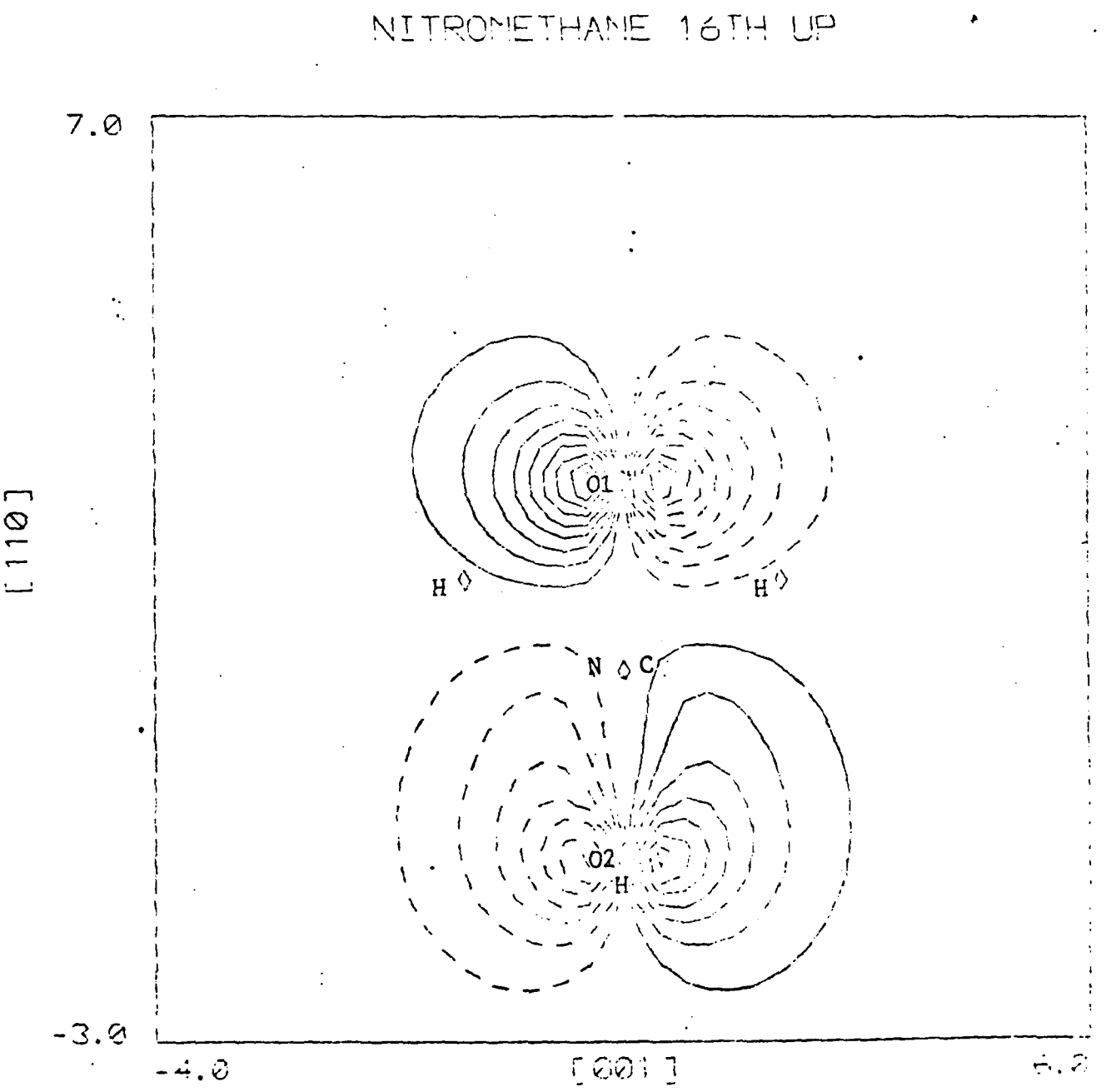

Orbital Plot 10

X-Z Plane

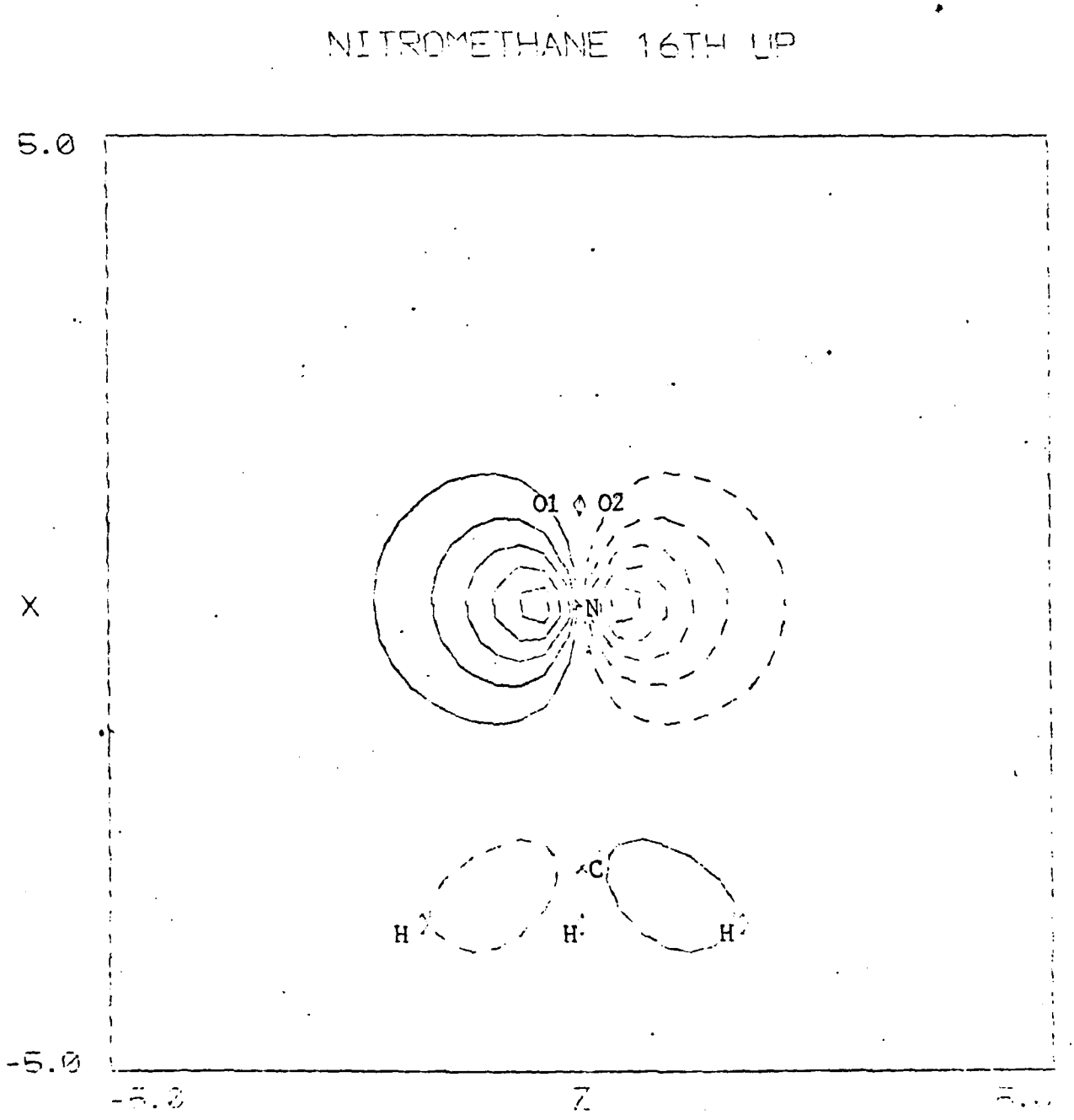

Orbital Plot 11

O1-O2 Plane

NITRO 16 RHF

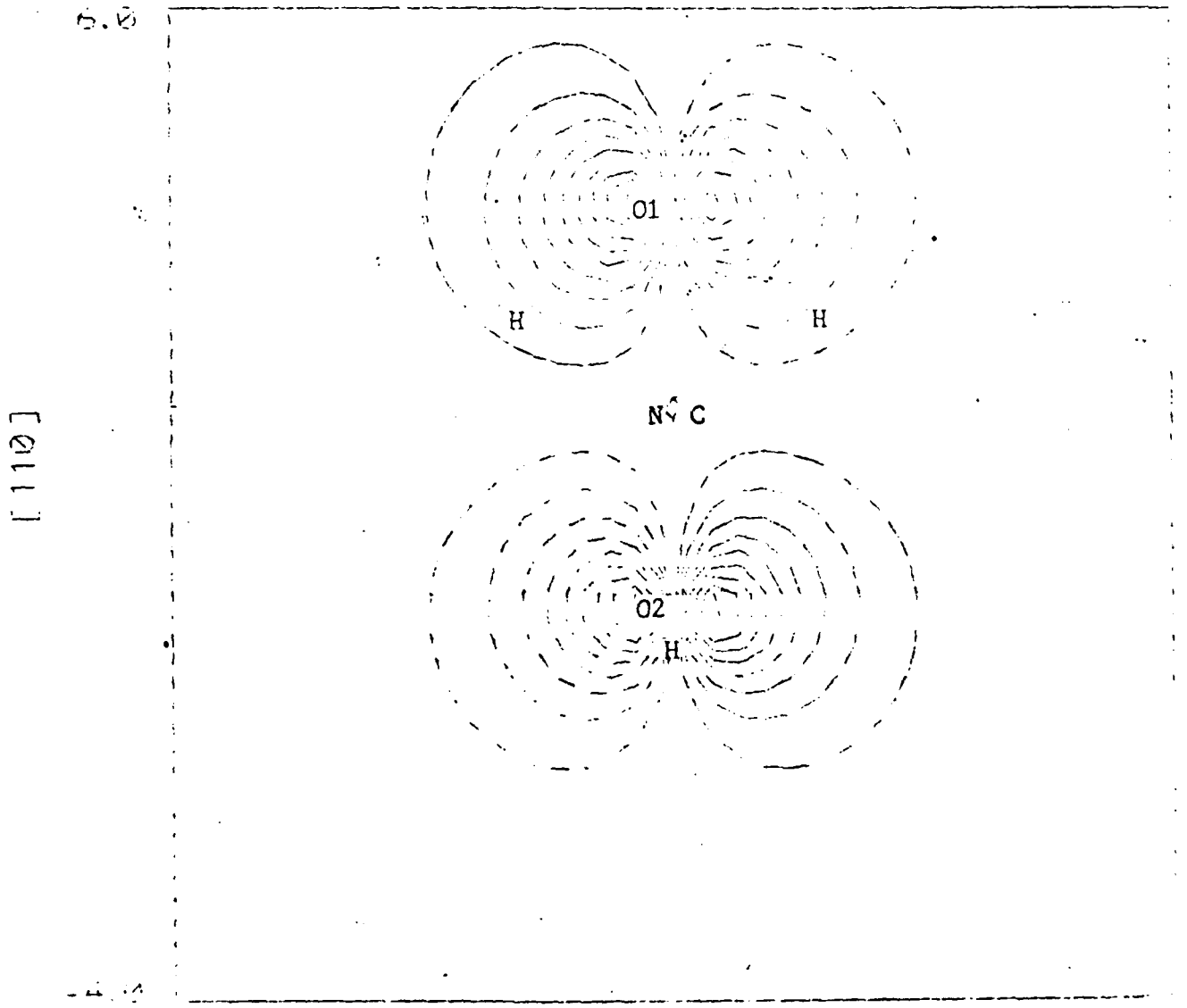

Ionization Potentials

First and second ionization potentials were calculated through the HF stage using 48, 57, and 81 functions. The 48 and 57 function sets were also correlated. As can be seen in Table 4.8, the results are in reasonable agreement with experiment. The discrepancy in ordering between experiment and theory is indicated by the symmetry type of the ionized orbital. The values reported in this work are closer to the experimental values than those previously reported. However, the 57 function data is anomalous in that its values appear to be reversed. This may have something to do with the orbital ordering problem and may be an indication that the outer orbital is that of a_2 symmetry. Also, a more precise calculation involving relaxation of bond angles and correlation of these relaxed systems after ionization should really be done. Although some bond angle and bond length relaxation work was done by the author on the first ionized state, it was not correlated. The indications were that the O-N-O bond angle relaxed from the ground state value of 125.3° to about 120° at the HF stage. The values listed in Table 4.8 by this author are for fixed ground state geometries only.

Also shown in Table 4.8 is a comparison of the 48, 57 and 81 function HF results. The 81 function set has a tendency to give the lowest value of the three sets for both ionization potentials.

Table 4.8

Nitromethane 1st and 2nd Ionization Potentials

Reference	1st I.P. (eV)	Sym	2nd I.P. (eV)	Sym
This work 48 fns	11.16	a_2	11.33	a_1
This work 57 fns	11.53	a_2	11.39	a_1
Murrel (47)	10.95	a_2	12.39	a_1
Murdoch (49)	11.98		13.38	
Rabalais (13)*	11.32	a_1	11.73	a_2
Kobayashi (57)*	11.31	a_1	11.81	a_2
Fujikawa (58)*		11.50		
48 fn HF only	9.51		9.88	
57 fn HF only	9.61		10.06	
81 fn HF only	9.49		9.76	

* Fujikawa was unable to resolve these two peaks individually using x-ray spectroscopy. Rabalais and Kobayashi used HeI ,584 A, 21.22 eV as their ionizing source for photoelectron spectroscopy .

Excited States

Excited states of nitromethane have not been well studied. McEwen[66] did semi-empirical work and arrived at a list of possible excitation energies, the lowest-lying state at 3.01 eV representing a transition of $a_2^{-1} \rightarrow b_1^*$ ($\pi \rightarrow \pi^*$:an electron is removed from the a_2 orbital and excited to an orbital of b_1 symmetry, both orbitals being π-like). Kleier and Lipton [1], in what they term an 'approximate ab initio method', report a lowest lying excited state of 1.45 eV. They also state that this value is not expected to be accurate but that the symmetry of the excitation is $\pi \rightarrow \pi^*$. They also state that evidence for the existence of such a low-lying excited state of this symmetry is inconclusive. Rabalais [13] insists the lowest lying excited state is the $\sigma \rightarrow \pi^*$ transition and that the $\pi \rightarrow \pi^*$ transition is at a higher energy. Again, this goes back to the discrepancy in the ordering of the outer ground state orbitals. His prediction is that the $\pi \rightarrow \pi^*$ excitation lies at about 6.27 eV. This author calculated a correlated low-lying excited state at 3.46 eV using both the 48 and 57 function basis sets. The excited orbital was π-like and of b_1 symmetry, indicating a $\pi \rightarrow \pi^*$ transition. The HF energy yielded a difference of 1.4 eV with respect to the 48 function ground state, 1.8 eV for the 57 function system, and 1.8 eV for the 84 function system, all values being similar to that

reported by Kleier. Electron correlation brought the difference in both the 48 and 57 systems with respect to the correlated ground states, to 3.46 eV. The 84 function system was not correlated. Also, the spin for these results was S=1, indicating convergence to the triplet. Further confirmation of the existence of this state came from two RHF runs (uncorrelated) using the 57 function and 84 function sets.

Very recently, Kaufman [50] did some calculations using CI methods for several low-lying excited states of nitromethane. (see Table 4.9). Her lowest state lies at 0.1763 (4.8 eV) above the ground state, using the full CI estimate. Her singles+doubles CI work shows this difference to be 0.2029 Hy (5.52 eV) and her extrapolated CI calculation lowers this to 0.1802 Hy (4.9 eV). The value reported in this work for the lowest state (3.46 eV) is not in good agreement with her work. It is difficult to determine the reason for this relatively large discrepancy. One possibility is that the excited state in this work is the triplet whereas it is assumed Kaufman converged to the singlet in her CI calculation (the singlet lying above the triplet). Also, there could again be differences due to the relative sizes of the basis sets used in her calculation compared to those used in this work. The difference could be related to either the multiconfiguration character of the system or to the approximations in Kaufman's CI values. It is unlikely that higher orders of MBPT would make repulsive contributions as large as 1.5 eV, the difference in

Table 4.9

Summary of Excited State Results

and Comparison to Other Work

	E_{tot} (gs)	E_{tot} (exc.)	Δ Energy hy (eV)	Spin
*This work 48	-244.0699	-243.9428	0.1271 (3.46)	1.0
*This work 57	-244.2082	-244.0725	0.1277 (3.47)	1.0
**Kaufman	-243.8135	-243.6106	0.2029 (5.52)	
**Kaufman	-243.8749	-243.6947	0.1802 (4.90)	
**Kaufman	-243.8962	-243.7199	0.1763 (4.79)	
M.DR	-242.2547		& 0.0390 (1.06)	
M.DG	-242.3082		&& 0.0925 (2.52)	
M.DRO		-242.2157		
M.PDR	-242.4284		# 0.0681 (1.85)	
M.PDG	-242.4712		## 0.1105 (3.01)	
M.PDRO		-242.3606		

*$E_{tot} = E_{HF} + E_{MBPT}$

E_{MBPT} = -0.429168 (g.s. 48), = -0.509799 (g.s. 57)
= -0.354409 (exc. 48), = -0.449676 (exc. 57)

**Kaufman's work shown at three levels of calculation, CI, Extrapolated CI and 'Full CI Estimate'.
M.=Marynick [85], gs=ground state, D=double zeta,P=polarized, G=GVB,R=RHF,RO=ROHF &value=M.DRO-M.DR, &&value=M.DRO-M.DG, #value=M.PDRO-M.PDR, ##value=M.PDRO-M.PDG

Table 4.9a

Singlet-Triplet Splitting: Excited State of Nitromethane

Energies in hy (eV)

	E gs*	E s*	E t	ΔE s-gs	ΔE t-gs	ΔE s-t
57fn	-.690	-.607	-.621	.083 (2.3)	.069 (1.9)	.014 (.38)
84fn	-.716	-.629	-.644	.087 (2.4)	.073 (2.0)	.015 (.40)

57fn,84fn (this work, RHF),
* values shown to be prefixed with 243., i.e., -243.690 for gs 57.

energy between the excited states of this work and Kaufman's. It should also be noted that Kaufman's quoted values are the roots extracted from the diagonalization of her CI matrix. This may not yield accurate results unless the basis set used was a very good one.

For 57 functions the open shell singlet lies at 2.26 eV above the ground state and 0.39 eV above the triplet. The triplet lies 1.87 eV above the ground state. For 84 functions the singlet is 2.37 eV above the ground state and 0.40 eV above the triplett which is 1.97 eV above the ground state. These results were uncorrelated. A better estimate of the energy difference between the ground state and excited singlet would be to use the value of 3.46 eV (48 functions + correlation) and add the 0.40 eV singlet-triplet splitting since the triplet is the state converged to in this work (to be shown later) and the singlet is assumed to lie above the triplet. This shows a value of 3.86 eV for this energy difference. Recent work by Marynick [52] and co-workers using GVB methods indicates the splitting between the ground state singlet and the first excited state triplet to lie somewhere between 1.0 and 3.01 eV. The large variation in values (see Table 4.9) is a function of the method used. His best calculation, which gives the result of 3.01 eV supports the work done by this author (3.47 eV) for the energy difference between the ground state and first excited triplet state.

Kleier and Lipton show the lowest lying state to be a

triplet (1.45 eV above the ground state) followed by a triplet and singlet (2.54 eV and 2.64 eV) separated by 0.1 eV.

The work done by this author is strong confirmation of the existence of a low-lying excited state, 3.46 eV above the ground state with the symmetry of a $\pi \rightarrow \pi^*$ transition. A summary of the above discussion is given in Tables 4.9 and 4.9a.

Plots For Excited State Molecular Orbitals 14,15,16,17

The following pages show wavefunction amplitude plots for the top four spin-up orbitals of nitromethane in its first excited state. As in the ground state plots, there may be more than one view of an orbital to see all of its character. Again, the individual contours are in increments of 0.05 au with 'x' implying in-plane atoms and diamonds, out-of-plane atoms of the molecule.

MO 14 has strong carbon character and also oxygen lobes. The orbital is of b_1 symmetry and consists of π bonding lobes on the oxygen. This orbital is similar to MO 13 of the ground state except that a nitrogen lobe occurred in that MO. It appears that charge was transferred to the oxygens in going from the ground to the excited state. MO 15 is of b_2 symmetry. It appears to be a modification of the ground state MO 14. In that orbital a spin-up electron was primarily centered on one oxygen. In MO 15 (excited), this electron is shared by the two oxygens. MO 16

(excited) is another modification of MO 14 or MO 15 (ground state). This is of a_1 symmetry and looks somewhat more like the a_1 orbital Rabalais proposes for the outermost ground state orbital. The oxygen's lobes are aligned more along the x direction. Three views are shown of the outermost excited state orbital, MO 17. Plots in the x-z and y-z plane show a large nitrogen π double lobe. A plot through a plane containing both oxygens shows them both holding π lobes also. The orbital possesses b_1 symmetry, and the oxygen lobes are bonding to each other and non-bonding to the nitrogen lobes.

Orbital Plot 12

X-Z Plane

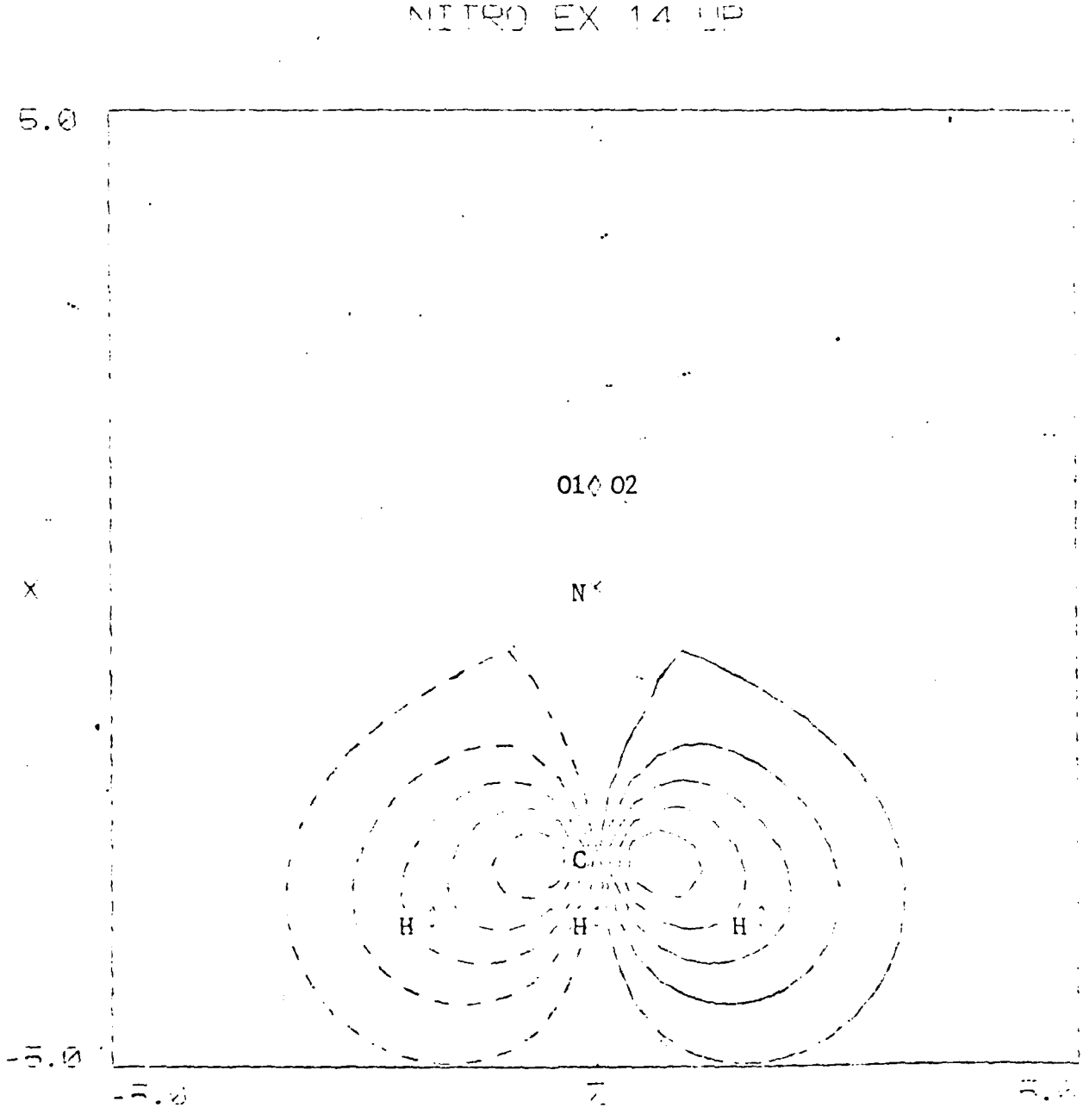

Orbital Plot 13

01-02 Plane

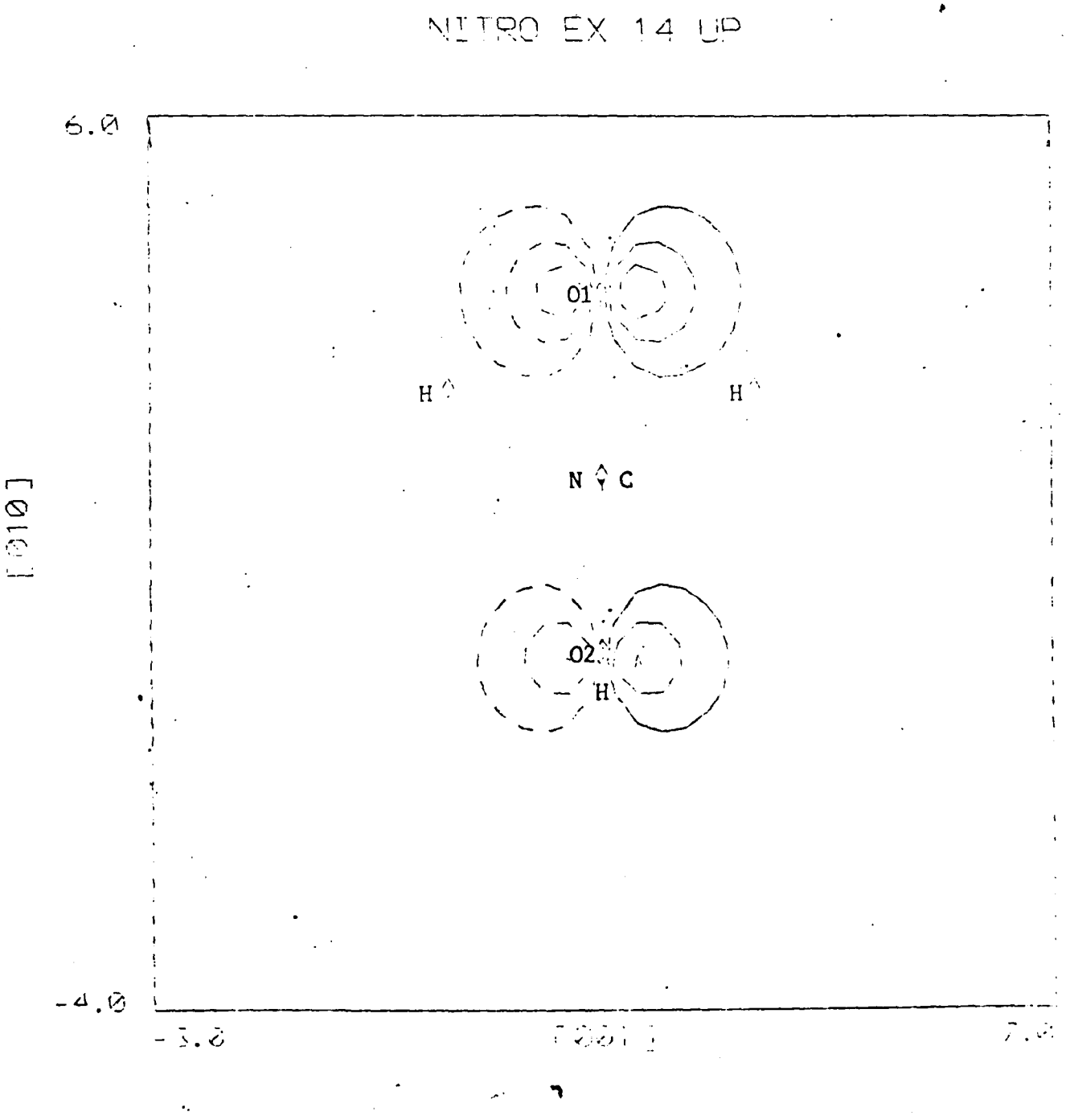

Orbital Plot 14

X-Y Plane

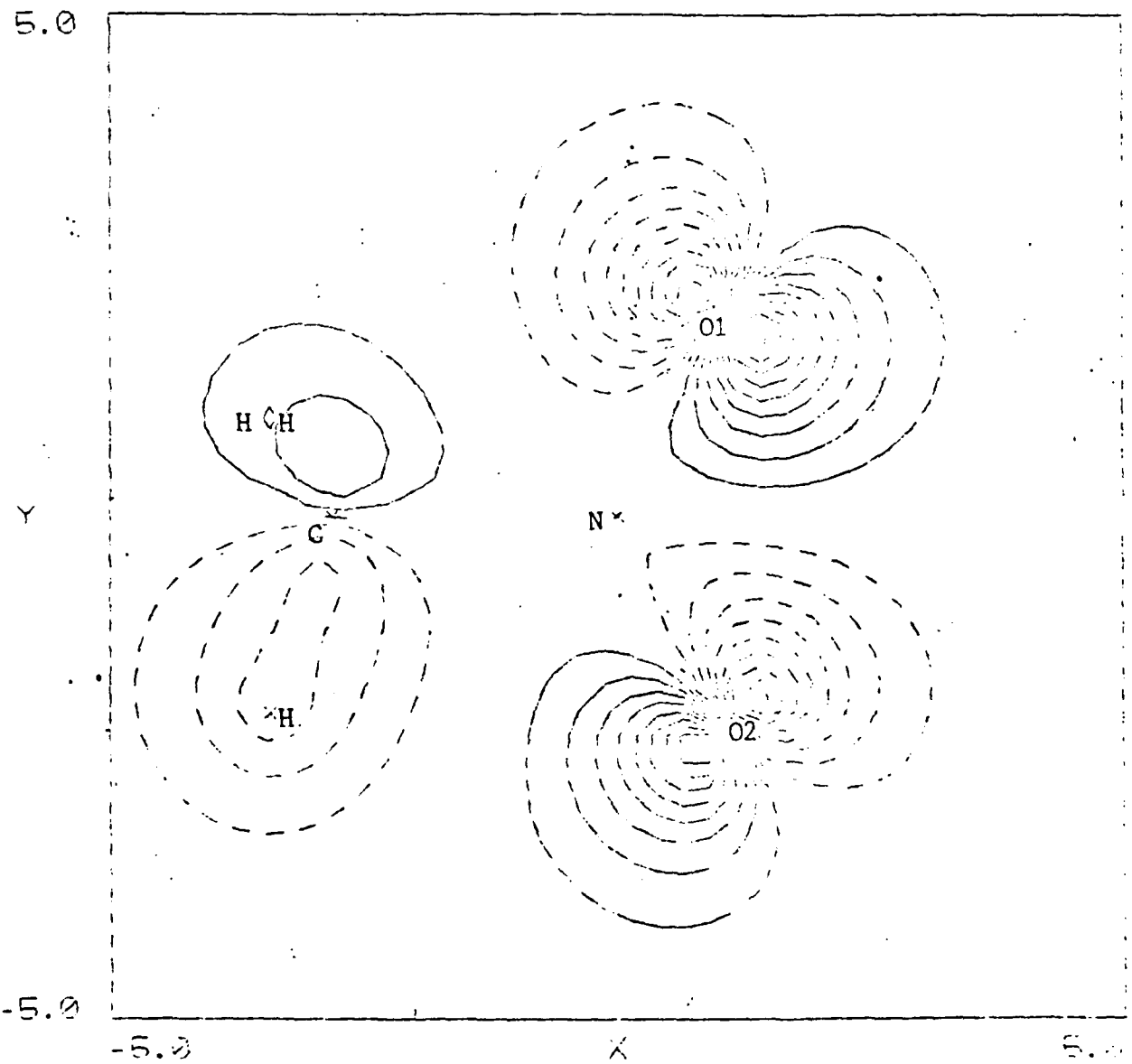

Orbital Plot 15

X-Y Plane

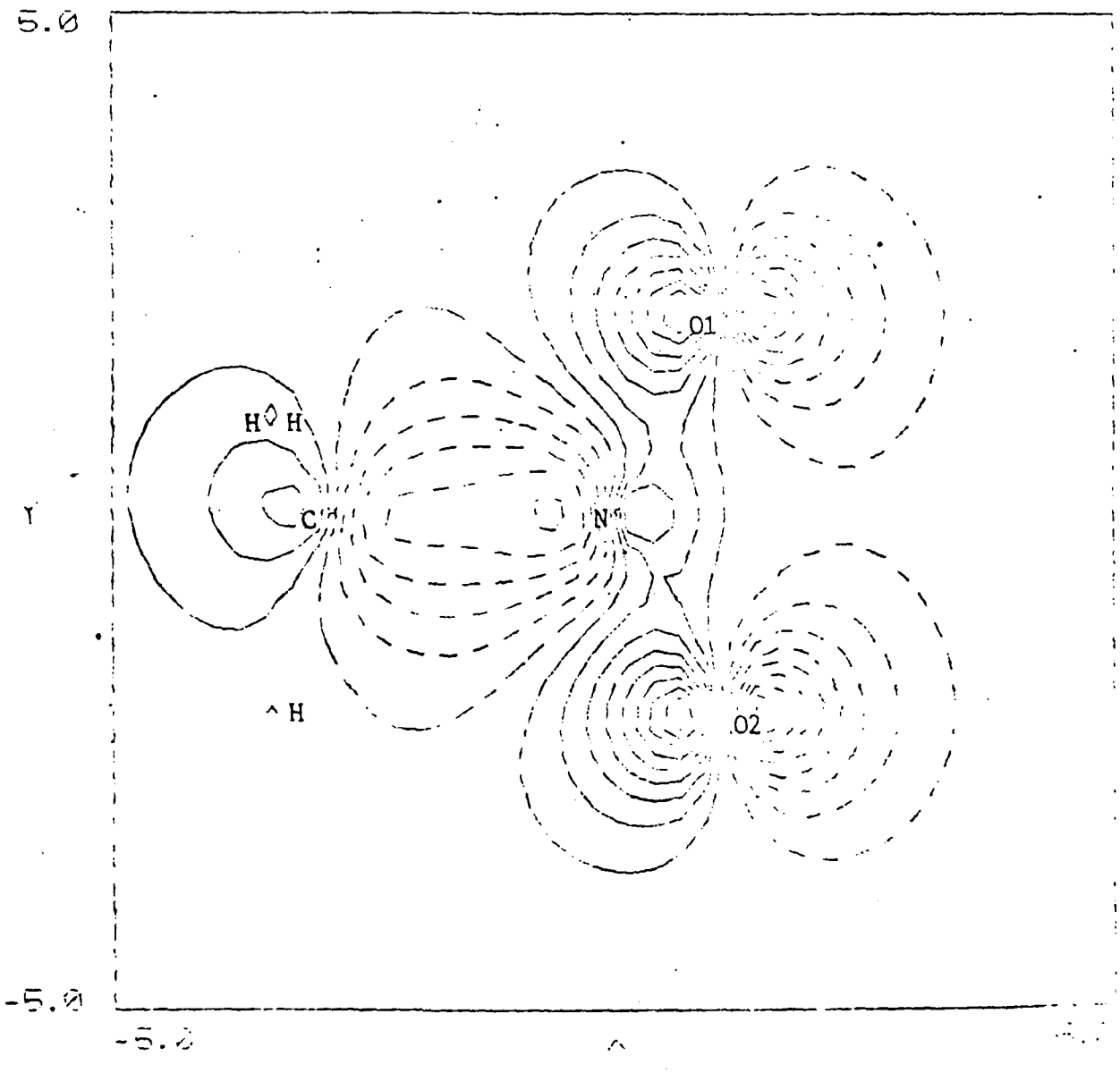

Orbital Plot 16

X-Z Plane

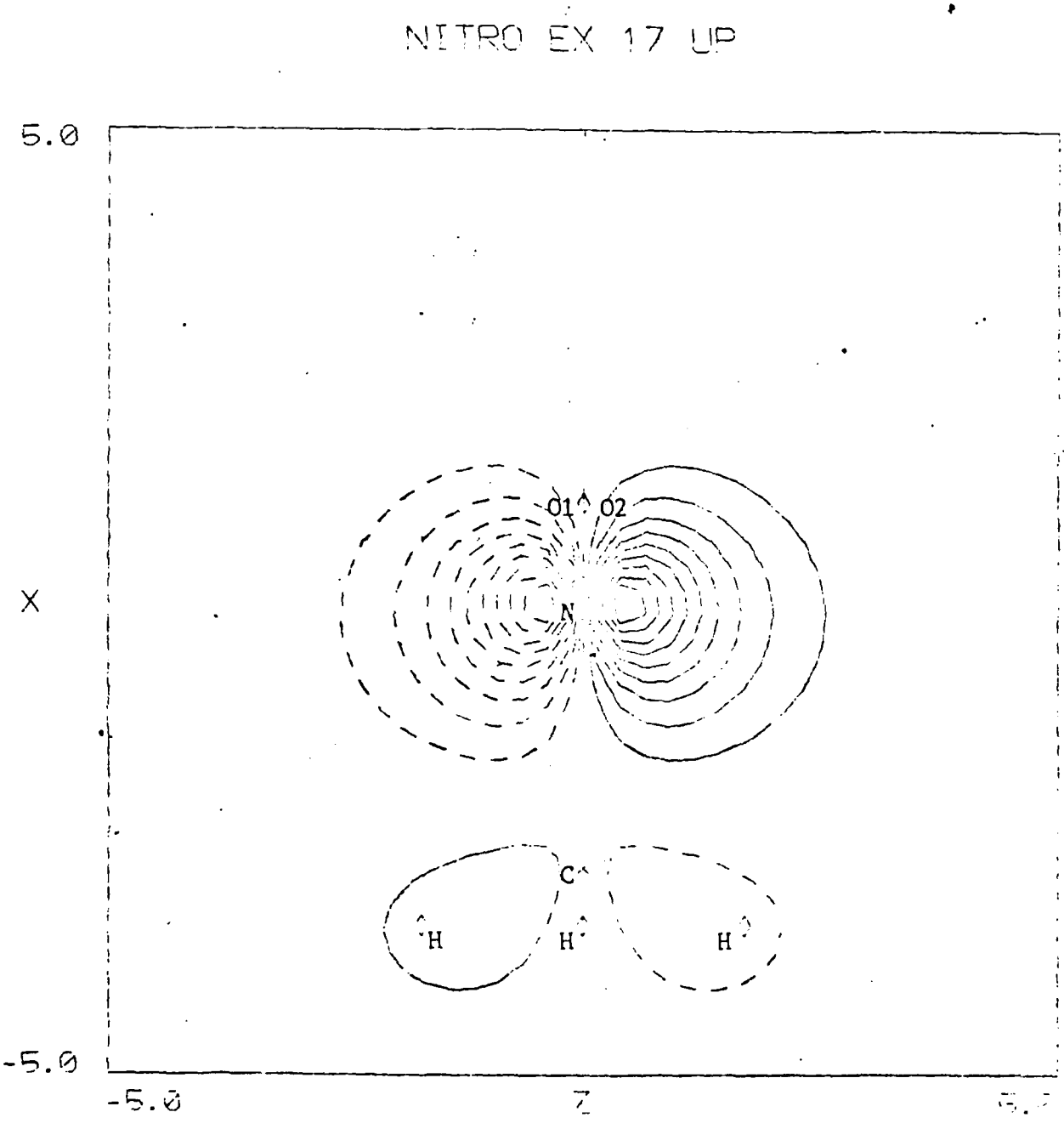

Orbital Plot 17

Y-Z Plane

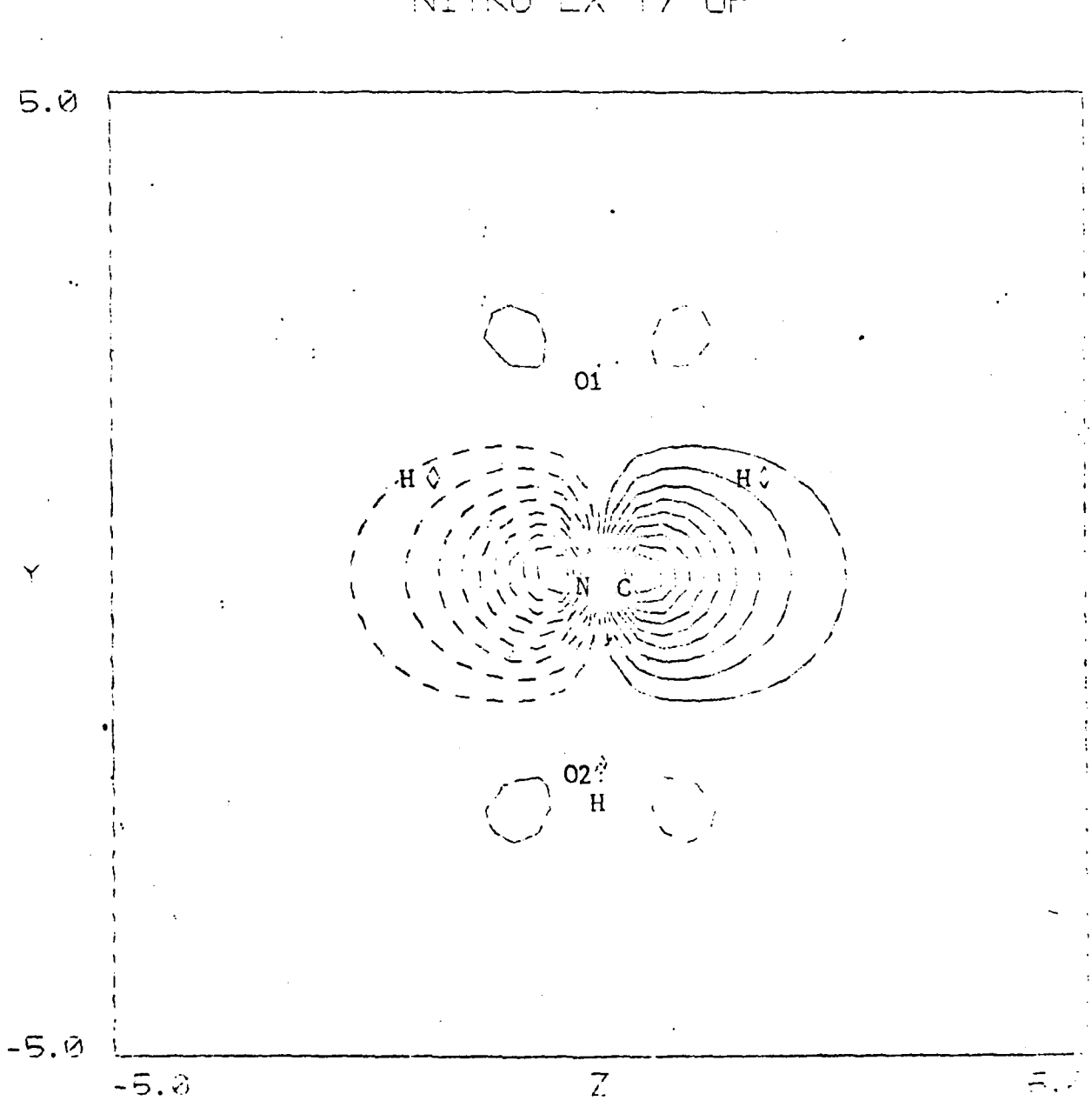

Orbital Plot 18

O1-O2 Plane

NITRO EX 17 UP

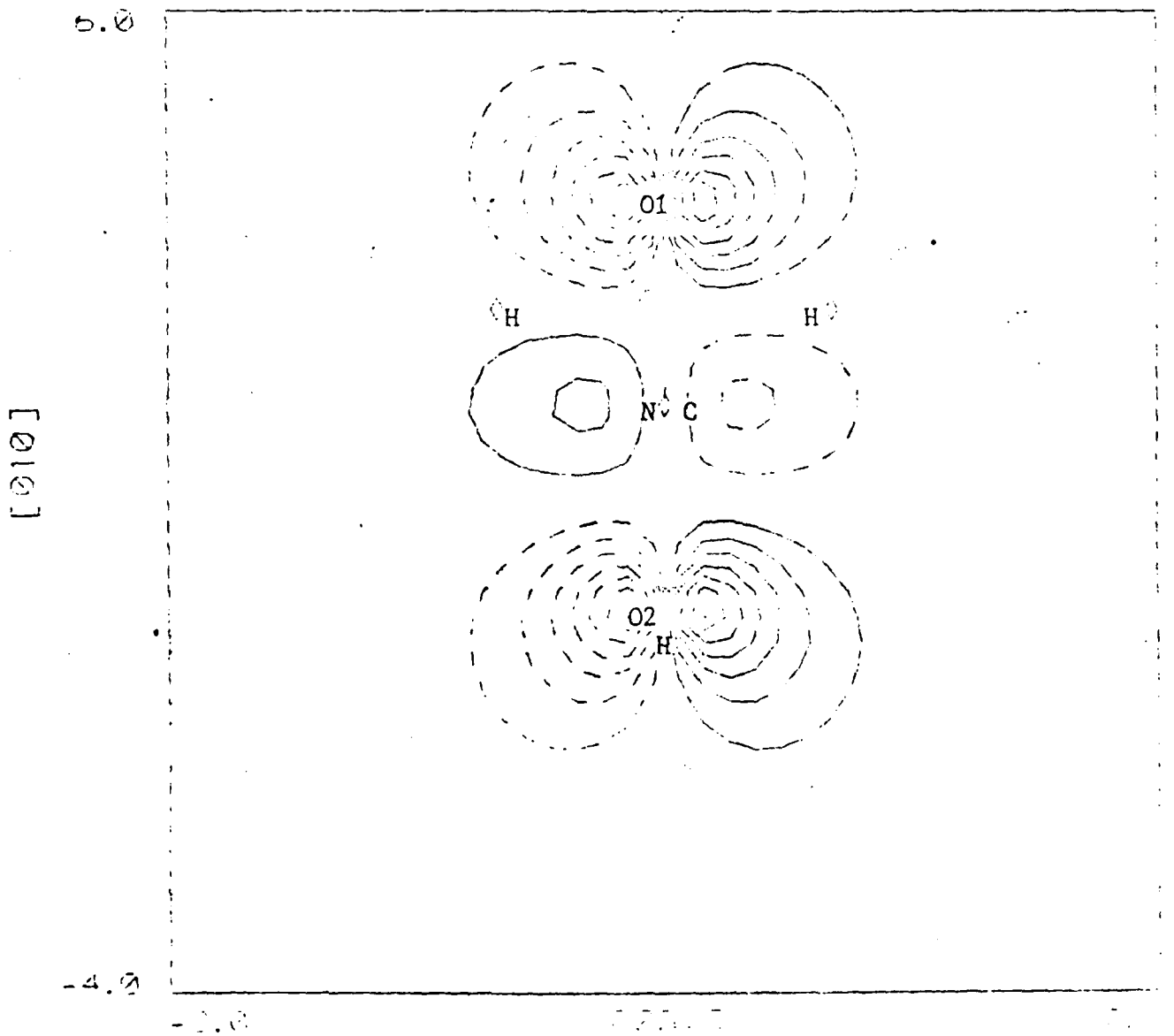

Plots For the Singlet and Triplet Contributions To the First Excited State of Nitromethane

The first four plots of this section show MO's 15, 16 and 17 for the triplet contribution to the first excited state of nitromethane. These should be compared with the same orbitals of the previous section to see that the excited state referred to there was the triplet state (both sets of orbitals are identical). The following four plots show the same 3 orbitals for the singlet contribution. It should be noted that the singlet contains 2 orbitals which are identical to the triplet except in order. That is, singlet 16 is the same as triplet 15 (b_2 symmetry) and singlet 17 is the same as triplet 16 (a_1 symmetry). Singlet 15 consists of double lobes on only one oxygen and a lobe on the nitrogen whereas the triplet 17 orbital is double lobed on both oxygens as well as the nitrogen (lone-pairs).

Orbital Plot 19

X-Y Plane

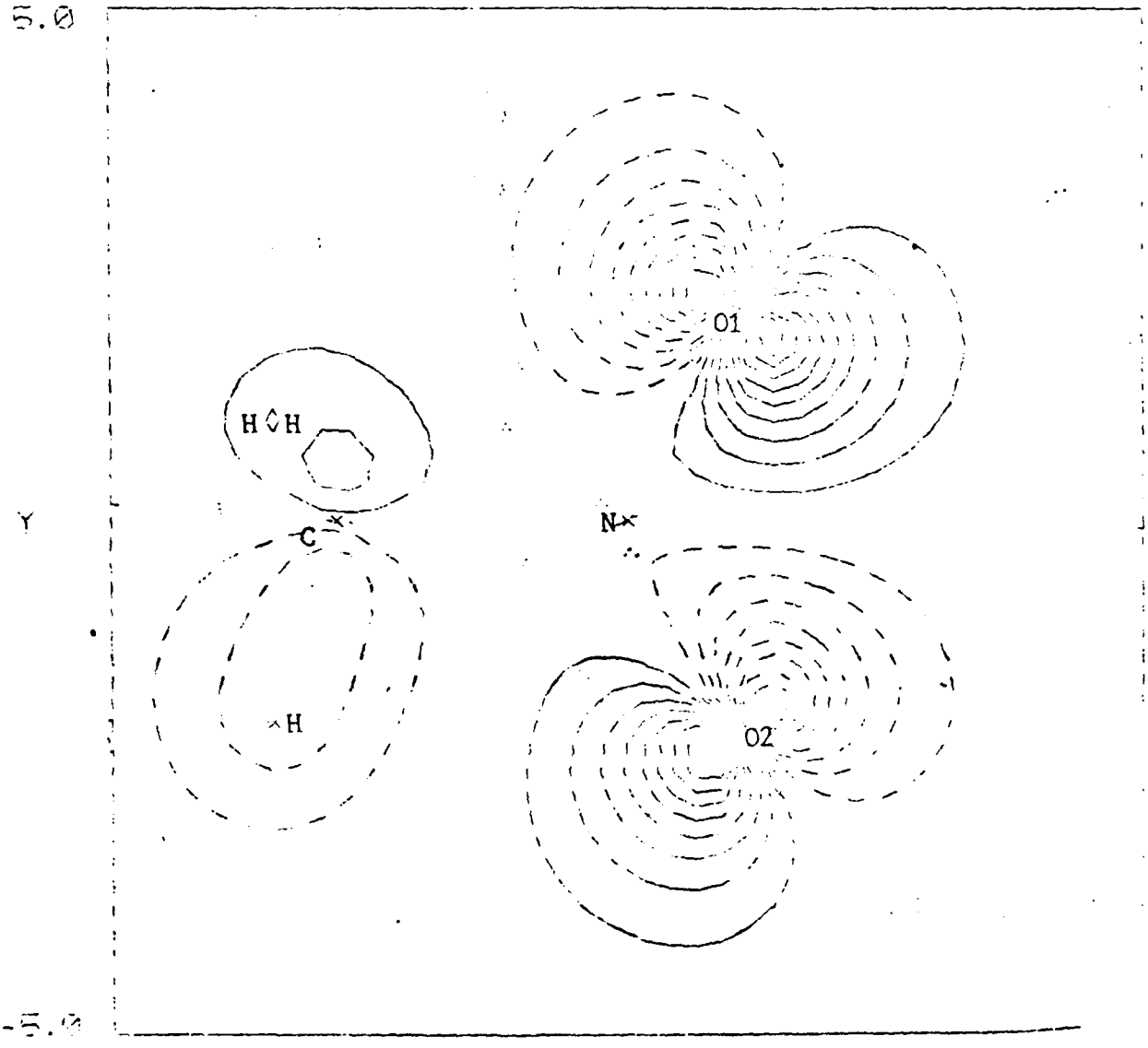

Orbital Plot 20

X-Y Plane

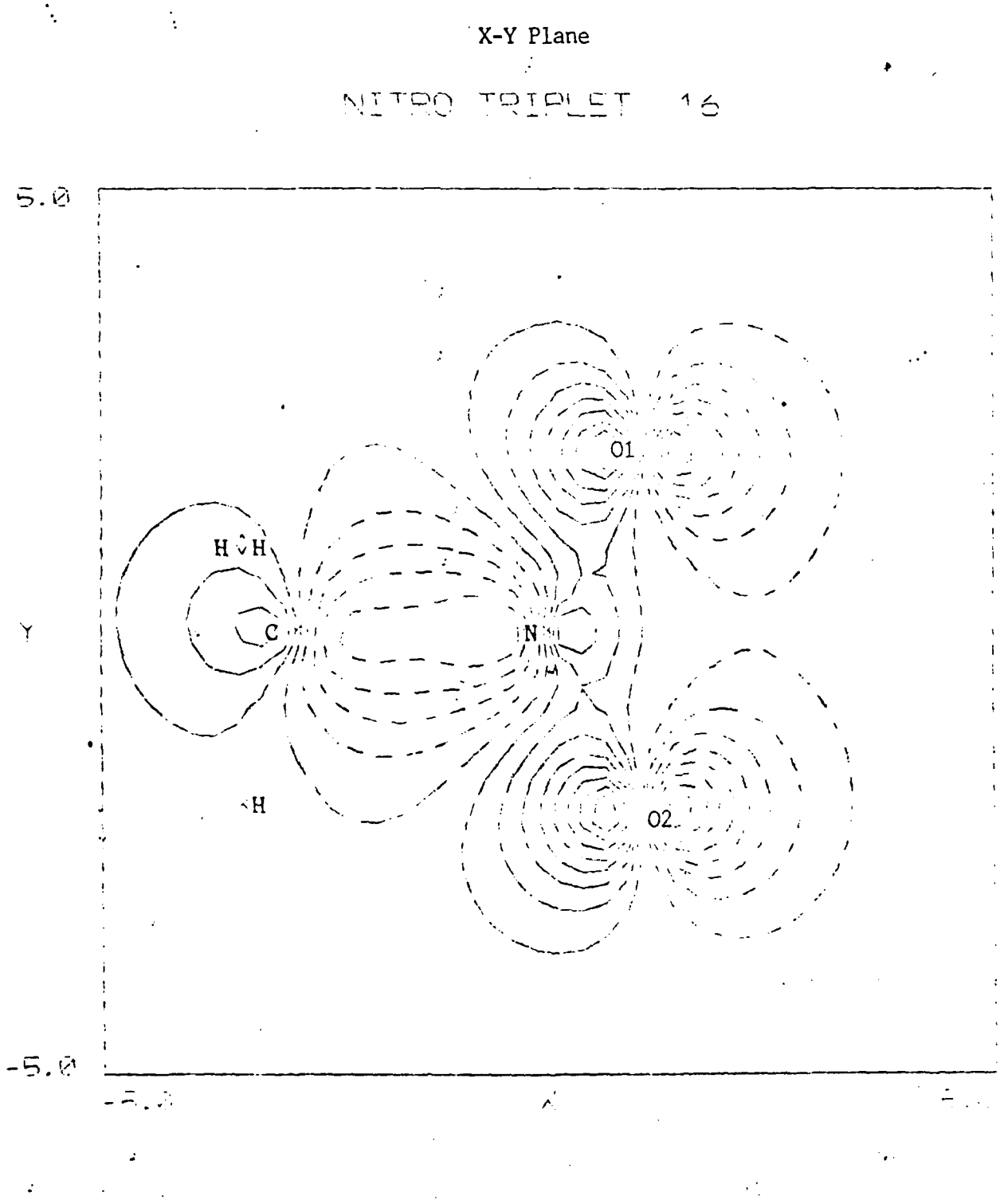

Orbital Plot 21

X-Z Plane

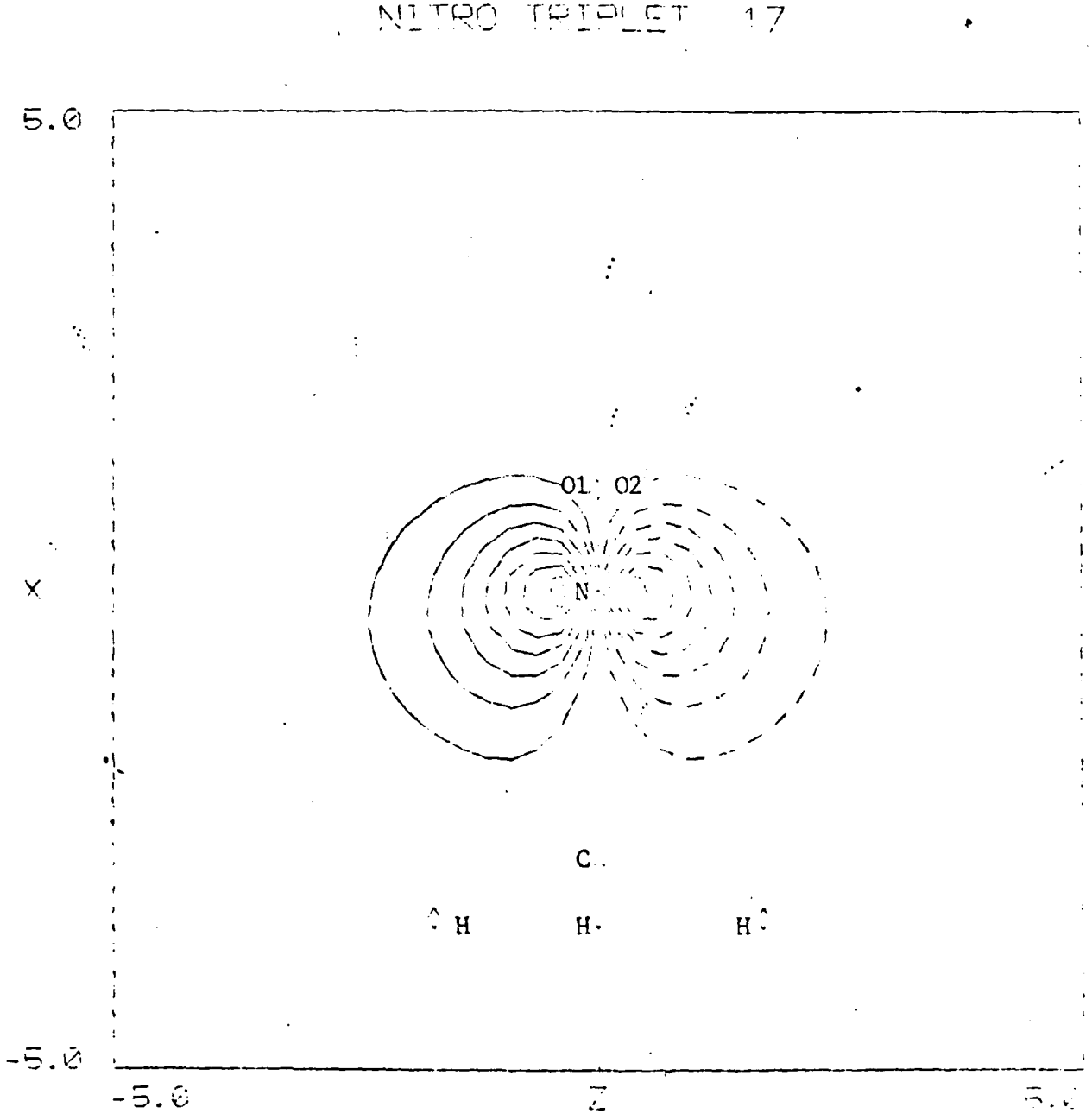

Orbital Plot 22

01-02 Plane

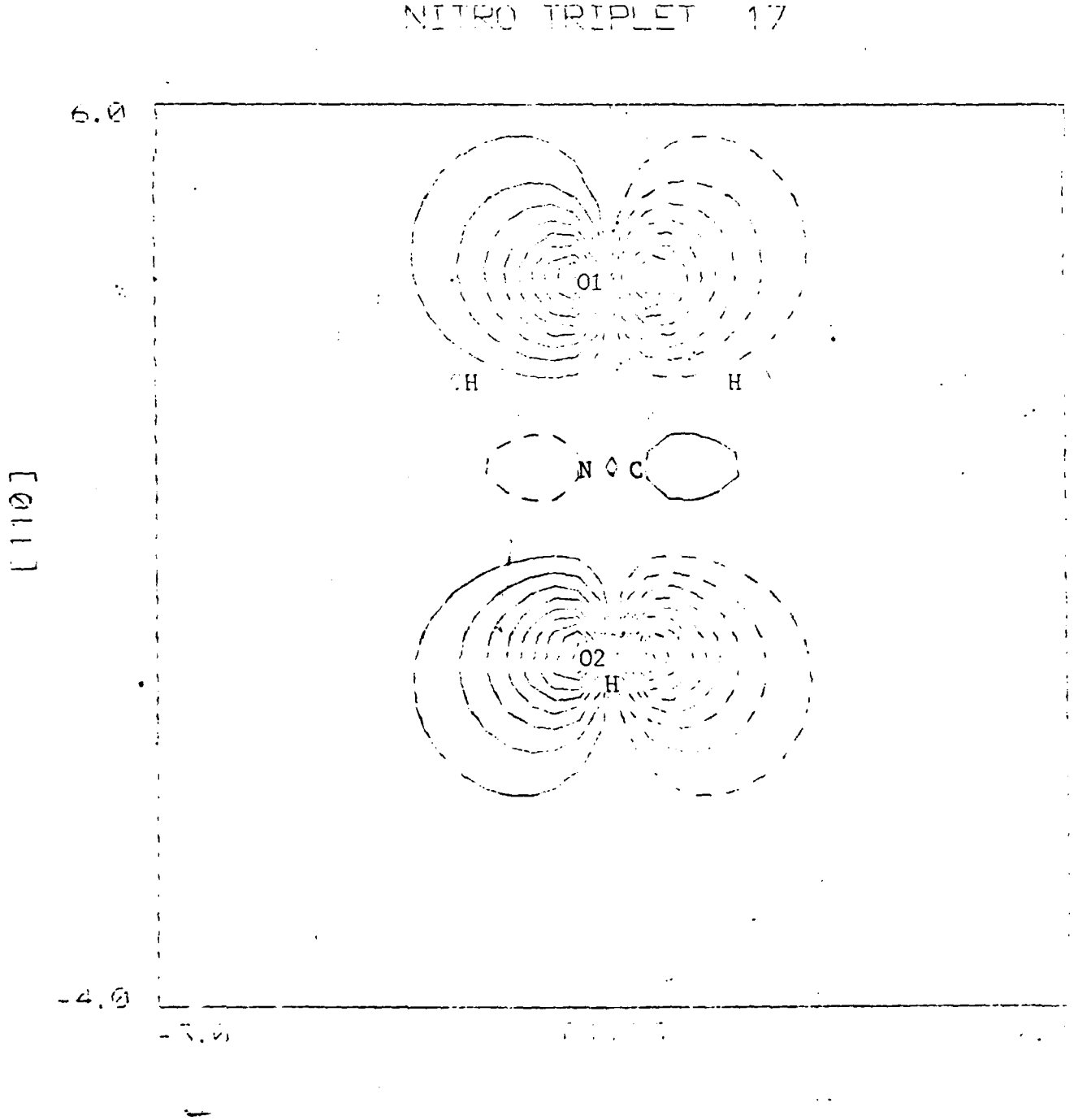

Orbital Plot 23

X-Z Plane

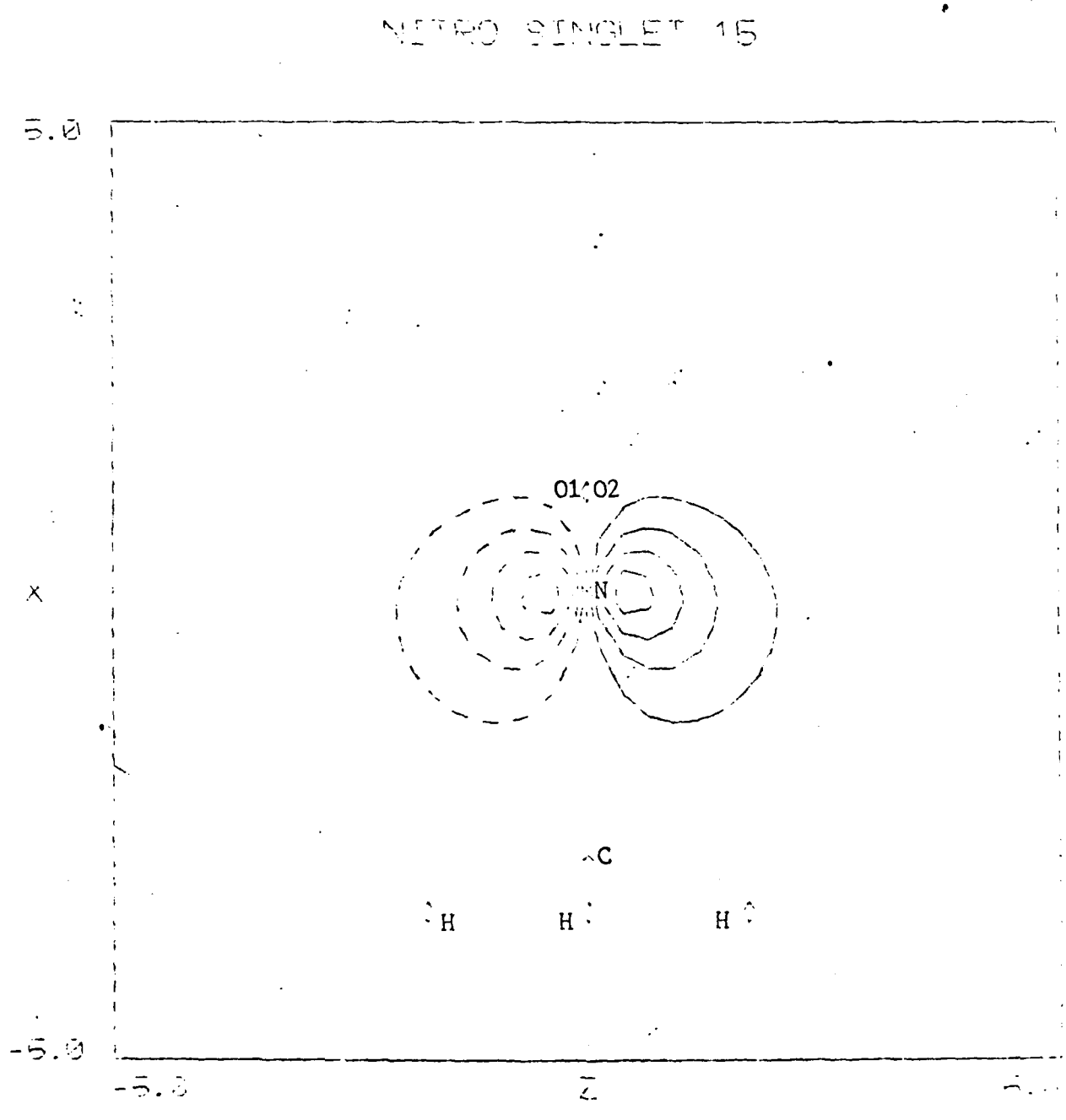

Orbital Plot 24

O1-O2 Plane

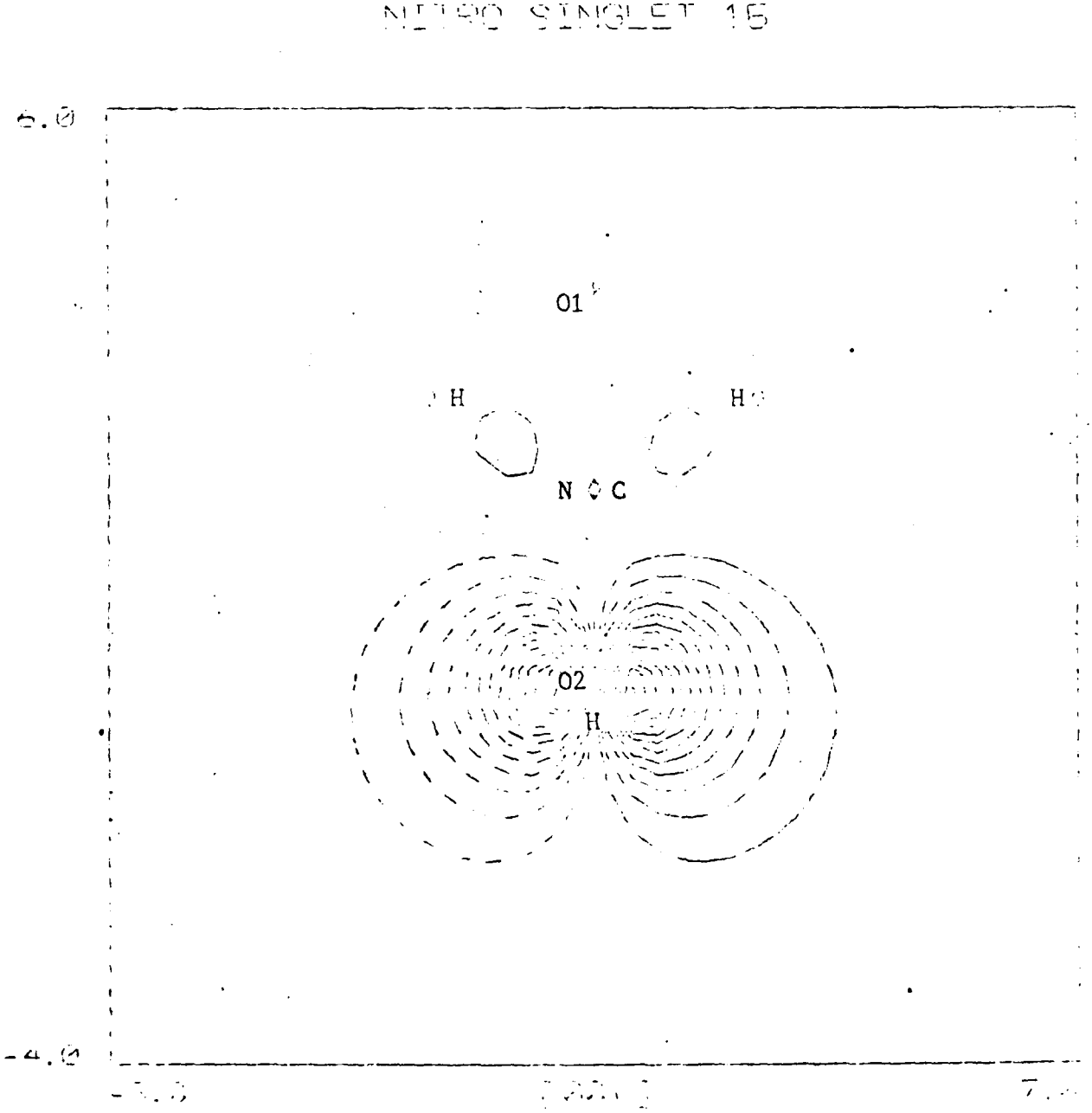

Orbital Plot 25

X-Y Plane

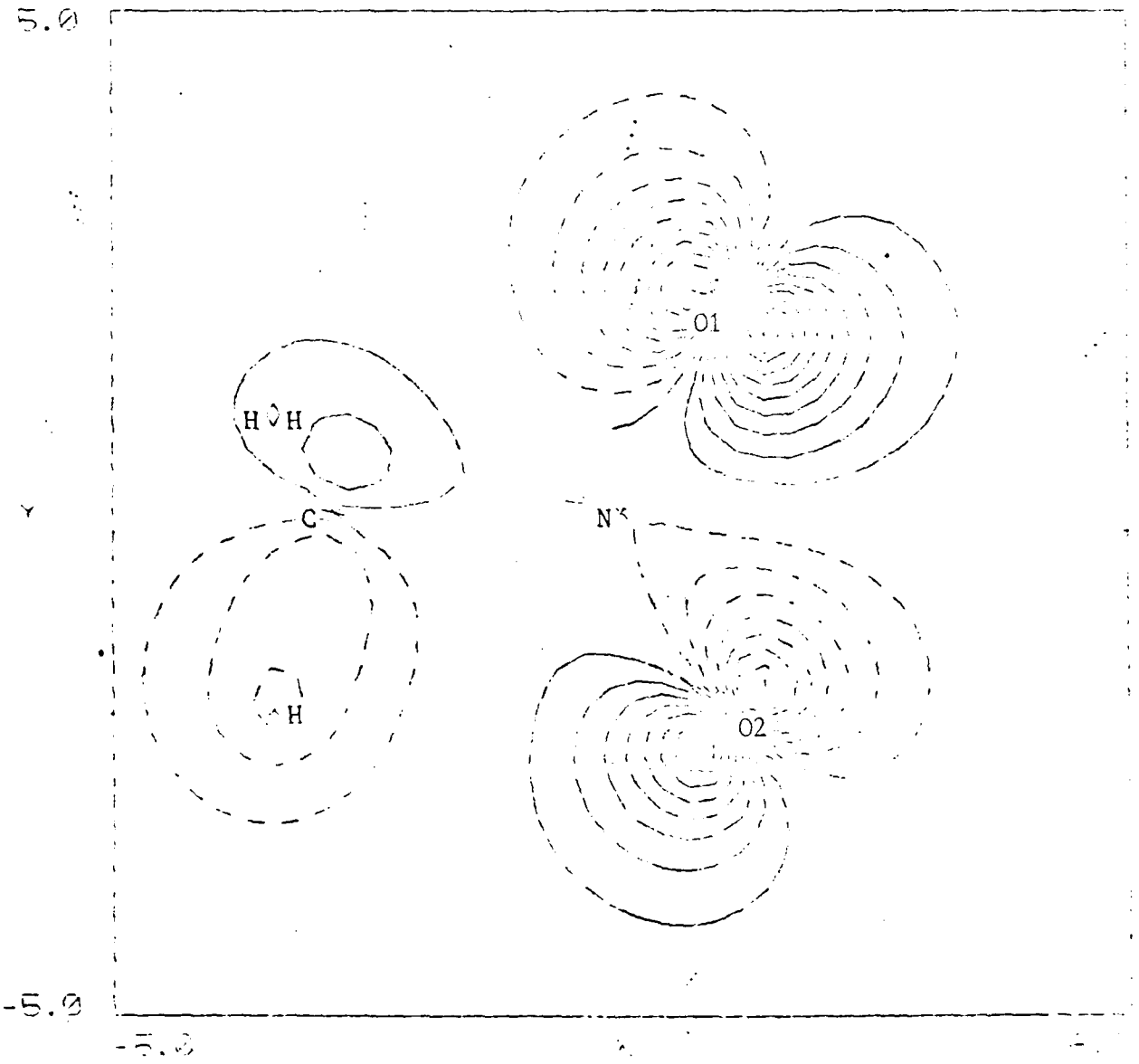

Orbital Plot 26

X-Y Plane

NITRO SINGLET 17

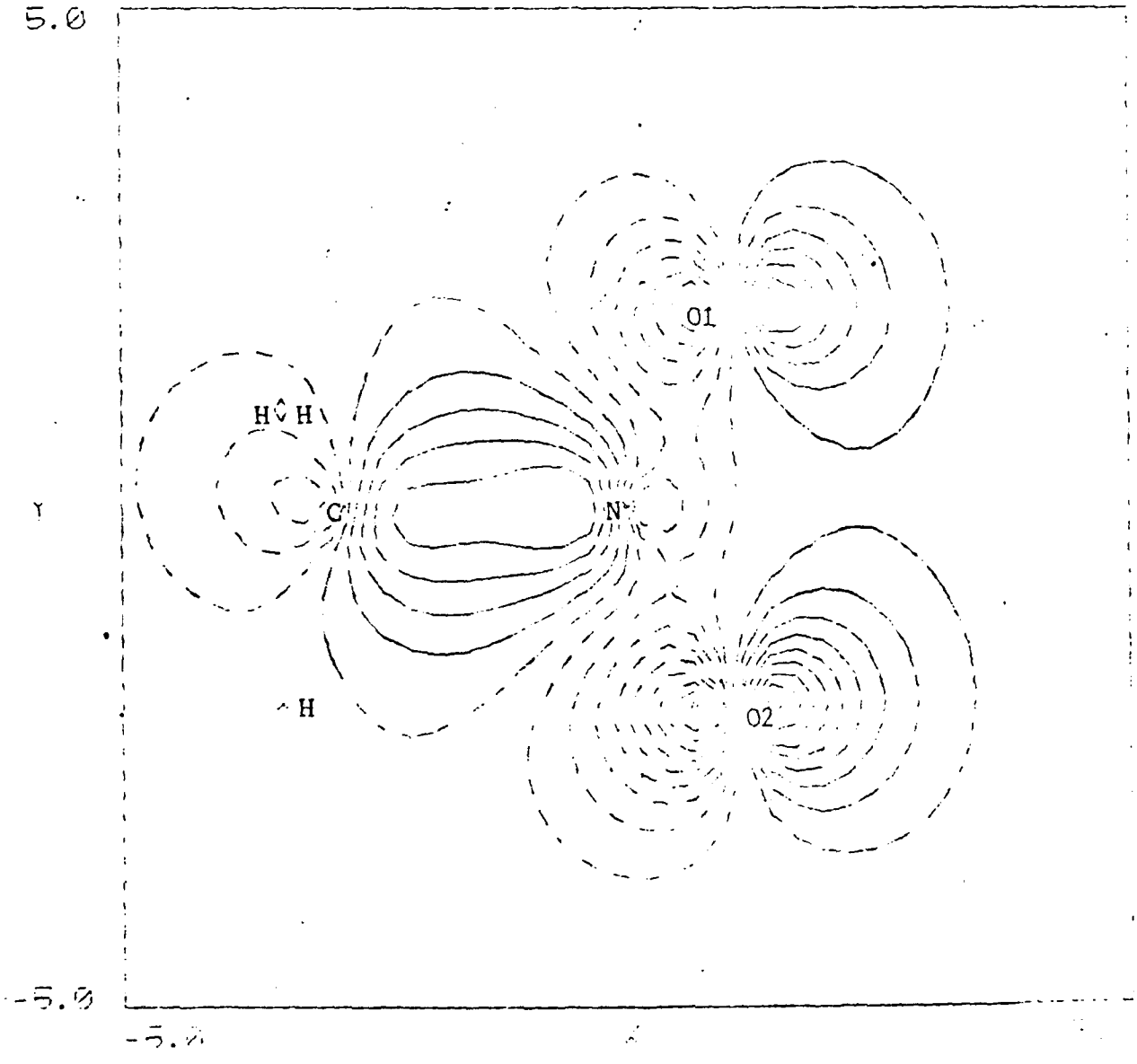

Dipole Moment

The dipole moment of nitromethane was calculated to be 1.45 au (3.696 Debye) using the 57 function set. No effort was made to determine correlation effects on this value. Current work by Beck [21] on methanol (CH_3OH) indicates that correlation effects on the dipole moment for that molecule are small. The experimental value is given by Tannenbaum [61] as 3.46 ± 0.2 D. The calculated result is in good agreement with experiment indicating the charge distribution within the MO's of the 57 function set give a reasonable representation of the nitromethane molecule.

Oscillator Strength

The oscillator strength (f) is a measure of the transition probability between two states. The f value is given by:

$$f_{ab} = 2/3\ (E_b - E_a)^*|\langle a|r|b\rangle|^2 \quad \text{(Ref.24, page 102)} \qquad (4.1)$$

Where E_b and E_a are the energies of the states of interest and the matrix element is referred to as the transition moment.

The calculation of f values is difficult because highly accurate wavefunctions are necessary to get reasonable agreement with experiment. It is even quite difficult to measure f values

experimentally in molecular systems. Part of the problem lies in the fact that the radiation the molecule in the solid actually sees is modified somewhat by the medium through which it travels. Corrections involving the index of refraction and dielectric constants of the bulk material are required in order to interpret results. The medium also has an effect on the molecule of interest (see Fowler, reference 74, for more details).

Another problem in the calculation of f values is a result of the Born-Oppenheimer approximation. The f value is proportional to the transition moment:

$$f \propto \langle \Psi | \Sigma \bar{r} | \Psi' \rangle \qquad (4.2)$$

where Ψ is the total (electron + nucleus) wavefunction for the ground state and Ψ' represents the excited state. The Born-Oppenheimer approximation separates nuclear and electronic motion:

$$\langle \Psi | \Sigma \bar{r} | \Psi' \rangle \rightarrow \langle \Psi_{el} \Psi_{nuc} | \Sigma \bar{r} | \Psi'_{el} \Psi'_{nuc} \rangle . \qquad (4.3)$$

The separation of the wavefunction allows for the approximate calculation of the electronic portion and it is the electronic part of the transition moment,

$$D_{el}(\bar{R}) = \langle \Psi_{el} | \Sigma \bar{r} | \Psi'_{el} \rangle \qquad (4.4)$$

which is calculated. Schaefer [24] shows that this can vary widely with internuclear separation. Therefore, for accurate f values, it is also necessary to calculate vibrational wavefunctions and their effects on D_{el}; i.e.,

$$\langle \Psi_{nuc}(\bar{R}) | D_{el} | \Psi'_{nuc}(\bar{R}) \rangle. \qquad (4.5)$$

Beck and Nicolaides [32] show that the approximation used for the transition moment (D_{el}) can vary from 10% to factors of 10 and that correlated wavefunctions yield much better results. There are also computational problems of non-orthonormality effects between ground state and excited state wavefunctions and the calculation of transition moments. However, these effects have recently been accounted for by D.R. Beck in the codes used to calculate f values.

The transition moment portion of f, where 'a' and 'b' represent the RHF ground state and excited state wavefunctions (Hartree-Fock) discussed previously, was calculated to be 2.8 for nitromethane. The difference in energy between these states at the RHF level was 0.06684 au (1.87 eV). Combining all terms yields the f value of 0.125 for nitromethane. It should be emphasized again that this could be off by a factor of up to 10 (more likely to be around a factor of 2 (Beck [21])).

The interpretation of this value in terms of classifying the strength of the transition is a difficult one. In comparing to

atomic systems, it appears that a value of 0.125 may be considered to represent a moderate transition. For example, measured f values for several transitions in nitrogen range from 0.093 to 0.350 (Ref. 24, page 105) where 0.350 would represent a strong transition. It appears that the transition studied here for nitromethane is not particularly strong and may, in fact, be very weak if errors due to wavefunction inaccuracy and the Born-Oppenheimer approximation are accounted for.

CH_3 and NO_2 Studies

During the course of investigation of the CH_3NO_2 molecule it was of some interest to study the CH_3 and NO_2 fragments individually. In doing so, some investigation into the energy of these two systems occurred as well as the implementation of the counterpoise (CP) method to aid in convergence as well as to be used to compare the two systems with and without pseudopotentials. Also, the C-N bond energy in the ground state was determined. Another hope here was that combining the UHF output of the separate systems into a single UHF input would result in improved spin for the nitromethane molecule.

Binding Energy of the CH_3 and NO_2 Fragments

Two different approaches were employed to investigate the energy associated with the C-N bond (rragmentation into CH_3 and NO_2 groups). First, this energy was calculated for the free molecule and then it was calculated in the presence of a +1 or -1 au charge, situated at the location a neighbor nitrogen or carbon atom would have in the crystal. This step was suggested by A.B Kunz to see what effect ions moving into vacancies in the lattice would have on the strength of this bond. The CP method was used for all calculations. It should be recalled that, in this method, one calculates the energy of a fragment in the presence of the

functions of the other fragment, these functions being situated at the location they would have in the whole molecule, but without associated charges. The analogous calculation is done for the second fragment. The sum of the energies of these two fragments subtracted from the energy of the molecule, gives the energy required to break the bond.

Tables 4.10 and 4.11 summarize these calculations. The first calculations done, using the 81 function set and MBPT, indicated a value of 82.8 Kcal/mole for this bond energy (multiply hy/molecule by 627.07 to get Kcal/mole). Work done by Corey and Firestone [62] show a number of possible ways in which the molecule may fragment. They indicate that irradiation of gaseous or liquid nitromethane with photons of wavelength 253.7 nm results in C-N bond breakage. This is equivalent to absorption of 112.8 Kcal/mole. Their work suggests the molecule first makes a transition to an excited state and then the bond breaks. The value of 82.8 Kcal/mole is not in good agreement with experiment. A better calculation of ground state correlation energy may help to bring the calculated value closer to experiment. Also, rotational and vibrational excitations as well as electronic transitions could be considered.

Results of the effect of the presence of a single charge near the molecule are shown in Table 4.11. The motivation behind this study was the possibility of changing bond strength within the molecule if a nearby lattice site was occupied by a free ion. The C-N bond was of primary interest. Calculations were performed

Table 4.10

CH_3 and NO_2: HF-MBPT CP Results 81 Function

	HF Energy (hy)	MBPT	Total
CH_3	-39.560296	-0.125111	-39.685406
NO_2	-204.016393	-0.488029	-204.504422
CH_3NO_2	-243.723297	-0.598611	-244.321905

ΔE $\{CH_3NO_2 - (CH_3 + NO_2)\}$ = 0.13208 hy/molecule = 82.8 Kcal/mole

Experiment = 112.8 Kcal/mole

Comparison with other work is given in the following section of text.

Table 4.11

Effects of Ion (±1au) on C-N Bond Strength: 57 Fns, Crystal Geom.

Ch	Loc	CH_3NO_2	CH_3(CP)	NO_2(CP)	Bond Energy ,hy
0		-243.6974	-39.5491	-204.0538	-0.0946 (-2.57eV)
-1	-11103N	-243.7100	-39.5491	-204.0603+ch	-0.1007 (-2.74eV)
+1	-11103N	-243.6910	-39.5491	-204.0493+ch	-0.0927 (-2.52eV)
-1	-11103C	-243.7036	-39.5504+ch	-204.0538	-0.0994 (-2.71eV)
+1	-11103C	-243.6933	-39.5495+ch	-204.0538	-0.0901 (-2.45eV)
-1	⊥ C-N	-243.7048	-39.5491	-204.0538	-0.1020 (-2.77eV)
+1	⊥ C-N	-243.6933	-39.5491	-204.0538	-0.0905 (-2.46eV)

Ch=charge(au), loc=location of the charge (see Appendix A for notation), CP=counterpoise, +ch=energy calculated as charge stayed with fragment, ⊥=perpendicular to the C-N bond length midpoint of the main molecule, about 8 au towards -11103.

Coordinates: -11103N=(-1.7028,-0.0854,7.4013)au (x,y,z)
-11103C=(-2.5127,-1.6703,9.6919)au
⊥ =(-1.3990,-0.8750,8.5450)au

Note: The main molecule's nitrogen is located at (0,0,0)

using a single molecule in its crystal geometry and a ±1 au charge located at a position in the lattice where a nitrogen or carbon would exist in a nearby molecule. In particular, the main molecule used was (000 01) and the charge was placed at the nitrogen or carbon position in molecule (-111 03). See Appendix A for an explanation of this notation. The charge was also placed at a position perpendicular to the C-N bond of (000 01) at a distance and in the direction of (-111 03). The bond energy was defined to be the difference between the energy of the molecule and the sum of the counterpoised fragments. The additional charge was assumed to be a part of a fragment (either CH_3 or NO_2) for counterpoised runs except in the perpendicular case where the charge was assumed to separate independently of the other fragments. The bond energy was determined to be 2.57 eV for the free molecule (no correlation). A rather large strengthening occurred by placing the -1 charge at (-111 03)N, (-111 03)C and at the perpendicular location (increases of about 0.2 eV). The +1 charge had a tendency to weaken the bond, especially if located at (-111 03)C or at the perpendicular position (by about 0.2 eV). It should be noted that the distance from the charge locations to the center of the nitromethane molecule was about 8 au. The effects of charge rearrangement on the central molecule due to the presence of a single charge are rather pronounced when considering the distance involved.

These calculations indicate that free ions within the crystal lattice may have a substantial effect on the C-N bond strength of nitromethane.

CH_3 and NO_2

The energy of the CH_3 group at the UHF and MBPT level was -39.560296 hy which is in good agreement with Pople's [63] exact value of -39.57268 hy. No effort was made in this work to improve upon this value. The spin for this fragment was 0.5, a correct value for the one unpaired electron in the system.

A bit more work was done on the $^2A_1$ ground state of NO_2. Handy [64] and co-workers, using a (4s,2p,1d) set and the configuration interaction method (CI) found an energy of -204.42460 (-204.06816 SCF) where they froze the 5 lowest MO's. A 56 fuhction set (4s,2p,1d) was developed in this work, also freezing the 5 lowest MO's and using 2nd order MBPT. A total energy of -204.47778 (-204.083902 SCF) was calculated, about 0.0532 Hy (1.45 eV) below Handy. The spin was 0.5, correct for the single unpaired electron in this system. The geometry used was that given by Bird [65] et.al.

It is interesting to note that upon combining counterpoised CH_3 and NO_2 outputs, both of which yield correct spin, the spin at the UHF level for the entire molecule is still incorrect. This

indicates that it may not be possible to get a correct spin for this system without using more than one configuration. Kleier and Lipton [1] make reference to this problem in obtaining a ground state singlet using GVB descriptions where they claim these states cannot be described at the RHF level. No mention is made of problems at the UHF level.

Comparison of Pseudopotential to All Electron Fragments

Since pseudopotentials were to be used in place of core electrons on neighbor molecules in the calculations involving larger groups of molecules, it was useful to develop a basis for the molecule which would be small, use pseudopotentials and still maintain some semblance of the orbital characteristics obtained from the 81 function set. It was practical and convenient to work on the individual fragments (CH_3 and NO_2) since good spin could be obtained at the UHF level for both. Eventually, a 35 function set plus pseudopotentials was developed for the neighbors. A (2s,2p) set for each of C,N, O1 and O2 (8 functions on each) and a (1s) set for each hydrogen was chosen. Some experimentation had been done with even smaller sets but it was clear they were not adequate to properly describe the molecule. Of the 35 functions, 11 were on the CH_3 group and 24 on the NO_2 group.

Table 4.12 shows, for a given set of exponents, the orbital

energies and major contributors for those MOs which exist in both the CH_3 81 function, CP set and the CH_3 11 function set. Of course the total energy of the CP group is much lower since there are more functions and the core electrons are removed from the small set. There is about a 0.1 eV difference in orbital eigenvalues between the CP and all electron cases for CH_3 (This is also true for the NO_2 fragment). The CP values are forced lower in value. Ideally, one would hope the pseudopotentials which replace the core electrons would have minimal effect on both the character and eigenvalues of the outer orbitals. This could indicate a need for work to be done on pseudopotentials which more correctly describe the inner orbitals of molecules. However, the table shows reasonable agreement in characteristics between the two (also in orbital energy). The spin for both cases was 0.5. The 1↑ MO for the 11 function set corresponds to the 2↑ MO for the 81 function set since core orbitals (1↑ and 1↓) are removed from the smaller set. Table 4.13 shows the same information for the NO_2 spin up space fragment. Here, the 4↑ orbital for the large set corresponds to the 1↑ orbital in the small set. The CH_3 data compares quite nicely. The NO_2 data shows some ordering problems, especially in the 5 middle orbitals (3↑ through 7↑). There are also some discrepancies in the character of at least 2 of these. Note that 3, 4 and 7 for the small set are very similar to 10, 9 and 8 respectively of the larger set. Orbitals 5 and 6 for the small set have no clear counterpart in the large set. The spin in

both cases is correct and the Mulliken populations are very reasonable. These discrepancies are probably due to the minimal basis set used. NO_2 is an active fragment which is probably difficult to describe using a small number of functions. Nevertheless, since the outer orbitals looked reasonable and the expense of including more functions on the NO_2 group would be prohibitive, computationally, the small set was deemed acceptable. Upon combining the two fragments basis sets with pseudopotentials, exponent variation resulted in a UHF output which, in orbital character, compared favorably with the 61 function output for nitromethane. In particular, the orbitals which were purely z-type were ordered identically to the corresponding z orbitals in the output of the large set.

Table 4.12

Orbital Comparison: CH_3 (CP) vs CH_3 (11)

MO(CP)	MO(11)	Char.(CP)	Energy (hy)	Char.(11)	Energy (hy)
2 ↑	1 ↑	Cs+Cx	-0.945	Cs+Cx	-0.837
3 ↑	2 ↑	Cy	-0.579	Cz	-0.668
4 ↑	3 ↑	Cz	-0.579	Cy	-0.668
5 ↑	4 ↑	Cx	-0.387	Cs+Cx	-0.494
2 ↓	1 ↓	Cs+Cx	-0.855	Cs+Cx	-0.798
3 ↓	2 ↓	Cy	-0.565	Cy	-0.654
4 ↓	3 ↓	Cz	-0.565	Cz	-0.654
Total Energy			-39.56		-6.44
Spin			0.5		0.5

CP=counterpoised 81 function set.
11=11 function set plus pseudopotentials (core electrons removed)

Mulpops	CP	11
C	6.3	5.3
H1	0.82	0.58
H2	0.82	0.58
H3	0.82	0.58
BCH1	0.08	
BCH2	0.08	
BCH3	0.08	
Total	9.0	7.0

11 function set has no bond functions.

Table 4.13

. Orbital Comparison: NO_2 (CP) vs NO_2 (24) (Spin up only)

MO(CP)	MO(24)	Char.(CP)	Energy (hy)	Char.(24)	Energy (hy)
4↑	1↑	Os,Oy,Ns	-1.681	Os,Oy,Ns	-1.726
5↑	2↑	Os,Ny	-1.499	Os,Ny	-1.571
6↑	3↑	Os,Ns	-0.970	Ox,Nx	-1.130
7↑	4↑	Ny	-0.835	Oz,Nz	-1.083
8↑	5↑	Os,Ox,Ny	-0.802	Ox,Oy	-0.887
9↑	6↑	Oz,Nz	-0.766	Os,Ox,Oy	-0.837
1↑	7↑	Ox	-0.596	Os,Oy,Ny	-0.836
1↑	8↑	Oz	-0.528	Oz	-0.808
12↑	9↑	Ox,Nx	-0.503	Ox,Ns,Nx	-0.759
Total Energy			-204.083902		-36.619178
Spin			0.51		0.51

Mulpops	CP	24
N	6.35	4.64
O1	8.15	6.18
O2	8.15	6.18
BNO1	0.17	
BNO2	0.17	
Total Charge	22.99	17.0

NO_2 has 23 electron (6 core electrons).

Chapter 5

Nitromethane Dimer Calculations

This section discusses ab initio calculations performed on dimers of nitromethane oriented in the relative positions they would have in the crystal configuration. Crystallographic work on solid nitromethane was done primarily by Trevino [66] and associates. Appendix A describes the general method used to transform crystallographic coordinates into the coordinates of the molecules in the crystal. The geometry of a single molecule within the crystal differs slightly from that of the free molecule. The primary reason for working on dimers initially was to:

a) show that convergence could be obtained for the dimer system. There is no reported work at all on interactions of more than one nitromethane molecule.

b) develop a basis set that would be manageable and adaptable for larger groups of molecules.

c) observe the excited state determined in the gas phase calculation to see what effect (if any) the presence of one near neighbor might have.

Since the intermolecular system is assumed to be weakly interacting (see Trevino [67] and Pastine [68]), the presence of the near neighbor is not expected to have much effect on the exciton

of the other molecule in the dimer.

The study of dimers followed a path which would lead up to the study of larger groups of molecules. A minimal cluster of nitromethane molecules would contain a central molecule surrounded by 8 near neighbors (see Figure 5.1 and Appendix A for the geometry involved). One can view this cluster as being comprised of essentially 8 dimers, the central molecule plus each neighbor. It was desirable to use a basis set for the dimer which, when applied to the larger groups would still be reasonably manageable. An 81 function set on each molecule would certainly not be feasible from the computational point of view. Therefore it was decided to use the 57 function basis set for the central site. This set yields a good description of the molecule as shown previously in this thesis. A reduction of this set to 35 functions was done and applied to the neighbors (see the preceding section). This set evolved after considering many different basis set contractions. Also, in all calculations involving dimers or larger groups of molecules, the core electrons on the neighbors were removed and replaced with pseudopotentials developed by Topiol [69] (See Appendix C for basis sets and pseudopotential parameters used in these calculations). Christopher Woodward's [70] extensive tests indicate that the use of pseudopotentials in place of core electrons give excellent agreement with experiment when investigating excited states in metallic clusters. The use of pseudopotentials reduces the number of basis functions required in

the system since core electrons no longer exist. The argument here is that only valence electrons are important in determining the chemical characteristics of the system as core electrons are bound too tightly to the nucleus. Pseudopotentials represent the effects of core electrons on outer shells of electrons.

A brief summary of the dimer basis set follows.

1) 57 function set applied to what would be the central molecule in a cluster (designated CEN). The 57 functions consist of (3s),[7,2,1] and (2p),[4,1] on each of O1, O2, N and C, (2s),[4,1] on each hydrogen, and one s and one p bond function on each of the bonds N-O1, N-O2, N-C and finally, one s function on each C-H bond. (a total of 57 functions and 127 Gaussian primitives.

2) 35 function set applied to any molecule which would be a near neighbor in the cluster, designated NEI1 through NEI8. This set consists of a (2s),[1,1] and (2p),[1,1] on each of O1, O2, N and C and (1s),[1] on each hydrogen, with no bond functions for a total of 35 functions and 35 Gaussian primitives. The central molecule and any near neighbor would constitute a dimer (e.g., CEN-NEI1= dimer 1 = D1, etc.)

3) Any neighbor in a dimer (or larger group) will also have pseudopotentials to replace the core electrons. Since

a single nitromethane molecule has 32 electrons, an all-electron dimer would have 64 electrons. Removing the two 1s electrons from O1, O2, N and C (8 electrons all together) reduces the total number to 56 electrons in a dimer (32 on CEN and 24 on any NEI).

Figure 5.1 is a schematic diagram of the nitromethane cluster, the geometry being derived from Trevino's [66] work (Appendix A). The central molecule (CEN) is shown surrounded by 8 near neighbors. There is essentially no symmetry in this cluster to aid in reducing the number of integrals required by the UHF method. Based on the basis sets mentioned above, each dimer has 92 functions (57+35) and 162 primitive Gaussians (127+35). This results in a total number of two electron integrals equal to 8822323. Initially, a very limited amount of symmetry was invoked for CEN, a coordinate transformation placing the x-axis along the C-N bond and the NO_2 group in the x-y plane (same orientation as the free molecule--see Figure 4.1). This reduced the total number of unique integrals to 8317090, not a great reduction. Much later it was realized that the oxygens don't see quite the same electrostatic potential and the potential energy integrals involving them were slightly incorrect. It may be useful to invoke a symmetry test in the POLYATOM integrals code at the potential energy stage (VINTS) to catch this problem.

A major gain was made, however, in the realization that a

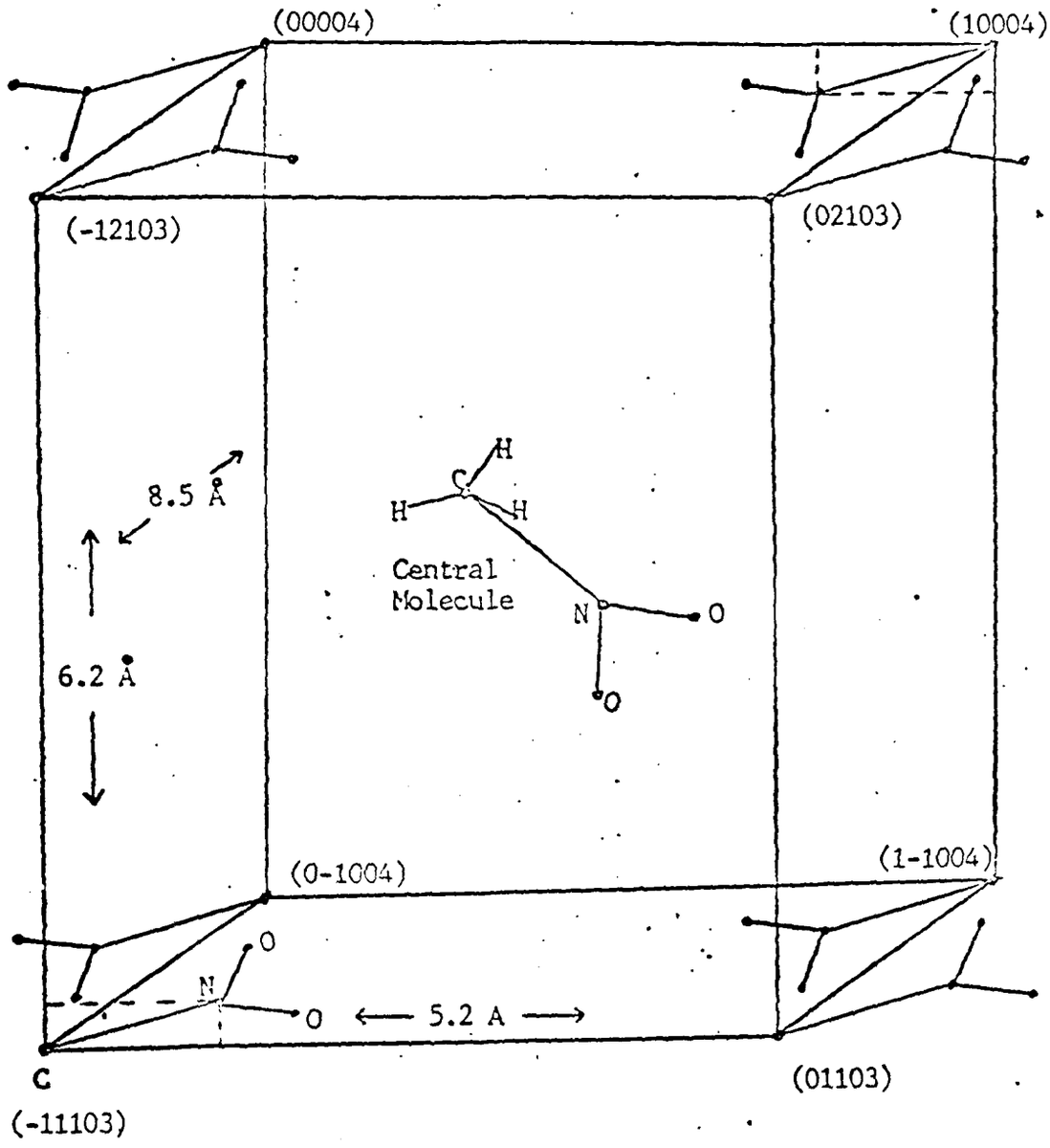

Figure 5.1

Schematic diagram of the Nitromethane Cluster. The bond lengths are not to scale. The front 4 molecules are oriented with the C-N bond in the front plane (The back 4 have this bond in the back plane). The central molecule has a unique orientation with respect to the other 8 shown here. The distance from the corner to the center of the parallelepiped is about 5.9 Å. The C-N bond length is about 1.5 Å. Neighbor hydrogens not shown for simplicity.

great deal of the two electron (2e) integrals were extremely small ($<10^{-6}$ in absolute value). A tolerance of 10^{-6} in absolute value was placed on the two electron integrals. This resulted in a reduction for D1 from 8822323 integrals to 2453781. This value varies with the dimer referred to since none of the 8 dimers are geometrically equivalent. The FPS164/MAX takes approximately 6 hours to calculate the 8.8 million 2e integrals. This reduces to about 1.7 hours when they are scrubbed at 10^{-6}. Using counterpoised input data from the 57 and 35 function sets, relatively rapid convergence occurred for D1. In 37 iterations the energy converged to -290.562604 Hy for the unscrubbed case. Again, there was a problem with the spin as a value of S=0.43 wascalculated for an S=0 system. The Mulliken populations were very reasonable (see Table 5.1). The scrubbed integrals yield convergence in 37 iterations to a value of -290.562599 and spin of 0.43 with reasonable Mulpops. The unscrubbed case showed an iteration time at the UHF stage of 13 minutes/iteration while the scrubbed case took only 3.8 minutes/iteration. Neither case was correlated due to the excessive computation time that would be required to do so. It should be noted that the same calculation performed on the VAX would take approximately 5 to 6 times longer. As noted above, since each dimer was geometrically different, the scrubbed integrals savings varied, as shown in Table 5.2 (the total number of unscrubbed integrals is the same for each dimer). Convergence criteria was based on an energy difference of 10^{-6}.

Table 5.1

Mulliken Populations for Dimer 1 and Dimer 8

Compared to the Monomer

Center	D1(unscrub)	D1(scrub)	D8(scrub)	Monomer
N (CEN)	6.3482	6.3487	6.3365	6.3675
O1 "	8.0965	8.0962	8.1022	8.0876
O2 "	8.0965	8.0962	8.1056	8.0876
C "	5.9775	5.9774	6.0061	5.9794
H1 "	0.8093	0.8093	0.7904	0.7945
H2 "	0.8285	0.8287	0.8139	0.7906
H3 "	0.8043	0.8043	0.8006	0.7945
BNO1 "	0.3150	0.3151	0.3154	0.3147
BNO2 "	0.3149	0.3150	0.3153	0.3147
BNC "	0.0770	0.0770	0.0771	0.0761
BCH1 "	0.1305	0.1305	0.1309	0.1309
BCH2 "	0.1302	0.1302	0.1310	0.1311
BCH3 "	0.1306	0.1306	0.1306	0.1309
N (NEI)	4.6254	4.6254	4.6214	
O1 "	6.2519	6.2519	6.2518	
O2 "	6.2455	6.2455	6.2658	
C "	5.3498	5.3498	5.3649	
H1 "	0.4926	0.4926	0.4933	
H2 "	0.4859	0.4859	0.4933	
H3 "	0.4899	0.4899	0.4603	

Table 5.2

Two Electron Integral Savings Due to 10^{-6} Scrubbing

Dimer	Total Integrals	Total Saved	Total Unique*
1	8822323	2453781	1999469
2	"	2483156	2028844
3	"	2122725	1668423
4	"	2179175	1724863
5	"	2217949	1763637
6	"	2164527	1710215
7	"	2392283	1937971
8	"	2406099	1951787
Totals	**70578584**	**18419705**	**14785209**

* Unique integrals apply only when symmetry operations are allowed on CEN. As noted in the text, these operations introduce slight errors in the potential energy integrals involving the oxygen functions.

There is nearly a 4-fold savings in total integrals when scrubbing is implemented.

Table 5.1 shows there is little difference between the monomer and D1's CEN Mulpops, indicating little charge rearrangement upon dimerization in this geometry and therefore a relatively weakly interacting system. Dimer 8 Mulpops are also shown in Table 5.1. The oxygen and carbon atoms have made slight gains in charge at the expense of nitrogen and hydrogens. This is due to the difference in orientation of the two molecules in the two different dimers.

Table 5.3 is a summary of the dimer characteristics. There are 28 spin up and 28 spin down electrons, 8 removed by pseudopotentials. The molecular orbitals showed minor CEN-NEI interactions. They separated into primarily CEN or NEI centered MOs. Of course, there was adequate contribution within any orbital from both molecules to indicate they were weakly interacting. Table 5.3 also shows the energy and character of the top 5 orbitals of the dimer. The z-type orbitals remain with the central molecule but not with the neighbor since the coordinate system was oriented to favor the central site in this respect. The relatively small error induced by the use of symmetry on the central site did not warrant recalculation of this systems energy. The largest error in any VINTS integral was 1.63 eV. While this may seem like a large number, it must be remembered that the symmetry problem involved only the oxygen atomic orbitals and of

Table 5.3

Results for Dimer 1 Ground State

Molecules (000 01) and (-111 03)

92 Functions, 56 Electrons and Pseudopotentials

	Unscrubbed Integrals	Scrubbed Integrals
Total integrals	8822323	2453781
Energy (hy)	-290.562404	-290.562599
Convergence	0.65×10^{-6}	0.66×10^{-6}
Iterations	37	37
Minutes/Iter.	13.8	3.8
Integrals Calc time	6 hours	1.8 hours
Spin	0.33	0.33

Top 5 Orbitals

ORB	Char.	Energy	Char	Energy
24	CEN Ox,Oy,Nx,Cx	-0.463247	CEN Ox,Oy,Nx,Cx	-0.463264
25	CEN Z-type	-0.434348	CEN Z-type	-0.434359
26	NEI Ox,Oy,Oz,N, Cz,CEN H2s	-0.399734	NEI Ox,Oy,Oz,Nz, Cz,CEN H2s	-0.399749
27	NEI Ox,Oy,Oz,Cz	-0.396385	NEI Ox,Oy,Oz,Cz	-0.396391
28	NEI Ox,Oy,Oz	-0.370486	NEI Ox,Oy,Oz	-0.370494

these, errors this large occurred in very few. Also, due to the means in which these ao's are combined at the UHF stage to create the Hamiltonian matrix elements, these errors are not expected to contribute to a significant error in the final result.

Table 5.2 shows the approximation of scrubbing the integrals at 10^{-6} tolerance is an excellent one. It also shows the distinct separation of neighbor orbitals from central ones and also the large number of nearly degenerate orbitals. In this orientation the most weakly bound MO is primarily centered on the neighbor. Note, the system was not geometry optimized since the primary goal here is to work within the crystal geometry.

Each of the other dimers in the cluster were also briefly studied. D8 was also brought to full convergence with its scrubbed integrals. Its energy was -290.565751, spin=0.42. The orbital ordering was identical to D1 except 16 and 15 were reversed (they are nearly degenerate). Dimers 2 through 7, although not brought to convergence, after 10 iterations exhibit good Mulpops and orbital eigenvalues (see Table 5.4). It is interesting to note that although none of the dimers is geometrically equivalent, they all appear to behave in a very similar manner. This is an indication that this energetic system is a weakly interacting one.

Table 5.4

Ground State Energy After 10 Iterations, D1 → D8

Dimer	Its., Con.*	Energy (hy)	Mulpops
1	37 converged	-290.562404	OK
2	10, 10^{-3}	-290.555154	OK
3	10, 10^{-2}	-290.556447	OK
4	10, 10^{-2}	-290.567864	OK
5	10, 10^{-1}	-290.579741	OK
6	10, 10^{-1}	-290.566704	OK
7	10, 10^{-1}	-290.566730	OK
8	49 converged	-290.565751	OK

Note: Under 'Mulpops', OK implies that the Mulliken populations looked reasonable, i.e., there were no charge imbalances with respect to the monomer case.

* Its. = Iterations, Con. = convergence. 10^{-6} was considered to be converged.

Molecular Orbital Plots for the Nitromethane Dimer

in the Crystal Configuration

Orbitals 25 and 28

The following three plots show 2 views of D1 MO 25 up and one view of D1 MO 28 up. MO25 is localized on CEN, atoms O1, O2, N and C and is π anti-bonding of b_1 symmetry. Plot 27 (xz) shows the nitrogen and carbon lobes. The seven diamonds to the right are the atoms of NEI1. Note some sharing of charge between CEN nitrogen and NEI1 oxygen. The contours are at intervals of 0.005 au resulting in an extremely dense plot near the atoms but necessary to show the slight interaction between molecules. The neighbor in these plots is oriented in such a way as to look skewed, i.e., the NO_2 group points in, to the left and slightly down in the xz plot. The yz plot shows the oxygen lobes of CEN. Also, the lower lobe shows some nitrogen contribution. This view shows a little more clearly how the weak bonding occurs between the two molecules. Plot 29 shows the outermost orbital (28) of the dimer, which is heavily localized on the oxygens of the

neighbor. There is some charge shown distributed near the nitrogen and oxygens of the central site but a finer contour would be needed to show the interaction more graphically. The orbitals of the dimer all had similar character, heavy localization on one or the other molecule and weak interaction with the neighbor.

Orbital Plot 27

X-Z Plane

DIMER 25 UP

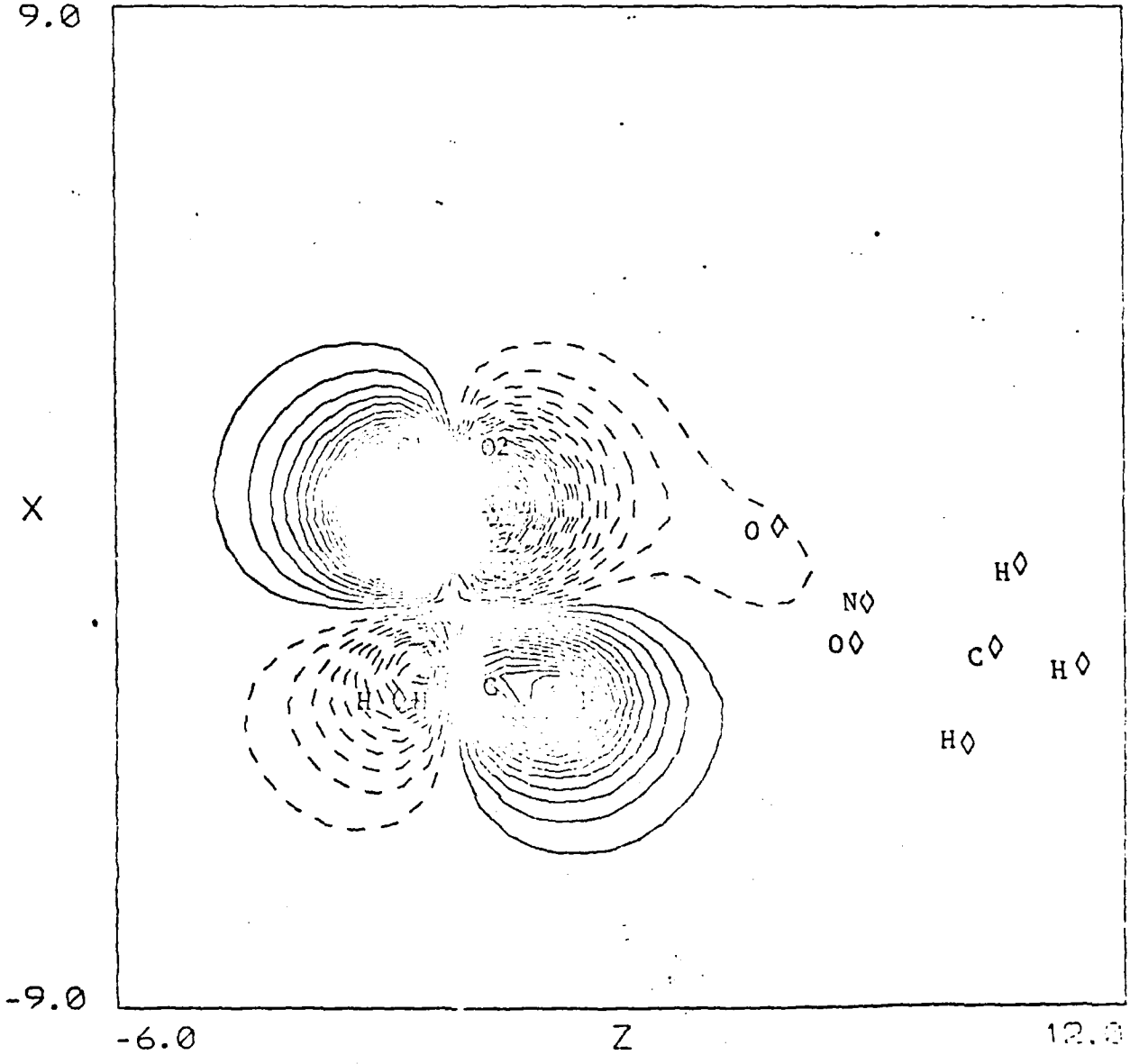

Orbital Plot 28

Y-Z Plane

DIMER 25 UP

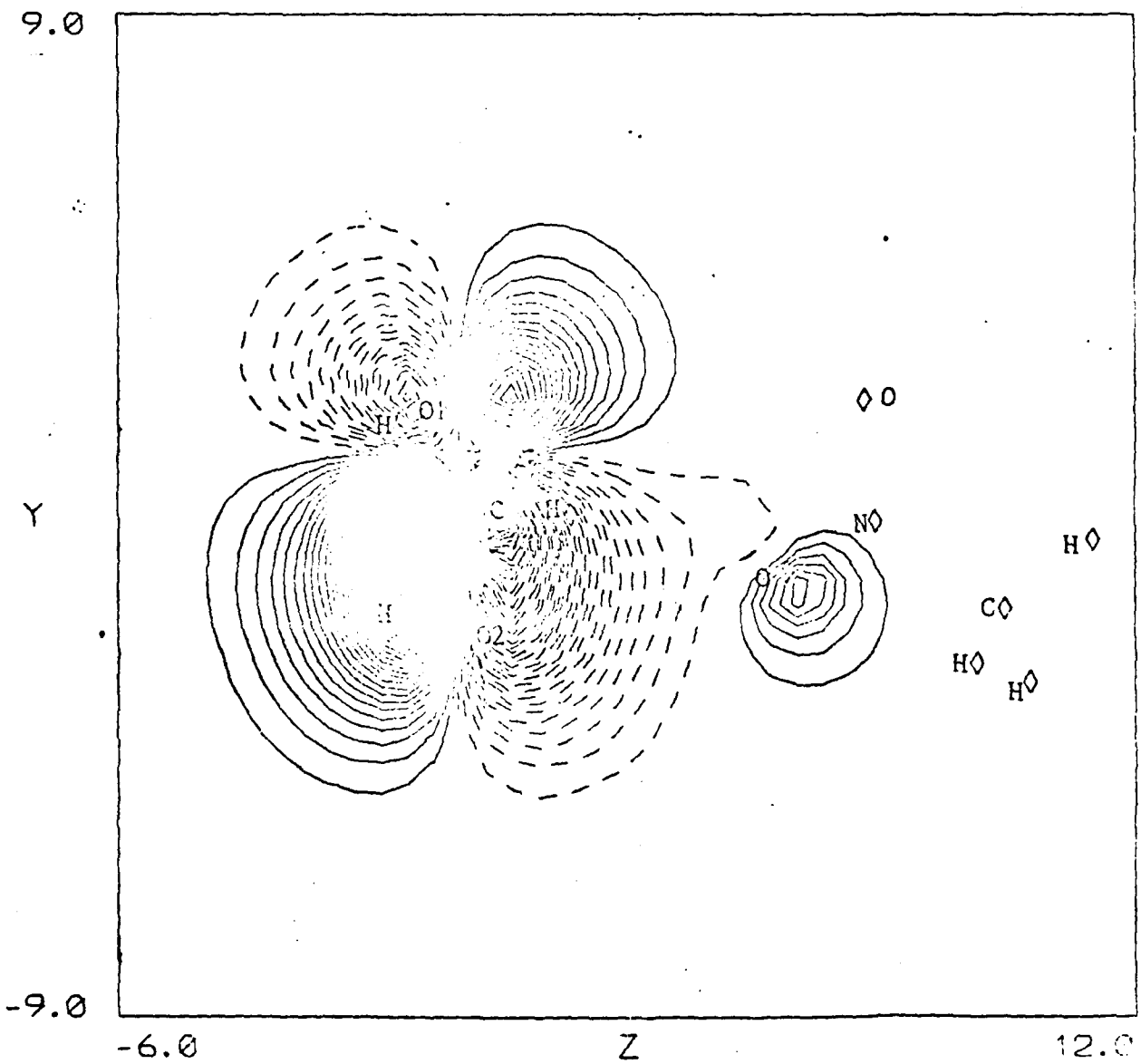

Orbital Plot 29
Y-Z Plane

DIMER 28 UP

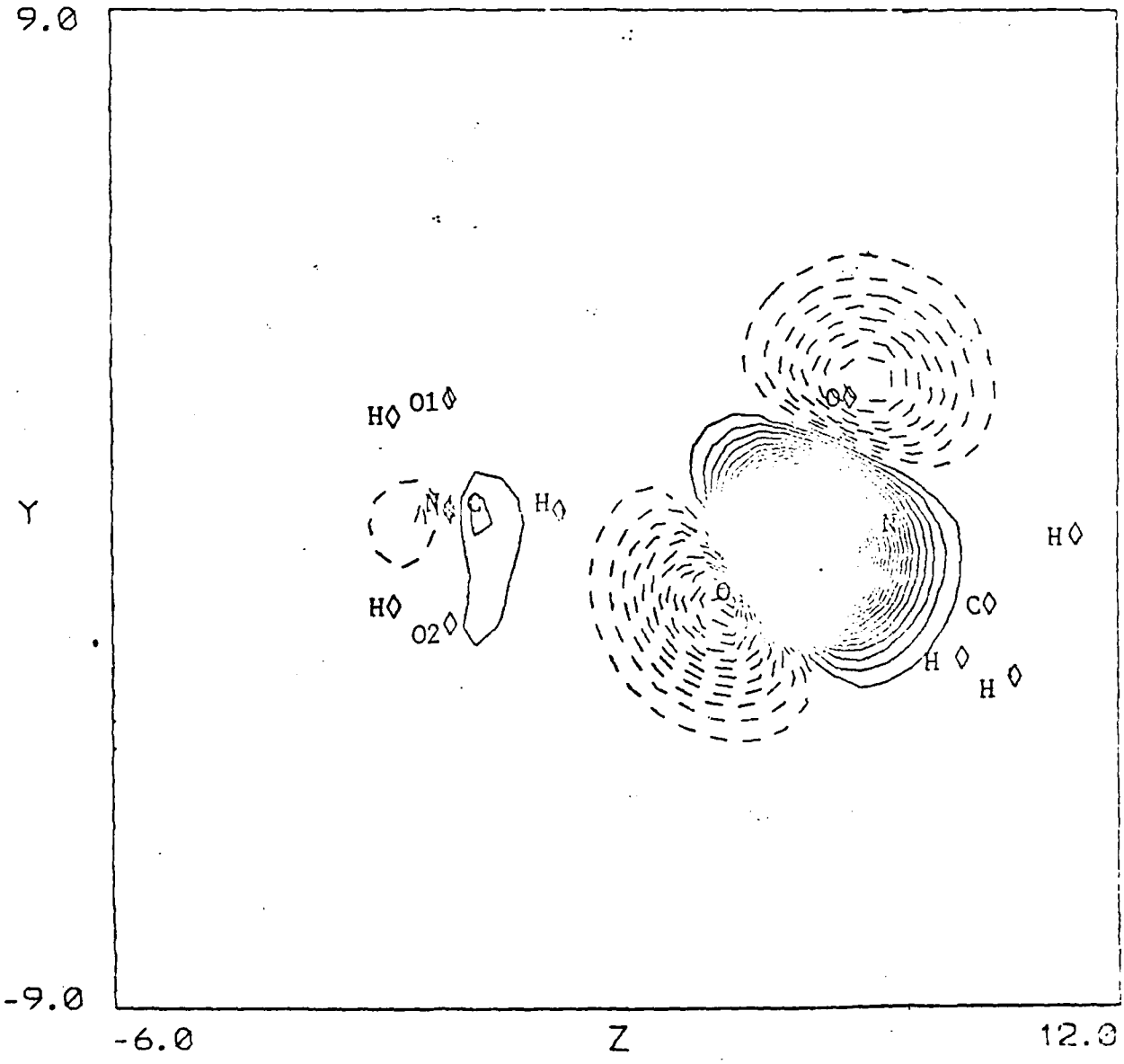

D1 Excited State

An excited state of the dimer was determined by removal of the 28↓ orbital and the addition of 29↑. The input guess for this orbital was that it be located on the central site and have z character. An overlap criteria was used which, after each iteration, determined which of the HF orbitals would be 29↑. After 40 iterations, convergence to nearly 10^{-5} in energy difference was attained. The energy of the excited dimer was -290.493572 Hy. The top most orbital was localized on the central site and exhibited the same π^* character as the monomer excited state. The system spin was calculated to be S=1, indicating convergence to a triplett. The difference in energy with respect to the ground state dimer is 0.068832 Hy (1.9 eV), close to the value recorded at the HF stage (1.8 eV) for the monomer. The central molecule had a total of 4 z-type orbitals in the spin up space for the excited state and 2 in the spin down space, the same as for the monomer. In the dimer these orbitals were numbers 29, 21, 19 and 13 with symmetry b_1, b_1, a_2 and b_1 respectively. The monomer z-type orbitals were 17, 14, 12 and 9 with the same relative symmetry as in the dimer. A good comparison can be made between monomer orbital 17 and dimer orbital 29 by looking at orbital plots 16 and 17 (monomer 17 up, xz and yz) and orbital plots 30 and 31 (dimer 29 up, xz and yz) shown on the following

pages. In both cases, the xz plots show major nitrogen contribution and some carbon contribution and the yz plots show nitrogen and oxygen contributions at the yz plane. The apparent difference in density of the plots is due to the fact that the dimer plots have contours of 0.005 au while the monomer plots have contours of 0.01au. Since the energy difference from ground to excited state is essentially the same at the Hartree-Fock level for both the monomer and dimer and the relative ordering and symmetries are also the same, it appears the presence of a single neighbor molecule oriented in the crystal configuration has little effect on the excited state of the central molecule. The excited orbital remains heavily localized on the central site. It is this type of phenomena which is amenable to study by cluster methods.

Orbital Plot 30

X-Z Plane

DIMER EXC. 29 UP

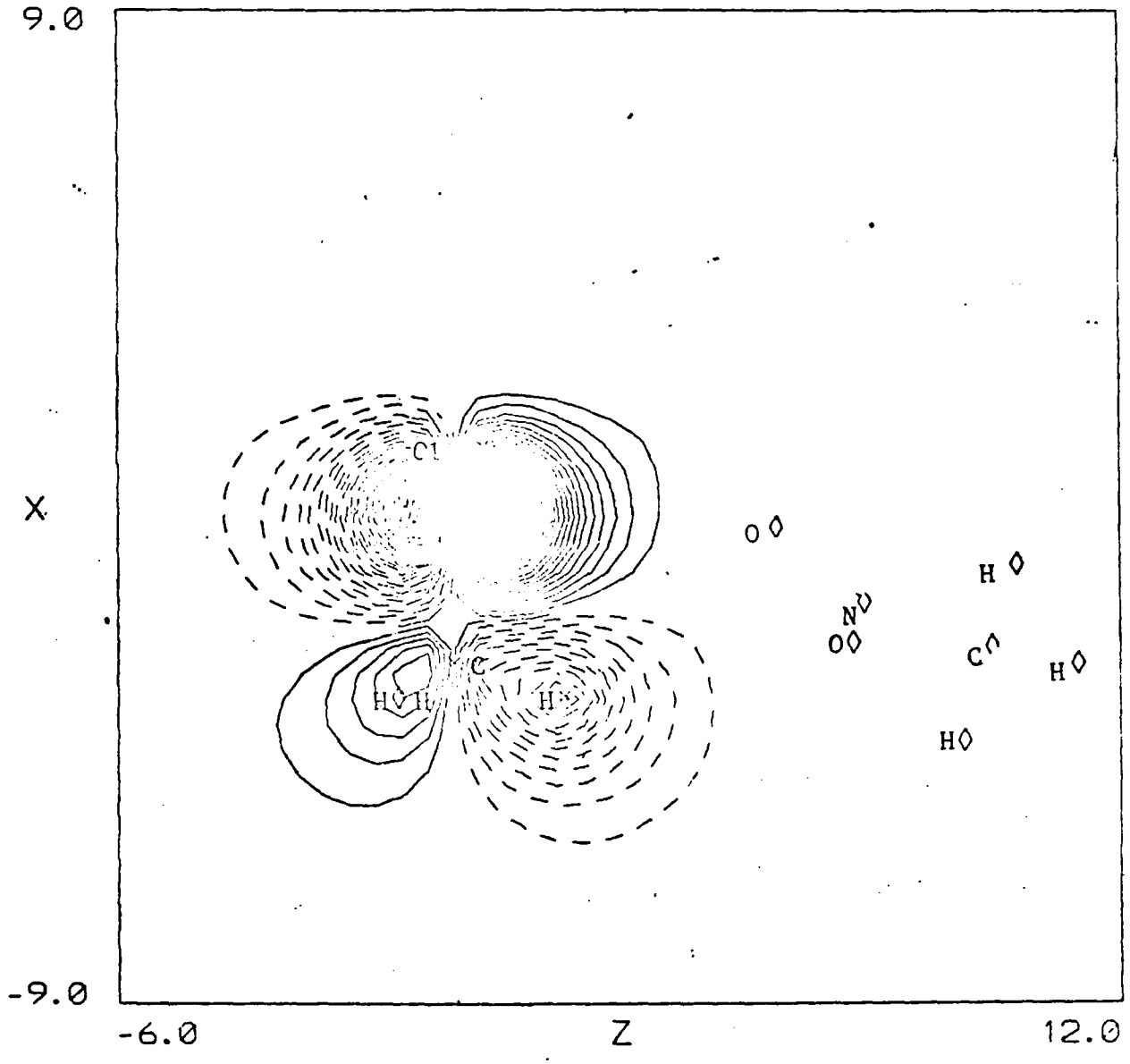

Orbital Plot 31

Y-Z Plane

DIMER EXC. 29 UP

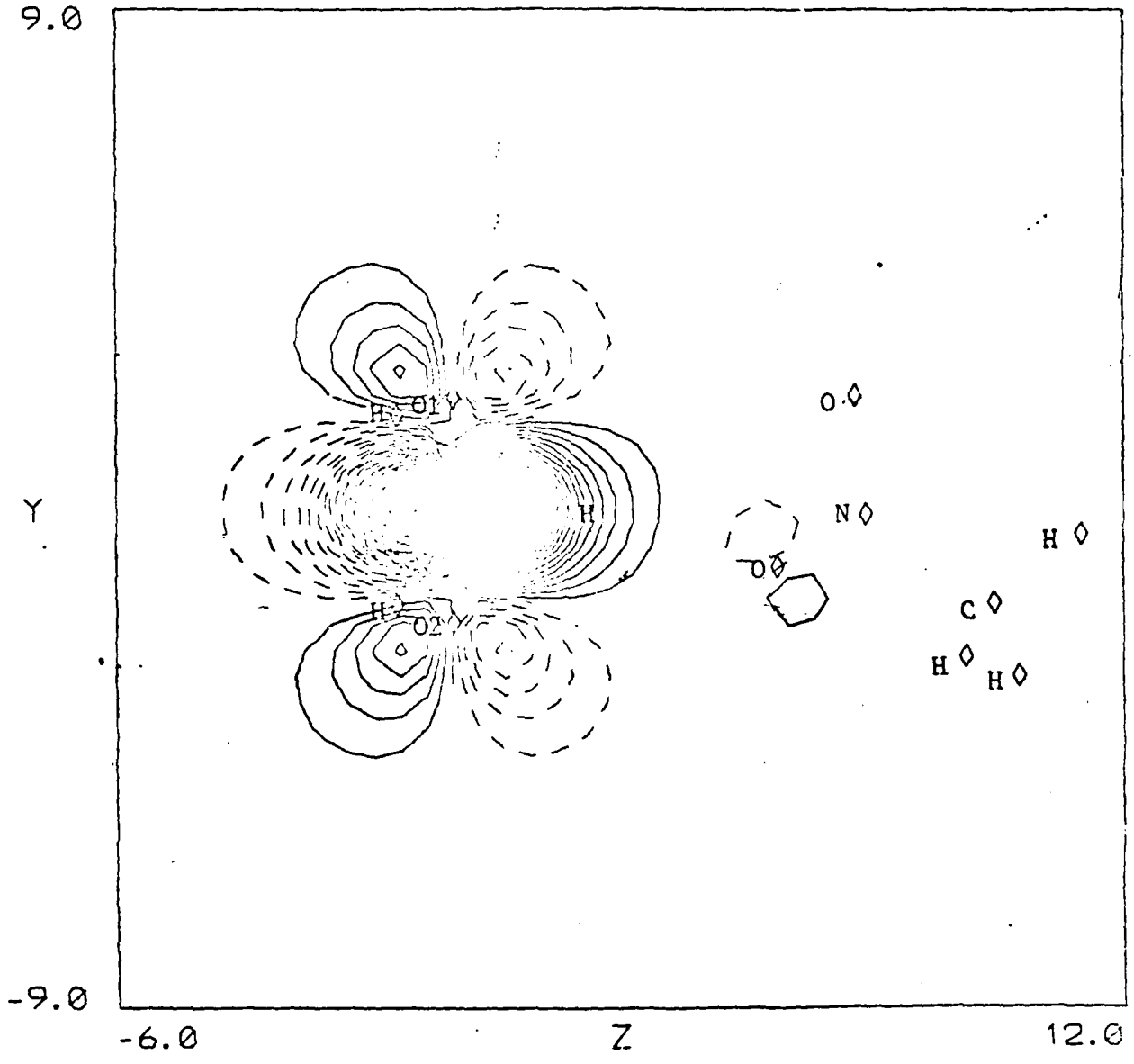

Chapter 6

Preliminary Trimer and Cluster Calculations

The computational procedures outlined in Chapter 3 have recently undergone preliminary testing to determine if:

a.) the fortran codes and complicated file structure and bookkeeping required was working properly.

b.) the approximations used (scrubbing of integrals and neglect of n-n interactions) were reasonable in their applications to the nitromethane system.

Initial attempts to converge the cluster of 9 molecules were unsuccessful. The general tendency in these runs was to cause a slight charge imbalance in the oxygen atoms of the central molecule which resulted in a convergence hang-up between two different energy values on alternate iterations. There were about 15×10^6 integrals used for this cluster (reduced from 1.6×10^9 by neglect of n-n interactions and scrubbing at 10^{-6} tolerance). Care was taken to ensure a correct potential energy calculation at the central site. The expected energy for the cluster is on the order of -619 hy based on the energy of a single dimer (-290 hy of which -47 hy comes from the neighbor and -243 comes from the central molecule: (8 x -47) + (-243) =-619). The HF code took about 1 hour per iteration for the cluster. Dimer orbital output

was used as the input guess for the cluster under the assumption that all 8 dimers acted in the same manner in terms of orbital structure and energy (This was shown to be the case in Chapter 5).

Since the dimers converged quite well, it was expected that the cluster would also and that one would see a weakly interacting system with orbitals characteristic of either the central molecule or a neighbor with essentially the same types of Mulliken populations on the central site as in the dimer. The charge imbalance which occurred on the oxygen atoms (shown to degrade after each iteration) was not expected. A careful check of the code to see if all the labels and integrals expected to be available were actually present indicated the codes to be performing properly. The problem was then scaled down to a calculation of trimer characteristics to see if the convergence problem could be pinpointed. This also failed to converge. The tendency here was to attain a very reasonable value for the energy after one iteration (expected to be about -337 hy), show inclinations to converge and then again become stuck between two energy values. The charge imbalance on the oxygens again showed up and appeared to be the cause of this problem. Also, a calculation involving all interactions (including n-n) but scrubbed at 10^{-6} tolerance and run using the original file structure with a code which was known to function properly lead to the same type of results.

A final attempt was made to develop reasonable trimer input

by stripping the central molecule of all but core electrons (32-8 = 24 electrons removed), and performing a counterpoised run in the presence of both sets of neighbor functions. The trimer being investigated contained the central molecule plus neighbors (-11103) and (01103); see Figure 5.1). This also failed to converge. This is extremely puzzling. The core oxygens refuse to settle into a stable orientation. The tendency in these runs is to show slight convergence and then to make a circuitous route around where convergence should be. The current effort is aimed towards getting this ionized central molecule to converge with the aim of creating better input for the trimer.

It should be mentioned that a trimer of lithium atoms run under a geometry similar to that of the nitromethane trimer and spaced such that the overlap of functions between atoms was similar to that between molecules of the nitromethane trimer, resulted in a converged system when run under both the original computational method employing all interactions and the new method utilizing the new labels and integrals file structures, scrubbing and neglecting n-n interactions. This was an indication that the codes worked properly since with the small basis set applied, all the integrals and corresponding labels could be monitored to be sure the appropriate ones in the limit of the approximation were all there. The lithium runs also indicate that the approximations used show some promise. It should be noted, however, that a very small basis set was used for the Li trimer (6 fully contracted

functions) and that there are only 9 electrons (and 9 protons) in this system. The nitromethane trimer has 127 functions and 80 electrons (96 total electrons minus 16 core electrons on the neighbors). The cluster has 337 functions and 224 electrons with the core electrons removed from the neighbor molecules. So direct comparison between these two systems should be made with caution. There is a great deal of electrostatic potential involved at the central site of the cluster and this may have an affect on the delicate charge balance of the NO_2 group there. There may be a very fine region of stability in terms of NO_2 electron population when working with the limited cluster of 9 molecules.

The trimer and cluster work is quite important. If the convergence problems can be pinpointed and overcome, a lot will be learned about the way in which systems of this type must be handled from the computational viewpoint. If the cluster can be converged and reasonable results extracted under the given approximations, the ability to perform ab initio calculations on systems of large molecules will have been demonstrated. It is important that an effort be continued to study convergence problems in systems of this type.

Chapter 7

Conclusions

Hartree-Fock and many-body perturbation theory have been used to investigate the electronic structure of the energetic molecule, nitromethane. Both ground and excited states have been studied in the free molecule (monomer) as well as in a dimer configuration. A preliminary investigation has been done on the molecule in trimer (3 molecules) and cluster (9 molecules) configurations in the crystal geometry. In order to make these investigations feasible, new computer codes (as well as modifications to existing Hartree-Fock codes) were necessary.

Studies of the monomer have resulted in the lowest reported ground state energy (-244.3219 hy) and the first correlated result using extended basis sets and many-body perturbation theory for the lowest lying excited state (3.47 eV above the ground state). The outermost orbital of the ground state was found to be a pi-type anti-bonding orbital of a_2 symmetry and the second orbital in to be a sigma-type bonding orbital of a_1 symmetry. This is in contradiction to experimental results which have these reversed. All results have been disputed due to the close energy spacing between these orbitals. It may be necessary to use a correlated wave function to determine the proper order of these orbitals since they are so closely spaced in energy (about 0.5 eV).

Calculations of first and second ionization potentials yield the best reported results so far when compared to experiment.

The correlated excited state shows its outermost orbital to be a pi-type bonding orbital of b_1 symmetry. Other recent work using small basis sets places this state either higher in energy by about 1.3 eV than reported here or lower by about 0.5 eV. The excited state converged to in this work was a triplet. The singlet-triplet splitting for this state (singlet above triplet) was calculated to be approximately 0.4 eV, results which were consistent using both a small and large basis set.

The calculation of nitromethane's dipole moment resulted in an uncorrelated value of 3.696 Debye, which compares well to experiment (3.46 ± .2 D).

The electronic transition moment for the ground to first excited state was calculated. Based on this value (2.8) an oscillator strength (f value) of 0.125 was calculated for this transition. Arguments are presented to indicate this to represent a moderate to weak transition. This transition has not yet been observed experimentally.

An investigation was done on both the CH_3 and NO_2 fragments of the molecule. A calculation of the C-N bond energy resulted in a value which was low compared to experiment (82.8 Kcal/mole vs 112.8 Kcal/mole for experiment).

An important analysis was made concerning the effect on the C-N bond strength due to a free charge near the nitromethane

molecule. A crystal configuration was used where the main molecule was located at the central position of the proposed cluster and the single +1 or -1 au charge was located at various positions within what would normally be near-neighbor (-11103). It was found that the C-N bond strength of the central molecule could change by up to 0.2 eV depending on the location and sign of the single charge. The implications are that within the crystal, it may be possible for free ions located at vacancies to cause weakening of the C-N bond of other molecules resulting in a possibility of bond scissioning and release of energy into the crystal.

Calculations on the NO_2 group resulted in the lowest reported energy for that molecule. It was also demonstrated that the use of atomic pseudopotentials gave reasonable descriptions of the CH_3 and NO_2 fragments.

This thesis also reports the first known computational work on groups of more than one nitromethane molecule. It was shown that it is possible to gain convergence for a dimer in the crystal configuration. It was also demonstrated that a large reduction in the size of the problem could be attained by scrubbing the integrals over atomic functions without a very great loss in accuracy. The dimer system was demonstrated to be weakly interacting in that molecular orbitals are well delineated with respect to central or neighbor domination.

The first excited state of the dimer was also studied. The

excited orbital was of b_1 symmetry as in the ground state with possibly a slightly greater contribution from the carbon atom than in the ground state. This orbital was very well localized, on the central molecule with only a weak interaction with the neighbor.

A methodology was developed for studying much larger groups of molecules. Scrubbing of integrals (highly successful for the dimer) as well as the neglect of neighbor-neighbor interactions are proposed as initial steps to reduce the problem size while hoping to gain reasonable physical results for study of the cluster. Problems in gaining convergence for the cluster and a trimer configuration have currently refocused the effort on the study of convergence criteria for energetic systems of this type. The approximations mentioned above were shown to be highly successful in studying a lithium trimer. Extensive code modification and development was necessary to attempt the cluster calculation.

The initial proposal for this study, the investigation of excited states in nitromethane and the effect of the environment on them, has been partially successfully completed (dimer work). Many other successes were attained in the mean time as noted above.

Suggestions for continued work are:

a.) an investigation of the presence of free charges on excited states of nitromethane and, and once the cluste is successfully completed, the same sort of study where

a neighbor is replaced by a free charge.

b.) work on molecular pseudopotentials to attain better descriptions of outer orbitals when core electrons are removed.

c.) most importantly, to gain convergence of the trimer and cluster. Success here will demonstrate that the methodology developed can be applied to systems of relatively large, weakly interacting molecules. Also, much can be learned about the subtleties of convergence problems in energetic systems.

Appendix A

Calculation of Cartesian Coordinates From Crystallographic Data

This appendix is intended as a tutorial on how to determine the cartesian coordinates of any molecule in a crystal given the fractional coordinates of the atoms of one molecule, data which is derived from diffraction studies. Much of what follows evolved from private communication with S.F. Trevino, who along with E. Prince and C.R. Hubbard has done the primary work on the structure of solid nitromethane.

The crystallographic data (at T = 4.2K) was taken from Trevino's [66] paper. Neutron diffraction data yield what are called fractional coordinates, i.e., x, y and z coordinates of an atom within a molecule in terms of fractions of the lengths of the sides (a,b,c) of the unit cell. Also, a, b and c are determined from the data.

The unit cell dimensions for solid CH_3NO_2 were determined to be:

a = 5.1832 A b = 6.2357 A c = 8.5181 A

Table A1 shows the fractional coordinates (X,Y,Z) of each atom (C,N,O1,O2,D1,D2,D3) in nitromethane. The D's represent the hydrogen atoms. The cartesian coordinates of any atom is then simply given by the product of the fractional coordinates and the corresponding lattice parameter:

x' = X*a y' = Y*b z' = Z*c

For example, the cartesian coordinates of carbon are given by:

$$x'_c = 0.1330 * 5.1832 = 0.6894 \text{ A}$$
$$y'_c = 1.0548 * 6.2357 = 6.5774 \text{ A}$$
$$z'_c = 0.3772 * 8.5181 = 3.2130 \text{ A}$$

where X, Y and Z are from Table A1. These coordinates are with respect to the origin of the unit cell. All other atomic coordinates are given in the same manner.

Nitromethane has 4 molecules in the primitive cell. The above procedure gives the position of one of them. The other three are determined by the space group symmetry of the unit cell. Nitromethane was determined to have orthorhombic space group symmetry, $P_{2_1 2_1 2_1}$. The International Tables for X-ray Crystallography [71] give pertinent information regarding all possible space groups. Page 105 of that reference pertains to $P_{2_1 2_1 2_1}$ symmetry (see Figure A1). Four transformations are shown in this figure, representing the four molecules in the unit cell. These transformations are given in matrix representation as:

$$x,y,z \rightarrow \begin{bmatrix} 1 & 0 & 0 \\ 0 & 1 & 0 \\ 0 & 0 & 1 \end{bmatrix} \qquad (1)$$

L6
which corresponds to the original molecule as calculated above.

$$\frac{1}{2} - x,\ \bar{y},\ \frac{1}{2} + z \longrightarrow \begin{bmatrix} -1 & 0 & 0 \\ 0 & -1 & 0 \\ 0 & 0 & 1 \end{bmatrix} + \begin{bmatrix} \frac{1}{2} \\ 0 \\ \frac{1}{2} \end{bmatrix} \qquad (2)$$

$$\frac{1}{2} + x,\ \frac{1}{2} - y,\ \bar{z} \longrightarrow \begin{bmatrix} 1 & 0 & 0 \\ 0 & -1 & 0 \\ 0 & 0 & -1 \end{bmatrix} + \begin{bmatrix} \frac{1}{2} \\ \frac{1}{2} \\ 0 \end{bmatrix} \qquad (3)$$

$$\bar{x},\ \frac{1}{2} + y,\ \frac{1}{2} - z \longrightarrow \begin{bmatrix} -1 & 0 & 0 \\ 0 & 1 & 0 \\ 0 & 0 & -1 \end{bmatrix} + \begin{bmatrix} 0 \\ \frac{1}{2} \\ \frac{1}{2} \end{bmatrix} \qquad (4)$$

Each transformation is used to find the coordinates of the other atoms (and therefore molecules) in the primitive cell. As an example, to calculate the coordinates of the carbon atom of molecule 2 we do the following:

$$\begin{bmatrix} x_C^2 \\ y_C^2 \\ z_C^2 \end{bmatrix} = \begin{bmatrix} -1 & 0 & 0 \\ 0 & -1 & 0 \\ 0 & 0 & 1 \end{bmatrix} * \begin{bmatrix} x_C^1 \\ y_C^1 \\ z_C^1 \end{bmatrix} + \begin{bmatrix} \frac{1}{2} \\ 0 \\ \frac{1}{2} \end{bmatrix}$$

$$\begin{bmatrix} x_c^2 \\ y_c^2 \\ z_c^2 \end{bmatrix} = \begin{bmatrix} -1 & 0 & 0 \\ 0 & -1 & 0 \\ 0 & 0 & 1 \end{bmatrix} * \begin{bmatrix} 0.1330 \\ 1.0548 \\ 0.3772 \end{bmatrix} + \begin{bmatrix} \frac{1}{2} \\ 0 \\ \frac{1}{2} \end{bmatrix} = \begin{bmatrix} 0.3670 \\ -1.0548 \\ 0.8772 \end{bmatrix}$$

The results on the right are the fractional coordinates, which then have to be multiplied by the lattice parameters to give the final cartesian coordinates of molecule 2's carbon atom.

$$x_c^2 = 0.3670 * 5.1832 = 1.9022 \text{ A}$$
$$y_c^2 = -1.0548 * 6.2357 = -6.5774 \text{ A}$$
$$z_c^2 = 0.8772 * 8.5181 = 7.4721 \text{ A}$$

Applying this transformation to the other atoms creates the position of molecule 2. Molecules 3 and 4 are obtained analogously using transformations 3 and 4 above. The molecules in adjacent unit cells are determined by adding to the coordinates in the primitive cell a vector joining the origins of the two cells. The above coordinates are for unit cell (0,0,0). For the (1,0,0) coordinates of carbon in molecule 1 ((1,0,0) is the unit cell adjacent to (0,0,0) in the direction of a) we have:

$$x_c^1(1,0,0) = 0.6894 + (1 * 5.1832) = 5.8726 \text{ A}$$
$$y_c^1(1,0,0) = 6.5774 + (0 * 6.2357) = 6.5774 \text{ A}$$
$$z_c^1(1,0,0) = 3.2130 + (0 * 8.5181) = 3.2130 \text{ A}$$

or in general:

$$x_c^n(h,k,l) = x_c^n(0,0,0) + (h * a)$$
$$y_c^n(h,k,l) = y_c^n(0,0,0) + (k * b)$$
$$z_c^n(h,k,l) = z_c^n(0,0,0) + (l * c)$$

where h, k and l are allowed all integer values and n represents the transformation involved. Application of the above procedure will allow one to obtain the location of any atom in any molecule in the crystal.

Molecule (0,0,0)01 was used as the central molecule. Its 8 nearest neighbors were determined to be:

(-1,1,1)03, (0,1,1)03, (0,2,1)03, (-1,2,1)03
(0,0,0)04, (0,-1,0)04, (1,-1,0)04, (1,0,0)04

Note that molecule 2 (02) is not one of the nearest neighbors. The coordinates of (0,0,0)03 and (0,0,0)04 were determined as above and then translated to corresponding unit cells.

A coordinate transformation was performed to place the origin at the nitrogen molecule of (0,0,0)01 and the x-axis along the C-N bond with atoms O1, N, O2 and c in the x-y plane. This was done to invoke what little local point group symmetry there was on the

central site. It was later determined that the oxygen atoms in the central molecule don't quite see the same potential and use of symmetry introduced a slight error in the potential energy integrals.

The general procedure for performing this translation and rotation is as follows. Determine the coordinates, in A, of (0,0,0)01 atoms from the fractional coordinates. Subtract the nitrogen coordinates from those of each atom to translated the molecule to the new origin. Trevino [66] also gives the interatom distances and bond angles. From these, it is easy to determine what the x, y and z coordinates in the final reference frame should be. One then determines the direction cosines for the rotation from the following:

$$x' = (l_{11} * x) + (l_{12} * y) + (l_{13} * z)$$
$$y' = (l_{21} * x) + (l_{22} * y) + (l_{23} * z)$$
$$z' = (l_{31} * x) + (l_{32} * y) + (l_{33} * z)$$

where the l_{ij} are direction cosines, x, y and z are the original (translated) coordinates of the atom and x', y' and z' are the desired coordinates. Both the unprimed and primed coordinates are known for each atom of (0,0,0)01, the first from the crystallographic data (after conversion to cartesian coordinates and translating to the nitrogen atom) and the second from the

relative positions of the atoms in the molecule.

Therefore, one can obtain 3 equations in 3 unknowns for each of x', y' and z' using the desired and known coordinates of 3 atoms. The direction cosines are then solved for.

Once the positions of the other molecules of the cluster are determined from the crystallographic data, one then translates them based on the coordinates of the central site nitrogen atom. Then the rotations given above are applied, based on the calculated direction cosines. Finally, all coordinates are converted to atomic units (au) to be used in the POLYATOM integrals code (1 au =0.529 A).

Table A1.

Atom	Parameter	4.2 K	78 K
C	X	0.1330(5)	0.1290(9)
	Y	1.0548(3)	1.0527(5)
	Z	0.3772(2)	0.3973(5)
	U_{11}	0.0149(6)	0.0217(10)
	U_{22}	0.0115(5)	0.0198(11)
	U_{33}	0.0075(7)	0.0177(16)
	U_{12}	−0.0055(5)	−0.0029(11)
	U_{13}	−0.0001(0)	−0.0000(0)
	U_{23}	0.0001(0)	0.0000(0)
N	X	0.3626(3)	0.3609(5)
	Y	0.9136(3)	0.9128(5)
	Z	0.3749(3)	0.3771(5)
	B	0.34(4)	0.78(7)
O1	X	0.5179(6)	0.5158(10)
	Y	0.9271(6)	0.9278(10)
	Z	0.4804(4)	0.4809(6)
	B	0.82(4)	1.72(8)
O2	X	0.3817(7)	0.3820(11)
	Y	0.7846(5)	0.7835(9)
	Z	0.2674(5)	0.2699(7)
	B	0.82(4)	1.72(8)
D1	X	0.0755(6)	0.0686(12)
	Y	1.0818(5)	1.0730(11)
	Z	0.2577(4)	0.2694(9)
	U_{11}	0.0325(7)	0.0698(16)
	U_{22}	0.0438(10)	0.1119(27)
	U_{33}	0.0088(6)	0.0320(16)
	U_{12}	0.0183(9)	0.0637(21)
	U_{13}	−0.0013(1)	−0.0063(2)
	U_{23}	−0.0015(1)	−0.0089(2)
D2	X	−0.0150(3)	−0.0071(5)
	Y	0.9737(4)	0.9808(7)
	Z	0.4420(4)	0.4433(8)
	U_{11}	0.0205(6)	0.0415(11)
	U_{22}	0.0211(5)	0.0553(14)
	U_{33}	0.0434(11)	0.1169(31)
	U_{12}	0.0019(5)	0.0230(13)
	U_{13}	0.0133(5)	0.0362(9)
	U_{23}	0.0175(6)	0.0479(12)
D3	X	0.1875(4)	0.1775(8)
	Y	1.2022(3)	1.1934(6)
	Z	0.4335(4)	0.4268(9)
	U_{11}	0.0188(6)	0.0336(10)
	U_{22}	0.0193(5)	0.0442(12)
	U_{33}	0.0469(12)	0.1359(35)
	U_{12}	0.0000(0)	0.0141(12)
	U_{13}	−0.0116(4)	−0.0276(7)
	U_{23}	−0.0163(6)	−0.0406(11)

Fractional Coordinates for Nitromethane
From Trevino (Ref. 66)

Orthorhombic 222 $P\,2_1\,2_1\,2_1$ No. 19 $P\,2_1\,2_1\,2_1$ D_2^4

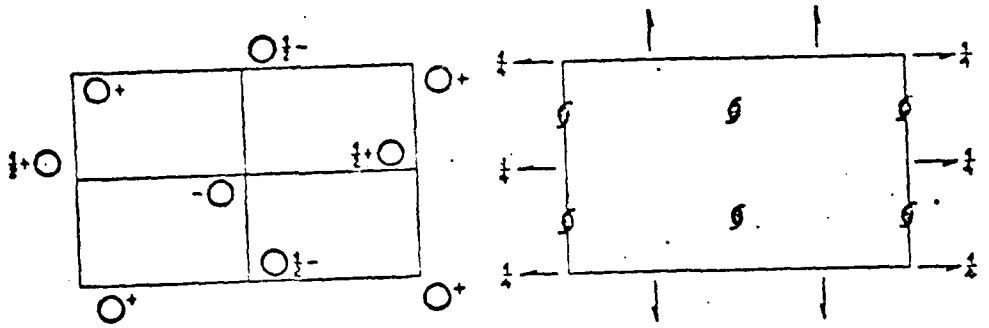

Origin halfway between three pairs of non-intersecting screw axes

Number of positions, Wyckoff notation, and point symmetry			Co-ordinates of equivalent positions	Conditions limiting possible reflections
4	a	1	x,y,z; $\frac{1}{2}-x,\bar{y},\frac{1}{2}+z$; $\frac{1}{2}+x,\frac{1}{2}-y,\bar{z}$; $\bar{x},\frac{1}{2}+y,\frac{1}{2}-z$.	hkl: No conditions $0kl$: No conditions $h0l$: No conditions $hk0$: No conditions $h00$: $h=2n$ $0k0$: $k=2n$ $00l$: $l=2n$

Symmetry of special projections

(001) pgg; $a'=a, b'=b$

(100) pgg; $b'=b, c'=c$

(010) pgg; $c'=c, a'=a$

Figure A1.

Orthorhombic Space Group Symmetry $P2_12_12_1$

From Ref. 71

Appendix B

Notation and Meaning of Symmetry Operations and Orbital Bonds

When discussing the character of molecular orbitals, mention is usually made of the symmetry of a given MO. Table B1. is the character table for C_{2v} symmetry operations. This group has for independent operations; identity (E), 2-fold rotation about the symmetry axis (C_2), and reflection in two different planes (σ_v and σ_v'). Figure B1. shows these operations when applied to the C-N-O1-O2 group of atoms in nitromethane.

Symmetry element a_1 implies that whenever any of the four operations are applied to the molecule, the molecule looks exactly as it did before the application. Symmetry element a_2 indicates the the identity and 2-fold rotation operations leave the molecule unchanged but either of the reflection operations reverse the sign of the wavefunction (orbital) of the molecule. An example is shown in Figure B2. Applying a 2-fold rotation about the x-axis (symmetry axis) brings the (-) lobe of O2 into the (-) lobe of O1 (and + → +), i.e., the molecule is unchanged. However, reflection in the x-z or the x-y planes cause a (+) lobe of an oxygen to go to a (-) lobe on the other oxygen, etc. Therefore, a -1 is associated with both σ(xy) and σ(xz) in the character table. Similarly, b_1 symmetry implies the identity and σ(xz) operations leave the molecule unchanged and C_2 and σ(xy) cause a sign change. For b_2 symmetry, the identity and σ(xy) operations leave it

unchanged while C_2 and $\sigma(xz)$ cause a sign change.

Figure B3. shows what is meant by σ and π bonding. The top part of the diagram shows how a σ bond may be formed by the overlap of various types of orbitals. A molecular orbital which is symmetric about the line joining the two atoms is called a sigma (σ) bond. Pi (π) bonds are shown in the lower half of Figure B3. These are created by the lateral overlap of orbitals and result in the line joining the two atoms to be free of electronic charge. Also shown is a σ bond formed by 2 p-type orbitals. Combinations of more p orbitals can yield the toroidal charge distribution of the overlap of two π bonds as shown at the bottom of the figure. Again, no charge overlaps the interatom radius vector. The diagrams of Figure B3. were taken from reference 72 and the character table from reference 73.

Table B1

Character Table for C_{2v} Symmetry

C_{2v}	E	C_2	$\sigma_v(xz)$	$\sigma_v(xy)$	
a_1	1	1	1	1	x
a_2	1	1	-1	-1	R_x
b_1	1	-1	1	-1	z, R_y
b_2	1	-1	-1	1	y, R_z

Note: x is the axis of symmetry.

AD-A174 012 ENERGY TRAPPING RELEASE AND TRANSPORT IN THREE DIMENSIONAL ENERGETIC SOLI..(U) MICHIGAN TECHNOLOGICAL UNIV HOUGHTON A B KUNZ 30 JUN 86 N00014-81-K-0620 3/4

UNCLASSIFIED F/G 7/3 NL

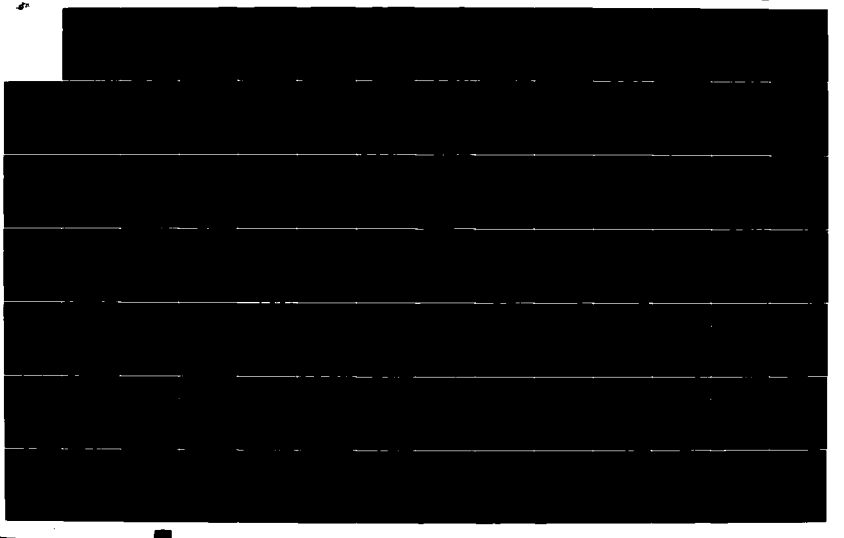

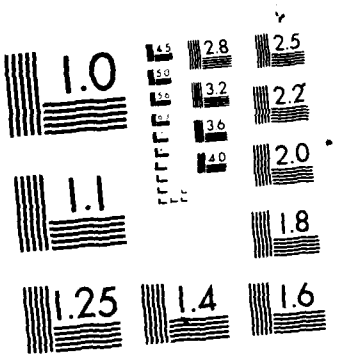

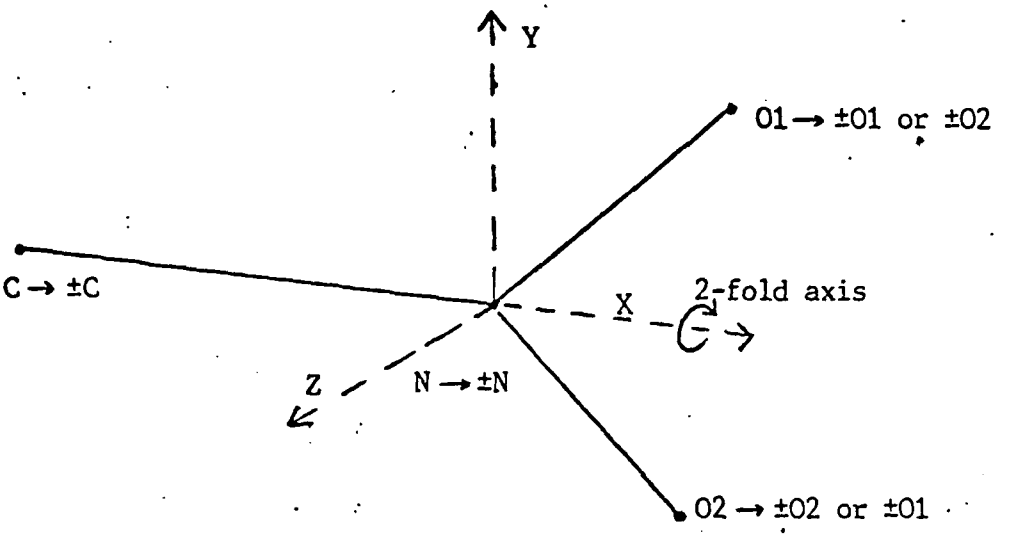

Figure B1

The sign change depends upon the type and orientation of the function located at the atom as well as the applied symmetry operation.

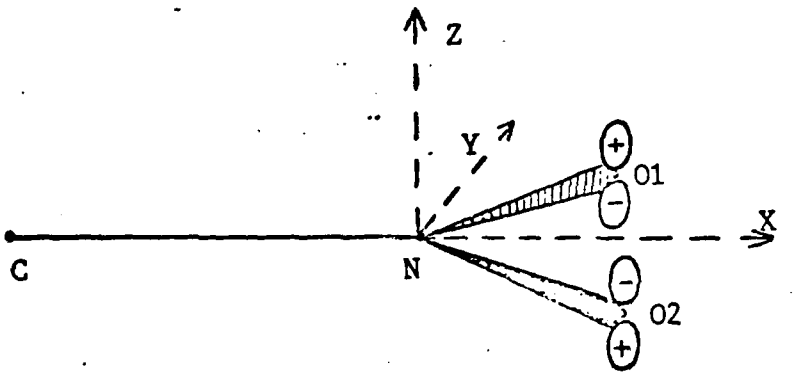

Figure B2

2-fold rotation about X places the (-) lobe of O2 at the (-) lobe of O1 whereas reflection in the x-z pland places the (-) lobe of O2 at the (+) lobe of O1.

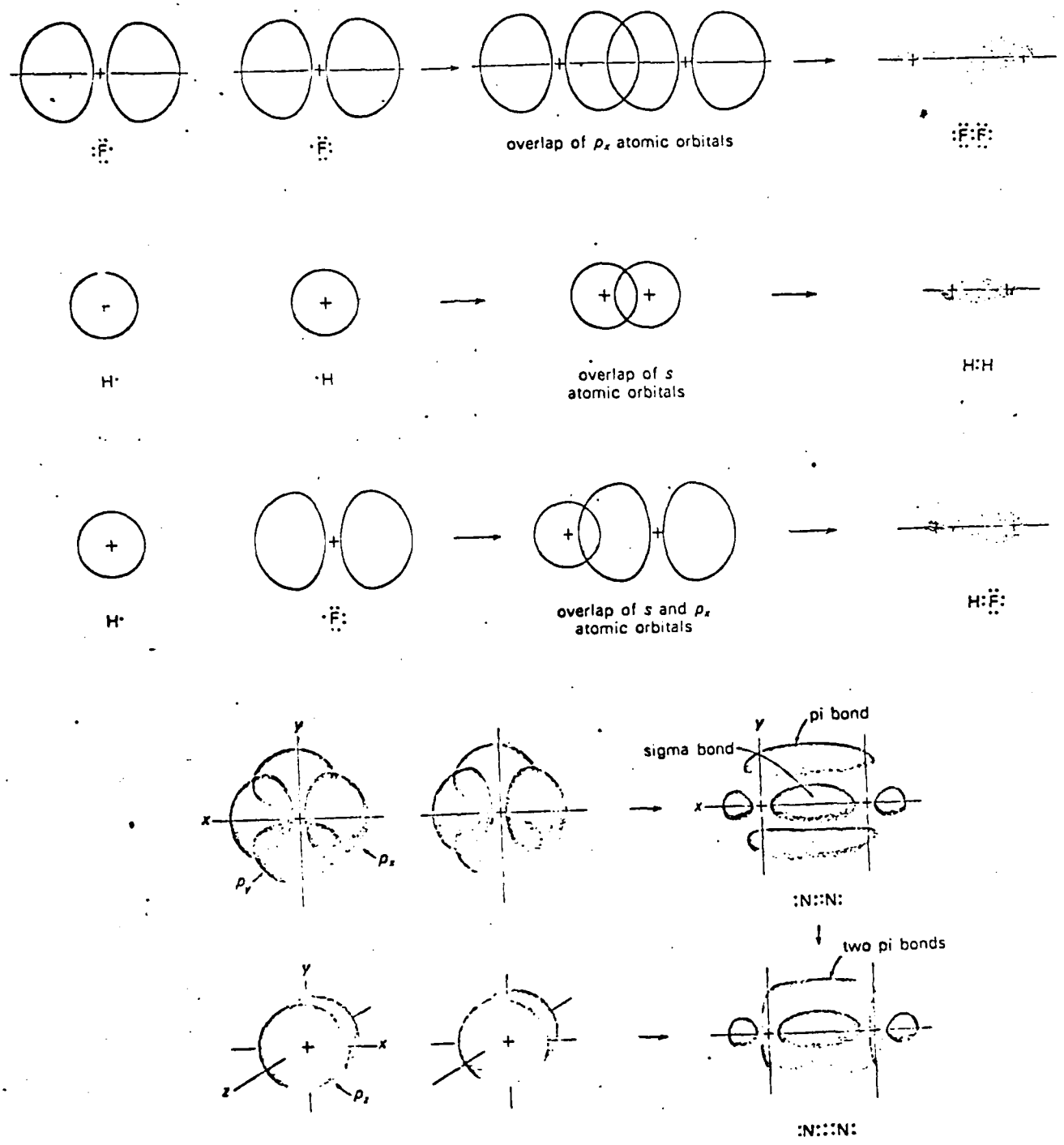

Figure B3.
Examples of Sigma and Pi Bonds
From Ref. 72

Appendix C

Tables of Basis Sets

This appendix lists tables of basis sets used for nitromethane monomer, dimer, trimer and cluster calculations in this thesis as well as molecular coordinates for these systems. Main features shown in the tables are the atomic center (oxygen = O1 or O2, etc.), the type of function (Gaussian) associated with that center (s, x,y,z (p-type), etc.), and the exponent and coefficient used in the function. The column containing the much larger numbers (such as 7817. for O1, s) holds the exponents. The beginning of each table shows the x,y and z coordinates of each center (in au) as well as the charge associated with that center and sometimes a code (such as NLP) which indicates that pseudopotentials are to be used to replace the 1s electrons for that center (in which case the corresponding charge is reduced by 2).

Table C1. .....48 function set used for the monomer. (Note: The final four bond coordinates <BNC,BCH1,BCH2,BCH3> are not correct in this table.)

Table C2. .....57 function set used in both the free molecule and crystal geometry (shown) and for the central (main) molecule in calculations involving more than one molecule..

Table C3. .....80 function set used for the monomer.

Table C4. .....81 function set used for the monomer. This set is the same as the 80 function set except for the addition of the carbon d function (YY).

Table C5. .....84 function set used for the monomer. This set is slightly uncontracted (oxygen and nitrogen s functions) compared to the 81 function set.

Table C6. .....Coordinates (au) of the central molecule and 8 nearest neighbors in the cluster.

```
NITROMETHANE, MAY SET, 5 BONDS, NBF=48,
  7  6
N          0.0           0.0           0.0           7.0
O1         1.062041      2.054916      0.0           8.0
O2         1.062041     -2.054916      0.0           8.0
C         -2.813085      0.0           0.0           6.0
H1        -3.419281      .9819151     -1.700777      1.0
H2        -3.419281      .9819151      1.700777      1.0
H3        -3.419281     -1.963830      0.0           1.0
BNO1       .5310205      1.027458      0.0
BNO2       .5310205     -1.027458      0.0
BNC       -1.336716      0.0           0.0
BCH1      -1.709641      .4909576     -.8503885
BCH2      -1.709641      .4909576      .8503885
BCH3      -1.709641     -.981915       0.0
118 48
 7 2 1 7 2 1 4 1 4 1 4 1 4 1 4 1 7 2 1 4 1 4 1 4 1 7 2 1 4 1 4 1 4 1
 1 1 1 3 1 3 1 3 1 1 1 1 1
O1         S             7817.         .001176
O1         S             1176.         .008968
O1         S             273.2         .042868
O1         S             81.17         .143930
O1         S             27.18         .355630
O1         S             9.532         .461248
O1         S             3.414         .140206
O1         S             9.532        -.154153
O1         S              .9398        1.056914
O1         S              .2846        1.0
O2         S      1
O2         S      2
O2         S      3
O1         X             35.18         .019580
O1         X             7.904         .124200
O1         X             2.305         .394718
O1         X              .7171        .627376
O1         X              .2137        1.0
O2         X      7
O2         X      8
O1         Y      7
O1         Y      8
O2         Y      7
O2         Y      8
O1         Z      7
O1         Z      8
O2         Z      7
O2         Z      8
N          S             5909.         .003190
N          S             887.5         .009099
N          S             204.7         .044145
N          S             59.84         .150468
N          S             20.00         .356741
N          S             7.193         .486533
N          S             2.686         .145603
N          S             7.193        -.160405
N          S              .7000        1.056215
N          S              .3133        1.0000
N          X             26.79         .018254
N          X             5.996         .118481
N          X             1.707         .340178
N          X              .5314        .637102
N          X              .1654        1.0000
N          Y     22
N          Y     23
N          Z     22
N          Z     23
C          S             4233.         .001220
C          S             634.9         .009342
C          S             146.1         .045452
C          S             42.50         .154657
C          S             14.19         .358866
C          S             5.148         .438632
C          S             1.967         .145918
C          S             5.148        -.166367
C          S              .4962        1.060091
C          S              .1533        1.00000
C          X             18.16         .018539
C          X             3.986         .115436
C          X             1.143         .386188
C          X              .3594        .640114
C          X              .1146        1.00000
C          Y     31
C          Y     32
C          Z     31
C          Z     32
BNO1       S             1.5000000
BNO2       S             1.5000000
BNC        S             1.2870000
H1         S             13.36         .032828
H1         S             2.013         .231204
H1         S              .4538        .817226
H1         S              .1233        1.00000
H2         S     40
H2         S     41
H3         S     40
H3         S     41
BCH1       S              .75
BCH2       S              .75
BCH3       S              .75
```

Table C1.

57 FUNCTION SET, NEW (CRYSTAL) GEOMETRY ONLY

NW	0,0	0,0	0,0	7,0
O1W	1,091	2,023	0,0	8,0
O2W	1,091	-2,023	0,0	8,0
CW	-2,798	0,0	0,0	4,0
H1W	-3,417	-1,716	-0,991	1,0
H2W	-3,417	0,0	1,982	1,0
H3W	-3,417	1,716	-0,991	1,0
BNO1	0,545	1,011	0,0	
BNO2	0,545	-1,011	0,0	
BNC	-1,399	0,0	0,0	
BCH1	-3,108	-0,858	-0,495	
BCH2	-3,108	0,0	0,991	
BCH3	-3,108	0,858	-0,495	

127 57

7 2 1 7 2 1 4 1 4 1 4 1 4 1 4 1 7 2 1 4 1 4 1 4 1 7 2 1 4 1 4 1 4 1
1 1 1 1 1 1 1 1 1 1 3 1 3 1 3 1 1 1 1

O1W	S		7017,	,001176
O1W	S		1176,	,008968
O1W	S		273,2	,042068
O1W	S		81,17	,143930
O1W	S		27,18	,355630
O1W	S		9,532	,441248
O1W	S		3,414	,[illegible]96
O1W	S		9,532	-,154153
O1W	S		,9398	1,056914
O1W	S		,2846	1,0
O2W	S	1		
O2W	S	2		
O2W	S	3		
O1W	X		35,18	,019580
O1W	X		7,904	,124200
O1W	X		2,305	,394714
O1W	X		,7171	,627376
O1W	Y		,2137	1,0
O2W	X	7		
O2W	X	8		
O1W	Y	7		
O1W	Y	8		
O2W	Y	7		
O2W	Y	8		
O1W	Z	7		
O1W	Z		,2137	
O2W	Z	7		
O2W	Z		,2137	
NW	S		5909,	,001190
NW	S		887,5	,009099
NW	S		204,7	,044145
NW	S		59,84	,150464
NW	S		20,00	,356741
NW	S		7,193	,446533
NW	S		2,686	,145603
NW	S		7,193	-,162405
NW	S		,7000	1,050215
NW	S		,3133	1,0000
NW	X		26,79	,016254
NW	X		5,956	,116461
NW	X		1,707	,340178
NW	X		,5318	,637102
NW	X		,1654	1,0000
NW	Y	22		
NW	Y	23		
NW	Z	22		
NW	Z	23		
CW	S		4233,	,001220
CW	S		634,9	,009342
CW	S		146,1	,045452
CW	S		42,50	,154657
CW	S		14,19	,358866
CW	S		5,148	,430632
CW	S		1,967	,145918
CW	S		5,148	-,160367
CW	S		,4962	1,000091
CW	S		,1533	1,00000
CW	X		18,16	,018539
CW	X		3,986	,115436
CW	X		1,143	,366188
CW	X		,3594	,640114
CW	X		,1146	1,00000
CW	Y	31		
CW	Y	32		
CW	Z	31		
CW	Z	32		
BNO1	S		1,5000000	
BNO2	S		1,5000000	
BNC	S		1,287	
BNO1	X		,88	
BNO2	X		,88	
BNO1	Y		,88	
BNO2	Y		,88	
BNO1	Z		,88	
BNO2	Z		,88	
BNC	X		,75	
BNC	Y		,75	
BNC	Z		,75	
H1W	S		13,36	,032828
H1W	S		2,013	,231204
H1W	S		,4538	,817226
H1W	S		,1233	1,00000
H2W	S	49		
H2W	S	50		
H3W	S	49		
H3W	S	50		
BCH1	S		,75	
BCH2	S		,75	
BCH3	S		,75	

Table C2.

```
NITRO, S,P,O FNS, NBF=88
  7  6
N          0.0           0.0           0.0           7.0
O1         1.062081      2.054916      0.0           8.0
O2         1.062041     -2.054916      0.0           8.0
C         -2.813085      0.0           0.0           6.0
H1        -3.419281      .9819151     -1.700777      1.0
H2        -3.419281      .9819151      1.700777      1.0
H3        -3.419281     -1.963830      0.0           1.0
BNO1       .5310205      1.027458      0.0
BNO2       .5310205     -1.027458      0.0
BNC       -1.400543      0.0           0.0
BCH1      -3.116163      .4909576     -.8503885
BCH2      -3.116163      .4909576      .8503885
BCH3      -3.116163     -.981915       0.0
150 88
 7 2 1 7 2 1 4 1 4 1 4 1 4 1 4 1 4 1 1 1 1 1 1 1 1 1 1 1 1 1 7 2 1 4 1 4
 1 4 1 1 1 1 1 1 1 7 2 1 4 1 4 1 4 1 1 1 1 1 1 1 1 1 1 1 1 1 1 1 1 1 1 3
 1 3 1 3 1 1 1 1
O1         S             7817.         .001176
O1         S             1176.         .000968
O1         S             273.2         .042688
O1         S             81.17         .143930
O1         S             27.18         .355030
O1         S             9.532         .461248
O1         S             3.414         .140206
O1         S             9.532        -.154153
O1         S              .9398        1.006914
O1         S              .2846        1.0
O2         S     1
O2         S     2
O2         S     3
O1         X             35.18         .019580
O1         X             7.904         .124200
O1         X             2.305         .394714
O1         X              .7171        .627376
O1         X              .2137        1.0
O2         X     7
O2         X     8
O1         Y     7
O1         Y     8
O2         Y     7
O2         Y     8
O1         Z     7
O1         Z              .2137
O2         Z     7
O2         Z              .2137
O1         XX            1.0
O2         XX            1.0
O1         YY            1.0
O2         YY            1.0
O1         ZZ            1.0
O2         ZZ            1.0
O1         XY            1.0
O2         XY            1.0
O1         XZ            1.0
O2         XZ            1.0
O1         YZ            1.0
O2         YZ            1.0
N          S             5909.         .001190
N          S             887.5         .009099
N          S             204.7         .044145
N          S             59.84         .150464
N          S             20.00         .356741
N          S             7.193         .446533
N          S             2.886         .145603
N          S             7.193        -.160405
N          S              .7000        1.058215
N          S              .3133        1.0000
N          X             26.79         .018254
N          X             5.956         .116461
N          X             1.707         .390178
N          X              .5314        .637102
N          X              .1654        1.0000
N          Y     34
N          Y     35
N          Z     34
N          Z     35
N          XX             .800
N          YY             .800
N          ZZ             .800
N          XZ             .800
N          YZ             .800
N          XY             .800
C          S             4233.         .001220
C          S              634.9        .009342
C          S              146.1        .045452
C          S              42.50        .154657
C          S              14.19        .358666
C          S              5.148        .438632
C          S              1.967        .145918
C          S              5.148       -.168367
C          S              .4962        1.060091
C          S              .1533        1.00000
C          X             18.16         .018539
C          X             3.986         .115436
C          X             1.143         .386188
C          X              .3594        .640114
C          X              .1146        1.00000
C          Y     49
C          Y     50
C          Z     49
C          Z     50
C          XX             .800        BNC       Z              .75
C          ZZ             .800        H1        S             13.36         .03282
C          XZ             .800        H1        S              2.013        .23123
C          YZ             .800        H1        S              .4538        .81723
C          XY             .800        H1        S              .1233        1.0003
BNO1       S             1.5000000    H2        S     73
BNO2       S             1.5000000    H2        S     74
BNC        S             1.287        H3        S     73
BNO1       X              .88         H3        S     74
BNO2       X              .88         BCH1      S              .75
BNO1       Y              .88         BCH2      S              .75
BNO2       Y              .88         BCH3      S              .75
BNO1       Z              .88
BNO2       Z              .88
BNC        X              .75
BNC        Y              .75
```

Table C3.

```
NITRO, S,P,D FNS, NBF=81,                                                    1
  7  6
N          0,0             0,0             0,0             7,0
O1         1,062041        2,054916        0,0             8,0
O2         1,062041        -2,054916       0,0             8,0
C          -2,813085       0,0             0,0             6,0
H1         -3,419281       ,9819151        -1,700777       1,0
H2         -3,419281       ,9819151        1,700777        1,0
H3         -3,419281       -1,963830       0,0             1,0
BNO1       ,5310205        1,027458        0,0
BNO2       ,5310205        -1,027458       0,0
BNC        -1,466543       0,0             0,0
BCM1       -3,116183       ,4909576        -,8503885
BCM2       -3,116183       ,4909576        ,8503885
BCM3       -3,116183       -,981916        0,0
151 81
 7 2 1 7 2 1 4 1 4 1 4 1 4 1 4 1 1 1 1 1 1 1 1 1 1 1 1 7 2 1 4 1 4
  1 4 1 1 1 1 1 1 7 2 1 4 1 4 1 4 1 1 1 1 1 1 1 1 1 1 1 1 1 1 1 1 1
  3 1 3 1 3 1 1 1 1
O1         S               7817,           ,001176
O1         S               1176,           ,008968
O1         S               273,2           ,042668
O1         S               81,17           ,143930
O1         S               27,18           ,355630
O1         S               9,532           ,461248
O1         S               3,414           ,140206
O1         S               9,532           -,154153
O1         S               ,9398           1,056914
O1         S               ,2846           1,0
O2         S       1
O2         S       2
O2         S       3
O1         X               35,18           ,019580
O1         X               7,904           ,124200
O1         X               2,305           ,394714
O1         X               ,7171           ,627376
O1         X               ,2137           1,0
O2         X       7
O2         X       8
O1         Y       7
O1         Y       8
O2         Y       7
O2         Y       8
O1         Z       7
O1         Z               ,2137
O2         Z       7
O2         Z               ,2137
O1         XX              1,0
O2         XX              1,0
O1         YY              1,0
O2         YY              1,0
O1         ZZ              1,0
O2         ZZ              1,0
O1         XY              1,0
O2         XY              1,0
O1         XZ              1,0
O2         XZ              1,0
O1         YZ              1,0
O2         YZ              1,0
N          S               5909,           ,001190
N          S               887,5           ,009099
N          S               204,7           ,044145
N          S               59,88           ,150464
N          S               20,00           ,356741
N          S               7,193           ,446533
N          S               2,686           ,145603
N          S               7,193           -,160405
N          S               ,7000           1,058215
N          S               ,3133           1,0000
N          X               26,79           ,018254
N          X               5,956           ,116461
N          X               1,707           ,390178
N          X               ,5314           ,637102
N          X               ,1654           1,0000
N          Y       34
N          Y       35
N          Z       34
N          Z       35
N          XX              ,800
N          YY              ,800
N          ZZ              ,800
N          XZ              ,800
N          YZ              ,800
N          XY              ,800
C          S               4233,           ,001220
C          S               634,9           ,009342
C          S               146,1           ,045452
C          S               42,50           ,154657
C          S               14,19           ,358066
C          S               5,148           ,438632
C          S               1,967           ,145918
C          S               5,148           -,168367
C          S               ,4962           1,060091
C          S               ,1533           1,00000
C          X               18,16           ,018539
C          X               3,986           ,115436
C          X               1,143           ,386168
C          X               ,3594           ,640114
C          X               ,1146           1,00000
C          Y       49
C          Y       50
C          Z       49
C          Z       50
C          XX              ,800
C          ZZ              ,800
C          XZ              ,800
C          YZ              ,800
C          XY              ,800
BNO1       S               1,5000000
BNO2       S               1,5000000
BNC        S               1,287
BNO1       X               ,88
BNO2       X               ,88
BNO1       Y               ,88
BNO2       Y               ,88
BNO1       Z               ,88
BNO2       Z               ,88
BNC        X               ,75
BNC        Y               ,75
BNC        Z               ,75
C          YY              1,00
H1         S               13,36           ,0328
H1         S               2,013           ,2312
H1         S               ,4538           ,8172
H1         S               ,1233           1,000
H2         S       73
H2         S       74
H3         S       73
H3         S       74
BCM1       S               ,75
BCM2       S               ,75
BCM3       S               ,75
```

Table C4.

```
NITRO, 4S,2P,1D ON NO2, 3S,2P,1D ON C W/BOND8                                  1
  7  6
N          0.0           0.0           0.0           7.0
O1         1.062041      2.054916      0.0           8.0
O2         1.062041     -2.054916      0.0           8.0
C         -2.813085      0.0           0.0           6.0
H1        -3.419281      .9819151     -1.700777      1.0
H2        -3.419281      .9819151      1.700777      1.0
H3        -3.419281     -1.963830      0.0           1.0
BNO1       .5310205      1.027458      0.0
BNO2       .5310205     -1.027458      0.0
BNC       -1.406543      0.0           0.0
BCH1      -3.116183      .4909576     -.8503885
BCH2      -3.116183      .4909576      .8503883
BCH3      -3.116183     -.981915       0.0
148 88
 6 1 1 1 6 1 1 1 4 1 4 1 4 . 4 1 4 1 4 1 1 1 1 1 1 1 1 1 1 1 1 1 6 1 1 1
 4 1 4 1 4 1 1 1 1 1 1 1 7 2 1 4 1 4 1 4 1 1 1 1 1 1 1 1 1 1 1 1 1 1 1 1
 1 1 1 3 1 3 1 3 1 1 1 1
O1         S             7817.         .002031
O1         S             1176.         .015436
O1         S             273.2         .073771
O1         S             81.17         .247606
O1         S             27.18         .611032
O1         S             3.414         .241205
O1         S             9.532         1.0
O1         S             .9398         1.0
O1         S             .2846         1.0
O2         S     1
O2         S     2
O2         S     3
O2         S     4
O1         X             35.18         .019500
O1         X             7.904         .124189
O1         X             2.305         .394727
O1         X             .7171         .627376
O1         X             .2137         1.0
O2         X     9
O2         X    10
O1         Y     9
O1         Y    10
O2         Y     9
O2         Y    10
O1         Z     9
O1         Z    10
O2         Z     9
O2         Z    10
O1         XX            .8
O2         XX            .8
O1         YY            .8
O2         YY            .8
O1         ZZ            .8
O2         ZZ            .8
O1         XY            .8
O2         XY            .8
O1         XZ            .8
O2         XZ            .8
O1         YZ            .8
O2         YZ            .8

BNC        Z             .75
H1         S             13.36         .032828
H1         S             2.013         .231204
H1         S             .4538         .817226
H1         S             .1233         1.00000
H2         S     76
H2         S     77
H3         S     76
H3         S     77
BCH1       S             .75
BCH2       S             .75
BCH3       S             .75

N          S             5909.         .002004
N          S             887.5         .015310
N          S             204.7         .074293
N          S             59.84         .253364
N          S             20.00         .600576
N          S             2.606         .245111
N          S             7.193         1.0
N          S             .7000         1.0
N          S             .2133         1.0
N          X             26.79         .018257
N          X             5.956         .116407
N          X             1.707         .390111
N          X             .5314         .637221
N          X             .1654         1.0000
N          Y     37
N          Y     38
N          Z     37
N          Z     38
N          XX            .800
N          YY            .800
N          ZZ            .800
N          XZ            .800
N          YZ            .800
N          XY            .800
C          S             4233.         .001220
C          S             634.9         .009342
C          S             146.1         .045452
C          S             42.50         .154657
C          S             14.19         .358866
C          S             5.148         .438632
C          S             1.967         .145918
C          S             5.148         -.168367
C          S             .4962         1.060091
C          S             .1533         1.00000
C          X             18.16         .018539
C          X             3.986         .115436
C          X             1.143         .366188
C          X             .3594         .640114
C          X             .1146         1.00000
C          Y     52
C          Y     53
C          Z     52
C          Z     53
C          XX            .800
C          ZZ            .800
C          XZ            .800
C          YZ            .800
C          XY            .800
C          YY            .800
BNO1       S             1.5000000
BNO2       S             1.5000000
BNC        S             1.287
BNO1       X             .88
BNO2       X             .88
BNO1       Y             .88
BNO2       Y             .88
BNO1       Z             .88
BNO2       Z             .88
BNC        X             .75
BNC        Y             .75
```

Table C5.

CENTRAL NITRO

14 6

NN	0.0	0.0	0.0	7.0
O1N	1.091	2.023	0.0	8.0
O2N	1.091	-2.023	0.0	8.0
CN	-2.798	0.0	0.0	6.0
H1N	-3.417	-1.716	-0.991	1.0
H2N	-3.417	0.0	1.982	1.0
H3N	-3.417	1.716	-0.991	1.0
BN01	0.545	1.011	0.0	
BN02	0.545	-1.011	0.0	
BNC	-1.399	0.0	0.0	
BCH1	-3.108	-0.858	-0.495	
BCH2	-3.108	0.0	0.991	
BCH3	-3.108	0.858	-0.495	

NEAR NEIGHBOR -111 03

	NA	-1.7634	-0.1076	7.4015	5.0
NLP	O1A	-0.3554	-1.0323	5.8079	6.0
OLP	O2A	-2.4940	2.0501	7.1896	6.0
OLP	CA	-2.5138	-1.6709	9.6919	4.0
CLP	H1A	-2.8121	-0.4212	11.2556	1.0
	H2A	-4.2335	-2.6446	9.1917	1.0
	H3A	-1.0314	-2.9800	10.1388	1.0

NEAR NEIGHBOR 011 03

	NA	6.1286	3.4267	2.4153	5.0
NLP	O1A	7.5066	2.5019	0.8217	6.0
OLP	O2A	5.3081	5.5843	2.2032	6.0
OLP	CA	5.3442	1.8631	4.7055	4.0
CLP	H1A	5.0499	3.1130	6.2692	1.0
	H2A	3.6285	0.8896	4.2055	1.0
	H3A	6.8301	0.5543	5.1526	1.0

NEAR NEIGHBOR 021 03

	NA	-0.8811	8.5353	-5.8408	5.0
NLP	O1A	0.4071	7.6108	-7.4344	6.0
OLP	O2A	-1.6715	10.6932	-6.0529	6.0
OLP	CA	-1.6913	8.9720	-3.5505	4.0
CLP	H1A	-1.9096	8.2217	-1.9870	1.0
	H2A	-3.4110	5.9983	-4.0507	1.0
	H3A	-0.2096	5.6629	-3.1036	1.0

NEAR NEIGHBOR -121 03

	NA	-8.7431	5.0013	-0.8546	5.0
NLP	O1A	-7.3949	4.0766	-2.4482	6.0
OLP	O2A	-9.5335	7.1590	-1.0665	6.0
OLP	CA	-9.5533	3.4378	1.4357	4.0
CLP	H1A	-9.8516	4.6075	2.9994	1.0
	H2A	-11.2730	2.4641	0.9355	1.0
	H3A	-8.0715	2.1289	1.8026	1.0

NEAR NEIGHBOR 000 04

	NA	-9.1457	-3.3342	-2.7155	5.0
NLP	O1A	-10.4299	-5.2165	-2.9832	6.0
OLP	O2A	-8.4202	-2.6295	-0.6070	6.0
OLP	CA	-8.3340	-1.8319	-5.0465	4.0
CLP	H1A	-8.1079	0.1000	-4.5019	1.0
	H2A	-6.5762	-2.5837	-5.6096	1.0
	H3A	-9.7817	-2.0221	-6.4866	1.0

NEAR NEIGHBOR 0-10 04

	NA	-2.1060	-8.4429	5.5406	5.0
NLP	O1A	-3.3402	-10.3274	5.2730	6.0
OLP	O2A	-1.3807	-7.7384	7.6491	6.0
OLP	CA	-1.2443	-6.9408	3.2096	4.0
CLP	H1A	-1.0684	-5.0087	3.7541	1.0
	H2A	0.4647	-7.6926	2.5665	1.0
	H3A	-2.7422	-7.1308	1.7696	1.0

NEAR NEIGHBOR 1-10 04

	NA	5.7560	-4.9087	0.5543	5.0
NLP	O1A	4.4718	-6.7932	0.2868	6.0
OLP	O2A	6.4813	-4.2042	2.6628	6.0
OLP	CA	6.5677	-3.4066	-1.7766	4.0
CLP	H1A	6.7936	-1.4745	-1.2321	1.0
	H2A	8.3267	-4.1584	-2.4197	1.0
	H3A	5.1198	-3.5966	-3.2166	1.0

NEAR NEIGHBOR 100 04

	NA	-1.2837	0.2000	-7.7019	5.0
NLP	O1A	-2.5679	-1.6843	-7.9694	6.0
OLP	O2A	-0.5562	0.9047	-5.5934	6.0
OLP	CA	-0.4720	1.7023	-10.0327	4.0
CLP	H1A	-0.2459	3.6342	-9.4883	1.0
	H2A	1.2670	0.9503	-10.6758	1.0
	H3A	-2.0848	1.5121	-11.4728	1.0

Table C6.

```
NITROMETHANE,CONTRACTED SLT W/PSEUDOPOTS FOR CLUSTER
                                                                    1
  7
N          0.0           0.0           0.0           5.0          NLP
O1         1.062041      2.054916      0.0           6.0          OLP
O2         1.062041     -2.054916      0.0           6.0          OLP
C         -2.813085      0.0           0.0           4.0          CLP
H1        -3.419281      .9819151     -1.700777      1.0
H2        -3.419281      .9819151      1.700777      1.0
H3        -3.419281     -1.963830      0.0           1.0
 35 35
  1  2  3  4  5  6  7  8  9 10 11 12 13 14 15 16 17 18 19 20 21 22 23 24 25 26 27 28 29 30 31 32 33 34 35
O1         S                14.0          1.0
O1         S                 .75          1.0
O2         S     1
O2         S     2
O1         X                2.3           1.0
O1         X                 .40          1.0
O2         X     5
O2         X     6
O1         Y     5
O1         Y     6
O2         Y     5
O2         Y     6
O1         Z     5
O1         Z     6
O2         Z     5
O2         Z     6
N          S                12.0          1.0
N          S                 .50          1.0
N          X                1.5           1.0
N          X                 .40          1.0
N          Y    19
N          Y    20
N          Z    19
N          Z    20
C          S                6.0           1.0
C          S                 .30          1.0
C          X                1.25          1.0
C          X                 .225         1.0
C          Y    27
C          Y    28
C          Z    27
C          Z    28
H1         S                0.9           1.0
H2         S    33
H3         S    33

  NITROGEN LOCAL POTENTIAL
    2
  V(D)
    3
1                8.00000000D+01-1.60000000D+00
1                3.00000000D+01-0.40000000D+00
2                0.76280000D+00-0.04990000D+00
  V(P-D)
    2
2                1.94884000D+01-1.11778000D+01
2                2.83756000D+01 1.21413000D+01
  V(S-D)
    3
0                0.87220000D+00 0.52790000D+00
0                4.81739600D+01 3.51510000D+00
2                9.38610000D+00 2.01290000D+01

  OXYGEN LOCAL POTENTIAL
    2
  V(D)
    3
1                8.00000000D+01-1.60000000D+00
1                3.00000000D+01-0.40000000D+00
2                1.09540000D+00-0.06620000D+00
  V(P-D)
    2
2                5.23427000D+01 2.79779000D+01
2                3.07220000D+01-1.64963000D+01
  V(S-D)
    3
0                0.92130000D+00 0.39550000D+00
0                2.86422000D+01 2.51650000D+00
2                9.30330000D+00 1.70486000D+01
  CARBON LOCAL POTENTIAL
    2
  V(D)
    3
1                8.00000000D+01-1.60000000D+00
1                3.00000000D+01-0.40000000D+00
2                0.54960000D+00-0.03990000D+00
  V(P-D)
    2
2                1.06864000D+01-3.24680000D+00
2                2.34980000D+01 0.78510000D+00
  V(S-D)
    3
0                0.73750000D+00 0.63810000D+00
0                1.35235500D+02 1.10092000D+01
2                8.56864000D+00 2.01360000D+01
```

Table C7.

CENTRAL NITRO WITH ONE NEAR NEIGHBOR

```
 14  6
NW          0.0          0.0          0.0          7.0
O1W         1.091        2.023        0.0          8.0
O2W         1.091       -2.023        0.0          8.0
CW         -2.798        0.0          0.0          6.0
H1W        -3.417       -1.716       -0.991        1.0
H2W        -3.417        0.0          1.982        1.0
H3W        -3.417        1.716       -0.991        1.0
NA         -1.7028      -0.8854       7.4013       5.0          NLP
O1A        -0.3539      -1.0316       5.8085       6.0          OLP
O2A        -2.4298       2.0805       7.1890       6.0          OLP
CA         -2.5127      -1.6703       9.6919       4.0          CLP
H1A        -2.8112      -0.4200      11.2552       1.0
H2A        -4.2121      -2.6435       9.1909       1.0
H3A        -1.0314      -2.4785      10.1399       1.0
BNO1        0.545        1.011        0.0
BNO2        0.545       -1.011        0.0
BNC        -1.399        0.0          0.0
BCH1       -3.108       -0.858       -0.495
BCH2       -3.108        0.0          0.991
BCH3       -3.108        0.858       -0.495
162 92
 7 2 1 7 2 1 4 1 4 1 4 1 4 1 4 1 4 1 4 1 7 2 1 4 1 4 1 4 1 7 2 1 4 1 4 1 4 1
 1 1 1 1 1 1 1 1 1 1 1 1 1 1 3 1 3 1 3 1 1 1 1 1 1 1 1 1 1 1 1 1 1 1 1 1 1 1
 1 1 1 1 1 1 1 1 1 1 1 1 1 1 1 1 1 1 1 1 1 1 1 1 1 1 1 1 1 1 1 1 1 1 1 1 1 1
O1W         S                 7617.        .001176
O1W         S                 1176.        .006968
O1W         S                 273.2        .042668
O1W         S                 61.17        .143930
O1W         S                 27.18        .356830
O1W         S                 9.532        .461248
O1W         S                 3.414        .140206
O1W         S                 9.532       -.154153
O1W         S                 .9398        1.056914
O1W         S                 .2846        1.0
O2W         S        1
O2W         S        2
O2W         S        3
O1W         X                 35.18        .019580
O1W         X                 7.904        .124200
O1W         X                 2.305        .394714
O1W         X                 .7171        .627376
O1W         X                 .2137        1.0
O2W         X        7
O2W         X        8
O1W         Y        7
O1W         Y        8
O2W         Y        7
O2W         Y        8
O1W         Z        7
O1W         Z                 .2137
O2W         Z        7
O2W         Z                 .2137
NW          S                 5909.        .001190
NW          S                 887.5        .009099
NW          S                 204.7        .044145
NW          S                 59.84        .150464
NW          S                 20.00        .356741
NW          S                 7.193        .846533
NW          S                 2.686        .145603
NW          S                 7.193       -.160405
NW          S                 .7000        1.058215
NW          S                 .3133        1.0000
NW          X                 26.79        .018254
NW          X                 5.956        .116461
NW          X                 1.707        .390178
NW          X                 .5314        .637102
NW          X                 .1654        1.0000
NW          Y        22
NW          Y        23
NW          Z        22
NW          Z        23
CW          S                 4233.        .001220
CW          S                 634.9        .009342
CW          S                 146.1        .045452
CW          S                 42.50        .158657
CW          S                 14.19        .358866
CW          S                 5.148        .838632
CW          S                 1.967        .145918
CW          S                 5.148       -.168367
CW          S                 .4962        1.000091
CW          S                 .1533        1.00000
CW          X                 18.16        .019439
CW          X                 3.966        .115436
CW          X                 1.143        .356178
CW          X                 .3594        .642114
CW          X                 .1146        1.00000
CW          Y        31
CW          Y        32
CW          Z        31
CW          Z        32
BNO1        S                 1.5000000
BNO2        S                 1.5000000.
BNC         S                 1.287
BNO1        X                 .88
BNO2        X                 .88
BNO1        Y                 .88
BNO2        Y                 .88
BNO1        Z                 .88
BNO2        Z                 .88
BNC         X                 .75
BNC         Y                 .75
BNC         Z                 .75
H1W         S                 13.36        .032828
H1W         S                 2.013        .231204
H1W         S                 .4538        .617226
H1W         S                 .1233        1.00000
H2W         S        49
H2W         S        50
H3W         S        49
H3W         S        50
BCH1        S                 .75
BCH2        S                 .75
BCH3        S                 .75
O1A         S                 14.0         1.0
O1A         S                 .75          1.0
O2A         S        58
O2A         S        59
```

Table C8.

```
O1A       X          2.3          1.0
O1A       X          .80          1.0
O2A       X    62
O2A       X    63
O1A       Y    62
O1A       Y    63
O2A       Y    62
O2A       Y    63
O1A       Z    62
O1A       Z    63
O2A       Z    62
O2A       Z    63
NA        S         12.0          1.0
NA        S          .50          1.0
NA        X          1.5          1.0
NA        X          .40          1.0
NA        Y    76
NA        Y    77
NA        Z    76
NA        Z    77
CA        S          6.0          1.0
CA        S          .30          1.0
CA        X          1.25         1.0
CA        X          .225         1.0
CA        Y    84
CA        Y    85
CA        Z    84
CA        Z    85
H1A       S          0.9           1.0
H2A       S    90
H3A       S    90
1.0D-9
```

```
 NITROGEN LOCAL POTENTIAL
   2
 V(D)
   3
1                 8.00000000D+01-1.60000000D+00
1                 3.00000000D+01-0.40000000D+00
2                 0.76280000D+00-0.04990000D+00
 V(P-D)
   2
2                 1.94884000D+01-1.11778000D+01
2                 2.83756000D+01 1.21413000D+01
 V(S-D)
   3
0                 0.87220000D+00 0.52790000D+00
0                 4.81734000D+01 3.51510000D+00
2                 9.36610000D+00 2.01298000D+01
 OXYGEN LOCAL POTENTIAL
   2
 V(D)
   3
1                 8.00000000D+01-1.60000000D+00
1                 3.00000000D+01-0.40000000D+00
2                 1.09540000D+00-0.06620000D+00
 V(P-D)
   2
2                 5.23427000D+01 2.79779000D+01
2                 3.07220000D+01-1.64963000D+01
 V(S-D)
   3
0                 0.92130000D+00 0.39550000D+00
0                 2.86452000D+01 2.51650000D+00
2                 9.30330000D+00 1.70448000D+01
 CARBON LOCAL POTENTIAL
   2
 V(D)
   3
1                 8.00000000D+01-1.60000000D+00
1                 3.00000000D+01-0.40000000D+00
2                 0.54980000D+00-0.03990000D+00
 V(P-D)
   2
2                 1.06864000D+01-3.24660000D+00
2                 2.34960000D+01 0.78510000D+00
 V(S-D)
   3
0                 0.73750000D+00 0.63810000D+00
0                 1.35235500D+02 1.10920000D+01
2                 8.56060000D+00 2.01380000D+01
```

Table C8. (continued)

```
NITRO TRIMER -111 03 AND 011 03
 21  6                                                                  1
NW          0,0           0,0           0,0           7,0
O1W         1,091         2,023         0,0           8,0
O2W         1,091         -2,023        0,0           8,0
CW          -2,798        0,0           0,0           6,0
H1W         -3,417        -1,716        -0,991        1,0
H2W         -3,417        0,0           1,982         1,0
H3W         -3,417        1,716         -0,991        1,0
NA          -1,7038       -0,1076       7,4015        5,0           NLP
O1A         -0,3558       -1,0323       5,8079        6,0           OLP
O2A         -2,4940       2,0501        7,1896        6,0           OLP
CA          -2,5138       -1,6709       9,6919        4,0           CLP
H1A         -2,8121       -0,4212       11,2556       1,0
H2A         -4,2335       -2,5446       9,1917        1,0
H3A         -1,0314       -2,9806       10,1388       1,0
NB          6,1596        3,4267        2,4153        5,0           NLP
O1B         7,5066        2,5019        0,8217        6,0           OLP
O2B         5,3681        5,5943        2,2032        6,0           OLP
CB          5,3482        1,8631        4,7055        4,0           CLP
H1B         5,0499        3,1130        6,2692        1,0
H2B         3,6285        0,8896        4,2055        1,0
H3B         6,8301        0,5543        5,1526        1,0
BND1        0,545         1,011         0,0
BND2        0,545         -1,011        0,0
BNC         -1,399        0,0           0,0
BCH1        -3,168        -0,858        -0,495
BCH2        -3,108        0,0           0,991
BCH3        -3,108        0,858         -0,495
19712?
 7 2 1 7 2 1 4 1 4 1 4 1 4 1 4 1 7 2 1 4 1 4 1 4 1 7 2 1 4 1 4 1 4 1
 1 1 1 1 1 1 1 1 1 1 1 3 1 3 1 3 1 1 1 1 1 1 1 1 1 1 1 1 1 1 1 1 1 1
 1 1 1 1 1 1 1 1 1 1 1 1 1 1 1 1 1 1 1 1 1 1 1 1 1 1 1 1 1 1 1 1 1 1
 1 1 1 1 1 1 1 1 1 1 1 1 1 1 1 1 1 1 1 1 1 1 1 1 1 1 1 1 1 1 1 1 1 1
O1W         S             7817,         ,001176
O1W         S             1176,         ,008968
O1W         S             273,2         ,042868
O1W         S             81,17         ,143930
O1W         S             27,18         ,355030
O1W         S             7,532         ,461248
O1W         S             3,414         ,140206
O1W         S             9,532         -,154153
O1W         S             ,9398         1,056914
O1W         S             ,2846         1,0
O2W         S     1
O2W         S     2
O2W         S     3
O1W         X             35,18         ,019580
O1W         X             7,904         ,124200
O1W         X             2,305         ,394714
O1W         X             ,7171         ,627376
O1W         X             ,2137         1,0
O2W         X     7
O2W         X     8
O1W         Y     7
O1W         Y     8
O2W         Y     7
O2W         Y     8
O1W         Z     7
O1W         Z           ,2137
O2W         Z     7
O2W         Z           ,2137
NW          S           5909,         ,001190
NW          S           887,5         ,009099
NW          S           204,7         ,044145
NW          S           59,84         ,150464
NW          S           20,00         ,356741
NW          S           7,193         ,446533
NW          S           2,686         ,145603
NW          S           7,193         -,160405
NW          S           ,7000         1,058215
NW          S           ,3133         1,0000
NW          X           26,79         ,018254
NW          X           5,956         ,110461
NW          X           1,707         ,360178
NW          X           ,5314         ,637102
NW          X           ,1654         1,0000
NW          Y     22
NW          Y     23
NW          Z     22
NW          Z     23
CW          S           4233,         ,001220
CW          S           634,9         ,009342
CW          S           146,1         ,045452
CW          S           42,50         ,156657
CW          S           14,19         ,350866
CW          S           5,148         ,439632
CW          S           1,967         ,145818
CW          S           5,148         -,108367
CW          S           ,4962         1,000091
CW          S           ,1533         1,00000
CW          X           18,16         ,015539
CW          X           3,986         ,115436
CW          X           1,143         ,361188
CW          X           ,3594         ,640114
CW          X           ,1146         1,00000
CW          Y     31
CW          Y     32
CW          Z     31
CW          Z     32
BND1        S           1,5000000
BND2        S           1,5000000
BNC         S           1,287
BND1        X           ,88
BND2        X           ,88
BND1        Y           ,88
BND2        Y           ,88
BND1        Z           ,88
BND2        Z           ,88
BNC         X           ,75
BNC         Y           ,75
BNC         Z           ,75
H1W         S           13,36         ,032828
H1W         S           2,013         ,231204
H1W         S           ,4538         ,817226
H1W         S           ,1233         1,00000
H2W         S     49
H2W         S     50
H3W         S     49
```

Table C9.

```
H3M      S  50
BCH1     S                .75
BCH2     S                .75
BCH3     S                .75
O1A      S                1.0      1.0
O1A      S                .75
O2A      S  58
O2A      S  59
O1A      X                2.3      1.0
O1A      X                .40      1.0
O2A      X  62
O2A      X  63
O1A      Y  62
O1A      Y  63
O2A      Y  62
O2A      Y  63
O1A      Z  62
O1A      Z  63
O2A      Z  62
O2A      Z  63
NA       S                12.0     1.0
NA       S                .50      1.0
NA       X                1.5      1.0
NA       X                .40      1.0
NA       Y  76
NA       Y  77
NA       Z  76
NA       Z  77
CA       S                8.0      1.0
CA       S                .30      1.0
CA       X                1.25     1.0
CA       X                .225     1.0
CA       Y  84
CA       Y  85
CA       Z  84
CA       Z  85
H1A      S                0.9      1.0
H2A      S  90
H3A      S  90
O1B      S                18.0     1.0
O1B      S                .75      1.0
O2B      S  58
O2B      S  59
O1B      X                2.3      1.0
O1B      X                .40      1.0
O2B      X  62
O2B      X  63
O1B      Y  62
O1B      Y  63
O2B      Y  62
O2B      Y  63
O1B      Z  62
O1B      Z  63
O2B      Z  62
O2B      Z  63
NB       S                12.0     1.0
NB       S                .50      1.0
NB       X                1.5      1.0
NB       X                .40      1.0
NB       Y  76
NB       Y  77
NB       Z  76
NB       Z  77
CB       S                8.0      1.0
CB       S                .30      1.0
CB       X                1.25     1.0
CB       X                .225     1.0
CB       Y  84
CB       Y  85
CB       Z  84
CB       Z  85
H1B      S                0.9      1.0
H2B      S  90
H3B      S  90

  NITROGEN LOCAL POTENTIAL
    2
  V(D)
    3
1                8.00000000D+01-1.60000000D+00
1                3.00000000D+01-0.40000000D+00
2                0.76280000D+00-0.04990000D+00
  V(P-D)
    2
2                1.94804000D+01-1.11778000D+01
2                2.83756000D+01 1.21413000D+01
  V(S-D)
    3
0                0.87220000D+00 0.52790000D+00
0                4.81739000D+01 3.51510000D+00
2                9.38610000D+00 2.01298000D+01
  OXYGEN LOCAL POTENTIAL
    2
  V(D)
    3
1                8.00000000D+01-1.60000000D+00
1                3.00000000D+01-0.40000000D+00
2                1.09540000D+00-0.06620000D+00
  V(P-D)
    2
2                5.23427000D+01 2.79779000D+01
2                3.07220000D+01-1.64963000D+01
  V(S-D)
    3
0                0.92130000D+00 0.39550000D+00
0                2.86482000D+01 2.51650000D+00
2                9.30330000D+00 1.70448000D+01
  CARBON LOCAL POTENTIAL
    2
  V(D)
    3
1                8.00000000D+01-1.60000000D+00
1                3.00000000D+01-0.40000000D+00
2                0.54980000D+00-0.03990000D+00
  V(P-D)
    2
2                1.06864000D+01-3.24680000D+00
2                2.34940000D+01 0.78510000D+00
  V(S-D)
    3
0                0.73750000D+00 0.63810000D+00
0                1.35235000D+02 1.10092000D+01
2                8.56000000D+00 2.01360000D+01
```

Table C9. (continued)

```
NO2 (4S,2P,1D) SET FROM DUNNING, 56 FNS.
  3  2
N          0.0           0.0           0.0          7.0
O1         0.879659      2.077386      0.0          8.0
O2         0.879659     -2.077386      0.0          8.0
BNO1       .4398295      1.038693      0.0
BNO2       .4398295     -1.038693      0.0
 98 56
 6 1 1 1 6 1 1 1 4 1 4 1 4 1 4 1 4 1 4 1 1 1 1 1 1 1 1 1 1 1 1 6 1 1 1
 4 1 4 1 4 1 1 1 1 1 1 1 1 1 1 1 1 1 1 1 1 1 1 1 1 1 1 1 1 1 1 1 1 1
O1         S             7817.         .002031
O1         S             1176.         .015436
O1         S             273.2         .073771
O1         S             81.17         .247606
O1         S             27.18         .611832
O1         S             3.414         .241205
O1         S             9.532         1.0
O1         S             .9398         1.0
O1         S             .2846         1.0
O2         S      1
O2         S      2
O2         S      3
O2         S      4
O1         X             35.18         .019580
O1         X             7.904         .124189
O1         X             2.305         .394727
O1         X             .7171         .627376
O1         X             .2137         1.0
O2         X      9
O2         X     10
O1         Y      9
O1         Y     10
O2         Y      9
O2         Y     10
O1         Z      9
O1         Z     10
O2         Z      9
O2         Z     10
O1         XX            .8
O2         XX            .8
O1         YY            .8
O2         YY            .80
O1         ZZ            .80
O2         ZZ            .80
O1         XY            .80
O2         XY            .80
O1         XZ            .80
O2         XZ            .60
O1         YZ            .80
O2         YZ            .80
N          S             5909.         .002004
N          S             [illegible]   [illegible]
N          S             204.7         .074293
N          S             59.84         .253364
N          S             20.00         .600576
N          S             2.686         .245111
N          S             7.193         1.0
N          S             .7000         1.0
N          S             .2133         1.0

N          X             26.79         .018257
N          X             5.956         .116407
N          X             1.707         .390111
N          X             .5314         .637221
N          X             .1654         1.0000
N          Y     37
N          Y     38
N          Z     37
N          Z     38
N          XX            .600
N          YY            .800
N          ZZ            .800
N          XZ            .800
N          YZ            .800
N          XY            .800
BNO1       S             1.5000000
BNO2       S             1.5000000
BNO1       X             .88
BNO2       X             .88
BNO1       Y             .88
BNO2       Y             .88
BNO1       Z             .88
BNO2       Z             .88
```

Table C10.

REFERENCES

1. D. A. Kleier and M. A. Lipton, J. Mol. Struct. (Theochem) 109, 39 (1984).

2. A. B. Kunz, Technical Report to the Office of Naval Research, (Dec. 1983), unpublished.

3. F. J. Zerilli and E. T. Toton, Phys. Rev. B 29 (10), 5891 (1984).

4. D. Cavagnat, A. Magerl, C. Vettier, I. S. Andersen and S. F. Trevino, Phys. Rev. Letts. 54 (3), 193 (1985).

5. E. Tannenbaum, R. J. Meyers and W. P. Gwinn, J. Chem. Phys. 25, 42 (1956).

6. D. Cavagnat, J. Lascombe, J. C. Lassegues, A. J. Horsewill, A. Heidemann and J. B. Suck, J. Phys. (Paris) 45, 67 (1984).

7. D. H. Tsai and S. F. Trevino, J. Chem. Phys. 79 (4), 1684 (Aug.15, 1983).

8. S. F. Trevino and D. H. Tsai, J. Chem. Phys. 81 (1), 248 (1984).

9. D. H. Tsai and S. F. Trevino, J. Chem. Phys. 81 (12), 5636 (1984).

10. R. H. Guirguis, JAYCOR Document, #J206-83-011/6223, (1983).

11. S. Nagakura, Mol. Phys. 3, 152 (1960).

12. E. S. Stern and J. C. Timmons, Electronic Absorption Spectroscopy in Organic Chemistry, 3rd edn. (St. Martin's Press, New York, 1971).

13. J. W. Rabalais, J. Chem. Phys. 57 (2), 960 (1972).

14. K. Lenore McEwen, J. Chem. Phys. 32 (6), 1801 (1960).

15. D. R. Beck and A. B. Kunz, J. Phys. B: At. Mol. Phys 17, 2159 (1984).

16. B. DiBartolo, ed., Energy Transfer Processes in Condensed Matter, NATO ASI Series: Series B: Physics, Vol. 114 (Plenum Press, New York, 1984).

17. R. S. Knox, Theory of Excitons (Academic Press, New York, 1984).

18. O. Madelung, Introduction to Solid-State Theory (Springer-Verlag, Berlin, 1981).

19. M. Born and R. Oppenheimer, Ann. Physik 84, 457 (1927).

20. D. R. Hartree, Proc. Cambridge Phil. Soc. 24, 111 (1928).

21. D. R. Beck, private communication.

22. J. C. Slater, Phys. Rev. 35, 210 (1930).

23. R. McWeeny and B. T. Sutcliffe, Methods of Molecular Quantum Mechanics (Academic Press, London, 1976).

24. H. F. Schaefer III, The Electronic Structure of Atoms and Molecules (Addison-Wesley, Reading, Mass., 1972).

25. W. G. Richards and D. L. Cooper, Ab Initio Molecular Orbital Calculations for Chemists, 2nd ed. (Clarendon Press, Oxford, 1983).

26. E. Clementi, J. Chem. Phys. 38, 2248 (1963).

27. E. Clementi and D. R. Davis, J. Comput. Phys. 2, 223 (1967).

28. S. Wilson, Electron Correlation in Molecules (Clarendon Press, Oxford, 1984).

29. P. O. Lowdin, Advan. Chem. Phys. 2, 207 (1959).

30. R. J. Bartlett and G. D. Purvis, Physica Scripta (Sweden) 21, 255 (1980).

31. H. P. Kelly, Phys. Rev. 131, 690 (1963).

32. D. R. Beck and C. A. Nicolaides, Excited States in Quantum Chemistry, D. R. Beck and C. A. Nicolaides, eds. (D. Reidel Publishers, Dordrecht, Holland, 1978).

33. S. F. Boys and F. Bernardi, Mol. Phys. 19 (4), 553 (1970).

34. P. D. Dacre, Mol. Phys. 37 (5), 1529 (1979).

35. B. J. Ransil, J. Chem. Phys. 34, 2109 (1961).

36. W. Kolos, G. Ranghino and E. Clementi, Int. J. Quan. Chem. 17, 429 (1980).

37. I. G. Csizmadia et. al., QCPE 11, 47 (1964).

38. P. Goalwin, private communication.

39. A. Cox and S. Waring, J. Chem. Soc. Far. Trans. 2 68, 1060 (1972).

40. T. H. Dunning, Jr., J. Chem. Phys. 53 (7), 2823 (1970)

41. S. Huzinaga, J. Chem. Phys. 42, 1293 (1965).

42. R. Ditchfield, W. J. Hehre and J. A. Pople, J. Chem. Phys. 52, 5001 (1970).

43. R. F. Stewart, J. Chem. Phys. 50, 2485 (1969)..

44. D. T. Clark and J. Miller, Theo. Chim. Acta. 41, 193 (1976).

45. D. B. Adams, J. Chem. Soc. Far. Trans. 2 72, 383 (1976).

46. I. H. Hillier, J. Kendrick, F. E. Mabbs and C. D. Gardner, J. Am. Chem. Soc. 98, 395 (1976).

47. J. M. Murrell and B. Vidal, J. Chem. Soc. Far. Trans. 2 71, 1577 (1975).

48. P. G. Mezey, A. J. Kresge and I. G. Csizmadia, Can. J. Chem. 54, 2526 (1976).

49. J. R. Murdoch, A. Streitwieser, Jr. and S. Gabriel, J. Am. Chem. Soc. 100 (20), 6338 (1978).

50. J. J. Kaufman, P. C. Hariharan, C. Chabalowski and M. Hotokaa, Int. J. Quan. Chem: Quantum Chemistry Symposium 19, 221 (1986).

51. E. R. Davidson, The World of Quantum Chemistry, R. Daudel and B. Pullman, eds. (Reidel Publishers, Dordercht, Holland, 1974).

52. J. Paldus, P. E. S. Wormer, F. Visser and A. van der Avoird Proceedings of the 5th Seminar on Computational Methods in Quantum Chemistry, Groningen, Netherlands, September 1983.

53. J. J. Kaufman, P. C. Hariharan and H. E. Popkie, Int. J. Quan. Chem. 515, 199 (1981).

54. D. S. Marynick, A. K. Ray, J. L. Fry and D. A. Kleier, J. Mol. Struct. 108, 45 (1984).

55. A. B. Kunz, private communication.

56. M. J. S. Dewar, M. Shansol and S. D. Worley, J. Am. Chem. Soc. 91, 3590 (1969).

57. T. Kobayashi and S. Nagakura, Chem. Letts., 903 (1972).

58. T. Fujikawa, T. Ohta and H. Kuroda, Chem. Phys. Letts. 28 (3), 433 (1974).

59. H. M. Niemeyer, Tetrahedron 35, 1297 (1979).

60. D. S. Marynick, A. K. Ray and J. L. Fry, Chem. Phys. Letts. 116 (5), 429 (1985).

61. E. Tannenbaum, R. J. Myers and W. D. Gwinn, J. Chem. Phys. 25, 42 (1956).

62. J. L. Corey and R. F. Firestone, J. Phys. Chem, 74 (7), 1425 (1970).

63. J. A. Pople and J. S. Binkley, Mol. Phys. 29 (2), 599 (1975).

64. N. C. Handy, J. D. Goddard and H. F. Schaefer III, J. Chem. Phys. 71 (1), 426 (1979).

65. G. R. Bird, J. C. Baird, A. W. Jacke, J. A. Hodgeson, R. F. Curl, Jr., A. C. Kunkle, J. W. Bransford, J. Rastrup-Anderson and J. Rosenthal, J. Chem. Phys. 40, 3378 (1964).

66. S. F. Trevino, E. Prince and C. R. Hubbbard, J. Chem. Phys. 73 (6), 2996 (1980).

67. S. F. Trevino, J. Chem. Phys. 71, 1973 (1979).

68. D. J. Pastine, D. J. Edwards, H. D Jones, C. T. Richmond and K. Kim, High Pressure Science and Technology, K. D. Timerhaus and M. S. Barber, eds., (Plenum Press, New York, 1979), Vol.2.

69. S. Topiol, J. W. Moskowitz, C. F. Melius, M. D. Newton and J. Jafri, Ab Initio Effective Potentials for First Three Rows of the Periodic Table, ERDA Research and Development Report, Chemistry, New York University, January, 1976.

70. C. Woodward, Ph.D. Thesis (University of Illinois, 1986).

71. International Tables for X-ray Crystallography: Vol. 1 Symmetry Groups, N. F. M. Henry and K. Lonsdale, eds., (Kynoch Press, Birmingham, England, 1965).

72. C. W. Keenan and J. H. Wood, General College Chemistry, 4th ed. (Harper Row, New York, 1971).

73. G. Burns, Introduction to Group Theory with Applications (Academic Press, New York, 1977).

74. W. Beall Fowler, Reprint from Physics of Color Centers (Academic Press, New York, 1968).

VITA

David J. Lucas was born in Ironwood, Michigan on August 23, 1953. He is a 1971 graduate of Luther L. Wright High School in Ironwood, after which he attended Gogebic Community College in Ironwood from 1971 through 1973. He received his Bachelor of Science degree in physics from Michigan State University, E. Lansing, Michigan, in 1975 and his Master of Science degree in physics from Michigan Technological University in Houghton, Michigan, in 1977. He was an instructor in the MTU physics department from 1977 through 1978, then worked as a research engineer for the Eastman Kodak Company in Rochester, New York through 1981. He returned to MTU in 1983 to pursue his Ph.D. in Metallurgical Engineering under the Physics of Solids option and was a part-time instructor in the Physics Department during that time. He is married to Marsha J. Erickson, also formerly of Ironwood and has two sons, Adam and Evan.

Appendix D: – Harris

The ICECAP method for Defect Properties in Solids

Appendix D

IMPLEMENTATION OF KUNZ-KLEIN LOCALIZATION IN ICECAP AND AN APPLICATION TO THE PROBLEM OF OFF-CENTER ISOVALENT SUBSTITUTIONAL IMPURITIES IN ALKALI HALIDES

BY

PHILLIP BROOKS KEEGSTRA

B.A., Calvin College, 1982
M.S., University of Illinois at Urbana-Champaign, 1984

Part of Final rept, 30 Jun 86

THESIS

Submitted in partial fulfillment of the requirements
for the degree of Doctor of Philosophy in Physics
in the Graduate College of the
University of Illinois at Urbana-Champaign, 1986

N0014-81-K-0620
NSF-DMR-83-16981

Urbana, Illinois

PACS NOS. 61.70.Bv
71.55.Ht
71.10.+x
63.20.Pw

IMPLEMENTATION OF KUNZ-KLEIN LOCALIZATION IN ICECAP AND AN APPLICATION TO THE PROBLEM OF OFF CENTER ISOVALENT SUBSTITUTIONAL IMPURITIES IN ALKALI HALIDES

BY

PHILLIP BROOKS KEEGSTRA

B.A., Calvin College, 1982
M.S., University of Illinois at Urbana-Champaign, 1984

THESIS

Submitted in partial fulfillment of the requirements
for the degree of Doctor of Philosophy in Physics
in the Graduate College of the
University of Illinois at Urbana-Champaign, 1986

Urbana, Illinois

IMPLEMENTATION OF KUNZ-KLEIN LOCALIZATION IN ICECAP AND AN APPLICATION TO THE PROBLEM OF OFF-CENTER ISOVALENT SUBSTITUTIONAL IMPURITIES IN ALKALI HALIDES

Phillip Brooks Keegstra, Ph.D.
Department of Physics
University of Illinois at Urbana-Champaign

ABSTRACT

Theoretical models of off-center isovalent substitutional impurities in alkali halides are examined. Calculations have been performed on Li^+ in KCl, a representative system known experimentally to exhibit off-center behavior. The potential seen by the Li^+ ion in the lattice has been calculated within the shell model using the computer program HADES and by means of an Unrestricted Hartree-Fock (UHF) cluster embedded in a shell model lattice using the computer program ICECAP. For the case using HADES, off-center behavior was predicted, and the resulting potential was used to predict the tunnelling splitting of the system and the Grueneisen parameter. The tunnelling splitting was calculated to be 1.19 meV for $^7Li^+$ and 1.26 meV for $^6Li^+$, compared to experimental results of 0.10 meV and 0.14 meV, respectively. The Grueneisen parameters were found to be 60 for $^7Li^+$ and 66 for $^6Li^+$, compared to experimental results of 150 for both isotopes. For the cases using ICECAP and UHF, off-center behavior was predicted, but the quantitative agreement with experimental barrier heights was not as good as that for HADES.

ACKNOWLEDGEMENTS

I would like to start by thanking my research advisor, Professor A. Barry Kunz, for his guidance and support and the way he has provided an environment conducive to research. I am especially grateful for his allowing me to be a part of an international collaboration, and his provision of state-of-the-art computing equipment.

I would also like to thank fellow group members John Blaisdell, Joe Boisvert, Maki Bacalis, Pat Goalwin, Chris Woodward, Dave Groh, and Phil Kaldon. Each of them has contributed advice helpful to my research, and to each of them I am indebted. Of the faculty of Michigan Tech I am also grateful to Professor Donald Beck, who on several occasions has had helpful discussions with me.

I would like to thank Joel Graber for implementing QUICKSORT for me in non-recursive FORTRAN; he has saved me a great deal of computer time.

I am also grateful to the members of our international collaboration, recognizing especially Dr. John Vail and Mr. Ravi Pandey of the University of Manitoba and Dr. Tony Harker, Dr. John Harding, and Dr. Marshall Stoneham of AERE Harwell.

I acknowledge the use of two fine computer centers: that of the Materials Research Laboratory of the University of Illinois, run by Mrs. Virginia Metze, and at Michigan Tech what last time I checked was called the Center for Experimental Computation, administered by Mr. Ron Winsauer.

For proofreading this manuscript I am indebted to Jane Kulina, Phil Kaldon, and David Groh. For teaching me to use PROOFWRITER and putting up with my rearrangements of their office after hours I am indebted to Julie Walter, Gloria Strieter, and Helene Hiner.

From the Department of Physics of the University of Illinois at Urbana-Champaign I am grateful for having received a summer fellowship for 1982, a fellowship for the academic year 1982-1983, and a travel grant allowing me to spend the summer of 1984 at AERE Harwell. This research was supported in part by the National Science Foundation under grant NSF-DMR-83-16981 and in part by the Office of Naval Research under contract ONR-N00014-81-K-0620.

TABLE OF CONTENTS

CHAPTER 1

INTRODUCTION

The computer program ICECAP promises to offer a reliable method to calculate energies of point defects in ionic crystals.(1) The approach used by this program is to perform an Unrestricted Hartree-Fock self-consistent field cluster computation embedded in a lattice described by the classical shell model. An important problem in such embedded-cluster calculations has to do with quantum-mechanical cluster boundary conditions, since the classical shell-model lattice does not provide any Pauli exclusion of the cluster wavefunction. A mechanism called Kunz-Klein localization(2) has been implemented to provide a systematic, mathematically rigorous boundary for the quantum-mechanical cluster.

Considerable work, both theoretical and experimental, has over the past two decades gone into investigating low-lying energy levels of defects in crystalline solids.(3) These levels may arise when the potential seen by a defect in a crystalline solid possesses two or more equivalent minima rather than a single minimum at the site of substitution. Tunnelling between these minima may then split the ground state of the defect into two or more states with very closely spaced energies.(4) These level splittings may be very small compared to the excited energy

states of the impurity which remain thermally inaccessible at low temperatures. These energy levels may also be very small with respect to the Debye energies of the crystalline lattice, making it possible, in many cases, to separate the tunnelling behavior from the lattice phonons.(3) Among the systems which exhibit these properties are certain systems of small isovalent substitutional impurities in alkali halides, the classic example being Li^+ in KCl. Due to the relative simplicity of these systems, it is hoped that they will be particularly amenable to quantitative theoretical analysis. Such a theoretical analysis has been undertaken, using ICECAP or the classical shell-model program HADES(5) to obtain potentials for these impurities, and the computer programs DYNFIT and DYNNUC to solve for the dynamics of these impurities in the potentials so calculated.

1.1 Background to ICECAP

In 1984 Vail et. al.(6) analyzed the F^+ center in MgO, a single electron trapped in an oxygen vacancy. Because of the net positive charge of this defect, lattice relaxation and polarization could not be ignored. A relaxed, polarized lattice was generated by the classical shell-model program HADES(5) in response to the multipole moments of a second-nearest neighbor Hartree-Fock cluster determined by the ATMOL program.(7) Qualitative agreement with experiment was obtained, but it was noted that a more systematic approach to quantum-mechanical

cluster boundary conditions was necessary, and that automation of the iterative cycle was desirable.

Such automation was achieved in 1985, with the computer program ICECAP.(1) This program combines the HADES classical shell-model lattice program with the UHFABK(8) Hartree-Fock cluster program, under the control of a driver program which automates the iterative interaction between the two. Since it was written, it has been tested and enhanced, but the need for systematic boundary conditions for the quantum-mechanical cluster has remained. In the absence of such systematic boundary conditions, the Pauli exclusion of the cluster wavefunction by the point ions in the classical shell-model lattice must be provided for by using suitably localized cluster basis functions or by choosing the quantum-mechanical region so that it is surrounded by cations which bear complete-ion pseudopotentials.

1.2 Background to Off-Center Impurities

It is now understood that in certain systems of small isovalent substitutional impurities in alkali halides, the impurity tunnels between equivalent off-center minima. The existence of off-center minima is due to the fact that for these small impurities the gain in polarization energy due to locating off-center is not cancelled by a corresponding cost in Pauli repulsion energy. Since in the pressure regime of interest (less

than 10 kbar) the alkali halides are cubic crystals, symmetry dictates that there be either 6, 8, or 12 equivalent minima, corresponding to displacement along the <100>, <111>, or <110> directions, respectively. The known off-center systems and the directions of their displacement are summarized in Table 1.1A and Table 1.1B. Let us review the experimental and theoretical work which has led to this level of understanding.

1.2.1 Existing Experimental Results

The first indication of the unusual properties of Li^+ defects in KCl was in 1964, when a dip in the low temperature thermal conductivity, indicating a strong resonant scattering, was reported.(9) Subsequently a large polarization in an applied electric field(10) and an electrocaloric effect, i. e. paraelectric cooling,(11) were observed. That the potential minima in this system lie along the <111> direction was confirmed by measurements of the sound velocity(12) and by nuclear magnetic resonance experiments.(13)

The energy level diagram for the ground tunnelling multiplet of Figure 1.1 results from very general assumptions concerning the form of a potential with minima along the <111> direction. The splittings, however, depend on the relative importance of tunnelling along edges, face diagonals, and body diagonals. Unfortunately, most experiments are unable to distinguish the

TABLE 1.1A

List of systems with substitutional alkalis exhibiting off-center behavior
(Blanks imply no experimental data)

System	Off-center?
Li^+ in NaF	
Li^+ in NaCl	no
Li^+ in NaBr	no
Li^+ in NaI	
Li^+ in KF	
Li^+ in KCl	<111>
Li^+ in KBr	no
Li^+ in KI	
Li^+ in RbF	
Li^+ in RbCl	no
Li^+ in RbBr	
Li^+ in RbI	
Na^+ in KF	

TABLE 1.1B

List of systems with substitutional halides exhibiting off-center behavior
(Blanks imply no experimental data)

System	Off-center?
F^- in LiCl	
F^- in NaCl	no
F^- in KCl	no
F^- in NaBr	<110>
F^- in KBr	no
F^- in RbBr	no
F^- in NaI	no
F^- in KI	<110>
F^- in RbI	<110>
Cl^- in KBr	
Cl^- in KI	
Cl^- in RbI	

FIGURE 1.1

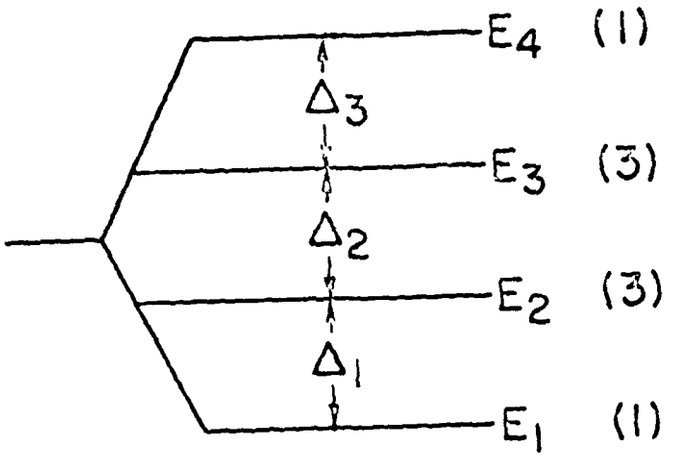

Energy level diagram for the ground tunnelling multiplet of a system with minima along the <111> direction (dipole allowed transitions indicated)

individual splittings. However, an unique phonon spectrometer experiment(14) has determined that for $^{7}Li^{+}$ equal splittings of about $^{7}\Delta$ = 0.095 meV are appropriate, whereas for $^{6}Li^{+}$ unequal splittings were found, with $^{6}\Delta_1 = {}^{6}\Delta_3$ = 0.121 meV and $^{6}\Delta_2$ = 0.086 meV. Specific heat measurements(15) interpreted on the basis of equal splittings have determined $^{7}\Delta$ and $^{6}\Delta$ to be 0.102 meV and 0.143 meV, respectively.

A very interesting feature of these off-center impurity systems is that due to the delicate balance of polarization and Pauli repulsion energies, they are very sensitive to changes in the lattice constant, e. g. by hydrostatic pressure. It has been observed by Kahan et. al.(16) that a pressure of about 4 kbar, corresponding to a strain dr/r of 0.58%, suffices to drive Li^{+} back on-center in KCl. This experiment, far infrared spectroscopy in a pressure cell, produced data only for strains dr/r greater than about 0.3%, corresponding to pressures greater than about 1.3 kbar. To obtain information on the zero-strain dependence of the tunnelling states, Dobbs and Anderson(17) have determined the Grueneisen parameter for a single Li^{+} in KCl by specific heat and thermal expansion measurements. For these purposes we may define the Grueneisen parameter Γ due to a single impurity with energy levels E_i contributing a specific heat C_i as

$$\Gamma = \left(\sum_i \Gamma_i C_i\right) / \left(\sum_i C_i\right)$$

where

$$\Gamma_i = -d(\ln E_i)/d(\ln V)$$

For equally spaced levels with splitting Δ this simplifies to

$$\Gamma = -d(\ln\Delta)/d(\ln V)$$

They obtain $\Gamma = 150$ for both $^6Li^+$ and $^7Li^+$, which they contrast with the value obtained by extrapolating the previously mentioned results of Kahan et. al.(16) to zero strain of $\Gamma \approx 300$ and previous measurements of the thermal expansion(18) which also yielded $\Gamma \approx 300$.

1.2.2 Existing Theoretical Work

Theoretical work for Li^+ in KCl and related systems takes two forms, attempts to determine the nature of the potential well in which the Li^+ ion moves, and attempts to calculate the tunnelling splittings.

Several attempts have been made to apply classical lattice methods to the calculation of the potential wells in which such ions move. The displacement of such small substitutional ions to off-center sites depends on a balance between overlap and polarization terms in the lattice energy, and the successful

prediction of this effect in lattice calculations is therefore a very critical test of the lattice model used. Wilson et. al.(19), using a polarizable point ion (Born-Mayer) model and an ad hoc modification to the Li^+-Cl^- potential inferred from LiCl, found stable minima along the <111> direction for Li^+ in KCl. Quigley and Das(20) also used a polarizable point ion model, with a Born-Meyer-Verwey repulsive potential for Li^+-Cl^-, and obtained stable minima along the <111> for Li^+ in KCl, and predicted that at a strain dr/r of about 1%, corresponding to a pressure of about 7 kbar, the Li^+ should be driven on-center. Catlow et. al.(21) applied the shell model to Li^+ in KCl using potentials as given by standard prescriptions and also found stable minima along the <111>; they obtained values for dr/r the strain required to drive the Li^+ on-center of 1% for one standard potential and 2% for another.

Attempts have also been made to calculate the potential well in which Li^+ moves in KCl by fitting to the experimental absorption lines. Devaty and Sievers(22) reported such fits for lattice strains from 0.0% to 0.6%. They used the approximation $V(x,y,z) = V_0(x) + V_0(y) + V_0(z)$ and fit to forms $V_0 = Ax^2 + Bx^4$ and $V_0 = Ax^2 + Be^{-Cx^2}$.

Finally, the tunneling in such systems has been modelled by Gomez, Bowen, and Krumhansl.(4) They modelled the potential by harmonic wells centered on the minima, and considered minima

along the <100>, <110> and <111> directions. Their wavefunctions were harmonic oscillator functions also centered on the minima. They obtained explicit expressions for the energy levels within this model in terms of the overlap and Hamiltonian matrix elements, and considered two cases. For the case of isotropic harmonic wells with minima along the <111> (edge tunnelling dominating) they obtain a tunnelling multiplet consisting of four equally spaced states with degeneracies 1-3-3-1, i. e. Figure 1.1 with all Δ_1 equal. For the case of wells highly elongated along the body diagonal (diagonal tunnelling dominating) they obtain a tunnelling multiplet consisting of two states, each quadruply degenerate, i. e. Figure 1.1 with $\Delta_1 = \Delta_3 = 0$, Δ_2 nonzero.

CHAPTER 2

CALCULATIONAL TECHNIQUES

The goal of this study is to construct a theoretical model for an isovalent substitutional impurity in an ionic crystal. Of particular interest is the motion of the impurity. One can imagine the exact solution $\Psi(\vec{X},\vec{x})$ of the full system Hamiltonian. However, such a solution is neither practical nor useful. Even if the calculational difficulties could be overcome, interpretation of the results would be nearly impossible.

These difficulties are overcome by a series of approximations to be described in this chapter. The first of these is the Born-Oppenheimer approximation,(23) which separates the nuclear from the electronic coordinates. This allows the electronic structure to be calculated for a frozen lattice, giving the energy as a function of the lattice configuration. The nuclear motion can then in principle be calculated by treating this function as a potential for a quantum mechanical calculation. The section on the computer program ICECAP describes how the energy as a function of the lattice configuration is obtained, and the section on the computer programs DYNFIT and DYNNUC explains how nuclear motion is calculated from these potentials.

2.1 ICECAP

A computer program has been developed which combines a quantum-mechanical treatment of electrons in the vicinity of a point defect with a classical discrete-ion model for the rest of the crystal, which is only weakly perturbed by the defect. This program is named ICECAP: ionic crystal with electronic cluster, automatic program.(1) The portion of ICECAP responsible for the quantum-mechanical calculation is called the UHF sequence of programs,(8) which implements the Unrestricted Hartree-Fock equations, with extensions implementing Kunz-Klein localization.(24) The classical discrete-ion portion of ICECAP is called HADES,(5) and implements the shell model of Overhauser and Dick.(25)

2.1.1 The Hartree-Fock Approximation(26)

The immediate vicinity of the defect whose properties are being calculated is treated in the Unrestricted Hartree-Fock (UHF) approximation. This approximation can be derived from the non-relativistic Schroedinger equation for the total system wavefunction: $H\Psi(\vec{X},\vec{x}) = E\Psi(\vec{X},\vec{x})$ where the lower-case variable ($\vec{x}$) refers to electronic spatial and spin coordinates and the upper-case ($\vec{X}$) to nuclear coordinates.(27) The Hamiltonian is written as a sum of electronic, nuclear and interaction parts:

$$H = H_e + H_N + H_{int}$$

$$H_e = \sum_i \left[-\frac{1}{2}\nabla^2 + \frac{1}{2}\sum_{j\neq i} \frac{1}{|\vec{r}_j - \vec{r}_i|} \right]$$

$$H_N = \sum_I \left[-\frac{1}{2M_I}\nabla^2 + \frac{1}{2}\sum_{J\neq I} \frac{Z_I Z_J}{|\vec{R}_J - \vec{R}_I|} \right]$$

$$H_{int} = \sum_i \sum_I \frac{-Z_I}{|\vec{r}_i - \vec{R}_I|}$$

where we have adopted Hartree atomic units ($\hbar = e = m_e = 1$).

The next step in obtaining the UHF equations is to make the Born-Oppenheimer approximation,(23) separating the nuclear and electronic parts of the wavefunction. We calculate only the latter, in this context approximating the former by a fixed lattice which contributes to the total energy a constant shift called the nuclear repulsion energy.

The Schroedinger equation to be solved is now of the form $H\Psi(\vec{x}_1,\ldots\vec{x}_n) = E\Psi(\vec{x}_1,\ldots\vec{x}_n)$ where $\vec{x}_i$ represents the space and spin coordinates of the i-th electron. We now approximate the wavefunction Ψ by a single Slater determinant of one-electron spinorbitals $\psi_i(\vec{x})$:

$$\Psi(\vec{x}_1,\vec{x}_2,\ldots\vec{x}_n) = (n!)^{-1/2}\begin{vmatrix} \psi_1(\vec{x}_1) & \psi_2(\vec{x}_1) & \cdots & \psi_n(\vec{x}_1) \\ \psi_1(\vec{x}_2) & \psi_2(\vec{x}_2) & \cdots & \psi_n(\vec{x}_2) \\ & \vdots & & \\ \psi_1(\vec{x}_n) & \psi_2(\vec{x}_n) & \cdots & \psi_n(\vec{x}_n) \end{vmatrix}$$

The Slater determinant form is selected because it automatically provides the antisymmetry required by the Pauli exclusion principle.

The Hartree-Fock equations result from an application of the variational principle. The one-electron spinorbitals are varied to minimize $\langle\Psi|H|\Psi\rangle$ subject to the constraint that the spinorbitals form an orthonormal set. This constraint is enforced by introducing Lagrange multipliers λ_{ij}. The result of the minimization is $F\psi_i(\vec{x}) = \Sigma\lambda_{ij}\psi_j(\vec{x})$, where F is the Fock operator:

$$F(\rho)\psi_i(\vec{x}) = \left[-\frac{\hbar^2}{2}\nabla^2 - \sum_I \frac{Z_I}{|\vec{x}-\vec{R}_I|} + \sum_j \int \frac{\psi_j^*(\vec{y})\psi_j(\vec{y})}{|\vec{x}-\vec{y}|}\,d\vec{y} \right]\psi_i(\vec{x})$$

$$- \sum_j \psi_j(\vec{x}) \int \frac{\psi_j^*(\vec{y})\psi_i(\vec{y})}{|\vec{x}-\vec{y}|}\,d\vec{y}$$

and integrations include inner products over spin space. A unitary transformation will leave determinantal wavefunctions unchanged, so we apply a transformation such that the matrix of

Lagrange multipliers is diagonalized. This gives us the standard form of the Hartree-Fock equations $F\psi_i(\vec{x}) = \epsilon_i\psi_i(\vec{x})$.(28) Because the Fock operator depends on the one-electron spinorbitals, these equations must in general be solved by iterating to self-consistency. Koopmans' theorem suggests that we may interpret the ϵ_i in these equations as an approximation to the ionization energy of the i-th electron.(29)

Applying the Hamiltonian to the Hartree-Fock wavefunction thus defined gives us the expression for the energy of the system in the Hartree-Fock approximation:

$$E = \sum_i \left[\int \psi_i(\vec{x}) \left(-\frac{\hbar^2}{2}\nabla^2 - \sum_I \frac{Z_I}{|\vec{x} - \vec{R}_I|} \right) \psi_i(\vec{x}) d\vec{x} \right.$$

$$+ \frac{1}{2} \sum_j \int \frac{\psi_j^*(\vec{x})\psi_j^*(\vec{y})\psi_j(\vec{y})\psi_i(\vec{x})}{|\vec{x} - \vec{y}|} d\vec{y}d\vec{x}$$

$$\left. - \frac{1}{2} \sum_j \int \frac{\psi_i^*(\vec{x})\psi_j^*(\vec{y})\psi_i(\vec{y})\psi_j(\vec{x})}{|\vec{x} - \vec{y}|} d\vec{y}d\vec{x} \right]$$

$$+ \frac{1}{2} \sum_{I,J}{}' \frac{Z_I Z_J}{|\vec{R}_I - \vec{R}_I|}$$

We can use the Hartree-Fock equations to eliminate the Coulomb

and exchange terms from this expression in favor of the Hartree-Fock eigenvalues. We then obtain:

$$E = \frac{1}{2} \sum_i \left[\epsilon_i + \int \psi_i^*(\vec{x}) \left[-\frac{1}{2} \nabla^2 - \sum_I \frac{Z_I}{|\vec{x} - \vec{R}_I|} \right] \psi_i(\vec{x}) d\vec{x} \right]$$

$$+ \frac{1}{2} \sum_{I,J}{}' \frac{Z_I Z_J}{|\vec{R}_J - \vec{R}_I|}$$

The final term is the nuclear repulsion energy mentioned earlier.

One further simplification is made in deriving Unrestricted Hartree-Fock. The one-electron spinorbitals ψ_i are chosen to be the product of a spatial function and an eigenstate of spin (S_z). Because of the orthonormality of α and β the spin disappears from the problem almost completely. In contrast to the Restricted Hartree-Fock (RHF) equations, no requirements of symmetry are imposed on the spatial functions, nor must there necessarily be any correspondence between the spin up and spin down orbitals.(30)

Numerical integration can be used to solve the Hartree-Fock equations, but the calculations become much more tractable when the orbitals are expanded as linear combinations of basis functions. This separates the problem into an integration phase in which integrals over pairs and quartets of basis functions are calculated and an iterative phase in which standard numerical

matrix techniques are employed.(31) Calculations are performed using basis functions of Cartesian Gaussian type, i. e. of the form $x^{\ell}y^{m}z^{n}e^{-\alpha r^2}$. These have the advantage of exact analytic integrability, even for functions on different centers, although the disadvantage of lack of resemblance to hydrogen orbitals must be recognized.(32)

2.1.2 Kunz-Klein Localization(24)

In principle we would like to solve the Unrestricted Hartree-Fock (UHF) equations for an entire solid-state system,(33) in this case an ionic solid. These equations are:

$$F(\rho)\Phi_i = \epsilon_i \Phi_i$$

$$\rho(\vec{x},\vec{y}) = \sum_{i=\text{occ}} \Phi_i(\vec{x})\,\Phi_i(\vec{y})$$

$$F(\rho)\Phi_i(\vec{x}) = \left[-\frac{\hbar^2}{2}\nabla^2 - \sum_I \frac{Z_I}{|\vec{x}-\vec{R}_I|} + \int \frac{\rho(\vec{y},\vec{y})}{|\vec{x}-\vec{y}|}\,d\vec{y} \right]\Phi_i(\vec{x}) - \int \frac{\rho(\vec{x},\vec{y})}{|\vec{x}-\vec{y}|}\,\Phi_i(\vec{y})\,d\vec{y}$$

where the summation in the definition of ρ is over occupied orbitals only. The solution of this equation for an ionic crystal of realistic size is clearly impossible; we wish to treat quantum-mechanically only a finite cluster which we shall call A

and to treat with a classical discrete-ion model the remainder of the system, which we shall call the environment of A and denote by W.

Let us obtain a physically motivated derivation of the boundary conditions which must be applied by considering the local-orbital formalism of Adams and Gilbert.(34) A derivation which is mathematically exact also exists, and is given in an appendix to this work. Let us use F to denote the Fock operator for the entire system. We will assign m electrons to A, where for the sake of physical reasonability m will be taken to be the number of electrons on the ions inside A. We will write

$$F = F_A + U_A$$

where F_A is that part of F which includes the kinetic energy, nuclear attraction of the electrons and nuclei inside A, and the electron-electron potential including Coulomb and exchange parts for the electrons. Since we are considering an ionic crystal let us divide U_A into two parts, V_A^M, the long-range ionic (Madelung) contribution, and V_A^S, the short-range remainder. V_A^S may be considered to be made up of additive contributions from all the ions in the environment. It falls off very rapidly with distance, and so only contributions from ions in the immediate vicinity of the cluster need to be considered.

Let us consider the Adams-Gilbert equation:

$$(F_A + U_A - \rho T\rho^{-1})\Psi_i = \pi_i \Psi_i$$

where T is any Hermitian operator. They have shown that when a common T is used for all the electrons one can obtain orthonormal spinorbitals satisfying:

$$\rho = \sum_{i=occ} \Psi_i \Psi_i^\dagger = \sum_{i=occ} \Phi_i \Phi_i^\dagger$$

where Φ_i are the spinorbitals obtained by solving the normal Hartree Fock equation for the entire system:

$$(F_A + U_A)\Phi_i = \epsilon_i \Phi_i$$

We choose $T = V_A^S$ and rearrange to get

$$(F_A + V_A^M + V_A^S - \rho V_A^S \rho^{-1})\Psi_i = \pi_i \Psi_i$$

In the limit of self-consistency the terms involving V_A^S cancel, leaving an effective Fock operator for the localized cluster:

$$(F_A + V_A^M)\Psi_i = \pi_i \Psi_i$$

We wish to go beyond this level of approximation. Since we will always solve these equations by expansion in terms of basis

functions, let us consider the following matrix element between two basis functions χ_c and χ_d, which may be thought of as the correction to this effective Fock operator:

$$\langle \chi_c | V_A^S - \rho V_A^S \rho | \chi_d \rangle$$

The overlap between those orbitals in ρ from outside A and the basis function χ_c located inside A will be small, so approximate:

$$\rho = \rho_A \equiv \sum_{\substack{i=occ \\ i \text{ in } A}} |\Phi_i\rangle\langle\Phi_i|$$

to obtain:

$$\langle \chi_c | V_A^S | \chi_d \rangle - \sum_{\substack{i=occ \\ i \text{ in } A}} \sum_{\substack{j=occ \\ j \text{ in } A}} \langle \chi_c | \Psi_i \rangle \langle \Psi_i | V_A^S | \Psi_j \rangle \langle \Psi_j | \chi_d \rangle$$

which upon writing orbitals in terms of basis functions and their expansion coefficients p_a^i becomes:

$$\langle \chi_c | V_A^S | \chi_d \rangle -$$

$$\sum_a \sum_b \langle \chi_c | \chi_a \rangle \langle \chi_b | \chi_d \rangle \left\{ \sum_{a'} \sum_{b'} \langle \chi_{a'} | V_A^S | \chi_{b'} \rangle \left(\sum_{\substack{i=occ \\ i \text{ in } A}} p_a^i p_{a'}^i \right) \left(\sum_{\substack{j=occ \\ j \text{ in } A}} p_b^j p_{b'}^j \right) \right\}$$

Let us now obtain an expression for E, the energy of a system within this formalism.(35) We make the following

definitions, where we hav m states in our cluster A, and N states in total (recall we are using units in which $\hbar = e = m_e = 1$).

$$f = \left[-\frac{1}{2}\nabla^2 - \sum_I \frac{Z_I}{|\vec{r}_i - \vec{R}_I|} \right]$$

$$g = \frac{1}{|\vec{r} - \vec{r}'|}$$

$$V_{nn} = \frac{1}{2} \sum_{I,J}{}' \frac{Z_I Z_J}{|\vec{R}_I - \vec{R}_J|}$$

Applying the Hamiltonian to our wavefunction and expressing the result in terms of our definitions, we obtain:

$$E = \sum_{i=1}^{N} \langle i|f|i\rangle + \frac{1}{2} \sum_{i,j=1}^{N} \langle ij|g(1-\hat{P})|ij\rangle + V_{nn}$$

Rewriting the Kunz-Klein localization equation in matrix element form using our definitions, we obtain:

$$\langle i|f|i\rangle + \sum_{j=1}^{N} \langle ij|g(1-\hat{P})|ij\rangle = \pi_i + \langle i|\rho_A T \rho_A|i\rangle$$

We define:

$$\tilde{\pi}_i = \pi_i + \langle i|\rho_A T \rho_A|i\rangle = \begin{cases} \pi_i & i > m \\ \pi_i + \langle i|T|i\rangle & i \leq m \end{cases}$$

Note that the value of the matrix element $\langle i|T|i\rangle$ for i in A is known. We could eliminate the Coulomb and exchange terms in this expression in favor of the localization eigenvalues $\tilde{\pi}_i$ to obtain:

$$E = \frac{1}{2} \sum_{i \text{ in } A,W} \left[\bar{\pi}_i + \langle i|f|i\rangle \right]$$

However, let us instead consider this as motivation to define $\bar{E}$ as follows:

$$\bar{E} = \frac{1}{2} \sum_{i \text{ in } A} \left[\bar{\pi}_i + \langle i|f|i\rangle \right]$$

Note that each of the terms in this definition originates within A and is known. To find its relationship with E it is useful to rewrite $\bar{E}$ as:

$$\bar{E} = \sum_{i \text{ in } A} \langle i|f|i\rangle + \frac{1}{2} \sum_{i,j \text{ in } A} \langle ij|g(1-\hat{P})|ij\rangle + \sum_{\substack{i \text{ in } A \\ j \text{ in } W}} \langle ij|g(1-\hat{P})|ij\rangle$$

We now break up our expression for E into parts due to A and W, respectively:

$$E = \sum_{i \text{ in } A} \langle i|f|i\rangle + \frac{1}{2} \sum_{i,j \text{ in } A} \langle ij|g(1-\hat{P})|ij\rangle + \sum_{i \text{ in } W} \langle i|f|i\rangle + \frac{1}{2} \sum_{i,j \text{ in } W} \langle ij|g(1-\hat{P})|ij\rangle + \sum_{\substack{i \text{ in } A \\ j \text{ in } W}} \langle ij|g(1-\hat{P})|ij\rangle + \sum_{\substack{I \text{ in } A \\ J \text{ in } W}} \frac{Z_I Z_J}{|\vec{R}_I - \vec{R}_J|} + \frac{1}{2} \sum_{I,J \text{ in } A}{}' \frac{Z_I Z_J}{|\vec{R}_I - \vec{R}_J|} + \frac{1}{2} \sum_{I,J \text{ in } W}{}' \frac{Z_I Z_J}{|\vec{R}_I - \vec{R}_J|}$$

Identifying $\bar{E}$ in this expression gives:

$$E = \bar{E} + \sum_{i \text{ in } W} \langle i|f|i\rangle + \frac{1}{2} \sum_{i,j \text{ in } W} \langle ij|g(1-\hat{P})|ij\rangle$$

$$+ \frac{1}{2} \sum_{I,J \text{ in } A}{}' \frac{Z_I Z_J}{|\vec{R}_I - \vec{R}_J|} + \frac{1}{2} \sum_{I,J \text{ in } W}{}' \frac{Z_I Z_J}{|\vec{R}_I - \vec{R}_J|}$$

$$+ \sum_{\substack{I \text{ in } A \\ J \text{ in } W}} \frac{Z_I Z_J}{|\vec{R}_I - \vec{R}_J|}$$

We obtain a computationally tractable formula for E by deleting terms which remain approximately constant through the physical process under consideration. Recall A has been chosen to be large enough that the only terms which change are in A.

i. The kinetic energy part of the terms $\langle i|f|i\rangle$ for i in W does not change.

ii. The exchange terms $\langle ij|g|ji\rangle$ for i and j in W do not change.

Then:

$$E = \bar{E} + \sum_{i \text{ in } W} \langle i| \sum_I \frac{-Z_I}{|\vec{r}_i - \vec{R}_I|} |i\rangle + \frac{1}{2} \sum_{i,j \text{ in } W} \langle ij|g|ij\rangle$$

$$+ \frac{1}{2} \sum_{I,J \text{ in } A}{}' \frac{Z_I Z_J}{|\vec{R}_I - \vec{R}_J|} + \frac{1}{2} \sum_{I,J \text{ in } W}{}' \frac{Z_I Z_J}{|\vec{R}_I - \vec{R}_J|}$$

$$+ \sum_{\substack{I \text{ in } A \\ J \text{ in } W}} \frac{Z_I Z_J}{|\vec{R}_I - \vec{R}_J|}$$

If we call N_I the number of electrons at site I and recognize that $\langle i|-\frac{Z_I}{|\vec{r}_i - \vec{R}_I|}|i\rangle$ does not change for i on site I and $\langle ij|g|ij\rangle$ does not change for i and j on the same site, then we can rewrite this as:

$$E = \bar{E} - \sum_{I,J \text{ in } W}{}' \frac{N_I Z_J}{|\vec{R}_I - \vec{R}_J|} + \frac{1}{2} \sum_{I,J \text{ in } W}{}' \frac{N_I N_J}{|\vec{R}_I - \vec{R}_J|}$$

$$+ \frac{1}{2} \sum_{I,J \text{ in } A}{}' \frac{Z_I Z_J}{|\vec{R}_I - \vec{R}_J|} + \frac{1}{2} \sum_{I,J \text{ in } W}{}' \frac{Z_I Z_J}{|\vec{R}_I - \vec{R}_J|}$$

$$+ \sum_{\substack{I \text{ in } A \\ J \text{ in } W}} \frac{Z_I Z_J}{|\vec{R}_I - \vec{R}_J|}$$

Then if we define $Z_I - N_I$ to be the net ionic charge I_I the terms can be grouped together as follows to give our final expression:

$$E = \bar{E} + \frac{1}{2} \sum_{I,J \text{ in } W}{}' \frac{I_I I_J}{|\vec{R}_I - \vec{R}_J|} + \frac{1}{2} \sum_{I,J \text{ in } A}{}' \frac{Z_I Z_J}{|\vec{R}_I - \vec{R}_J|}$$

$$+ \sum_{\substack{I \text{ in } A \\ J \text{ in } W}} \frac{Z_I I_J}{|\vec{R}_I - \vec{R}_J|}$$

Note the similarity to the expression for the Hartree-Fock energy for a cluster in an array of ionic charges without Kunz-Klein localization.

It is envisioned that these Kunz-Klein potentials will be associated with the discrete ions nearest the quantum mechanical

region, and thus would reflect the non-coulombic part of the interaction between the electrons of this region and those of the neighboring ions. Herein lies a problem; in the classical discrete-ion model used, the shell model,(25) an ion is represented by two point charges, the core and the shell, and the net charge of the ion is distributed between the two in an empirical manner. Thus it is not obvious where to locate the coordinates of the center of the Kunz-Klein potential for an ion with respect to the coordinates for the core and shell of that ion. In a related context it was suggested to introduce a parameter α which would determine where along the line from the core to the shell to center the potential.(36) Of course, this simply restates the problem as one of determining the proper value of α. (There is not even any reason to expect the same value of α to be optimum for every ion, or even for different shell model parameterizations of the same ion.) Initially, however, the program has been written in such a way as to associate the center of the potential with the position of the core (i. e. fixing $\alpha = 0.0$).

2.1.3 The UHF Sequence of Programs

Calculations are performed in three stages. First the labels generation program LABELS uses any available information on the symmetry of the problem to generate a list of integrals to be computed. Then the polyatomic Gaussian integrals evaluation

program POLYIN evaluates the listed integrals. These two programs are from the Caltech POLYATOM program package, as modified by Kunz and his collaborators.(37) POLYIN also permits the user to replace the core electrons of one or more atoms in the problem with an effective potential or pseudopotential. Pseudopotentials may be of either Phillips-Kleinman(38) or norm-conserving(39) type. Finally the iterative program UHFABK of Kunz and his collaborators uses the integrals to form a self-consistent solution.(8)

The Kunz-Klein localization potentials appropriate to a particular crystal are generated by the program LOPAS written by A. B. Kunz.(8) The output of this program consists of a potential in tabular form, which is then fitted with Gaussians. There are two main reasons why we fit the tabulated Kunz-Klein localization potentials generated by LOPAS to Gaussians. First, evaluating the integrals in POLYIN is computationally more convenient when the potential is expressed in terms of Gaussians. Second, although the potentials are of interest in their own right, the publication of the number of pairs of mesh points and values required for a tabulated potential would be impractical because of both the excessive amount of space required and the proneness to error of the typesetting process.

The program KKLFIT of P. B. Keegstra performs the fitting process.(40) This program performs a linear least-squares fit to obtain the linear coefficients for n Gaussians, and then uses a nonlinear minimization subroutine to optimize the values of the Gaussian exponents used. Two minimization subroutines are available: the subroutine MINI which uses the quasi-Newton method and the subroutine MINPBK which uses the gradient method. The latter subroutine seems to be more dependable.

2.1.4 The Shell Model

The region to be treated quantum mechanically is embedded in a classical point-charge shell-model lattice. In the shell model an ion is represented as a point charge core coupled harmonically (force constant K) to an uniformly charged (charge Y) massless spherical shell of indeterminate radius. The cores and shells are treated as independant entities, referred to as species. Coulomb interactions apply between all species with the exception of the core and shell of the same ion. Short-range repulsive interactions may also be defined between any pairs of species, although they are conventionally chosen to act only between shells. The form of such interactions v(r) is exemplified by the Buckingham potential:

$$v(r) = B\, e^{-r/\rho} - C/r^6$$

where B, C, and ρ are parameters.(25) Tabulations of shell-model parameters, usually fitted to reproduce perfect-crystal bulk properties, are widely available.(41) The shell model has been widely successful in describing perfect-crystal and certain simple defect properties in ionic crystals. Some recent applications have been reviewed by Catlow and Mackrodt.(42) One significant shortcoming of the shell model is that, as a central force model, in rocksalt-structured crystals it cannot reproduce the departures from the Cauchy relations ($C_{12} = C_{44}$) actually observed.(43)

2.1.5 HADES

In applying the shell model to point defects, we use a concept first proposed by Mott and Littleton(44) in which the crystal is divided into an inner region I and an outer region II. In region I, which contains all the defects, the ions forming the lattice interact according to a specified model and the equilibrium distortion of the crystal is calculated by explicitly relaxing each ion until it is subject to no resultant force. The response of region II, comprising the remainder of the crystal, is calculated by considering the lattice as a dielectric continuum so that the ions are displaced in response to the electric field of any charged defects. Even for an ionic

crystal, these interactions need to be considered explicitly only for a small finite part of region II adjacent to the defect (called region IIa). The interaction with more distant ions (called region IIb) and any induced polarizations are calculated using lattice sums or continuum integrals.(5)

These methods have been implemented in the Harwell computer program HADES.(5) Two significant features of this program are its use of symmetry and its efficient minimization technique. The program applies all symmetry operations of the cubic or hexagonal group (set by the user) to the defect and crystal to see under which operations the system is invariant. Knowing the symmetry properties, the program works only with interactions differing in symmetry, together with weighting factors. The program carries out its minimization using a fast matrix method developed by Norgett and Fletcher.(45) This method uses first and approximate second derivatives of the energy function, which are easily evaluated for pair potentials of the forms used.

2.1.6 Interactions within ICECAP

The program ICECAP has been written to automate an iterative cycle containing both HADES and UHF and to keep track of the interactions between them. The system under investigation is partitioned into an environment which is controlled by HADES and a cluster to be treated quantum mechanically, where the cluster

contains any excess electrons (e. g. in a color center) and those ions whose positions or electronic structure are significantly perturbed by the defect. ICECAP is intended to perform a minimization of the total system energy with respect to the lattice configuration (shell and core coordinates to be varied by HADES), electronic configuration (linear coefficients of the UHF wavefunction), and the cluster configuration (coordinates of UHF and pseudopotential ions within the defect cluster). In practice a global minimization routine samples cluster configurations. For a given cluster configuration the excess electrons and UHF and pseudopotential ions are first simulated by fixed point charges, from which HADES determines the polarized, distorted lattice configuration. The shell-model point charges of the lattice, along with the nuclei and pseudopotentials of the given cluster configuration, are applied as a background potential for an UHF calculation, which yields the appropriate electronic configuration. Ideally, the point-charge simulation of the cluster in the HADES calculation should have all its electric multipole moments identical to those of the UHF cluster, but this is obviously not practical. One therefore matches only a finite set of low-order multipoles. This is accomplished by introducing into the HADES calculation additional point-charge simulators, representing a small dipole, quadrupole, etc., thus correcting for the discrepancies between HADES and UHF up to a given multipole order. After introducing these simulators, HADES is once again asked to determine a lattice configuration, which is

used as background to UHF, and the HADES/UHF sequence is iterated to consistency. This gives a value for the total energy associated with this cluster configuration, and the whole procedure is repeated until the cluster configuration of minimum total energy is found. A diagram of this procedure is given in figure 2.1.

There are two subtle "bookkeeping" matters pertaining to the different classes of defined entities which had to be dealt with in the construction of ICECAP. The first is that entities of each class must have their coordinates varied only in the appropriate portion of the program. The second is that the interaction between any two entities must be taken into account exactly once, that is, neither omitted nor double-counted. The classes of entities defined in ICECAP include:

1. Ions that will be replaced by bare nuclei plus electrons in UHF.
2. Ions that will be replaced by core pseudopotentials plus valence electrons in UHF.
3. Ions that will be replaced by complete-ion pseudopotentials or Kunz-Klein localization potentials.
4. Shell-model ions that will be explicitly moved about in minimizing total energy.
5. Point charges simulating excess electrons.
6. Point charges simulating multipole moment corrections.
7. Shell-model ions of the surrounding lattice.

FIGURE 2.1

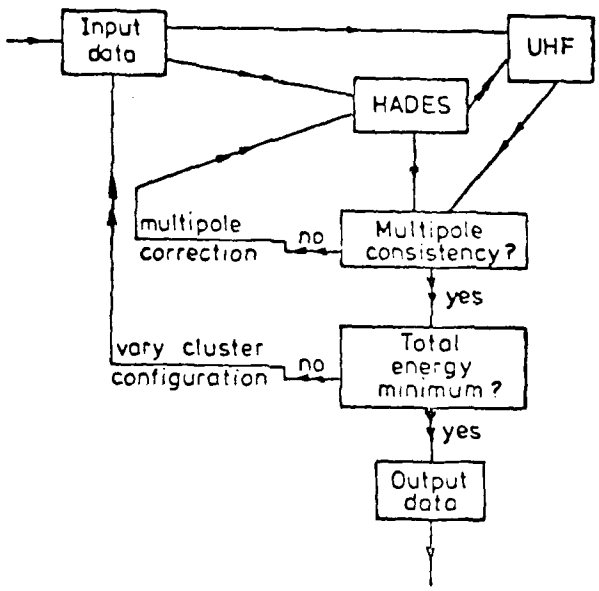

Block diagram of ICECAP

Double arrows define program flow.
Single arrows indicate data transmission paths.

Classes 1 through 6 are defined as the cluster, and classes 1 through 3 as the quantum-mechanical region.

The portions of the program within which entities of each class have their coordinates varied are as follows: Classes 1 through 4 have their coordinates varied by the DRIVER, that is, the overall minimization routine. By convention class 5 is never moved; the positions of these point charges are fixed as part of the input data. Entities in class 6 are regenerated by the multipole fitting routine each pass through the multipole consistency cycle, and also the magnitude of their displacements is user-selectable. Entities in class 7 are moved by HADES.

The proper counting of the interactions between entities of the various classes is insured by the way the total energy is defined. This energy is:

$$E = (E_H - E_S' - E_C') + (E_A + E_C + E_D)$$

In this expression E_H denotes the energy HADES calculates simulating the quantum-mechanical cluster by point charges. E_S' and E_C' are the shell-model short-range and Coulomb energies, respectively, of the quantum-mechanical cluster which are subtracted out because these interactions are accounted for in the quantum-mechanical calculation. E_A is the total electronic energy from the quantum-mechanical calculation. E_C is the

Coulomb energy between nuclei, pseudopotential centers, and Kunz-Klein localization centers. E_D corrects for the energy of the dipoles modelling the polarization of Kunz-Klein localization (or whole-ion pseudopotential) sites.

2.2 DYNFIT and DYNNUC

The computer programs DYNFIT and DYNNUC calculate the response of a substitutional ion in a potential which may be calculated either by ICECAP or HADES. The program DYNFIT takes the potentials as given by ICECAP or HADES and determines certain parameters necessary for the dynamical calculation and generates potentials of a form useful for the dynamical calculation. The program DYNNUC then takes these parameters and potentials and calculates the spectrum of motional states of the substitutional ion.

For computational efficiency, both HADES and ICECAP make heavy use of symmetry and are prohibitive in their use of computer time for systems without useable symmetry. Thus it is reasonable to restrict the computation of potentials by these programs to systems which exhibit useable symmetry. Such systems are those in which the substitutional ion is displaced along the <100> direction, the <110> direction, or the <111> direction.

The other constraint imposed on the potentials obtained from HADES or ICECAP has to do with the coordinates of the ions other than the substitutional ion under consideration. The complete treatment of the problem would require that the potential be plotted out in a 3N-dimensional space where N is the number of ions in the crystal, and that this potential be used in the Schroedinger equations for nuclear motion. In the interest both of computational feasability and of simplicity of interpretation we plot out the potential only for displacements of the substitutional ion, but we allow the crystal to relax fully during the energy calculation at each displacement. Thus these displacements may be thought of as an "effective coordinate." We assert that this "effective coordinate" exhibits the full symmetry of the cubic crystal.

2.2.1 DYNFIT

The computer program DYNFIT takes the potential seen by a substitutional ion in a cubic lattice and determines parameters and potentials necessary to calculate the dynamics of that substitutional ion. The potentials used as input are along the symmetry directions of a cubic crystal, that is, <100>, <110>, and <111>. In order to perform the calculation it is necessary to define the way in which these potentials are to be interpolated off these axes. An interpolation scheme widely used(16) is to write the potential as a sum of one-dimensional

potentials in the x, y, and z directions, respectively:

$$V(x,y,z) = V_0(x) + V_0(y) + V_0(z)$$

This form is calculationally very tractable, as the three-dimensional Schroedinger equation decomposes into three identical one-dimensional Schroedinger equations. The first calculation performed by DYNFIT is thus to construct such a V_0 to match the potential along one of the symmetry axes, as selected by the user. Following that the program finds the value of α which defines a basis of harmonic oscillator functions which gives the lowest energy for the ground state. Next the program calculates a correction to the form involving V_0. The way that is done is to add in a spherically symmetric potential V_S and a correction potential V_C such that:

$$\begin{aligned} V(x,y,z) = &(V_0(x)+V_C(x)) + (V_0(y)+V_C(y)) \\ &+ (V_0(z)+V_C(z)) + V_S(r) \end{aligned}$$

Given a table of values for V_S, V_C is chosen such that the fit is still exact along the same symmetry axis along which V_0 was defined. The best form for V_S is then obtained by means of the minimization routine MINPBK, which uses the gradient method. Following these calculations, the user has the option of having the program calculate the best approximations to V_0 of two different forms. The two forms are those used by Devaty and

Sievers;(22) the first form is $Ax^2 + Bx^4$ and the second form is $Ax^2 + Be^{-Cx^2}$. The way these fits were generated assumes that V_0 has its minimum away from the point x = 0. For the first potential form, $Ax^2 + Bx^4$, parameters were fit by requiring that the splitting between the first two states be the same for the original and fit potentials, and that the minima be in the same place. For the second potential form, $Ax^2 + Be^{-Cx^2}$, parameters were fit by imposing the same two conditions imposed on the first form, and in addition the condition that A be related to the optimum value of ω by the relation $2A = M\omega^2$ for M the mass of the isotope of the ion for which the fit was computed. That is, Ax^2 is the harmonic potential in which the ion has natural frequency ω.

2.2.2 DYNNUC

The computer program DYNNUC calculates the spectrum of motional states of the substitutional ion using the parameters calculated in DYNFIT. The first stage is called the one-dimensional calculation. There the one-dimensional Schroedinger equation with potential $V_0(x)$ is solved using matrix techniques with a basis set of harmonic oscillator functions with the frequency ω calculated in DYNFIT. The resulting one-dimensional orbitals are combined to form what we refer to as three-dimensional basis functions, so-called because of the way they will be used in the second stage of the calculation. The

addition of the energy eigenvalues for each component one-dimensional orbital gives the energy for the three-dimensional basis function in this approximation, which we call the energy from the one-dimensional calculation. The basis functions are sorted by the value of this energy, and grouped into multiplets. The multiplets of lowest energy, comprising up to 100 basis functions, are used in the second stage. In the second stage the Hamiltonian matrix with the potential $(V_0(x)+V_c(x))$ + $(V_0(y)+V_c(y))$ + $(V_0(z)+V_c(z))$ + $V_s(r)$ is calculated using these functions as a basis, and it is then diagonalized. This gives the final results, which are called the energies from the three-dimensional calculation.

CHAPTER 3

CALCULATIONS PERFORMED

Calculations have been performed on Li^+ in KCl, a representative system exhibiting off-center behavior. Calculations performed entirely within the classical shell model, using the computer program HADES, will be presented first. Then calculations performed with an Unrestricted Hartree-Fock cluster embedded within a classical shell-model lattice, using the computer program ICECAP, will be presented.

3.1 HADES-Generated Potentials

Catlow et. al.[21] have calculated the equilibrium position for displacements along the <100>, <110>, and <111> directions for Li^+ in KCl and related systems. We have extended their work by mapping out the potential seen by the Li^+ for displacements along these symmetry directions. This mapping was accomplished by fixing the position of the HADES core for the Li^+, leaving the HADES shell free to polarize. The potentials used for this calculation were identical to the Type I (Buckingham) potentials of Catlow et. al. with one exception: the Li^+-K^+ short-range interaction we used varied slightly from the form used by Catlow et. al., but the difference in results was negligible. Calculations were performed at three lattice constants to model

the effect of hydrostatic pressure on off-center behavior. The lattice constants used were 3.116 A, 3.105 A, and 3.096 A, corresponding to strains dr/r of 0.00%, 0.35%, and 0.64% respectively. The lattice constant of 3.116 A was obtained by extrapolating measured values to absolute zero(21,46) and the shell-model parameters used were fit to this value. The calculated potentials are presented in Tables 3.1A, 3.1B, and 3.1C.

These potentials were then used as input to the programs DYNFIT and DYNNUC to obtain the energy levels associated with the nuclear motion. The symmetry direction <111> was fitted exactly. The one-dimensional calculation was performed with 40 basis functions, i. e. harmonic oscillator functions with quantum numbers through 39. At least 64 three-dimensional basis functions were used in the three-dimensional calculation, with enough additional functions included to complete the last multiplet. The results for $^{7}Li^{+}$ for the three lattice constants are presented in Tables 3.2A, 3.2B, and 3.2C; those for $^{6}Li^{+}$ are presented in Tables 3.3A, 3.3B, and 3.3C. The results quoted are for the first three tunnelling multiplets. In some cases states from the fourth tunnelling multiplet were lower in energy than some of the states from the third tunnelling multiplet; these states have not been listed.

TABLE 3.1A

Potential from HADES Li^+ in KCl Lattice constant = 3.116 Å

X (Lattice) units	X (Å)	V100 (eV)	V110 (eV)	V111 (eV)
0.	0.	-1.07444	-1.07444	-1.07444
0.05	0.1558	-1.08256	-1.09054	-1.09887
0.10	0.3116	-1.09136	-1.11038	-1.12567
0.15	0.4674	-1.08563	-1.10594	-1.12685
0.20	0.6232	-1.06012	-1.06844	-1.09442
0.30	0.9348	-0.93592	-0.87808	-0.93588
0.40	1.2464	-0.70860	-0.56621	-0.73841
0.401	1.249516	-0.70580	-0.56266	-0.73695

TABLE 3.1B

Potential from HADES Li^+ in KCl Lattice constant = 3.105 Å

X (Lattice) units	X (Å)	V100 (eV)	V110 (eV)	V111 (eV)
0.	0.	-1.11852	-1.11852	-1.11852
0.05	0.15525	-1.12507	-1.13134	-1.13671
0.10	0.31050	-1.13084	-1.14480	-1.15501
0.15	0.46575	-1.12267	-1.13549	-1.14826
0.20	0.62100	-1.09423	-1.09319	-1.10854
0.30	0.93150	-0.96541	-0.89273	-0.93806
0.40	1.24200	-0.73077	-0.56696	-0.73530
0.401	1.245105	-0.72790	-0.56327	-0.73381

TABLE 3.1C

Potential from HADES Li^+ in KCl Lattice constant = 3.096 Å

X (Lattice) units	X (Å)	V100 (eV)	V110 (eV)	V111 (eV)
0.	0.	-1.15606	-1.15606	-1.15606
0.05	0.1548	-1.16107	-1.16569	-1.16953
0.10	0.3096	-1.16470	-1.17461	-1.18057
0.15	0.4644	-1.15448	-1.16111	-1.16750
0.20	0.6192	-1.12400	-1.11486	-1.12146
0.30	0.9288	-0.99075	-0.90660	-0.94025
0.40	1.2384	-0.75080	-0.56916	-0.73362
0.401	1.241496	-0.74787	-0.56535	-0.73212

TABLE 3.2A

Spectrum from HADES $^{7}Li^{+}$ in KCl Lattice constant = 3.116 A

Symmetry	Multiplicity	Energy (1-dim) (meV)	Energy (full) (meV)
A_{1g}	1	0.00000	0.00000
T_{1u}	3	1.00333	1.23948
T_{2g}	3	2.00666	2.38085
A_{2u}	1	3.01000	3.69150
A_{1g}	1	12.70836	12.41915
T_{1u}	3	13.71169	14.31878
E_{g}	2	12.70836	16.39985
T_{2g}	3	14.71502	16.46385
T_{2u}	3	13.71169	17.57417
A_{2u}	1	20.37060	21.20711
T_{2g}	3	19.36726	22.98523
T_{1u}	3	18.36393	23.66323
T_{1g}	3	19.36726	25.74398
E_{u}	2	20.37060	26.43655

Absolute energy for ground state:

(1-dim calculation) = -1.10862038 eV

(full calculation) = -1.10445106 eV

TABLE 3.3A

Spectrum from HADES $^{6}Li^{+}$ in KCl Lattice constant = 3.116 A

Symmetry	Multiplicity	Energy (1-dim) (meV)	Energy (full) (meV)
A_{1g}	1	0.00000	0.00000
T_{1u}	3	1.35553	1.68724
T_{2g}	3	2.71106	3.23067
A_{2u}	1	4.06659	4.91045
A_{1g}	1	13.72994	13.52077
T_{1u}	3	15.08547	15.86670
E_{g}	2	13.72994	17.71742
T_{2g}	3	16.44099	18.47260
T_{2u}	3	15.08547	19.30920
A_{2u}	1	23.16726	24.31652
T_{2g}	3	21.81173	25.98957
T_{1u}	3	20.45620	26.53393
T_{1g}	3	21.81173	28.98501
E_{u}	2	23.16726	29.92402

Absolute energy for ground state:

(1-dim calculation) = -1.10742789 eV

(full calculation) = -1.10308212 eV

TABLE 3.2B

Spectrum from HADES $^{7}Li^{+}$ in KCl Lattice constant = 3.105 A

Symmetry	Multiplicity	Energy (1-dim) (meV)	Energy (full) (meV)
A_{1g}	1	0.00000	0.00000
T_{1u}	3	2.06491	2.63369
T_{2g}	3	4.12983	5.07227
A_{2u}	1	6.19474	7.48192
A_{1g}	1	12.49671	12.90000
E_{g}	2	12.49671	15.58098
T_{1u}	3	14.56162	15.83729
T_{2u}	3	14.56162	18.06673
T_{2g}	3	16.62653	18.86246
T_{1u}	3	20.09107	26.11011
A_{2u}	1	24.22090	26.21371
T_{2g}	3	22.15598	26.57104
T_{1g}	3	22.15598	29.01482
E_{u}	2	24.22090	30.65382

Absolute energy for ground state:

(1-dim calculation) = -1.13760747 eV

(full calculation) = -1.13480878 eV

TABLE 3.3B

Spectrum from HADES $^{6}Li^{+}$ in KCl Lattice constant = 3.105 Å

Symmetry	Multiplicity	Energy (1-dim) (meV)	Energy (full) (meV)
A_{1g}	1	0.00000	0.00000
T_{1u}	3	2.58874	3.28484
T_{2g}	3	5.17748	6.32304
A_{2u}	1	7.76623	9.28258
A_{1g}	1	13.82501	14.46373
E_{g}	2	13.82501	17.29709
T_{1u}	3	16.41375	17.98298
T_{2u}	3	16.41375	20.37503
T_{2g}	3	19.00250	21.57985
T_{1u}	3	22.47613	29.36914
A_{2u}	1	27.65361	30.00528
T_{2g}	3	25.06487	30.15016
T_{1g}	3	25.06487	32.80254
E_{u}	2	27.65361	34.83988

Absolute energy for ground state:

(1-dim calculation) = -1.13673195 eV

(full calculation) = -1.13382648 eV

TABLE 3.2C

Spectrum from HADES $^{7}Li^{+}$ in KCl Lattice constant = 3.096 A

Symmetry	Multiplicity	Energy (1-dim) (meV)	Energy (full) (meV)
A_{1g}	1	0.00000	0.00000
T_{1u}	3	3.35972	4.07720
T_{2g}	3	6.71945	8.07992
A_{2u}	1	10.07917	11.81300
A_{1g}	1	13.26197	14.60429
E_{g}	2	13.26197	16.01807
T_{1u}	3	16.62170	18.57240
T_{2u}	3	16.62170	19.94617
T_{2g}	3	19.98142	22.63419
T_{1u}	3	22.17439	26.86913
T_{2g}	3	25.53412	30.68311
A_{2u}	1	28.89384	31.89225
T_{1g}	3	25.53412	32.58917
E_{u}	2	28.89384	35.54164

Absolute energy for ground state:

(1-dim calculation) = -1.16379057 eV

(full calculation) = -1.16540975 eV

TABLE 3.3C

Spectrum from HADES $^{6}Li^{+}$ in KCl Lattice constant = 3.096 A

Symmetry	Multiplicity	Energy (1-dim) (meV)	Energy (full) (meV)
A_{1g}	1	0.00000	0.00000
T_{1u}	3	4.00281	4.83966
T_{2g}	3	8.00562	9.56692
A_{2u}	1	12.00843	13.96878
A_{1g}	1	14.81755	16.41344
E_{g}	2	14.81755	17.96893
T_{1u}	3	18.82036	21.07897
T_{2u}	3	18.82036	22.60192
T_{2g}	3	22.82317	25.81806
T_{1u}	3	24.77582	30.11480
T_{2g}	3	28.77863	34.58995
A_{2u}	1	32.78144	36.12143
T_{1g}	3	28.77863	38.08290
E_{u}	2	32.78144	40.18444

Absolute energy for ground state:

(1-dim calculation) = -1.16466578 eV

(full calculation) = -1.16293246

To test the effect of changing the direction of exact fit, calculations were also performed for $^7Li^+$ using the data from lattice constant 3.116 A as fitted exactly along the <100> direction. The results of this test are presented in Table 3.4. While this caused results from the one-dimensional calculation to vary by a factor of two, the results from the full calculation differed by only 10-20%. Note that since the minima are located along the <111> direction, we expect the results to be the most reliable when this is the direction fitted exactly.

3.2 ICECAP-Generated Potentials

Difficulties were encountered in attempting to apply ICECAP to the problem of Li^+ in KCl. Specifically, HADES had trouble converging for certain cases, among which were all the cases involving Kunz-Klein localization. Thus all the cases for which numbers have been obtained were calculated using localization by means of orbitals with restricted spatial range and variational freedom. These cases are summarized in Table 3.5.

The quantum-mechanical cluster in each of the cases considered consisted of the Li^+ ion surrounded by its 6 nearest-neighbor Cl^- ions. The basis sets used for each ion were taken from Huzinaga.(47) For Li^+, 4 S Gaussians were used; for Cl^-, 9 S and 6 P Gaussians were used. Basis Set I consisted of just these functions, and used BHS norm-conserving pseudopotentials to

TABLE 3.4

Spectrum from HADES $^{7}Li^{+}$ in KCl Lattice constant = 3.116 Å
Potentials fitted exactly along the <100> direction

Symmetry	Multiplicity	Energy (1-dim) (meV)	Energy (full) (meV)
A_{1g}	1	0.00000	0.00000
T_{1u}	3	2.01898	1.03885
T_{2g}	3	4.03796	1.98211
A_{2u}	1	6.05694	3.15765
A_{1g}	1	15.28251	13.39703
T_{1u}	3	17.30149	15.33606
E_{g}	2	15.28251	16.12112
T_{2g}	3	19.32047	17.05272
T_{2u}	3	17.30149	17.14700
T_{1u}	3	24.44353	23.10798
T_{2g}	3	26.46251	23.15310
A_{2u}	1	28.48149	24.71604
T_{1g}	3	26.46251	24.73500
E_{u}	2	28.48149	26.14873

Absolute energy for ground state:

(1-dim calculation) = -1.10094867 eV

(full calculation) = -1.10538334 eV

replace the cores of the Cl^- ions.(40) In Basis Set II no such pseudopotentials were used, also an additional Gaussian was placed at the midpoint of each Li^+ - Cl^- bond.

The HADES potentials used were the same potentials used in the HADES-only phase of this investigation, that is, Buckingham potentials from Catlow et. al.(48)

All the cases reported were run with a lattice constant of 3.116 A. In the calculation listed as "Mobile QM Region" the overall minimization routine within ICECAP was allowed to vary the positions of the quantum-mechanical cluster; this calculation used considerable amounts of CPU time. To reduce the amount of CPU time required, other calculations were performed with the quantum-mechanical cluster fixed in the positions given by the HADES-only run from the first part of this investigation. The UHF-only run was performed in this same manner; the same nearest-neighbor quantum-mechanical cluster was embedded in a charge array extending out to the 15th shell of neighbors. The quantum-mechanical cluster had positions as determined by the HADES-only calculation; the point ions in the charge array were all at the perfect-lattice positions.

Due to constraints on available computer time, the complete potential predicted by UHF or ICECAP could not be mapped out; only the barrier heights along the <100> and <111> directions could be determined. Hence, DYNFIT and DYNNUC were not used in these cases.

TABLE 3.5

UHF and ICECAP Results Li^+ in KCl Lattice constant = 3.116 A

Calculation	HADES alone	UHF alone Basis Set II
<000>	E = -1.07444 eV	E = -76154.670 eV
<100>	E = -1.08536 eV	E = -76154.736 eV
<111>	E = -1.12685 eV	E = -76154.924 eV

Calculation	ICECAP Basis set I Fixed QM Region	ICECAP Basis set I Mobile QM Region
<000>	E = -2598.05768 eV	E = -2598.51849 eV
<100>	E = -2597.85779 eV	E = -2598.40526 eV
<111>	E = -2597.45252 eV	

Calculation	ICECAP Basis set II Fixed QM Region
<000>	E = -74886.10010 eV
<100>	E = -74885.79120 eV
<111>	E = -74885.12722 eV

<000> Configuration with Li^+ at 0. 0. 0. lattice constants.

<100> Configuration with Li^+ at 0.15 0. 0. lattice constants.

<111> Configuration with Li^+ at 0.15 0.15 0.15 lattice constants.

CHAPTER 4

CONCLUSIONS

The goal of this study has been to construct a theoretical model for an isovalent substitutional impurity in an ionic crystal. Two approaches to the construction of such a model have been presented, one using the classical lattice program HADES to generate the needed potentials, and the other using the embedded-cluster program ICECAP. Conclusions from each approach will be presented separately, followed by conclusions pertaining specifically to the programs DYNFIT and DYNNUC.

4.1 Conclusions from HADES Work

A classical shell-model approach with interactions defined by Buckingham potentials has been shown to reproduce well the qualitative behavior of Li^+ in KCl and other off-center systems. That is, it predicts off-center behavior in the systems known to be off-center, and similarly for on-center behavior with a few exceptions, and it successfully predicts that slightly decreasing the lattice constant will drive off-center systems back on-center. The two serious discrepancies reported by Catlow et. al.(21) were predictions of off-center behavior for Li^+ in RbCl and F^- in NaI where on-center behavior has been indicated experimentally; they suggest further experimental investigation

is warranted in these cases.

But that is not all we can learn from the paper of Catlow et. al. We can compare the difference in energy between on-center and off-center positions they report to the barrier heights calculated from measured absorption lines by Devaty and Sievers.(22) The results from Devaty and Sievers for the case of zero strain are that the barrier height is 7.4 meV for their fit to the form $Ax^2 + Bx^4$ and 9.9 meV for their fit to the form $Ax^2 + Be^{-Cx^2}$. The average of the results for the three symmetry directions from Catlow et. al. is 16 meV. Computing the tunnelling splittings provides a more stringent test of the form of the potential generated by HADES. Thus we compare the multiplicity-weighted average splittings

$$\bar{\Delta} = (\Delta_1 + 3\Delta_2 + \Delta_3)/5$$

(as defined in Figure 1.1) calculated from the HADES data at 3.116 Å:

$$^7\bar{\Delta} = 1.19485 \text{ meV}$$

$$^6\bar{\Delta} = 1.26201 \text{ meV}$$

to experimental data of:

$^{7}\bar{\Delta}$ = 0.102 meV

$^{6}\bar{\Delta}$ = 0.143 meV

from specific heat measurements(15) and

$^{7}\bar{\Delta}$ = 0.095 meV

$^{6}\bar{\Delta}$ = 0.100 meV

from phonon spectroscopy.(14) We note that the discrepancy in splittings is around a factor of ten, significantly worse than the factor of two discrepancy in barrier heights.

We are also interested in calculating the Grueneisen parameters at zero strain, as defined in Chapter 1. Calculating these from the multiplicity-weighted average splittings at 3.116 A and 3.105 A, we obtain $^{6}\Gamma$ = 66 and $^{7}\Gamma$ = 60. This can be compared with the best experimental determination, by Dobbs and Anderson,(17) of Γ = 150 independant of isotope. It can also be compared to a naive calculation using the model of Gomez et. al.(17,4) In this model the potential is taken to consist of isotropic harmonic oscillator potentials centered at the <111> minima (edge tunnelling dominating). It is assumed that small changes in the lattice parameter change only the separation between wells and not their oscillator frequencies ω_0. The splitting can then be written:

$$\Delta = 2x_0 S(x_0) K$$

for $2x_0$ the separation between wells along a cube edge, K a parameter independant of x_0, and $S(x_0)$ the overlap integral between wavefunctions on wells connected by a cube edge:

$$S(x_0) = e^{-M\omega_0 (x_0)^2/\hbar}$$

where M is the mass of the Li^+ ion. Assuming x_0 is proportional to the lattice constant, the logarithmic derivative can then be computed:

$$\Gamma = -d(\ln\Delta)/d(\ln V) = -3d(\ln\Delta)/d(\ln x_0) = 3[2M\omega_0 (x_0)^2/\hbar - 1]$$

Evaluating ω_0 from the observation of a second tunnelling multiplet at about 4.5 meV above the first tunnelling multiplet, taking x_0 = 0.7 A from an estimate of 1.2 A for the distance from the origin to the minimum,(3) and using M = 7 u, we obtain Γ = 19. Thus the HADES data does significantly better than this naive model at predicting the Grueneisen parameter.

4.2 Conclusions from ICECAP Work

Consider the barrier heights as given by the UHF and ICECAP calculations with basis set II. The barrier heights (for V_0 the one-dimensional potential) from the UHF calculation are

<100> 309 meV

<111> 324 meV

and those from the ICECAP calculation are

<100> 66 meV

<111> 85 meV

which may be compared with the previously cited fits to experimental data of 7.4 meV or 9.9 meV.

We must conclude that UHF and ICECAP in its present form are unable to match HADES for quantitative prediction of off-center behavior for Li^+ in KCl. In one sense, that is not surprising, as the energy differences between the on-center configuration and the off-center configuration along the <111> direction are on the order of 30 meV. Noone is claiming that even the component parts of ICECAP, i. e. HADES and UHF, are routinely capable of accuracies on that scale. With extreme care accuracies of a few tenths of an eV can be obtained with UHF when a correlation correction (MBPT) is applied. On appropriate classes of problems HADES may also be capable of accuracies on that order. Nevertheless, for this particular system we might hope that the random errors in both methods as used within ICECAP and in the interaction between them would remain constant. The main reason these errors might be hoped to remain constant is that the electronic wavefunction is in its ground state throughout this problem, and the changes in the wavefunction are not drastic.

Approaching the matter from another perspective, both HADES and UHF in principle include all the essential physics for a qualitative prediction of off-center behavior. Specifically, they each model Pauli repulsion and attraction due to induced polarization. The shortcomings of each model are different. The customary way of constructing an UHF model for this problem would be to use a point-charge array for sites not treated quantum-mechanically and ignore relaxation and polarization of these sites. HADES picks up this relaxation and polarization, but cannot model the changes in the interactions near the origin due to relaxation of the electronic wavefunction. Thus a combination of the two methods along the lines of ICECAP is an obvious way to attempt to overcome the shortcomings of both methods. With that in mind we may conclude that the features neglected by UHF are more important than those neglected by HADES for obtaining numerical predictions. As for why ICECAP is worse than both models taken separately, that can probably be ascribed to a mismatch between the HADES and UHF interactions. If the effective interaction between the quantum mechanical sites is different than the HADES interactions, a nonphysical strain will be observed at the boundary between the two regions. Since no attempt was made to match the HADES and UHF interactions, it is easy to assume that such an unphysical strain was affecting these calculations, causing ICECAP to give numerical results less reliable than either of its constituent models taken separately. Nevertheless, in conclusion, I suggest that when ICECAP is better

understood, and a way to insure consistency between the HADES and UHF portions of ICECAP is well developed, that this problem be taken up again as a test case because of its extreme sensitivity.

4.3 Conclusions Pertaining to DYNFIT and DYNNUC

The computer programs DYNNUC and DYNFIT seemed to work quite well within the approach used in constructing them. If a more efficient way of evaluating the Hamiltonian matrix elements for the three-dimensional calculation could be found, that would allow more three-dimensional functions to be used, which would improve convergence in the higher tunnelling multiplets. Beyond that, two improvements in the approach could be contemplated.

First, since three arbitrary functions are used as input to DYNFIT, one might consider whether it might generate a third independant function. Thinking along the lines of expanding the discrepancy between the form $V_0(x) + V_0(y) + V_0(z)$ and the exact function in angular momentum functions and recalling that the first functions consistent with cubic symmetry following $\ell = 0$ are $\ell = 4$, leads one to suggest adding a term $V_g(r,\theta,\phi)$. This might be expected to be especially important for systems with F^- off-center, as the minima in these systems have been determined experimentally to lie along the <110> direction. Hence the approximation $V_0(x) + V_0(y) + V_0(z)$ is not as good a

starting point for such systems.

Second, consider a way to take into account the motion of the nearest-neighbor nuclei. Let the effective coordinate q denote a spherically symmetric displacement of the nearest-neighbor nuclei from the configuration of minimum energy. The Hamiltonian then becomes:

$$H = H_0(\vec{r}) - \frac{1}{2M_q} \nabla^2 + V(q,\vec{r})$$

Pick V(q,r) harmonic in q:

$$V(q,\vec{r}) = \frac{1}{2} M_q \Omega^2(\vec{r})$$

Define $\Omega^2(0)$ to be $(\Omega_0)^2$ and expand the wavefunction associated with q in harmonic oscillator functions of frequency Ω_0. Then the potential energy matrix element simplifies to:

$$\frac{1}{2} M_q \langle\psi(\vec{r})|\Omega^2(\vec{r})|\psi'(\vec{r})\rangle \langle\psi(q)|q^2|\psi'(q)\rangle$$

The matrix element involving q is trivial from properties of harmonic oscillator functions. Choosing $\Omega^2(\vec{r}) = (\Omega_0)^2$ will leave the level structure unchanged, so to make this calculation physically significant we must include some non-constant term. An obvious choice is:

$$\Omega^2(\vec{r}) = (\Omega_0)^2 \ (1 + \frac{1}{2}\alpha r^2)$$

where α is determined from $\Omega^2(\vec{r})$ evaluated at the stable minimum.

Note that there is no obvious reason the α so defined must be positive. Since $r^2 = x^2 + y^2 + z^2$ this form will allow the matrix element $\langle\psi(\vec{r})|\Omega^2(\vec{r})|\psi(\vec{r})\rangle$ to factor into one-dimensional integrals, so it will be computationally very tractable. The use of only the basis function n=0 for the wavefunction in q ought to be sufficient, but n=2 might be included, if only to check convergence of the series.

APPENDIX

Mathematically rigorous derivation of the Kohn-Klein localization equations

Let

$$F = F_A + V_A^M + V_A^S$$

and

$$\rho = \sum_{\substack{i=occ \\ i \text{ in } A \text{ and} \\ i \text{ in } W}} \sum_{\substack{j=occ \\ j \text{ in } A \text{ and} \\ j \text{ in } W}} \Phi_i(\vec{x})\, S_{ij}^{-1}\, \Phi_j^+(\vec{x}')$$

and consider the exact solutions to the equation

$$(F_A + V_A^M + V_A^S - \rho T \rho)\Phi_i = \pi_i \Phi_i$$

where T is an arbitrary Hermitian operator.

We again denote the cluster by A, and we define

$$\rho_A = \sum_{\substack{i=occ \\ i \text{ in } A}} \Phi_i(\vec{x})\, \Phi_i^+(\vec{x}')$$

We recognize that for any k in the occupied space

$$\rho\Phi_k = \Phi_k \qquad \text{and} \qquad \Phi_k\rho = \Phi_k$$

and choose T to satisfy

$$T = \rho_A\, V_A^S\, \rho_A \quad .$$

Then the equation we are solving becomes

$$(F_A + V_A^M + V_A^S - \rho\rho_A V_A^S \rho_A \rho)\Phi_i = \pi_i \Phi_i$$

which can be rearranged into the form

$$(F_A + V_A^M + V_A^S - \rho_A V_A^S \rho_A)\Phi_i = \pi_i \Phi_i$$

which is the same equation derived approximately in the body of this paper.

REFERENCES

1. J. H. Harding, A. H. Harker, P. B. Keegstra, R. Pandey, J. M. Vail, and C. Woodward, Physica **131B**, 151 (1985).

2. A. Barry Kunz and David L. Klein, Phys. Rev B **17**, 4614 (1978).

3. V. Narayamurti and R. O. Pohl, Rev. Mod. Phys. **42**, 201 (1970).

4. M. Gomez, S. P. Bowen, and J. A. Krumhansl, Phys. Rev. **153**, 1009 (1967).

5. M. J. Norgett, Harwell Report No. AERE - R.7650 (1974).

6. J. M. Vail, A. H. Harker, J. M. Harding, and P. Saul, J. Phys. C **17**, 3401 (1984).

7. V. R. Saunders and M. F. Guest, Rutherford Laboratory Reports, ATMOL 3 (1976).

8. A. B. Kunz, University of Illinois and Michigan Technological University, unpublished.

9. F. C. Baumann, Bull. Am. Phys. Soc. **9**, 644 (1964).

10. H. S. Sack and M. C. Moriarty, Solid State Commun. **3**, 93 (1965).

11. G. Lombardo and R. O. Pohl, Phys. Rev. Lett. **15**, 291 (1965).

12. N. E. Byer and H. S. Sack, J. Phys. Chem. Solids **29**,677 (1968).

13. D. W. Alderman and R. M. Cotts, Phys. Rev B **1**, 2870 (1970).

14. M. C. Hetzler and D. Walton, Phys. Rev. B **8**, 4801 (1973).

15. J. P. Harrison, P. P. Peressini, and R. O. Pohl, Phys. Rev **171**, 1037 (1968).

16. A. M. Kahan, M. Patterson, and A. J. Sievers, Phys. Rev. B **14**, 5422 (1976).

17. J. N. Dobbs and A. C. Anderson, Phys. Rev. B (in press); J. N. Dobbs, Ph.D. thesis (University of Illinois, 1985) unpublished.

18. C. R. Case, K. O. McLean, C. A. Swenson, and G. K. White, in Thermal Expansion, M. G. Graham and H. E. Hagy, (eds.), (AIP, New York, 1971) p. 183.

19. W. D. Wilson, R. D. Hatcher, G. J. Dienes, and R. Smoluchowski, Phys. Rev. **161**, 888 (1967).

20. R. J. Quigley and T. P. Das, Solid State Commun. **5**, 487 (1967); Phys. Rev. **164**, 1185 (1967); Phys. Rev. **177**, 1340 (1969).

21. C. R. A. Catlow, K. M. Diller, M. J. Norgett, J. Corish, B. M. C. Parker, and P. W. M. Jacobs, Phys. Rev. B **18**, 2739 (1978).

22. R. P. Devaty and A. J. Sievers, Phys. Rev. B **19**, 2343 (1979).

23. M. Born and R. Oppenheimer, Ann. Phys. (Leipzig) **84**, 457 (1927).

24. A. Barry Kunz and David L. Klein, Phys. Rev B **17**, 4614 (1978); A. B. Kunz and P. B. Keegstra, "An ICECAP User's Guide to Kunz-Klein Localization Potentials", unpublished.

25. B. J. Dick and A. W. Overhauser, Phys. Rev. **112**, 90 (1958); W. Cochran, The Dynamics of Atoms in Crystals, (Edward Arnold, London, 1973).

26. H. A. Bethe and R. Jackiw, Intermediate Quantum Mechanics, (Benjamin/Cummings, Reading, Mass., 1968), p. 51 ff.

27. E. Schroedinger, Ann. Phys. (Leipzig) **79**, 361, 489; **80**, 437; **81**, 109 (1926).

28. D. R. Hartree, Proc. Cambridge Phil. Soc. **24**, 89, 111 (1928); V. Fock, Z. Physik **61**, 126 (1930); J. C. Slater, Phys. Rev. **35**, 210 (1930).

29. T. Koopmans, Physica **1**, 104 (1933).

30. P. O. Lowdin, "The Projected Hartree-Fock Method, An Extension of the Independant Particle Scheme" in Quantum Theory of Atoms, Molecules, and the Solid State, P. O. Lowdin, (ed.), (Academic Press, New York, 1966) p. 601.

31. C. C. J. Roothaan, Rev. Mod. Phys. **32**, 179 (1960).

32. S. F. Boys, Proc. R. Soc. London Ser. A **200**, 542 (1950).

33. R. F. Marshall, R. J. Blint, and A. B. Kunz, Solid State Commun. **18**, 731 (1976); Phys. Rev. B **13**, 3333 (1976).

34. W. Adams, J. Chem. Phys. **34**, 89 (1961); T. L. Gilbert, in Molecular Orbitals in Chemistry, Physics, and Biology, edited by P. O. Lowdin and B. Pullman (Academic Press, New York, 1964).

35. P. O. Lowdin, Adv. Phys. **5**, 1 (1956); A. B. Kunz, "Total Energy Algorithm for KKLP", unpublished.

36. J. Harding and A. H. Harker, private communication.

37. I. G. Csizmadia, M. C. Harrison, J. W. Moskowitz, S. Seung, B. T. Sutcliffe, and M. P. Barrett, Quantum Chemistry Program Exchange **11**, 47 (1964); D. R. Neumann, H. Basch, R. L. Kornegay, L. C. Snyder, J. W. Moskowitz, C. Hornback, and S. P. Liebman, Quantum Chemistry Program Exchange **11**, 199 (1971).

38. J. C. Phillips and L. Kleinman, Phys. Rev. **116**, 287 (1959).

39. G. B. Bachelet, D. R. Hamann, and M. Schluter, Phys. Rev. B **26**, 4199 (1982).

40. P. B. Keegstra, University of Illinois and Michigan Technological University, unpublished.

41. A. M. Stoneham, (ed.), Harwell Report No. AERE-R.9598 (corrected) (1981).

42. C. R. A. Catlow and W. C. Mackrodt, (eds.), Computer Simulation of Solids, (Springer-Verlag, Berlin, 1982).

AD-A174 012 ENERGY TRAPPING RELEASE AND TRANSPORT IN THREE DIMENSIONAL ENERGETIC SOLI..(U) MICHIGAN TECHNOLOGICAL UNIV HOUGHTON A B KUNZ 30 JUN 86 N00014-81-K-0620 4/4

UNCLASSIFIED F/G 7/3 NL

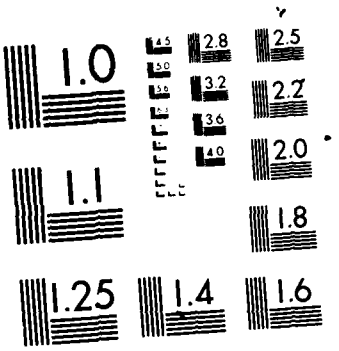

43. U. Schroeder, Solid State Commun. **4**, 347 (1966); C. R. A. Catlow, M. Dixon, and W. C. Mackrodt, "Interionic Potentials in Ionic Solids" in Computer Simulation of Solids, C. R. A. Catlow and W. C. Mackrodt, (eds.), (Springer-Verlag, Berlin, 1982).

44. N. F. Mott and M. J. Littleton, Trans. Faraday Soc. **34**, 485 (1938).

45. M. J. Norgett and R. Fletcher, J. Phys. C **3**, L190 (1970).

46. P. B. Ghate, Phys. Rev. **139**, A1666 (1965).

47. S. Huzinaga, (ed.), Gaussian Basis Sets for Molecular Calculations, (Elsevier, Amsterdam, 1984).

48. C. R. A. Catlow, K. M. Diller, and M. J. Norgett, J. Phys. C **10**, 1395 (1977).

VITA

Phillip Brooks Keegstra was born in Paterson, New Jersey on 23 July, 1959. He graduated from Eastern Christian High School in North Haledon, New Jersey in 1977. He attended Calvin College in Grand Rapids, Michigan from 1977 to 1982, receiving a B. A. in Math and a B. A. in Physics. In May, 1982 he enrolled in the Department of Physics at the University of Illinois at Urbana-Champaign. From May, 1982 to May, 1983 he was a departmental fellow. He served as a graduate teaching assistant during the 1982-1983 academic year. From May, 1983 to December, 1985 he served as a research assistant. In January, 1984 he received the M. S. degree in Physics. From January, 1986 through April, 1986 he served as a consultant to the Department of Physics at Michigan Technological University in Houghton, Michigan. He is a member of the American Physical Society.


FILM